SEISMIC PROBABILISTIC SAFETY ASSESSMENT AND RISK CONTROL OF NUCLEAR POWER PLANTS IN NORTHWEST EUROPE

A thesis submitted to The University of Manchester for the degree of

Doctor of Philosophy

in the Faculty of Engineering and Physical Sciences

2016

CARLOS MEDEL VERA

School of Mechanical, Aerospace and Civil Engineering

Table of Contents

Word count: 46848

List of Figures

List of Tables

Abstract

Nuclear power plays a crucial role in energy supply in the world: around 15% of the electricity generated worldwide is provided from nuclear stations avoiding around 2.5 billion tonnes of CO_2 emissions. As of January 2016, 442 reactors that generated 380+ GW were in operation and 66 new reactors were under construction. The seismic design of new nuclear power plants (NPPs) has gained much interest after the high-profile Fukushima Dai-ichi accident. In the UK, a tectonically stable continental region that possesses medium-to-low seismic activity, strong earthquakes capable of jeopardising the structural integrity of NPPs, although infrequent, can still occur. Despite that no NPP has been built in Great Britain after 1995, a New Build Programme intended to build 16 GW of new nuclear capacity by 2030 is currently under way. This PhD project provides a state-of-the-art framework for seismic probabilistic safety assessment and risk control of NPPs in Northwest Europe with particular application to the British Isles. It includes three progressive levels: (i) seismic input, (ii) seismic risk analysis, and (iii) seismic risk control.

For seismic input, a suitable model to rationally define inputs in the context of risk assessments is proposed. Such a model is based on the stochastic simulation of accelerograms that are compatible with seismic scenarios defined by magnitude $4 < M_w < 6.5$, epicentral distance 10 km $< R_{epi} <$ 100 km, and different types of soil (rock, stiff soil and soft soil). It was found to be a rational approach that streamlines the simulation of accelerograms to conduct nonlinear dynamic analyses for safety assessments. The model is a function of a few variables customarily known in structural engineering projects. In terms of PGA, PGV and spectral accelerations, the simulated accelerograms were validated by GMPEs calibrated for the UK, Europe and the Middle East, and other stable continental regions.

For seismic risk analysis, a straightforward and logical approach to probabilistically assess the risk of NPPs based on the stochastic simulation of accelerograms is studied. It effectively simplifies traditional approaches: for seismic inputs, it avoids the use of selecting/scaling procedures and GMPEs; for structural outputs, it does not use Monte Carlo algorithms to simulate the damage state. However, it demands more expensive computational resources as a large number of nonlinear dynamic analyses are needed.

For seismic risk control, strategies to control the risk using seismic protection systems are analysed. This is based on recent experience reported elsewhere of seismically protected nuclear reactor buildings in other areas of medium-to-low seismic activity. Finally, a scenario-based incremental dynamic analysis (IDA) is proposed aimed at the generation of surfaces for unacceptable performance of NPPs as function of earthquake magnitude and distance. It was found that viscous-based devices are more efficient than hysteretic-based devices in controlling the seismic risk of NPPs in the UK. Finally, using the proposed scenario-based IDA, it was found that when considering all controlling scenarios for a representative UK nuclear site, the risk is significantly reduced ranging from 3 to 5 orders of magnitude when using viscous-based devices.

This thesis is entitled “Seismic probabilistic safety assessment and risk control of nuclear power plants in Northwest Europe” and is submitted to The University of Manchester by Carlos Medel Vera for the degree of Doctor of Philosophy in March 2016.

Declaration

No portion of the work referred to in the thesis has been submitted in support of an application for another degree or qualification of this or any other university or other institute of learning.

Copyright statement

i. The author of this thesis (including any appendices and/or schedules to this thesis) owns certain copyright or related rights in it (the "Copyright") and s/he has given The University of Manchester certain rights to use such Copyright, including for administrative purposes.

ii. Copies of this thesis, either in full or in extracts and whether in hard or electronic copy, may be made **only** in accordance with the Copyright, Designs and Patents Act 1988 (as amended) and regulations issued under it or, where appropriate, in accordance with licensing agreements which the University has from time to time. This page must form part of any such copies made.

iii. The ownership of certain Copyright, patents, designs, trademarks and other intellectual property (the "Intellectual Property") and any reproductions of copyright works in the thesis, for example graphs and tables ("Reproductions"), which may be described in this thesis, may not be owned by the author and may be owned by third parties. Such Intellectual Property and Reproductions cannot and must not be made available for use without the prior written permission of the owner(s) of the relevant Intellectual Property and/or Reproductions.

iv. Further information on the conditions under which disclosure, publication and commercialisation of this thesis, the Copyright and any Intellectual Property and/or Reproductions described in it may take place is available in the University IP Policy (see http://documents.manchester.ac.uk/DocuInfo.aspx?DocID=487), in any relevant Thesis restriction declarations deposited in the University Library, The University Library's regulations and in The University's policy on Presentation of Theses (see http://www.manchester.ac.uk/library/aboutus/regulations).

Publications

Papers published or submitted to peer-reviewed journals:

1. Medel-Vera, C. and Ji T. (2014). "Seismic protection technology for nuclear power plants: a systematic review." *Journal of Nuclear Science and Technology* **52**(5): 607-632.

2. Medel-Vera, C. and Ji T. (2016). "A stochastic ground motion accelerogram model for Northwest Europe." *Soil Dynamics and Earthquake Engineering* **82**: 170-195.

3. Medel-Vera, C. and Ji T. (2016) "Seismic probabilistic risk analysis based on stochastic simulation of accelerograms for nuclear power plants in the UK" *Progress in Nuclear Energy* **91**: 373-388.

4. Medel-Vera, C. and Ji T. "Seismic risk control of nuclear power plants using seismic protection systems in stable continental regions: the UK case" *Nuclear Engineering and Design* (accepted subject to revisions).

Papers presented in conferences:

1. Medel-Vera, C. and Ji T. (2013). "Preliminary probabilistic seismic risk analysis for 3D seismically protected nuclear power plants" *SECED Young Engineers Conference*, Newcastle-upon-Tyne, UK.

2. Medel-Vera, C. and Ji T. (2015). “Seismic probabilistic risk assessment of nuclear power plants in the UK: an alternative procedure" *23rd International Conference on Structural Mechanics in Reactor Technology (SMiRT-23)*, Manchester, UK.

Dedication

To my parents,

for their endless love, support and encouragement.

Notation

A	Capacity of SSC of nuclear power plants (random variable)
$\bar{A}$	Median value for A
A^*	Gutenberg-Richter constant
A_{SSE}	Seismic response due to SSE
â	Deterministic value for $\bar{A}$
b^*	Gutenberg-Richter constant
C	Damping constant
$C_{1,..,9}$	Damping terms of soil impedances
D_1, D_2	Dummy variables to model type of soil
F	Factor of safety (random variable)
F_C	Capacity factor
F_{SR}	Structural response factor
$F_{\theta i}(\theta_1)$	Marginal cumulative distribution function fitted for θ_i
$\widehat{f}$	Median value for F
$f_M(m)$	Probability density function for earthquake recurrence
$f_R(r)$	Probability density function for earthquake attenuation with distance
H_0	Null hypothesis
$K_{1,..,9}$	Stiffness terms of soil impedances
M_L	Local magnitude scale (also known as Richter scale)
M_S	Surface-wave magnitude scale
M_w	Moment magnitude scale
m_b	Body-wave magnitude scale
Q	Confidence level of fragility curves
R_{epi}	Epicentral distance
R_{hyp}	Hypocentral distance
R_{JB}	Joyner-Boore distance
R_{rup}	Rupture distance
T	Trials
T_{obj}	Target fundamental period of vibration
z	Earthquake intensity
α	Damping exponent
$\beta_{1,...,9}$	Regression coefficients
β_r	Logarithmic standard deviation for ε_r
β_u	Logarithmic standard deviation for ε_u
ε_i	Residual of regressions for intra-event effects (random variable)

ε_r	Epistemic uncertainty (lognormal random variable)
ε_u	Aleatory uncertainty (lognormal random variable)
Φ	Standard normal distribution function
λ_m	Rate of exceedance of an earthquake equal or greater than magnitude M
η_i	Residual of regressions for inter-event earthquakes (random variables)
θ_i	Generic i-th random variable
σ_i	Standard deviation of ε_i
τ_i	Standard deviation of η_i
υ_i	Annual frequency of occurrence of earthquakes associated to an i-th source
ν_i	Transformation to Φ for an i-th variable originally in any space
ξ	Critical damping ratio

Acronyms

AFSA	Average floor spectral acceleration
AGR	Advanced Gas-Cooled Reactor
ALFRED	Advanced Lead Fast Reactor European Demonstrator
ASTRID	Advanced Sodium Technological Reactor for Industrial Demonstration
BWR	Boiling water reactor
CS	Containment structure
DBE	Design basis earthquake
DM	Damage measure
ENA	Eastern North America
FC	Fragility curves
FPS	Friction pendulum system
GMPE	Ground motion prediction equation
HCLPF	High confidence of low probability of failure
HDRB	High-damping rubber bearing
IAEA	International Atomic Energy Agency
IDA	Incremental Dynamic Analysis
IM	Intensity measure
IS	Internal structure
ISESD	Internet Site for European Strong-Motion Data
ITER	International Thermonuclear Experimental Reactor
JHR	Jules Horowitz Reactor
LDRB	Low-damping rubber bearing
LMR	Liquid-Metal-Cooled Reactor

LOCA	Loss-of-coolant accident
LOOP	Loss-of-off-site power
LRB	Lead-rubber bearing
LVD	Linear viscous dampers
MCE	Maximum credible earthquake
MMI	Modified Mercalli Intensity scale
MSK	Medvedev-Sponheuer-Karnik scale
NGA	Next Generation of Ground-Motion Attenuation Project (also known as NGA-West1 Project)
NGA-West2	NGA-West1 follow-up study
NPP	Nuclear power plant
NW	Northwest
PSA	Probabilistic safety assessment
PSHA	Probabilistic seismic hazard analysis
PWR	Pressurised water reactor
RESORCE	Reference Database for Seismic Ground-Motion in Europe
RV	Row vectors
SCR	Stable continental region
SMA	Seismic margin assessment
SME	Seismic margin earthquake
SPRA	Seismic probabilistic risk analysis
SPS	Seismic protection systems
SSC	Structures, systems and components
SSE	Safe shutdown earthquake
SSHAC	Senior Seismic Hazard Analysis Committee
SSI	Soil-structure interaction
UHS	Uniform hazard spectrum
URS	Uniform risk spectrum
VVER-1000	*Voda-Vodyanoi Energetichesky Reaktor*
WUS	Western United States

Chapter 1

Introduction

1.1 Background

1.1.1 Global nuclear industry: present situation

The current role played by nuclear power in the world is of crucial importance: as of January 2016, 442 commercial nuclear reactors housed in 191 power stations that generated 380+ GW were in operation [1] providing around 15% of the electricity generated worldwide [2]. Figure 1-1a shows the distribution by country of the currently operational nuclear reactors worldwide. They are major contributors towards a sustainable low-carbon electricity supply by avoiding the emission of around 2.5 billion tonnes of CO_2 [2]. Although the industry saw a marked decline by mid 1980s, it is in the early years of the present century that the so-called "nuclear renaissance" was underway. Such resurgence is mainly due to two necessities: (i) reducing greenhouse emissions, and (ii) ensuring stability of electricity supply, regardless of political uncertainties of fossil fuel imports [3]. As of January 2016, 66 new reactors were under

construction distributed in the countries shown in Figure 1-1b[1], most of which will have outputs from 1000 to 1600 MW [2]. Also, over 30 additional nations, including small and developing countries, are considering, planning or starting a new power programme supported by the International Atomic Energy Agency [4].

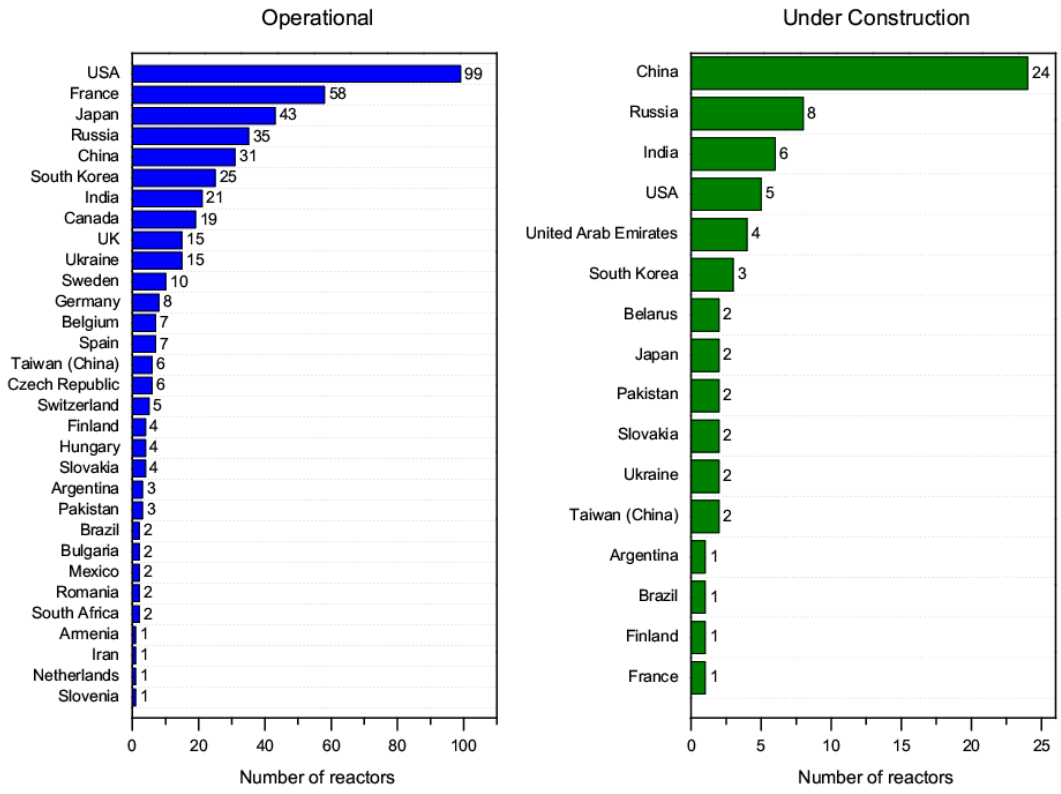

(a) (b)

Figure 1-1. Situation of the world nuclear industry as of January 2016: (a) 442 operational nuclear reactors, (b) 66 reactors under construction [1]

1.1.2 Nuclear power plants and earthquakes

A major technical challenge, that is often a matter of public controversy, is related to the assurance of a safe performance of nuclear installations against natural hazards, in particular, seismic actions. The World Nuclear Association has estimated that around 20% of nuclear reactors worldwide are operating in areas of significant seismic activity [5]. Figure 1-2 shows the location of the 5,814 earthquakes registered by the United States Geological Survey [6] during a period of 10 years (2005-2015) of magnitude 5.5+ and the location of the 191 currently operating nuclear power stations.

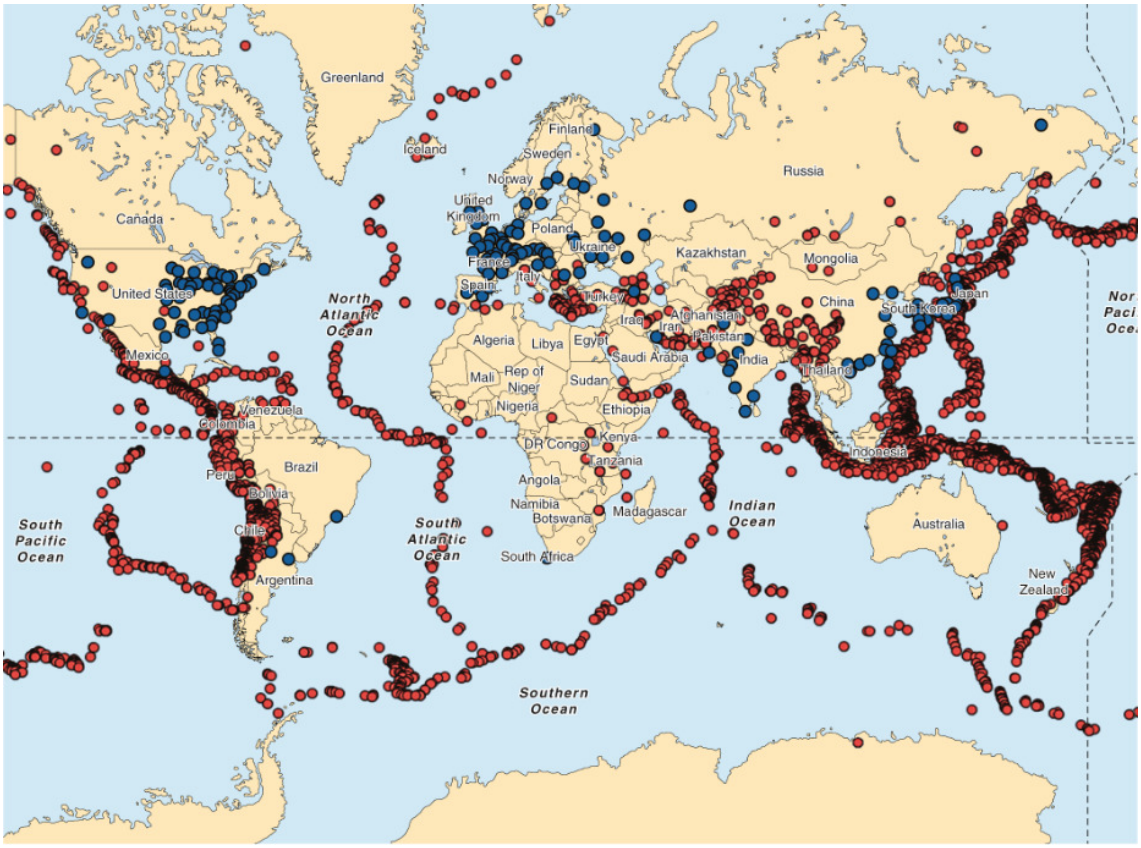

Figure 1-2. Earthquakes of magnitude 5.5+ registered between 2005 and 2015 (small red dots) and location of 191 currently operating nuclear power stations (big blue dots)

From Figure 1-2, it is possible to see that the majority of NPPs are located in seismically stable areas that possess medium-to-low seismic activity, in particular in Europe and Eastern USA. However, there is a number of NPPs located near active tectonic faults, such as in Western USA and Japan. The latter country recently experienced devastating consequences of nuclear facilities subjected to major seismic activity. On 11th March 2011, the Fukushima Dai-ichi reactors were hit by an unprecedented 15-metre tsunami triggered by the so-called Great East Japan Earthquake of magnitude M_w 9 [7]. Due to the occurrence of this accident, many nations, including those of medium-to-low seismic activity, commissioned comprehensive stress tests in order to re-assess the risk of their NPPs for events of similar nature as Fukushima's, i.e. extremely infrequent natural events that may lead to severe nuclear accidents [8]. Despite the severity of the Fukushima accident, the fundamental dynamics of global

energy policy did not suffer major changes: nuclear power will continue to be developed, recognising the need of improvements in regulations to ultimately increase structural safety as a matter of the utmost importance for new nuclear installations [9].

1.1.3 Seismic protection systems and nuclear power plants

In conventional civil structures, seismic protection systems (SPS), such as elastomeric-based bearings and energy dissipation devices, have been successfully used in more than 10,000 applications in 30 countries that possess a wide range of seismicity [10-11]. Nevertheless, their applications in the nuclear industry have been scarce: only two reactor buildings have been designed with such technology: Koeberg NPP in South Africa, with two isolated unit plants, and Cruas NPP in France, with four isolated unit plants [12]. The issues preventing the use of this technology in NPPs are mainly related to licensing and through life serviceability concerns, e.g. ageing, behaviour under radiation, stiffening, etc. Although Koeberg and Cruas NPPs were designed more than 40 years ago, extensive and valuable research has been conducted since then in order to include SPS in NPPs aimed at reaching a standardised seismic design of the nuclear island [13]. Nowadays, several new projects of isolated reactors in medium-to-low seismic areas are currently under way, e.g. the Jules Horowitz Reactor (JHR) [14] and the International Thermonuclear Experimental Reactor (ITER) [15], both under construction in Cadarache, France; plus the APR1400 currently under construction in South Korea [16]. Additionally, some other prominent projects of Generation IV reactors are currently in their early stages of preparation, e.g. the Advanced Sodium Technological Reactor for Industrial Demonstration (ASTRID) [17] to be built in France, and the Advanced Lead Fast Reactor European Demonstrator (ALFRED) to be built in Romania [18]. For the particular case of the UK, the benefits of using SPS was early recognised as a strategy to increase margins of safety of NPPs: in early 1990s,

laboratory tests were carried out on small-scale specimens of low-damping rubber bearings and viscous dampers for applications in Liquid-Metal-Cooled Reactors (LMRs) [19]. Nevertheless, no further analyses were reported and no real applications of seismically protected NPPs were built in the UK. Consequently, there is currently a knowledge gap on up-to-date investigations on the use of innovative strategies to control and reduce the risk of next generation NPPs in Britain using seismic protection devices.

1.1.4 UK nuclear industry: present situation

The UK nuclear industry has a long and well-established reputation of nearly 60 years of successful and, primarily, safe exploitation of nuclear power plants. Indeed, the UK was the first country that met all the scientific, technological and industrial challenges required to safely operate commercial nuclear stations [20]. At present, nearly 20% of the total electricity supply in the UK is provided by the 15 operational nuclear power reactors (14 Advanced Gas-Cooled Reactors and a single unit of a Pressurised Water Reactor) shown in Figure 1-3, most of which will stop operation by 2023.

Despite that no NPP has been built in the UK after Sizewell B in 1995, a New Build Programme intended to build 16 GW of new nuclear capacity by 2030 is in its early stages of development [21]. The investment, associated with at least 12 new reactors, is estimated at around £100 billion by the British government. Additionally, such programme is likely to be extended until 2050 with the development of reactors of Generation III+, IV and Small Modular Reactors [20]. This programme will be developed in five nuclear sites: Hinkley Point C (Somerset), Sizewell C (Suffolk), Wylfa Newydd (Anglesey), Oldbury (Gloucestershire) and Moorside (Cumbria).

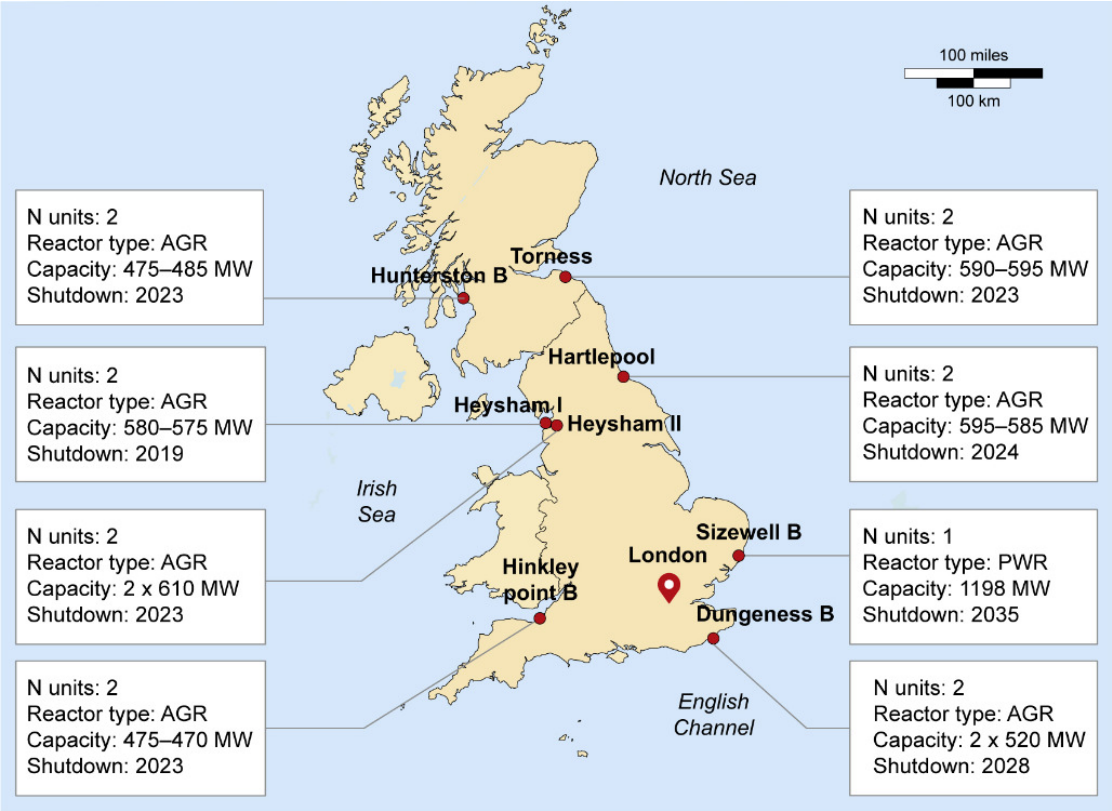

Figure 1-3. Situation of the UK nuclear industry as of January 2016.

Although the UK nuclear licensing regime is technically sound and does not have major weaknesses, after the Fukushima Dai-ichi accident, Her Majesty's Chief Inspector of Nuclear Installations [22] recommended that the British nuclear industry should conduct further studies to validate methodologies for analysing the seismic performance of structures, systems and safety-related components of NPPs. Currently, the safety of all reactors in the UK is carefully assessed on a regular basis as part of the Periodic Safety Reviews programme conducted every 10 years, which includes conducting a probabilistic assessment of risk [23]. Nevertheless, the seismic hazard has been characterised using an approach introduced in the late 1970s that was the subject of major research efforts during 1980s, the so-called "PML models" [24]. Such an approach possesses several shortcomings and limitations that have been reported in the literature [25]. Although it is acknowledged that the industry has made advances towards a better characterisation of the seismic hazard, no updated approaches have

been reported yet in the literature at the moment of writing of this PhD thesis. Consequently, there is currently a knowledge gap about a modern methodology to probabilistically assess the seismic risk of NPPs in the UK that includes an enhanced characterisation of the seismic hazard.

1.1.5 UK tectonics

In seismological terms, the UK is considered to be an intraplate region with moderate-to-low seismicity levels [26]. It is part of one of several Stable Continental Regions (SCRs), possessing unique tectonic features, mostly linked to the timing and nature of crustal deformation [27]. In spite of this fact, seismic hazard in the UK is non-negligible, as strong ground motions capable of compromising the structural integrity of strategic facilities can still occur [28]. Examples of significant earthquakes that have occurred in the UK are: an event magnitude M_w 5.5 in the Dover Straits region of the English Channel in 1580 and an event M_w 5.8 in the English Caledonides in 1931 [29]. It was also suggested that a major earthquake M_w 7 could have occurred offshore in recent geological times in the Northwest European passive margin near Britain [30]. Figure 1-4a shows the seismic events registered in the UK up to the end of 2010 and Figure 1-4b shows a PGA seismic hazard map for a return period event of 10,000 years.

In the context of seismic risk analysis of NPPs in the UK, there are three main barriers that make difficult to rationally define seismic inputs: (i) the underlying tectonic mechanism causing earthquakes in the British Isles is not yet fully understood [31]; (ii) there is little correlation between the pattern of earthquake occurrence and structural geology of Britain [26]; and (iii) the database of British earthquakes is mainly composed of small magnitude earthquakes, say, M_w 2 - 4.5. Consequently, there is currently a knowledge gap about the nature of accelerograms (intensity, frequency

content and time duration of the strong shaking phase) associated to earthquake magnitudes of interest for UK nuclear design, say, magnitude M_w 5~6.5 [25].

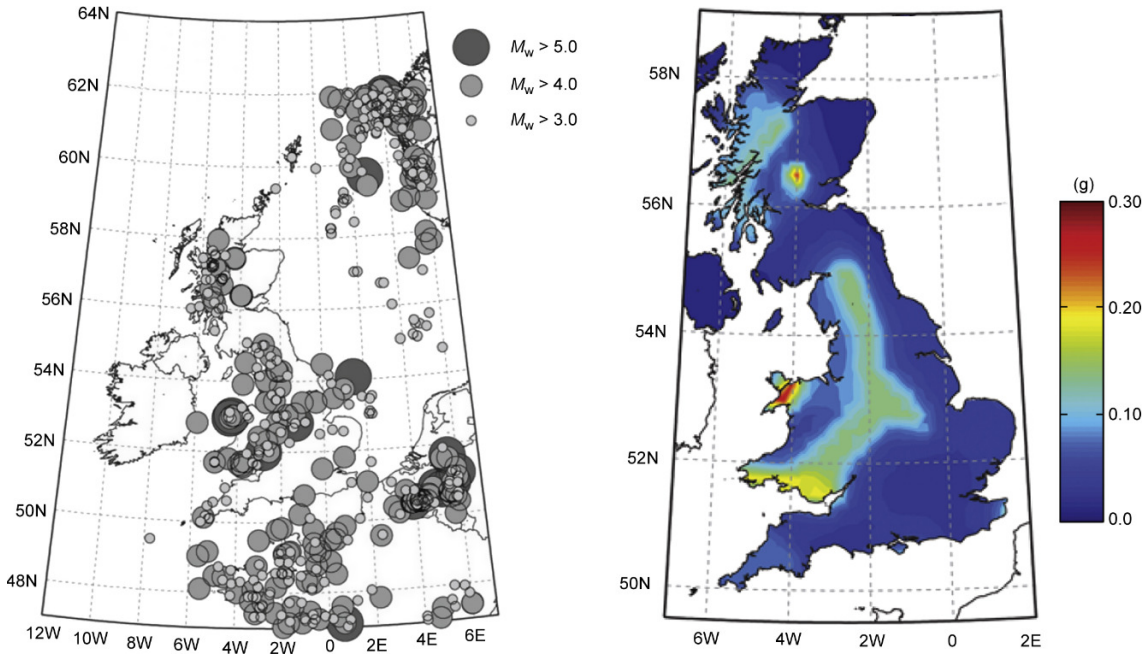

(a) (b)

Figure 1-4. Tectonics of the British isles: (a) seismic events in the UK up to the end of 2010, (b) seismic hazard contour map for PGA for a return period event of 10,000 years (redrawn from Goda et al. [32])

1.2 Aim and objectives

This research aims to bridge knowledge gaps in seismic ground inputs, seismic risk analysis and seismic risk control for making an original contribution to the development of the UK New Build Programme. The objectives are:

1. **Seismic input**: to establish a mathematical model, from a structural engineering perspective, that allows stochastic simulation of accelerograms for the UK nuclear industry taking account of intrinsic features of intensity, frequency content and time duration of earthquakes recorded in the same SCR to which the UK belongs.

2. **Seismic risk analysis**: based on Objective 1, to establish a rational and straightforward methodology that allows conducting seismic probabilistic risk analysis of NPPs in the UK.

3. **Seismic risk control:** based on Objectives 1 and 2, to determine the most efficient risk-informed approach on the use of seismic protection systems to control and reduce the seismic risk of NPPs in the UK.

The approach followed to make the contributions in the three gaps identified was progressive. At the basic level, the definition of the seismic input is the core contribution of this PhD project. The next level is based on the core contribution to propose a methodology to conduct seismic risk analysis. Finally, the top level is based on the basic and intermediate levels to analyse strategies of seismic risk control. The precise definition of each level of contribution including their justification, purposes, assumptions, scope, and limitations are described appropriately in the dedicated chapters that address such problems. The following section outlines the contents of this PhD thesis.

1.3 Thesis outline

This PhD thesis is organised as follows:

- Chapter 2 presents a literature review on: (i) seismic ground motion, (ii) seismic risk analysis, and (iii) seismic protection technology. Subjects (i) and (ii) are directly related to each other; hence, the review on seismic input initially provides a general yet complete description of approaches and it is further analysed when specifically addressing the definition of inputs for seismic risk analysis. Subject (iii) presents state-of-the-art seismic protection technology

devices intended to be used in nuclear deployments and a complete description of current applications of seismically protected nuclear reactor buildings.

- Chapter 3 presents the definition of a suitable model to rationally define seismic inputs in the context of risk analysis for NPPs in the UK. Such a model is based on the stochastic simulation of accelerograms that are compatible with seismic scenarios defined by magnitudes $4 < M_w < 6.5$, epicentral distances $10 \text{ km} < R_{epi} < 100 \text{ km}$, and different types of soil (rock, stiff soil and soft soil). The model is a set of predictive equations that define a stochastic process suitable to simulate accelerograms calibrated using a subset of accelerograms recorded in Northwest (NW) Europe. The model is validated in terms of peak ground acceleration (PGA), peak ground velocity (PGV) and spectral accelerations using ground motion prediction equations (GMPEs) for the UK, Europe and the Middle East, and other stable continental regions. This is the core contribution of this PhD project in which the remaining chapters of this thesis are based on.

- Chapter 4 presents an approach to probabilistically assess the seismic risk of NPPs in the UK based on the stochastic simulation of accelerograms described in Chapter 3. The approach is illustrated using an example of a 1000 MW Pressurised Water Reactor located in a representative UK nuclear site. A thorough comparison of risk assessment is also presented between the conventional and proposed approaches in order to highlight similarities and differences.

- Chapter 5 analyses three different strategies on the use of seismic protection systems for NPPs in the UK. Such strategies are based on the experience

reported elsewhere of seismically protected nuclear reactor buildings in other areas of medium-to-low seismic activity. Efficiency of protective systems is probabilistically assessed using the methodology described in Chapter 4 to achieve possible reduction of risk for both rock and soil sites in comparison with conventionally constructed NPPs. Further analyses are presented to study how the reduction of risk changes when all controlling scenarios of the site are included. This is done by introducing a scenario-based incremental dynamic analysis aimed at the generation of surfaces for unacceptable performance of NPPs as a function of earthquake magnitude and epicentral distance. Finally, general guidelines are proposed on the most suitable approach to potentially use seismic protection devices in next generation NPPs in the UK.

- Chapter 6 presents the conclusions of the work presented in this thesis and suggests topics for further related research.

Figure 1-5 shows the relationship among chapters 2, 3, 4 and 5 described above in order to visualise their interaction in this PhD thesis.

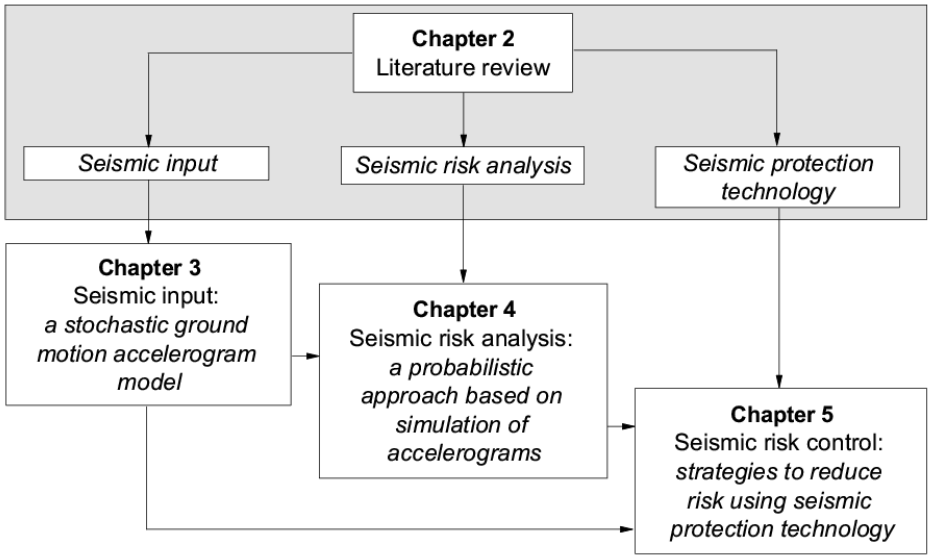

Figure 1-5. Relationship among chapters 2, 3, 4 and 5 of this PhD thesis

Chapter 2

Literature review

2.1 Introduction

Following the three topics identified in Section 1.2 suitable to make an original contribution, namely, seismic input, seismic risk analysis, and seismic protection technology, a dedicated literature review was conducted for each of them. For the first two topics, seismic input (Section 2.2) and seismic risk analysis (Section 2.3), the review was conducted as a traditional narrative review as is normally conducted in engineering. For the topic of seismic protection technology (Section 2.4), the review was innovatively conducted as a systematic review, a methodology widely used in health care and medical research, which was necessary to adapt in order to be applicable in engineering. Such work led to the publication of a peered literature review entitled "Seismic protection technology for nuclear power plants: a systematic review" [13] developed during the first year of this PhD project.

2.2 Seismic input

A major task in seismic design, analysis and assessment of structures is to appropriately define seismic loading conditions. Such definition of seismic loads depends on the type of analysis required, e.g. linear response spectrum, nonlinear dynamic, pushover, etc., and must satisfy certain conditions regarding their level and frequency of occurrence during the lifetime of a structure [33]. Currently, there is a wide variety of methodologies for predicting earthquake ground motions for engineering use (see Douglas and Aochi [34] for a comprehensive review of techniques). For the purposes of seismic hazard and risk analysis, in general, there are two main methods to define loading inputs: (i) ground motion prediction equations (GMPEs) or also referred to as attenuation relations and (ii) time-history acceleration records or simply referred to as accelerograms. The final product of these two types of models is essentially different: the following sections explain in detail similarities and differences between these two approaches.

2.2.1 Ground motion prediction equations

The predictive capacity of GMPEs is restricted to provide an estimation of a given ground motion intensity parameter for a specified earthquake scenario. These predictions, usually peak ground motion values (acceleration, velocity and displacement) and 5% damped spectral accelerations, are expressed as a function of a few independent parameters, e.g. earthquake magnitude, source-to-site distance, local soil conditions, fault mechanism, etc. They are calibrated using a dataset of earthquakes and defining a mathematical model for the ground motion parameter of interest which is derived by means of regression analysis given the independent variables selected [35]. Mathematical models used to define GMPEs normally have some physical basis, however, since all seismological aspects associated with the earthquake generation

phenomenon are not known, it is not possible to express a purely physical-based functional form for GMPEs [33]. As for datasets, GMPEs are normally calibrated using as much recorded accelerograms as possible; however, generally speaking, there are still "insufficient data to robustly characterise the expected range of ground motions over the entire magnitude-distance range of interest" [36]. In order to fill gaps in datasets of real accelerograms, GMPE developers routinely use the following approaches: (i) to use real accelerograms recorded in other areas that are thought of having a similar tectonic behaviour, (ii) to use simulated accelerograms, and (iii) a hybrid approach that combines (i) and (ii). Approach (i) is widely accepted in the literature: for example, GMPEs intended for use in active crustal regions normally include earthquake data from California, Turkey, Taiwan, Alaska, Italy, Mexico, New Zealand, etc. [37-38]. Approach (ii), also possessing high acceptance in research, is normally based on the stochastic simulation of accelerograms. As GMPE developers are mainly seismologists, the preferred model used to simulate accelerograms is the physics-based stochastic method based on the work of Hanks and McGuire [39] and Brune [40]. As such a stochastic model is heavily based on the physics of earthquake generation phenomenon, a deep knowledge of the underlying seismological governing process of the area of interest is needed. This model has been extensively used in research to help develop GMPEs: Boore [41] compiled more than 100 models published that made use of the stochastic model described. Approach (iii) takes advantage of both approaches previously described in order to produce robust datasets suitable for GMPEs calibration [42-44]. Figure 2-1 shows examples of typical final products of GMPEs for two different target regions, (a) Eastern North America [45], and (b) Europe and the Middle East [46]: they show median peak ground acceleration (PGA) predictions for three earthquake magnitudes, namely, M_w 5, 6 and 7, for epicentral distances between 10 km

< R_{epi} < 100 km, in rock conditions. From this figure, it is possible to see how PGA intensities and attenuation rates differ between them for the same earthquake magnitudes.

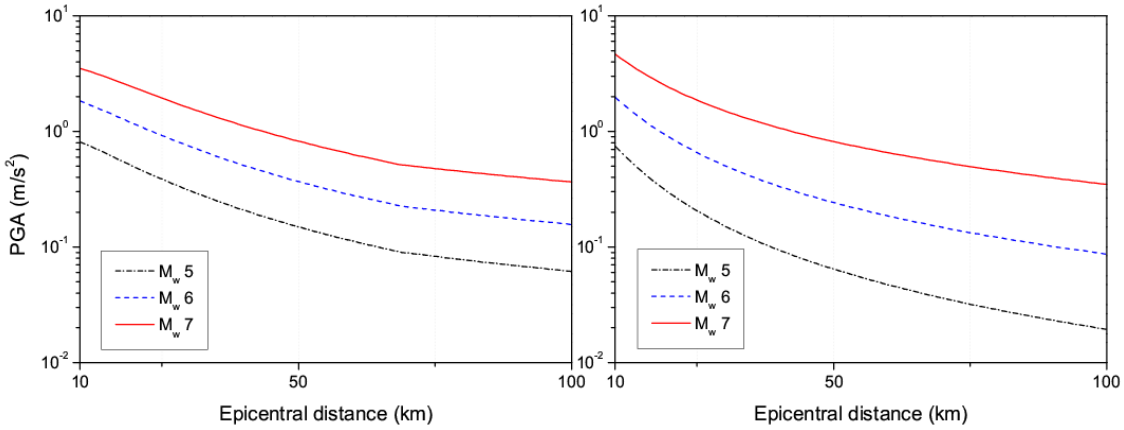

(a) (b)

Figure 2-1. Examples of PGA attenuation predicted by GMPEs: (a) Eastern North America [45]; (b) Europe and the Middle East [46]

GMPEs have rapidly evolved in recent years mainly due to an extensive growth of accelerogram databases: up to the year 2010, Douglas [47] showed that, on average, around 10 of these models are published every year. Recent GMPEs reported in the literature have been calibrated comprising a broad variety of sizes of their target geographical regions: e.g. Japan [48-49], Chile [50], New Zealand [51], Mexico [52], Turkey [53], Italy [54-57], Colombia [58], South Korea [59], India [60], Greece [61], Romania [62], Hawaii [63], the general region of Central and Eastern North America [64-67], the broader area of Europe and the Middle East [68], and even for generic active shallow crustal regions [37, 69]. In addition, two high-profile, multidisciplinary, long-term projects were finished in 2014 aimed at the generation of state-of-the-art GMPEs: (i) the NGA-West2 project that developed five attenuation models for shallow crustal active tectonic regions calibrated using a database composed of 21,332

recordings [38], and (ii) the RESORCE project that developed five attenuation models for the general region of Europe and the Middle East calibrated using a database composed of 5,882 recordings [70]. For the particular case of the UK, two models, PML [71-72], have been normally used in seismic risk assessments of critical structures, including nuclear power stations. These models were developed in the 1980s and were calibrated using small datasets of earthquake events recorded in areas that possess different tectonic regimes compared to the British Isles, such as, Central America, Greece, New Zealand and California. The latest GMPE reported in the literature for use in the UK, Rietbrock et al. [29], used simulated accelerograms obtained using a stochastic model calibrated using weak-motion data (events of magnitude $2 < M_l < 4.7$) recorded in Britain.

For a site-specific civil engineering project, the analyst is faced to the problem of choosing adequate GMPEs from a wealth of models available in the literature. Selection of appropriate GMPEs is a major task in itself and it is the subject of substantial research efforts [73-82]. Even if the selection of GMPEs is rationally performed, a significant issue that will normally cast doubt on the estimation needed for a given project is that GMPEs were calibrated combining data from different events in different regions [36]. Regional differences in ground motion attenuation can be observed even in relatively limited areas: for example, amplitudes in northern California are lower than those in southern California [83]. The wider the area of interest, the more likely is to include regional differences that may introduce bias in engineering applications. As it will be discussed in Section 2.3.3.1, GMPEs still play a key role in probabilistic seismic hazard analysis which in turn is performed to define site-specific loading for analysis and design of structures. Nevertheless, emerging trends in engineering seismology are

currently being developed as an alternative to GMPEs [36] that focus on judicious developments of accelerogram catalogues [84-85].

2.2.2 Accelerograms

In order to conduct risk analysis or performance assessment of structures, it is necessary to conduct nonlinear dynamic analyses of a structural model. Therefore, the type of input required is time-history acceleration records; hence, GMPEs by nature do not provide such type of input. Accelerograms suitable to perform nonlinear dynamic analyses of structures can be classified in three main groups: (i) real, (ii) synthetic, and (iii) artificial [86]. Real accelerograms, i.e. that have been recorded during an actual event, possess a wealth of information about the ground-motion characteristics of the site (amplitude, frequency content, energy content, time duration, etc.) and the underlying tectonics of the site (source mechanism, propagation path, etc.). Synthetic accelerograms are simulated recordings that are compatible with a given seismic scenario (magnitude, distance-to-site) obtained using seismological models or calibrating experimental models that use measured data of past earthquakes. Artificial accelerograms are recordings generated to match a target response spectrum using mathematical techniques. These types of recordings are not intended to represent accelerograms from actual earthquakes; rather, they are intended to represent the time-history version of a target spectrum used for design purposes.

As initially mentioned in Section 1.1.5, there is currently a lack of accelerograms in the UK associated to strong magnitude earthquakes suitable for seismic safety assessment of nuclear structures. This situation, also encountered in other areas of medium-to-low seismic activity, is due to two key reasons: (i) strong earthquakes rarely occur, and (ii) those areas have limited monitoring networks [87]. Consequently, a knowledge gap is

present in the UK nuclear industry to generate realistic sets of accelerograms compatible with controlling seismic scenarios likely to occur in British nuclear sites for use in probabilistic assessments of risk. As the simulation of synthetic accelerograms is a rational way to simulate earthquake recordings for areas that lack of real ones, only synthetics will be analysed in the remainder of this PhD thesis.

Currently, there are three techniques used to generate synthetic accelerograms [34]: (i) mathematical or source-based models based on physical/seismological principles (e.g. Halldórsson et al. [88]; Liu et al. [89]; Lam et al. [90]); (ii) experimental or site-based models using measured/experimental data (e.g. Mobarakeh et al. [91]; Rofooei et al. [92]; Sgobba et al. [93]; Zentner [94]); and (iii) hybrid models that combine both approaches (e.g. Graves and Pitarka [95]; Shahjouei and Pezeshk [96]). As pointed out by Boore [97], source-based models are mostly developed by seismologists in an attempt to explain the physics behind earthquake generation (e.g. source mechanism and propagation path). On the other hand, experimental models are mainly developed by engineers to obtain accelerograms using fitting techniques. From a structural engineering point of view, the main setback in using source-based models is that a profound knowledge of the governing seismological features of the site of interest is needed. Such knowledge is largely limited for the British Isles, therefore, any source-based model intended for UK purposes will possess an inherently high epistemic uncertainty. Therefore, this PhD project examined site-based models following a pragmatic approach in an attempt to define a model able to simulate accelerograms as a function of a few variables normally used in structural engineering projects.

The main challenge in any site-based stochastic ground motion accelerogram model is the ability to appropriately represent the temporal and spectral nonstationarity that is

inherent to real accelerograms [98]. Temporal nonstationarity refers to the variation in the intensity over time whereas spectral nonstationarity refers to the variation in the frequency over time. Appropriate parameterisation of both nonstationarities have a direct impact on the final results obtained in seismic risk analysis of structures [99]. There are different ways to achieve fully nonstationarity of a stochastic process (see Zerva and Zervas [100] for a complete overview) which has led to the development of several site-based models to stochastically simulate accelerograms, e.g. Sabetta and Pugliese [101], Montaldo et al. [102], Pousse et al. [103], Lin [104], Jurkevics and Ulrych [105], Nau et al. [106], Rupakhety and Sigbjörnsson [107], Polhemus and Cakmak [108], Conte and Peng [109], Der Kiureghian and Crempien [110], Wen and Gu [111], etc. However, the fully nonstationary mathematical formulation proposed by Rezaeian and Der Kiureghian [112] was selected due to the following combination of factors that make it suitable for the purposes established in this PhD project: (i) temporal and spectral nonstationarities are totally decoupled; this eases the selection of functional parameters governing both nonstationarities, (ii) the model works exclusively in the time domain; hence Fourier analysis or other analyses in the frequency domain are not required, and (iii) the simulation of accelerograms essentially involves the generation of random variables, avoiding the use of more complex numerical analysis.

The fully nonstationary stochastic process proposed by Rezaeian and Der Kiureghian [112] involves the simulation of a zero-mean white noise process (that confers the character of stochastic to the process) to then be altered by two functions: a linear filter with time-varying properties in order to achieve spectral nonstationarity, and a time-modulating function in order to reach temporal nonstationarity. The linear filter with time-varying properties is intended to introduce into the white noise the frequency content inherent to real accelerograms. A real recording can be seen as a complex

mixture of different waves travelling thorough the Earth's surface. P-waves (compressional) are first recorded as they travel fastest and possess high frequency contents. S-waves (shear) arrive later as they have lower velocities and also lower frequency contents. Finally, the surface waves, namely, Love (perpendicular to the direction of propagation) and Rayleigh (elliptical), arrive last as they have even lower velocities and frequency contents [113]. After the white noise has been filtered, the time-modulating function is intended to introduce into the stochastic process the evolution of ground motion intensities over time: starting from zero to then achieve maximum intensities that define the strong shaking phase to finally decrease to zero again. At the end of the process, a time-modulated filtered white noise process is achieved that is fully nonstationary; however, a common feature of stochastic processes is that they are likely to overestimate structural responses at long periods [114]. A high-pass filter is required to adjust the low-frequency content of the stochastic process after which a simulated accelerogram is realised. Figure 2-2 shows a graphical summary for simulating accelerograms using the approach selected in this work.

In Rezaeian and Der Kiureghian [112], they used a total of 6 parameters to define the stochastic process: 3 parameters each for the linear filter with time-varying properties and the time-modulating function. When such parameters are fitted to a single real accelerogram, then stochastically simulated accelerograms compatible with the real recording can be made. As each simulation uses a randomly generated white noise process, these accelerograms incorporate the randomness associated to a specified set of model parameters. In a later study, Rezaeian and Der Kiureghian [115] fitted the 6 governing parameters of the stochastic process to a dataset of real accelerograms recorded in active crustal regions and proposed a predictive functional form of such parameters against four variables of interest in structural engineering, namely,

earthquake magnitude, distance-to-site, type of soil and faulting mechanism. In this light, a set of accelerograms can be simulated that are compatible with a given seismic scenario of interest, incorporating the randomness of the model parameters associated to the site studied. Consequently, these two studies [112, 115] defined a comprehensive approach to simulate sets of synthetic accelerograms as function of a given seismic scenario for active crustal regions. As it will be seen in Chapter 3, this PhD project explored the applicability of such an approach for their applicability in the stable continental region of interest for this work. As a result of that, several modifications/upgrades were necessary to introduce for applications in seismic hazard and risk analysis in the UK nuclear industry. Figure 2-2 shows a graphical summary of the steps involved in the simulation of single/sets of accelerograms when using the methodology selected in this work.

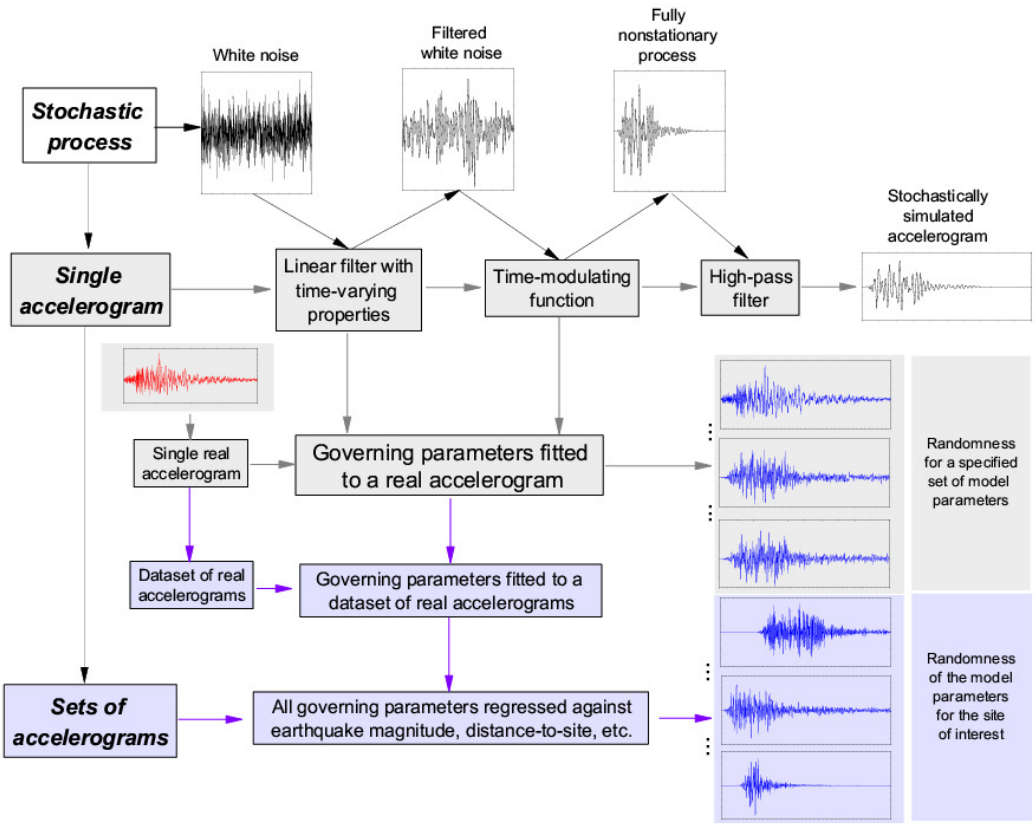

Figure 2-2. Generic procedure for simulating accelerograms under the methodology selected for this work

2.3 Seismic risk analysis

Seismic risk, in its broadest sense, is the potential probability of loss, be it human casualties, economic loss, cost of repair and replacement, loss of function, etc., due to the occurrence of an earthquake. In a strict sense, seismic risk analysis provides the foundations for seismic risk assessment, i.e. the judgment about its acceptability relative to a given threshold. Seismic risk assessment in turn provides the basis for seismic risk management, i.e. the mitigation actions, if necessary to take, to reduce it within acceptable levels [116]. Conceptually, seismic risk is the direct interaction between two analyses: the seismic hazard of a given site and the vulnerability (or fragility) of what is threatened by such seismic hazard [117].

In the nuclear industry, there are two customarily accepted methodologies to assess the seismic risk for power stations: the Seismic Margin Assessment (SMA) and the Seismic Probabilistic Risk Analysis, often abbreviated as Seismic PRA (or simply SPRA), or also referred to as Seismic Probabilistic Safety Assessment, abbreviated as Seismic PSA [118]. SMA is relatively straightforward in scope as it is a methodology that estimates the safety margin of a given design of a NPP by establishing the high-confidence-of-low-probability-of-failure (HCLPF) capacity of the critical components to be then verified against a given earthquake intensity called the Seismic Margin Earthquake (SME). Guidelines to conduct SMA for NPPs have been reported in the literature [119-121]. On the other hand, SPRA is more demanding as it is a comprehensive approach that fully integrates uncertainties in the seismic hazard, structural response and material capacity parameters that is aimed at estimating the probability of core damage and its consequences: potential release of radiation to the environment and the effects in the public health (see ASCE 4-98 [122] for an in-depth discussion of advantages and disadvantages between SMA and SPRA). In the UK nuclear industry, PRA (or PSA)

was introduced in mid 1980s as part of the Periodic Safety Reviews programme that involved comprehensive reviews of safety every 10 years [23]. Nevertheless, when assessing the seismic hazard, an approach developed more than 30 years ago is used to define it [24] possessing several limitations reported in the literature [25]. Consequently, a knowledge gap is present in the UK nuclear industry about a modern methodology to probabilistically assess the seismic risk of NPPs in Britain that includes an updated characterisation of the seismic ground inputs.

2.3.1 Probabilistic approach in the nuclear industry: general consideration

SPRA and its applications for NPPs were first endorsed by the American nuclear regulator: NUREG/CR-2300 [123] was the first guide published for using the methodology (see Garrick and Christie [124] and Keller and Modarres [125] for complete overviews on historical developments of SPRA in the nuclear industry). SPRA is traditionally used by owners in the nuclear industry in order to provide a thorough demonstration to the local nuclear regulator that any operation to be undertaken is adequately safe [23]. Nevertheless, the industry has also incorporated SPRA in the design process of NPPs [126]: the risk of a certain NPP design is assessed recurrently during the entire process for key decisions taken. This risk-informed approach towards NPP design has gained acceptance in the nuclear industry [127-130]. This approach is significantly useful for design of NPPs under the so-called "defence-in-depth" concept. This concept creates multiple independent, redundant and hierarchical barriers of defence in order to prevent and mitigate accidents that may lead to release of radiation or hazardous materials [131]. Several examples of such a concept of design in the nuclear industry have been reported in the literature [132-134]. It is worth mentioning that in the international practice of SPRA in the nuclear industry, three levels are established: Levels 1, 2 and 3. They are sequential analyses that provide

the foundations for the analysis in the next level. Level 1 SPRA [135] analyses the sequence of events that can lead to core damage, i.e. study the strengths and weaknesses of safety-related systems and safety case procedures designed to prevent core damage. Level 2 SPRA [136] takes the results of Level 1 SPRA to analyse the progression of events during core damage that can result in release of radiation to the environment. Level 3 SPRA [137] takes the results of Level 2 SPRA to study the impacts on public health and other societal consequences, such as contamination of land, water, food, etc. caused by release of radiation to the environment. As far as this PhD thesis is concerned, all analyses conducted and presented are simplified Level 1 SPRA.

There are two general methodologies to conduct SPRA of NPPs: (i) the Zion method [138], and (ii) the Seismic Safety Margin Research Program (SSMRP) method [139]. The latter is generally not used in practice [140] (hence, not pursued here), whereas the former is widely used in the nuclear industry (therefore, SPRA will refer to this methodology hereafter). Several approaches can be used to conduct SPRA possessing different levels of complexity depending on the type of project [126, 141]. However, the state-of-the-art SPRA procedure for NPPs reported in the literature has been proposed by Huang et al. [142-144]. Such a methodology is a combination of existing SPRA procedures enhanced with state-of-the-art tools of performance-based earthquake engineering (PBEE) methods for conventional buildings, in particular, the FEMA-P-58 project [145] (formerly, the ATC-58 project). PBEE, that incorporates a probabilistic approach, has gained much research interest and has experienced a remarkably rapid growth for applications in a wide range of mission-critical civil structures, such as tall buildings, hospitals, skewed bridges, etc. [146-149]. This PhD project has taken advantage of the methodology proposed by Huang et al. [142-144] to improve and

extend it, where possible, in order to be of use for the British nuclear industry. This methodology involves performing five steps: (i) perform plant-system and accident-sequence analyses, (ii) characterise seismic hazard, (iii) calculate and simulate structural response, (iv) assess damage of NPP components, and (v) compute the risk. These steps are summarised in Figure 2-3 and explained in detail in Sections 2.3.2 to 2.3.6.

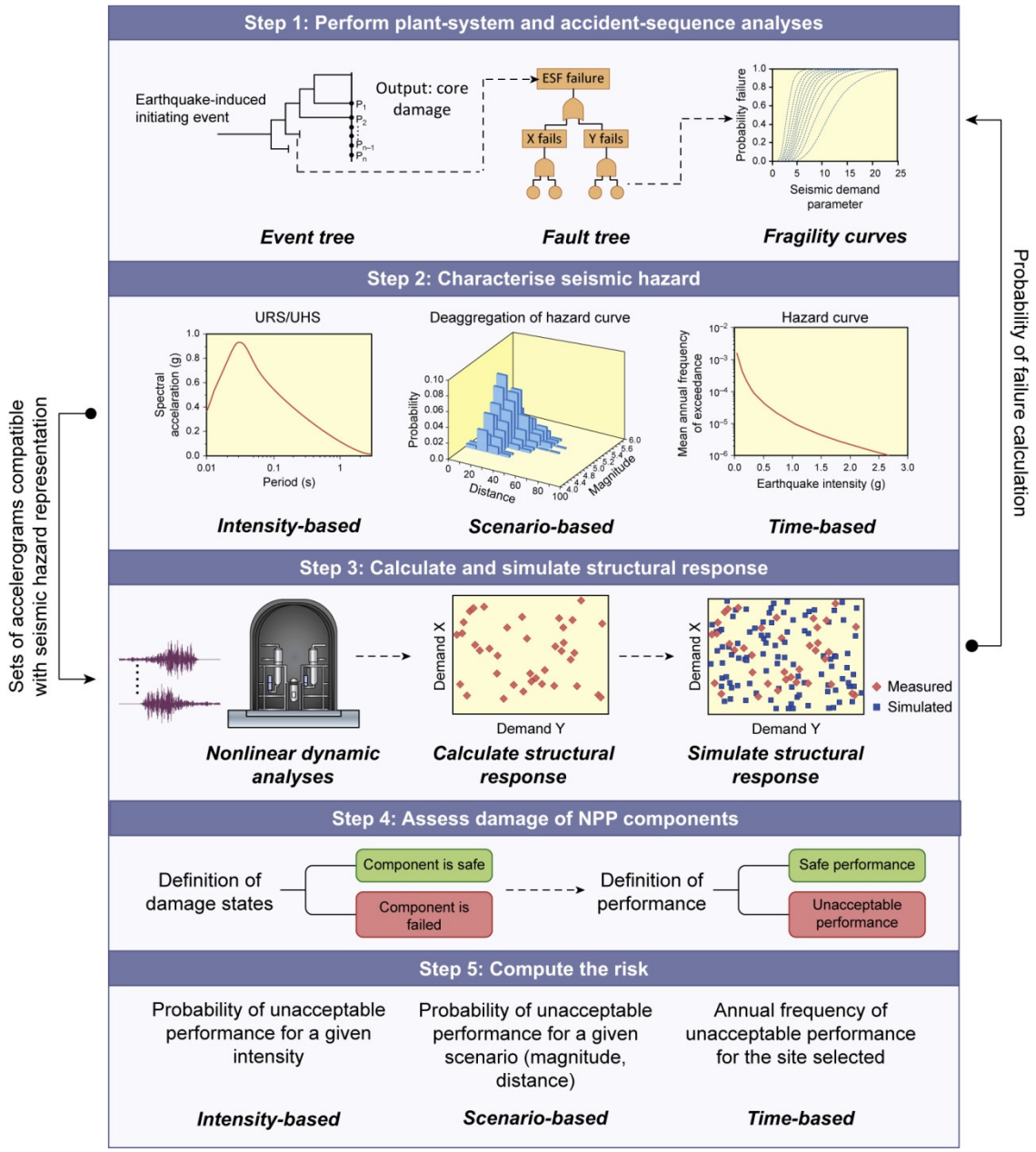

Figure 2-3. Graphical summary of steps to conduct state-of-the art SPRA for NPPs

2.3.2 Plant-system and accident-sequence analyses

This step comprises the identification of initiating events, i.e. occurrences that create disturbances, which may potentially cause a global failure of NPPs, e.g. core damage to then cause radiation release to the environment. There are different types of initiating events that normally need to be taken into account: guidelines to define initiating events for NPPs in the context of SPRA have been issued by the IAEA [150]. This PhD thesis is particularly concerned with earthquake-induced initiating events, for example: loss-of-coolant accident (LOCA), loss-of-off-site power (LOOP), reactor vessel rupture, etc. [151]. Identification of these events requires a deep understanding of the plant-system: i.e. how the plant responds to such perturbations, including responses of different nature: (i) physical (e.g. variations of temperature, water levels, etc.), (ii) automatic (e.g. actions that are automatically activated by mitigation/emergency equipment), and (iii) operator (e.g. actions that are manually activated by the plant operator according to the NPP's safety case procedures) [123]. After identification of initiating events, all possible paths that will progressively lead to the global failure are analysed by means of event and fault trees approach. Both methodologies are a pictorial representation of a statement in Boolean logic: event trees use "forward logic" to propagate an initiating event considering all possible paths that may lead to an accident; fault trees use "backward logic" to study the component failures that contribute to produce a prescribed failure of a system [152]. Then, seismic fragility curves need to be estimated for the NPP components at the lowest levels of the fault tree. Fragility curves give the local probability of failure of components as a function of a given seismic demand parameter. Sections 2.3.2.1 and 2.3.2.2 provide a description of event and fault trees, and fragility curves, respectively.

2.3.2.1 Event and fault trees

Event trees are a graphical representation of success/failure of several safety systems that may lead to an accident. Figure 2-4 shows a simplified event tree whose initiating event, e.g. a large pipe break, triggers two safety systems designed to prevent a failure event or accident, e.g. radiation release. If either of the safety systems operate properly, the system returns to normal; otherwise, an accident happens. The safety systems are considered to be independent from each other and they can either operate (upper branches) or fail (lower branches). Therefore, the probability of a whole path is simply obtained from direct multiplication of local event probabilities. A path that leads to an accident is referred to as accident sequence.

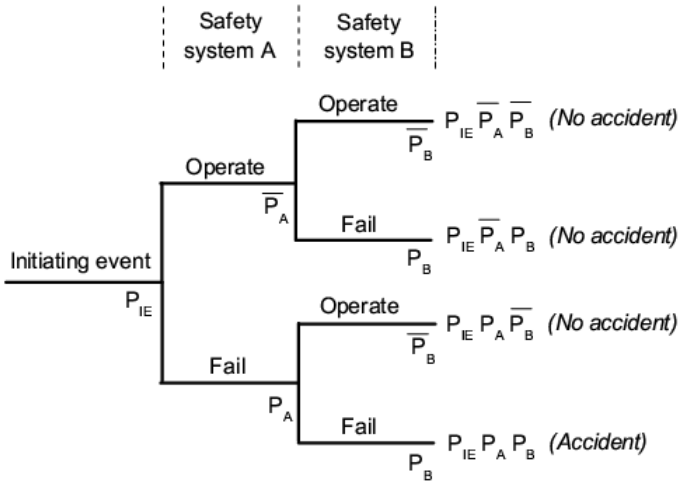

Figure 2-4. Example of a simplified event tree

In applications in the nuclear industry, it has been reported that event trees have problems for representing complex scenarios whose developments are affected by the plant operator's actions, i.e. they do not include the dynamic evolution in time of system component's interaction due to human behaviour [153-154]. In order to overcome this problem, the dynamic event trees methodology has been successfully used in nuclear applications [155-157]. Such a methodology effectively allows the simulation of the

evolution of systems and their dynamic interaction. Dynamic event trees are, however, beyond the scope of this PhD thesis; hence, not pursued here.

In an event tree, the local probabilities of failure of each safety system are needed in order to estimate the probability of occurrence for all of its paths. Such local probabilities can be estimated using fault trees. Fault trees are a graphical depiction of how a particular safety system can fail. The top event of a fault tree represents the occurrence of a given event which is dependent on several intermediate events until the basic events, at the lowest level of a fault tree, are reached. If the top event is a failure of a system, the basic events are normally failure of certain components of such a system [152]. Figure 2-5 shows an example of a fault tree of an engineered safety feature.

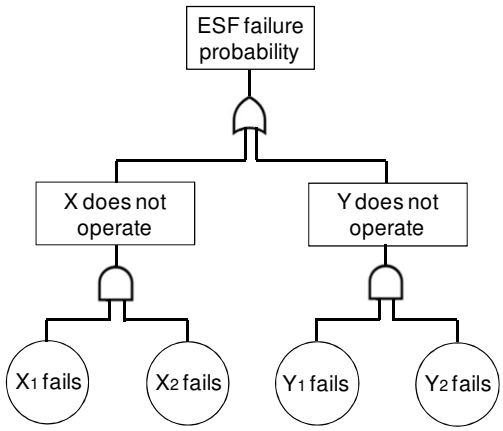

Figure 2-5. Example of a simplified fault tree

2.3.2.2 Fragility analysis

Seismic-related fragility curves for structures, systems and components (SSCs) in NPPs are needed to be estimated in SPRA. Industry-standard practice is largely based on the fragility analysis procedure used for the Zion NPP [138] and described in detail in Kennedy and Ravindra [158] and Kennedy et al. [159]. Thorough guidelines for conducting fragility analysis following such procedure in the context of SPRA were

later reported in EPRI [160] and then updated in EPRI [140]. It is acknowledged that alternative approaches to estimate fragility curves for NPP components are available in the literature [139, 161]. They are however beyond the scope of this PhD thesis, hence, not pursued here. See Pisharady and Basu [162] for a complete summary of methods to estimate fragility curves for NPP components.

Fragility curves are used to characterise the conditional probability of failure of SSCs under seismic loads; such failure occurs when its capacity, defined as a function of a predefined seismic demand parameter, is exceeded. The capacity of a component is defined by the double lognormal model as follows:

$$A = \overline{A} \cdot \varepsilon_r = \hat{a} \cdot \varepsilon_u \cdot \varepsilon_r \tag{2-1}$$

In this model, the capacity A is modelled as a random variable in which $\overline{A}$ is the median value of the capacity and ε_r is a lognormal random variable with unit median and logarithmic standard deviation β_r. The random variable ε_r accounts for the inherent randomness (aleatory uncertainty) naturally present in the seismic demand when determining the capacity of a component. As another source of uncertainty is the lack of complete knowledge (epistemic uncertainty) to determine the median capacity of the component, $\overline{A}$ is in turn modelled as a random variable in which $\hat{a}$ is a deterministic value that represents the best estimation for $\overline{A}$ and ε_u is a lognormal random variable with unit median and logarithmic standard deviation β_u. Using the capacity model indicated in (2-1), the probability of failure of a component for a given intensity *a* of the selected seismic demand parameter is

$$f = \Phi\left(\frac{\ln\left(a/\hat{a}\right) + \Phi^{-1}(Q)\cdot\beta_u}{\beta_r}\right) \tag{2-2}$$

where Φ is the standardised normal distribution function and Q is the probability (confidence level) that the median capacity of the component exceeds a predetermined value of the demand parameter. It is worth mentioning that the distinction between aleatory and epistemic uncertainty is subject of debate in the literature. It is widely accepted that aleatory uncertainty cannot be reduced as it is the inherent randomness associated to a given random variable whereas epistemic uncertainty can be reduced by improving the knowledge/data (by means of tests, simulations, etc.) associated to the random variable studied. In practice, such distinction between uncertainties is subjected to the analyst's modelling choices; hence, it is a subjective decision [163]. Some advocate for a rigorous separation between the two uncertainties [164-165] whereas others promote for a correct quantification of the total uncertainty (the sum of both) rather than an exhaustive distinction between them [166-167]. See Der Kiureghian and Ditlevsen [168] and Hofer [169] for thought-provoking discussions about the appropriateness of separating aleatory and epistemic uncertainties in risk analysis.

The capacity of a component, A, is normally obtained by using an intermediate random variable, regarded as factor of safety, F. This variable is defined as the ratio of the actual seismic capacity of the component analysed to the actual seismic response due to a given earthquake intensity of interest to the analyst, normally, the safe shutdown earthquake (SSE), i.e.:

$$F = \frac{A}{A_{SSE}} = \frac{Actual\ seismic\ capacity}{Actual\ seismic\ response\ due\ to\ SSE} \tag{2-3}$$

Equation 3 is re-written in such a way as to identify the conservatism in both the strength and the response:

$$F = \frac{Actual\ seismic\ capacity}{Design\ response\ due\ to\ SSE} \cdot \frac{Design\ response\ due\ to\ SSE}{Actual\ seismic\ response\ due\ to\ SSE}$$

$$F = F_C \cdot F_{SR} \tag{2-4}$$

where F_C is the capacity factor and F_{SR} is the structural response factor associated to the SSE. The factor of safety for structures considers both capacity and response parameters whereas for equipment and other components, the building structure and equipment response parameters as well as the capacity of equipment have to be included. The median value of F, $\hat{f}$, can be directly related to the deterministic capacity value, $\hat{a}$ using the equation:

$$\hat{f} = \frac{\hat{a}}{A_{SSE}} \tag{2-5}$$

Using Equations 2-3 to 2-5, the deterministic capacity value, $\hat{a}$, can be estimated for the component analysed. This method requires a great amount of knowledge [140, 158, 160, 162], such as plant specific information about seismic design and qualification test data. Such a procedure goes beyond the scope of this PhD thesis; hence, it is not studied further here. A straightforward alternative to estimate $\hat{a}$ when little information is available is based on a seismic margin approach. In seismic margin studies, it is of interest to determine the HCLPF capacity of a SSC. HCLPF is defined as the capacity level of a SSC in which the analyst has 95% confidence that the probability of failure is less than 5%. This benchmark capacity has a critical importance: the HCLPF capacity of

the weakest SSC in the safe shutdown path is considered the plant level HCLPF capacity [140]. When replacing Q=0.95 and f=0.05 in Equation 2-2, the HCLPF capacity is:

$$HCLPF = \hat{a} \cdot e^{-1.65 \cdot (\beta_r + \beta_u)} \tag{2-6}$$

Methodologies to determine the HCLPF capacity of NPP components have been reported in the literature, for example, the Conservative Deterministic Failure Margin (CDFM) method [121] or the Composite Fragility Curve approach [170]. In addition, values for β_u and β_r are recommended to be taken from published literature, if no analytic derivation is available [162] or when it is appropriate to use available generic information for standard components, as there is currently a wealth of experience from previous NPP projects for such values [171]. In this light, having determined values for HCLPF, β_u and β_r, it is possible to estimate the deterministic capacity value $\hat{a}$ and then, using Equation 2-2, a family of fragility curves can be defined for different confidence levels Q required by the analyst. Figure 2-6a shows three generic fragility curves for a given component considering 5%, 50% and 95% confidence levels as well as the HCLPF capacity level.

A seismic demand parameter needs to be selected to define fragility curves of NPP components. Traditionally, the peak ground acceleration (PGA) has been chosen in the nuclear industry [158, 172-174]. Such a practice is largely considered acceptable: a close example on the use of PGA to define seismic fragility curves for NPP components is the EU Stress Report of British NPPs, e.g. Hinkley Point B [175], as part of the response from the UK nuclear industry to the Fukushima accident. Nevertheless, it has been recently reported that structural response parameters provide a better correlation to

damage in comparison with ground-motion parameters [142, 176-177]. Several such parameters have been analysed and reported in the literature for nuclear applications, for example, pseudo-spectral acceleration, Arias intensity, cumulative absolute velocity intensity, among others [178]. In particular, the demand parameter used to define fragility curves in the methodology proposed by Huang et al. [142] is the average floor spectral acceleration (AFSA) over a given frequency range. This parameter is also in line with the industry-standard practice of specifying seismic demands on NPP components using floor response spectra [144]. For consistency purposes, AFSA is used in the remainder of this PhD thesis to define fragility curves: Figure 2-6b shows an example of a family of 11 fragility curves for a critical component of a sample NPP used later in this thesis.

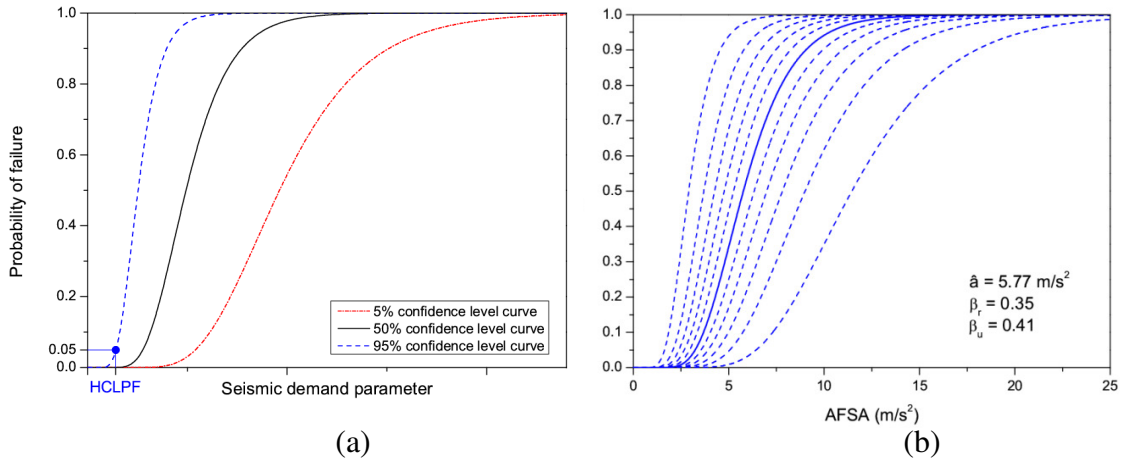

(a) (b)

Figure 2-6. Examples of fragility curves: (a) generic curves with 5% 50% and 95% confidence levels and HCLPF capacity level; (b) family of 11 fragility curves for a critical equipment of a sample NPP used later in this PhD thesis.

2.3.3 Seismic hazard and accelerograms

Seismic hazard analyses can be conducted in three ways: (i) deterministic, (ii) probabilistic, and (iii) an integrated approach of (i) and (ii) [179]. In a deterministic approach, a given earthquake magnitude and distance-to-site associated to the maximum credible earthquake (MCE) of the site analysed is selected as a representation of its

hazard. In this approach, the return period of the MCE is not directly addressed as the objective is to design against a "reasonable" event regardless of its time. In a probabilistic approach, the probability of exceedance of all possible earthquakes from all possible sources are estimated for a given exposure time. There is basically one fundamental difference between these approaches: a probabilistic approach carries units of time and a deterministic approach does not. An integrated approach is intended to benefit from both analyses: a probabilistic analysis is carried out to study which scenarios of magnitudes and distances contribute most strongly to the hazard of the site and then a deterministic analysis is performed to characterise such scenarios. There are different views in the literature about the appropriateness of deterministic and probabilistic approaches to characterise the seismic hazard for mission-critical structures [180-181]. Nevertheless, the difference between these two approaches has been regarded as an "exaggerated dichotomy" [182] as they have more commonalities than differences. Useful recommendations [183] have been reported about the better decision of using one or other approach based on: (i) the scope of project (e.g. regional risk, specific site, etc.); (ii) seismic environment (e.g. next to active fault, low hazard, etc.), and (iii) the type of seismic decision involved (e.g. emergency response, retrofit levels, etc.). Integrated approaches that are intended to benefit from the advantages of both methodologies have also been proposed in the nuclear industry [184-186].

2.3.3.1 Probabilistic Seismic Hazard Analysis

For the purposes of SPRA, characterisation of the seismic hazard is made by means of probabilistic seismic hazard assessment (PSHA). PSHA was formally introduced in late 1960s in the seminal paper of Cornell [187]. Later, in mid-1970s, McGuire [188] published an open source software for public domain that implemented the Cornell methodology. This software, which led the methodology to be known as the "Cornell-

McGuire" method, was the catalyst to an extensive recognition of PSHA as a tool for earthquake engineering in decision making (see McGuire [189] for a comprehensive note on the historical development of PSHA). PSHA is aimed at the generation of a family of curves depicting the frequency (usually the number of events per year) with which given values of a seismic hazard parameter, e.g. PGA, are expected to be exceeded [190]. Basically, PSHA consists of the four steps described as follows and graphically summarised in Figure 2-7.

1. Seismic source model: It is initially required the identification of the zone of influence which will define the area under study. For NPPs, it has been recommended to define a radial region of 200 miles (320 km) surrounding the facility for PSHA purposes [179]. All the relevant earthquakes and historical seismic activity occurred in such a zone are accounted for and grouped into the different seismic sources encountered. Seismic sources can consider: (i) points, to model distant or small sources (ii) lines, to model faults or (iii) areas, to model extensive areas with distinguishable patterns of seismicity and boundaries [191]. All this information is then compiled to define the "earthquake catalogue" for the influence zone. A typical earthquake catalogue comprises information such as: magnitude, location, date, focal depth, type of faulting, etc.

2. Recurrence law: Once the seismic source model is defined, a relationship between the average rate of occurrence of earthquakes and their magnitude must be developed for each source. In traditional PSHA, the recurrence law of Gutenberg-Richter [192] is commonly used. This law relates the rate of exceedance of an earthquake equal or greater than magnitude M per unit of time, λ_M, as $\log \lambda_M = A^* - b^* \cdot M$ where A^* and b^* are constants that depend on the particular source analysed. The Gutenberg-Richter

law has been shown to be valid for fairly vast regions, e.g. the entire southern California area, but it has been questioned in comparatively smaller areas that define a critical engineering project [180, 193]. In spite of this, it is still widely used in seismic hazard calculations for the nuclear industry, even when a microzonation process is involved [194]. The recurrence law is normally established by setting a minimum and a maximum earthquake magnitude for the purposes of the project. Once the recurrence law is compiled for each source of the site, it is possible to generalise such information by defining their probability density function, $f_M(m)$. This function is used to determine the frequency of exceedance of any earthquake of magnitude m within the magnitude range defined.

3. Ground motion intensity: Taking the seismic source model of step 1, it is of interest to determine how a given measure of earthquake intensity (e.g. peak ground acceleration or 5% damped spectral acceleration) decays as a function of the distance between each seismic source and the structure analysed. In traditional practice, this step heavily relies on the use of GMPEs (see Section 2.2.1). The aim is to generalise the attenuation-with-distance information for each source by defining their probability density function, $f_R(r)$. This function is used to determine how the demand parameter attenuates its intensity for any distance r for a given event magnitude m.

4. Seismic hazard curve: The seismic hazard curve is obtained by using the total probability theorem by summing up, within the ranges of validity defined, all possible earthquake magnitudes from every seismic source at every possible distance-to-site. The curve provides the total annual frequency of exceedance for any value of the earthquake intensity parameter used. Mathematically, the seismic hazard curve is the outcome of solving the integral indicated in Equation 2-7. Currently, there is software available to

solve the hazard integral: commercial packages (e.g. EZ-Frisk^{TM}) and public domain packages (e.g. OpenSHA) are available for practitioners and researchers involved in seismic hazard analyses.

$$\lambda(Z > z) = \sum_{i=1}^{n\,sources} \upsilon_i \iint P\left[Z > z \mid m, r\right] f_{Mi}(m) f_{Ri}(r)\, dm\, dr \qquad (2\text{-}7)$$

where:

$\lambda(Z > z)$: annual frequency of the earthquake intensity z is exceeded.

υ_i : annual frequency of occurrence of earthquakes of interest at the i-th source.

$P\left[Z > z \mid m, r\right]$: conditional probability that an earthquake intensity Z will exceed a value z, given an earthquake magnitude m and a distance r.

$f_{Mi}(m)$: probability density function for magnitudes in the i-th source.

$f_{Ri}(r)$: probability density function for distance-to-site in the i-th source.

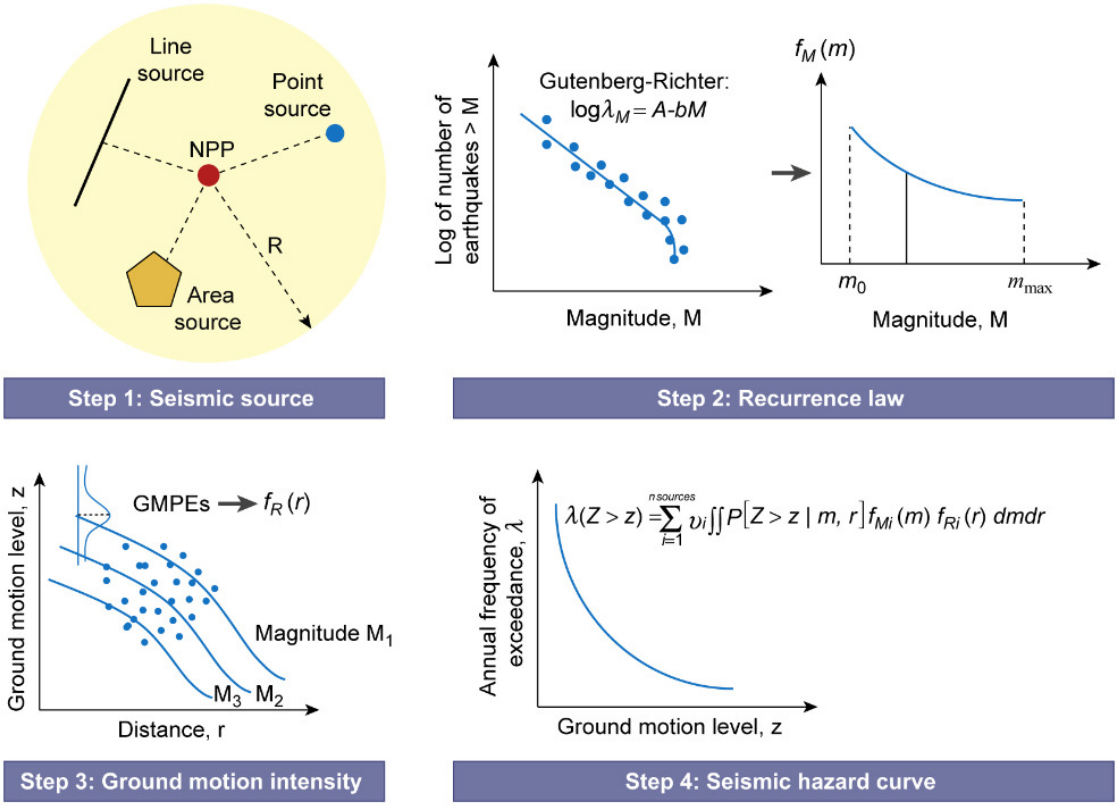

Figure 2-7. Steps for performing PSHA [190-191].

There is normally a great amount of uncertainty regarding steps 1, 2 and 3 which certainly will affect the results of step 4 [195-196]. Two types of uncertainty are traditionally included in PSHA: aleatory uncertainty or inherent randomness, e.g. location and magnitude of the next earthquake, ground motion amplitude for a given scenario magnitude and distance-to-site, etc., and epistemic uncertainty or lack of total knowledge, e.g. maximum magnitude for a given source, selection of ad-hoc GMPEs, etc. Aleatory uncertainty is completely included in the PSHA integration whereas epistemic uncertainty is modelled by means of logic trees. Extensive literature has been reported about the use of logic trees in PSHA [197-202]. They are a robust methodology to incorporate alternative models/parameters which are weighted according to the extent of belief that the analyst has on them. Certainly, there is a significant amount of expert judgment when accounting for the epistemic uncertainty in PSHA. It is believed that the epistemic uncertainty is likely to be reduced by combining assessments of several experts. This led the development of the Senior Seismic Hazard Analysis Committee (SSHAC) methodology [203]. In simple terms, the SSHAC methodology defines four levels that increase in sophistication and use of human and economic resources, from Level 1 to Level 4, to determine the hazard curve of a site. Recent examples of PSHA conducted using SSHAC Level 3 process for new nuclear sites can be found in Bommer et al. [204] and Coppersmith et al. [205].

PSHA can be considered standard practice in the global nuclear industry: it is customarily performed in countries with wide ranges of seismicity [206], e.g. the USA [205], UK [23], South Korea [207-208], India [209], Brazil [210], Switzerland [211], Slovenia [212], South Africa [204], among others. In addition, PSHA is not only used in the context of risk analysis, but also for design purposes: it provides basis to define the Uniform Hazard Spectrum (UHS) (or also called Uniform Hazard Response Spectrum

(UHRS)). In simple terms, UHS/UHRS is constructed for a given site by obtaining a series of hazard curves for a broad range of structural periods of interest. Then, a single return period of interest is selected, e.g. 10,000 years, and the corresponding demand parameter of the hazard curve is read for the structural periods of interest. In this way, a spectrum of demand parameter vs structural periods is obtained in which all points have equal probability of being exceeded, i.e. the hazard is uniform [191]. In US nuclear regulations [213], PSHA is the only methodology accepted to obtain the design basis earthquake (DBE), which in turn is obtained from the UHRS. The IAEA guidelines [214] have a broader scope to define the DBE: not only PSHA but also other probabilistic approaches in combination with deterministic methods are recommended.

PSHA is routinely used to define the seismic input required to conduct nonlinear dynamic analyses of a structural model of the NPP analysed when conducting SPRA. The type of input will depend on the type of seismic performance assessment required by the analyst. In the methodology selected for this work [142], three types to conduct risk assessments are defined: (i) intensity-based, (ii) scenario-based and (iii) time-based assessments. Intensity-based assessments are intended to estimate the probability of unacceptable performance when a NPP is subjected to a specific intensity of shaking (e.g. PGA=0.25g). Scenario-based assessments estimate the probability of unacceptable performance of a NPP under a specific earthquake, defined by a pair of magnitude and distance-to-site (e.g. M_w 6 and epicentral distance R_{epi} = 25 km). Finally, time-based assessments estimate the annual frequency of unacceptable performance of a NPP taking into account all potentially damaging earthquakes that may occur in the selected nuclear site. Although the nature of the seismic inputs for these three assessments is the same, i.e. accelerograms, they have to be compatible with different representations of the seismic hazard at the site. For intensity-based assessments, the hazard is represented

by a single spectrum, be it safe-shutdown response, design basis, uniform hazard, uniform risk, or any other type of spectrum required by the analyst. For scenario-based assessments, the hazard is represented by the deaggregation of the hazard curve of the site selected. Finally, for time-based assessments, the entire hazard curve of the nuclear site is needed. Figure 2-3 summarises the relationship between the representations of the seismic hazard for the three types of assessments. In the methodology selected for this work [142-143], 11 pairs of horizontal accelerograms compatible with the representation of the corresponding seismic hazard in intensity- and scenario-based assessment whereas it uses bins of 11 accelerograms for 8 discrete intensities of the hazard curve (i.e. 88 accelerograms) for time-based assessments. This is due to: (i) statistical basis to estimate structural responses with a minimum acceptable confidence for structural engineering purposes, (ii) the difficulty in obtaining suitable accelerograms compatible with the hazard representation, and (iii) to limit the use of computer resources.

2.3.3.2 Definition of accelerograms for nonlinear dynamic analyses

There are different methodologies available in the literature to select and scale accelerograms to match the different representations of the seismic hazard as well as ensuring un unbiased estimation of the structural response. A comprehensive review on methodologies for the selection of accelerograms developed until 2010 can be found in Katsanos et al. [215] and several other procedures have been published after such a review, for example, Kwong et al. [216], Jayaram et al. [217], Ay and Akkar [218], NIST [219], Baker [220], Huang et al. [221], and Bradley [222]. Even though the legitimacy and applicability of these procedures have been the subject of ample discussion in the literature [223-225], they are widely accepted and used by researchers and practitioners. The scaling procedures used in order to define suitable sets of

accelerograms to conduct nonlinear dynamic analyses for the three types of assessment are explained in the following paragraphs.

For intensity-based assessments, it is required to define the 5% damped response spectra (normally UHS/URS) for the nuclear site selected. Then, a target spectral acceleration for the fundamental period of NPP is determined and 11 accelerograms are scaled to match such a target. The accelerograms are scaled using the Amplitude Scaling Method [221] where all recordings are "anchored" to the target spectral acceleration without taking into account the variability in the spectral demand. Figure 2-8 shows a generic summary of the definition of accelerograms for nonlinear dynamic analyses in intensity-based SPRA.

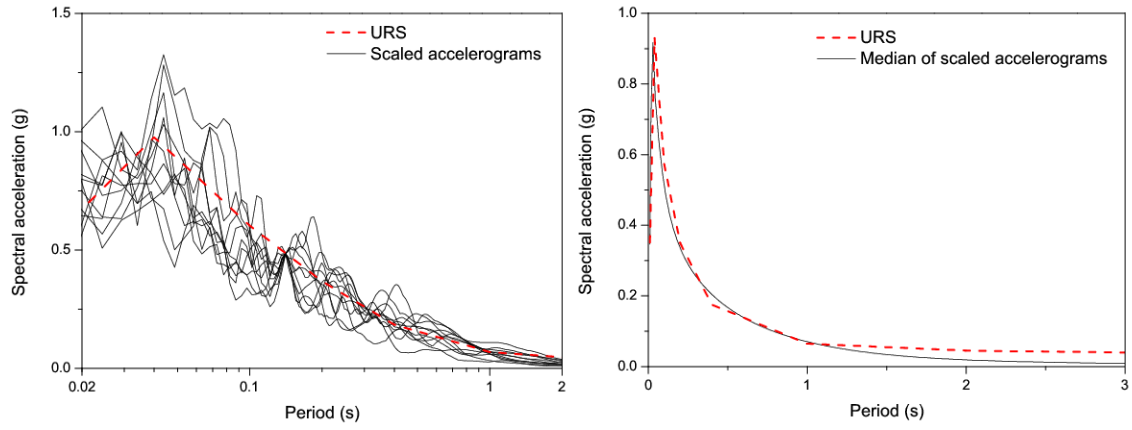

(a) (b)

Figure 2-8. Generic definition of accelerograms to conduct intensity-based SPRA: (a) URS and 11 scaled accelerograms anchored to a given target spectral acceleration; (b) URS and median of 11 scaled accelerograms

For scenario-based assessments, it is required to define the single scenario (or all scenarios of interest) that contributes most strongly to the hazard of the nuclear site selected. Such a scenario can be obtained by means of the deaggregation of the hazard curve of the site [32, 226]. Then, a spectral shape predicted by ad-hoc GMPE(s)

compatible with such scenario is estimated and 11 accelerograms are scaled to match such a spectral shape. The accelerograms are scaled using the Distribution Scaling Method [221] in order to capture the variability (median, 16th and 84th percentiles) predicted by the corresponding GMPE. Figure 2-9 shows a generic summary of the definition of accelerograms for nonlinear dynamic analyses in scenario-based SPRA.

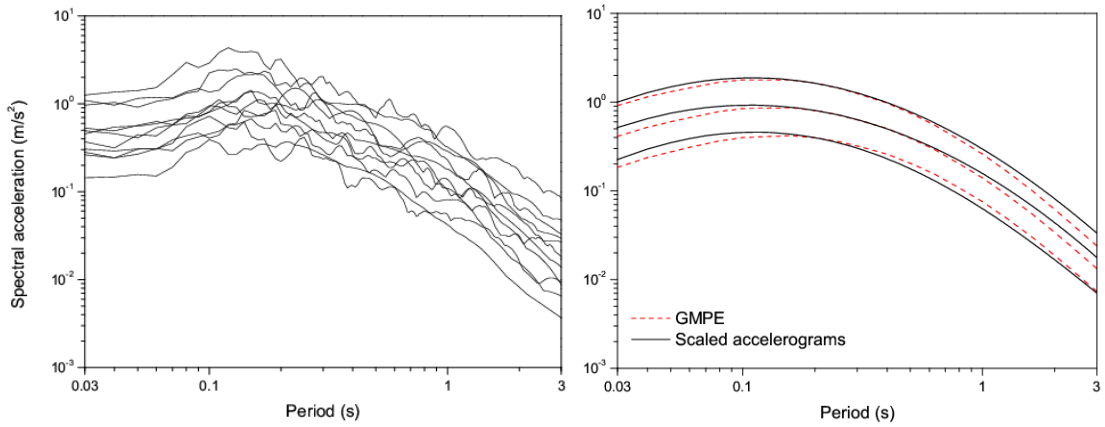

(a) (b)

Figure 2-9. Generic definition of accelerograms to conduct scenario-based SPRA: (a) 11 scaled accelerograms to match corresponding GMPE at a given structural period; (b) 16th, 50th and 84th percentiles for the 11 scaled accelerograms and the corresponding GMPE at a given structural period

For time-based assessments, it is required to use the mean hazard curve of the nuclear site selected. Then, such curve is equally divided, normally into 8 intervals, and the midpoint of each interval is selected as target intensity. Then, intensity-based assessments are conducted for each of the target intensities. Therefore, 8 bins of 11 accelerograms each are needed which in turn are scaled using the Amplitude Scaling Method. Figure 2-10 shows a generic summary of the definition of accelerograms for nonlinear dynamic analyses in time-based SPRA. A more complete version of this assessment could incorporate the variability in the hazard curve. Instead of only considering the median hazard curve, the 16th and 84th percentile hazard curves are

included in the analysis and the accelerograms of each bin are then scaled using the Distribution Scaling Method.

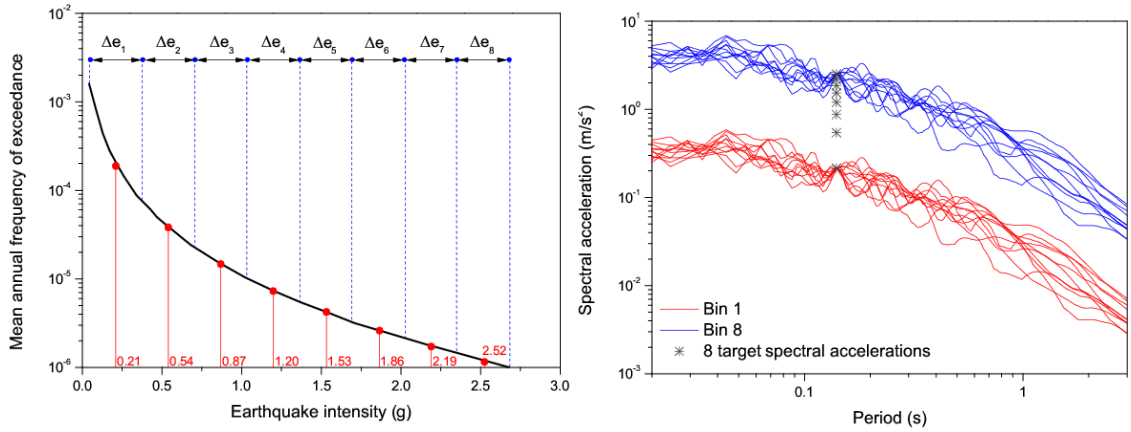

(a) (b)

Figure 2-10. Generic definition of accelerograms to conduct time-based SPRA: (a) mean hazard curve of a given site and 8 target intensities; (b) sample of 2 bins of accelerograms scaled to match the corresponding target intensity.

2.3.4 Calculation and simulation of structural response

After sets of suitable accelerograms compatible with the required type of assessment are defined, nonlinear time-history analyses are performed using an appropriate structural model of the NPP analysed. The aim is to estimate a statistical distribution of seismic demands on the critical components expressed in terms of the selected demand parameter used in the fragility analysis (see Section 2.3.2.2). Such statistical distribution of seismic demands should include the different types of uncertainty typically encountered in structural engineering projects, e.g. ground motion accelerograms, materials, soil-structure interaction, etc. The outcome of this step will produce one value of the response parameter for each nonlinear dynamic analysis for each critical component. This information is sorted in a demand-parameter matrix whose number of rows is the number of structural analyses performed (hence, the number of accelerograms used) and whose number of columns is the number of critical

components obtained from performing the plant-system and accident-sequence analysis. As an example, Table 2-1 shows a sample AFSA-based demand-parameter matrix obtained after performing 11 nonlinear dynamic analyses using a sample NPP that possesses five critical components.

Table 2-1. Sample demand-parameter matrix: AFSAs in m/s^2

GM	Reactor assembly	Feeders	Heat transport system	Steam generator	Maintenance crane
1	0.709	0.933	1.057	1.168	1.339
2	0.501	0.889	0.972	1.058	1.197
3	1.542	1.260	1.402	1.587	1.870
4	0.599	0.694	0.751	0.811	0.873
5	1.098	1.258	1.385	1.505	1.628
6	1.121	1.423	1.547	1.663	1.775
7	1.194	1.478	1.605	1.714	1.831
8	2.226	2.616	2.874	3.101	3.302
9	2.475	2.723	2.929	3.126	3.343
10	1.724	2.387	2.589	2.765	2.952
11	3.930	4.742	5.152	5.522	5.888

In order to estimate the seismic risk with high statistical confidence, it is normally required the demand-parameter matrix to possess hundreds or thousands of row vectors to robustly characterise the nonlinear structural response. Basically, there are two ways to achieve this: (i) directly, by conducting a large number of nonlinear time-history analyses that will undoubtedly require a great number of suitable accelerograms, or (ii) indirectly, making artificial enlargements of the demand-parameters by means of statistical simulations keeping the original correlation of the source data. The latter approach is favoured in the methodology reported by Huang et al. [142-144]. Several methodologies are available in the literature to simulate structural responses (e.g. Latin hypercube sampling [227]). However, the Monte Carlo simulation procedure reported in FEMA P-58 [145] is used by Huang et al. [142-144] as it is a straightforward

methodology, almost computationally inexpensive, to enlarge the demand-parameter matrix to any number of row vectors required by the analyst. As an example, Figure 2-11 shows an example of the demand-parameter matrix shown in Table 2-1 enlarged from 11 to 200 row vectors using Monte Carlo simulations: (a) first and second columns, i.e. reactor assembly vs feeders, and (b) fourth and fifth columns, i.e. steam generators vs maintenance crane.

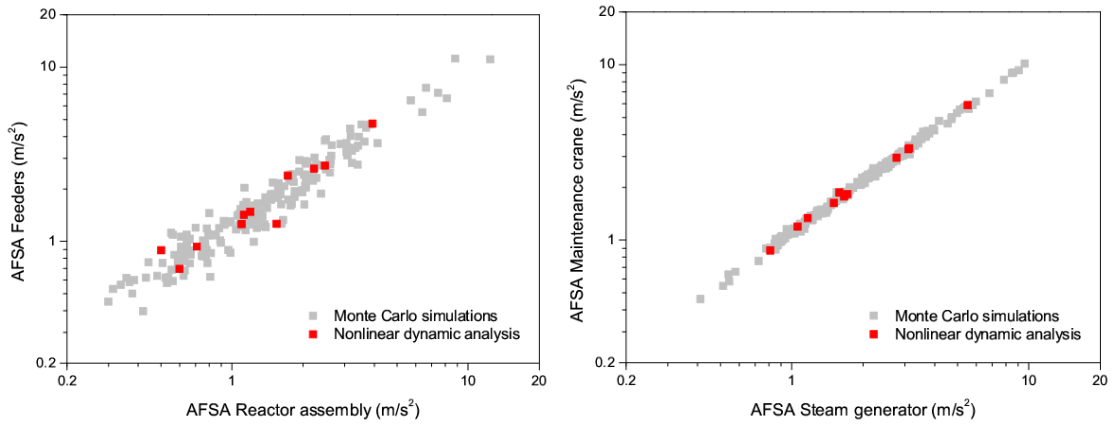

(a) (b)

Figure 2-11. Example of an augmented demand-parameter matrix, from 11 to 200 observations, using Monte Carlo simulations: (a) reactor assembly vs feeders; (b) steam generators vs maintenance crane.

As it will be seen in Chapter 4, this PhD project used the direct approach towards the characterisation of the nonlinear structural response. Such an approach is certainly computationally more demanding than the indirect approach as it involves performing a large number of nonlinear dynamic analyses. Nevertheless, it avoids the use of GMPEs and scaling/matching procedures when defining the seismic input for such analyses. In addition, as the structural response is directly calculated, assumptions regarding the statistical distribution of the demand-parameter matrix are also not needed as is done when using Monte Carlo simulations.

2.3.5 Damage assessment of NPP components

After a large number of observations of the nonlinear structural response have been obtained, the damage assessment of components is performed. For each component, its probability of failure for a given value of the demand parameter is obtained from the corresponding fragility curve. Two damage possibilities are defined in the methodology of Huang et al. [142-144]: the component has either failed or passed. This is assessed by a random test: a random number is generated between 0 and 1 and compared against the probability of failure. If the random number is smaller or equal than the probability of failure, the component is considered to have failed; otherwise, the component is considered safe. This procedure is repeated for all critical components obtained from performing the plant-system and accident-sequence analysis for a given row of the demand-parameter matrix. If any component has failed, then the given row vector is considered to have produced an unacceptable performance of the NPP.

2.3.6 Calculation of risk

In the final step, the probability of unacceptable performance of the NPP is calculated. This is done by assessing the damage state of components for all row vectors of the demand-parameter matrix. Then, the probability of unacceptable performance is simply calculated as follows:

$$\frac{\text{Number of row vectors with unacceptable performance}}{\text{Total number of row vectors}} \tag{2-8}$$

The value obtained from (2-8) is only one trial or realisation for the probability of unacceptable performance of the NPP. In order to obtain a statistical distribution for the probability of unacceptable performance, the entire process is repeated hundreds or thousands of times, each time using a new set of fragility curves randomly selected from

the corresponding family of curves associated to each component. After performing *n* trials, the probabilities of unacceptable performance are sorted from smallest to largest and frequencies of occurrence are assigned. For the smallest, the frequency of occurrence is assigned as 1/*n* and they are subsequently assigned in increments of 1/*n* until reaching the largest to which a frequency of occurrence of *n*/*n*=1 is assigned. The flowchart shown in Figure 2-12 summarises the steps involved in risk calculations following the methodology of Huang et al. [142-144].

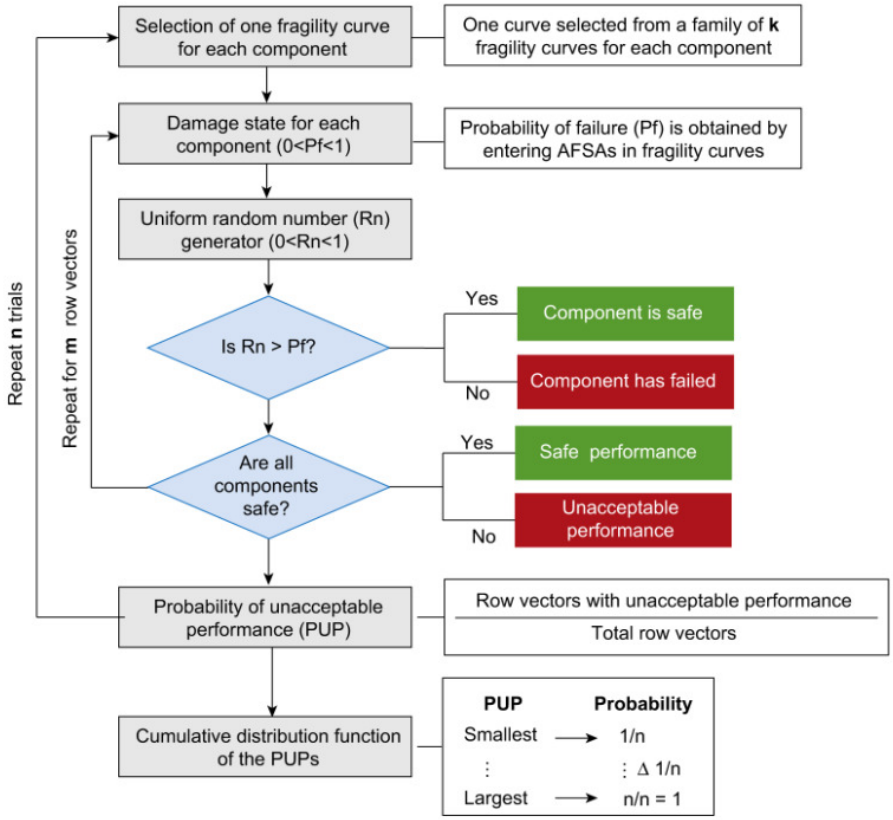

Figure 2-12. Summary for risk assessment calculations [142-143]

For intensity- and scenario-based assessments, the final product is a statistical distribution for the probability of unacceptable performance for a given intensity or scenario of the NPP analysed. A statistical indicator of such a distribution, e.g. median or mean, is normally selected as the benchmark value for the case studied. For time-

based assessments, as they are based on the entire seismic hazard curve which in turn incorporates frequencies of exceedance, the final product is the annual frequency of unacceptable performance for the case studied.

2.4 Seismic protection technology

This section is supported by the review article entitled "Seismic protection technology for nuclear power plants: a systematic review" [13] developed in the context of this PhD project. Such an article can be found in Appendix A. This section provides only a summary of its findings and an update that includes papers published after its time of writing.

2.4.1 Summary of review on seismic protection technology for nuclear power plants

2.4.1.1 General description

Seismic protection systems (SPS) have been successfully used in 30 countries, indicated in Figure 2-13, that posses wide ranges of seismicity to protect conventional civil structures against earthquake actions reaching more than 10,000 applications at present [10]. However, in the nuclear industry, their applications are rare: only two reactor buildings have been designed with such technology: Koeberg NPP in South Africa, with two isolated unit plants, and Cruas NPP in France, with four isolated unit plants [12]. Despite the reduced number of applications of SPS in NPPs, comprehensive theoretical and experimental research has been conducted in the last four decades in order to introduce such technology in the nuclear industry. The main objective of such research is to reach a standardised seismic design of the nuclear island, i.e. the NPP becomes site-independent of the local seismicity of the nuclear site. This allows the use of a

given NPP design in any geographical region, regardless of how severe their seismicity levels are.

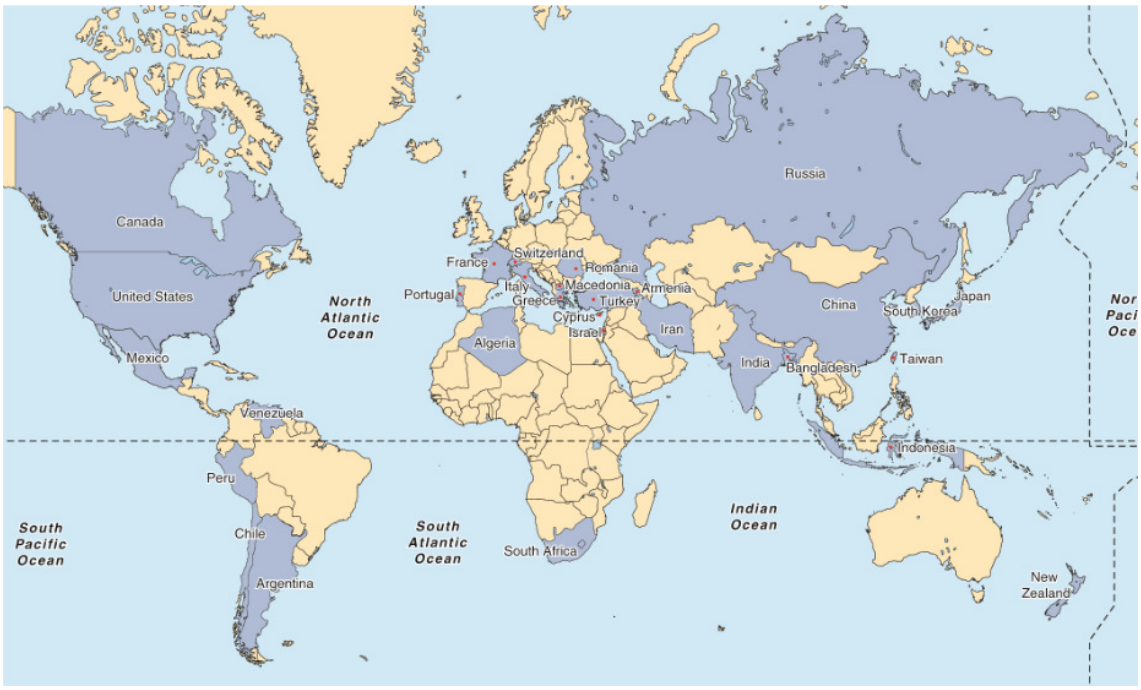

Figure 2-13. Countries that use seismic protection systems for civil structures (highlighted in blue)

The majority of the studies reported in the literature consider the use of devices that detach the superstructure from the foundation mat, isolating the nuclear island from the ground. Figure 2-14 shows a schematic view of a seismically isolated nuclear island.

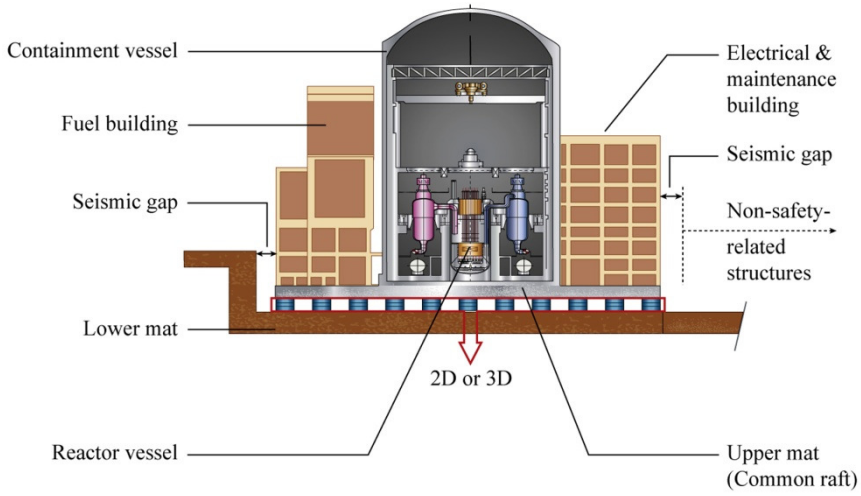

Figure 2-14. Nuclear island seismically isolated

Four key issues on the use of SPS in NPPs have been identified: cost, safety, applications and licensing [13]. In terms of cost, it is likely to reach an offset between a conventionally designed plant and its seismically protected counterpart. A seismically protected NPP needs to consider additional costs of the SPS plus additional structures (e.g. upper mat) to fit them in the plant. However, there is a reduction of costs due to a significant decrease of design seismic loads that allows reduction of the size of structural elements and seismic qualification of safety-related equipment. Regarding safety, the use of SPS allows the superstructure to remain in its elastic range as most of the demand of displacement imposed by earthquakes is absorbed by the SPS. No energy dissipation through structural and non-structural damage occurs in seismically isolated NPPs. Therefore, its overall safety increases by ensuring full structural integrity, safe shutdown of the reactor, and facilitating a quick return to operational condition after the occurrence of a significant earthquake. As for the number of applications of seismically protected NPPs, their scarcity seems to have prevented a widespread use of such technology in the nuclear industry. After Koeberg and Cruas NPPs, there were approximately 40+ years of a rather inflexible reluctance of the industry to incorporate SPS in actual applications. Nevertheless, such a tendency seems to have come to an end as several projects of seismically protected NPPs are either under construction or under development (see Section 2.4.1.3 for more details). Finally, in terms of licensing, the main hurdle that may have prevented granting licences for seismically protected NPPs is the lack of specific codes and design standards for such a purpose. At the moment of writing of this PhD thesis, there is only one specific code in the world that addresses the design of seismically isolated NPPs: the Japanese JEAG 4614-2000 [12]. Nevertheless, several other design guidelines have been issued in the USA [122], Europe [228], and by the IAEA [229]. It is expected that recently granted licences of seismically protected

NPPs will facilitate obtaining future licences of more applications. This will increase the economic competitiveness of nuclear energy in comparison with other sources of energy and will allow the deployment of nuclear power in more areas, such as developing countries and nations with increasingly higher demands for energy.

2.4.1.2 Types of devices

Most of the devices reported in the literature to provide seismic protection to NPPs are passive systems, i.e. they do not exert active forces to the structure to restore it to its normal position. Rather, they increase the energy dissipation capacity of a structure when subjected to earthquake actions. The types of devices that have taken most research interest in nuclear engineering research are elastomeric bearings and lead-rubber bearings. Elastomeric bearings (also known as seismic isolators or laminated rubber bearings) are composed of layers of natural rubber or neoprene with alternated steel plates bonded by vulcanisation. Depending on the type of rubber, natural rubber or enhanced-damping-capacity rubber, they are referred to as low-damping rubber bearing (LDRB) or high-damping rubber bearing (HDRB), respectively. Figure 2-15a shows a schematic view of a high-damping rubber bearing and Figure 2-15b shows a typical hysteresis loop of this type of bearings.

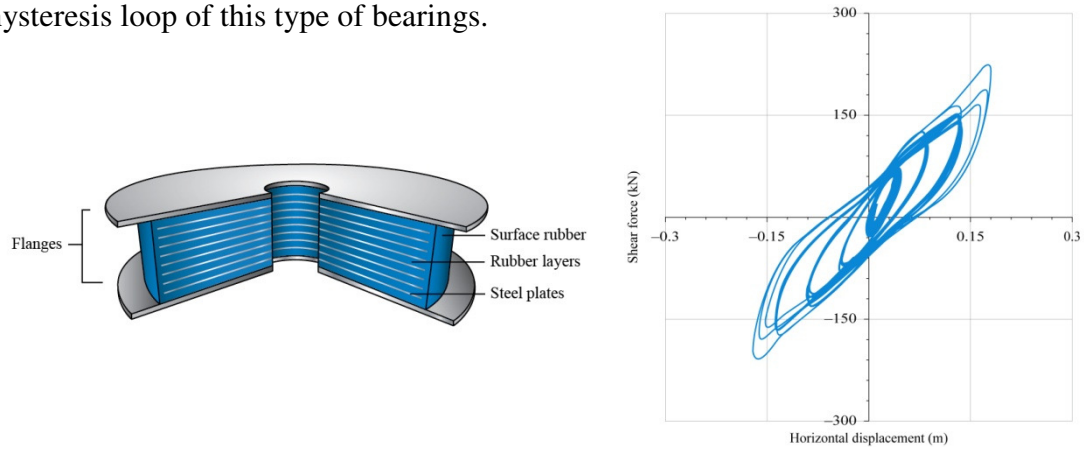

(a) (b)

Figure 2-15. High-damping rubber bearing: (a) schematic view, (b) hysteretic behaviour

LDRB exhibit a rather linear behaviour with little addition of supplemental damping, normally from 2% up to 10%. On the other hand, HDRB exhibit a nonlinear Bouc-Wen-type behaviour with added damping ranging from 10% to 20%.

Lead-rubber bearings (LRB) are also elastomeric-based, normally made of natural rubber, but a lead plug is inserted in the core of the bearing in order to substantially enhance the damping capacity of the bearing. This type of devices possesses a characteristic bilinear hysteretic behaviour as the natural rubber is roughly linear and the lead plug is elasto-plastic, giving the bearing the capacity to add supplemental damping from 20% to as high as 30%. Figure 2-16a shows a schematic view of a lead-rubber bearing and Figure 2-16b shows the hysteretic behaviour of this type of bearings.

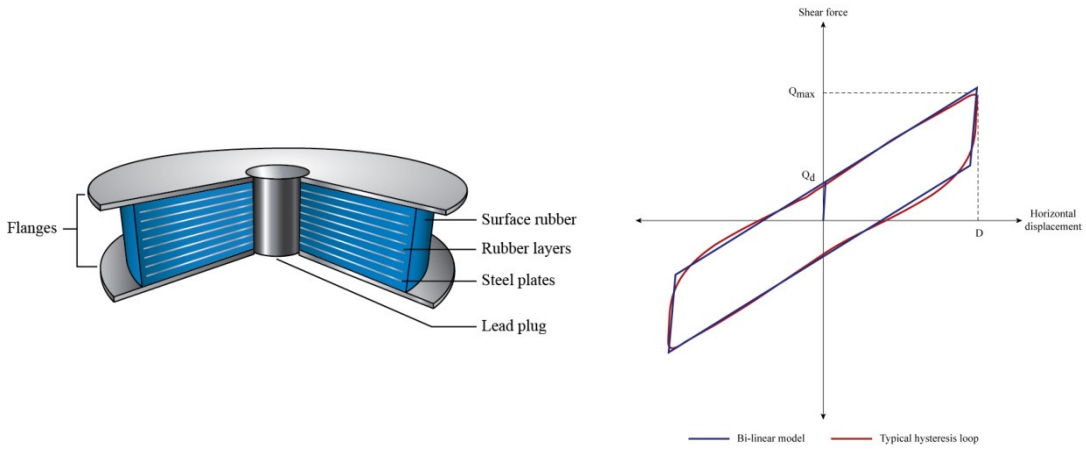

(a) (b)

Figure 2-16. Lead-rubber bearing: (a) schematic view, (b) hysteretic behaviour.

The three types of devices recently described, namely, LDRB, HDRB and LRB, were considered in more than 75% of the articles reported in the literature at the moment of writing of the review article [13]. Certainly, these devices possess the highest likelihood of being used in future nuclear deployments. This tendency is confirmed by the current applications of seismically isolated NPPs (addressed in detail in the next section). Such applications are all in areas of medium-to-low seismic activity. It is worth remembering

that these devices are intended to provide isolation in the horizontal direction (2D) only. For areas of high seismic activity, it seems that isolation both in the horizontal and vertical direction (3D) is needed to reach full standardisation of seismic design. Extensive research has been conducted, mainly in Japan [230-231], in order to fully isolate NPPs against earthquake actions. Examples of such devices are shown in Figure 2-17: (a) a composite device that provides horizontal isolation by elastomeric-based bearings and vertical isolation by an air spring; (b) a fully 3D air spring; (c) a composite device that provides horizontal isolation by elastomeric-based bearings and vertical isolation by metallic bellows; (d) a composite device that provides horizontal isolation by elastomeric-based bearings and vertical isolation by hydraulic dissipaters. Nevertheless, no actual application of NPPs protected with such devices is known to be under development at the moment of writing of this PhD thesis.

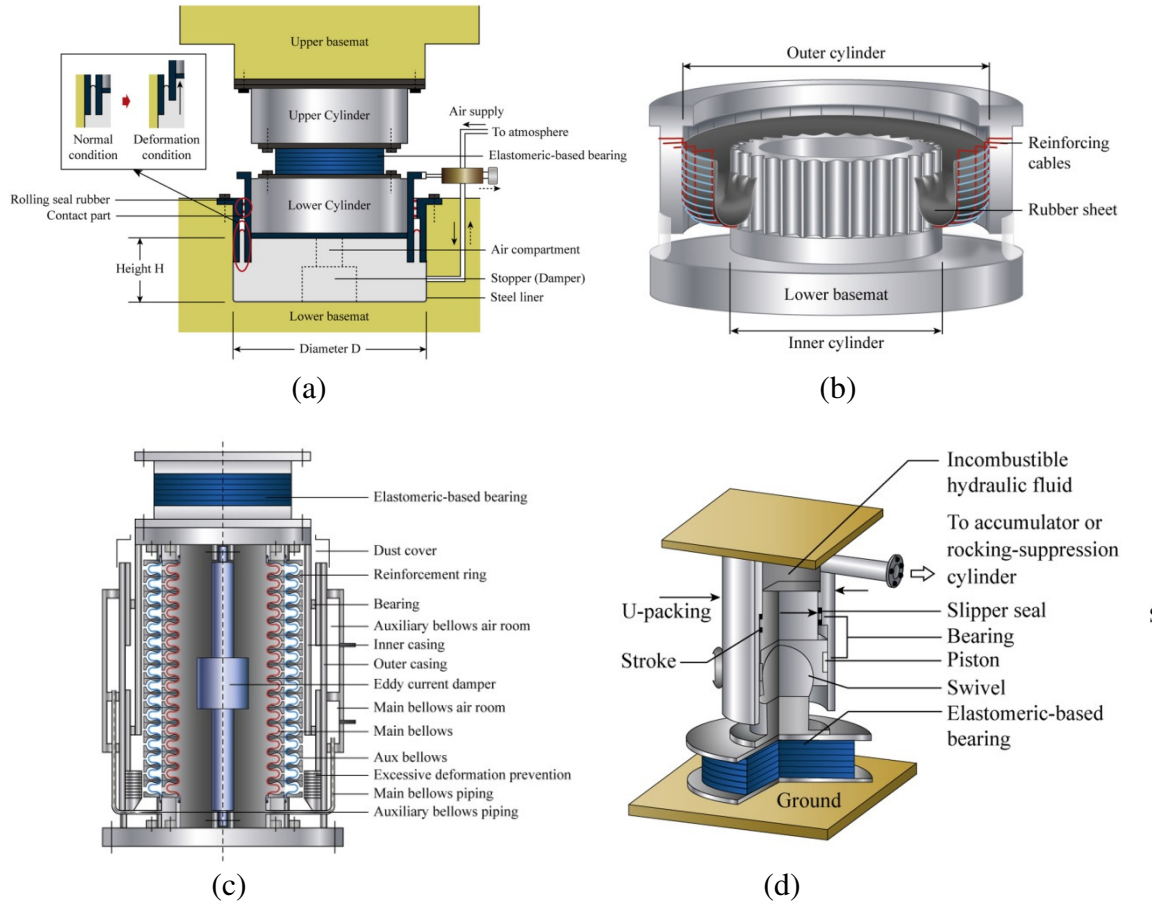

Figure 2-17. Examples of 3D seismic isolation devices (see text for description)

As 3D devices seem to be more suitable for nuclear deployments in areas of high seismic activity alongside the fact that current actual applications of isolated NPPs are all in areas of medium-to-low seismic activity and only consider 2D devices, such type of devices will not be analysed further in this PhD thesis.

2.4.1.3 Current applications

There are currently five actual applications of seismically isolated NPPs that are under construction or in advanced stages of development. Such applications are detailed in Table 2-2 and consider isolation in the horizontal direction only using LDRB, HDRB and LRB.

Table 2-2. Summary of actual seismically isolated NPPs

Application - country	Reactor description	Type of devices	Status	Reference
Jules Horowitz Reactor (**JHR**) – France	100 MW (thermal) Boiling Water Reactor	Low-damping rubber bearings	Under construction	[14]
International Thermonuclear Experimental Reactor (**ITER**) – France	500 MW Fusion Reactor	Low-damping rubber bearings	Under construction	[15]
APR1400 – South Korea	1400 MW Gen III Advanced Pressurised Water Reactor	Lead-rubber bearings	Under construction	[16]
Advanced Sodium Technological Reactor for Industrial Demonstration (**ASTRID**) - France	600 MW Fast Breeder Reactor	High-damping rubber bearings or lead-rubber bearings	Under development	[17]
Advanced Lead Fast Reactor European Demonstrator (**ALFRED**) - Romania	125 MW Lead-cooled Fast Reactor	High-damping rubber bearings or lead-rubber bearings	Under development	[18]

Although the UK explored the benefits of using SPS to increase margins of safety of NPPs in early 1990s [19], no further analyses were reported and no real applications of

seismically protected NPPs were built in the UK. Consequently, encouraged by recent developments on the use of seismically protected nuclear reactor buildings in other areas of medium-to-low seismic activity, a knowledge gap is present in the UK nuclear industry on up-to-date research on the use of strategies to control and reduce the risk of next generation NPPs in Britain using seismic protection devices.

2.4.2 Update of seismic protection technology for nuclear power plants

This section is intended to provide an update of the review article [13] summarised in Section 2.4.1 by analysing studies published after it. The outcome of this updating process did not produce significant changes in the results already obtained. Table 2-3 summarises studies that were intended to be developed for specific applications of seismically protected nuclear reactor buildings. Additionally, several other experimental and theoretical studies intended for generic nuclear reactor buildings were reported that considered LRB and LDRB [232-240]. Therefore, it is possible to see that all elastomeric-based isolators described in Section 2.4.1.2 continue to be the preferred type of devices to provide seismic protection to NPPs.

Three additional aspects are worth mentioning: (i) a new type of device not originally reported in the review article that seems to be gaining research interest for protecting reactor buildings is friction pendulum systems (FPS) [237-239, 241]; (ii) only a few studies have been reported addressing isolation in the vertical direction [242-243], and (iii) a major research programme is ongoing in Japan at the moment of writing of this PhD thesis intended to provide seismic protection to future PWRs and BWRs by means of LRBs [244-249]. The last aspect suggests that isolation in the vertical direction is not being explicitly considered for potential future deployments in an area of high

seismicity such as Japan. In any case, actual applications of seismically protected nuclear reactor buildings in Japan remain to be seen.

Table 2-3. Summary of research on SPS for nuclear islands

Study	Type of devices	Application	Achievements/Remarks
Chen et al. [250]	HDRB	AP1000 (China)	(1) Theoretical study on the effectiveness of HDRB for SSE (2) Accelerations are reduced ~70%
Lee et al. [16]	LRB	APR1400 (South Korea)	(1) Experimental study on a full-size device with enhanced rubber (2) Ultimate shear strain capacity > 400%
Jung et al. [251]	LRB	APR1400 (South Korea)	Theoretical study on the validation of simplified structural models of isolated NPPs
Shimizu et al. [244]	LRB	PWRs – BWRs (Japan)	Development of a complete framework for design of seismically isolated NPPs
Kubo et al. [252]	LRB	PWRs – BWRs (Japan)	Preliminary feasibility study on the use of seismic isolation in NPPs in Japan post-Fukushima
Forni et al. [253]	LRB - HDRB	Lead-cooled reactors, SILER project (Europe)	Comprehensive description of the seismic isolation system of the SILER project

Regarding seismic protection of components, equipments and machinery in NPPs, few studies were found in the literature considering: (i) innovative energy dissipation materials [254], (ii) a combination of steel springs and viscous dampers [255], and (iii) LRBs for an actual application to provide seismic protection for a diesel generation system in the Beznau NPP in Switzerland [256].

Chapter 3

Seismic input: a stochastic ground motion accelerogram model

3.1 Introduction

This section presents a stochastic ground motion accelerogram model to define seismic inputs in the context of SPRA for NPPs in the UK. Full details of the model can be found in Medel-Vera and Ji [257] which in turn is entirely reproduced in Appendix B; hence, this section only provides a concise yet complete description of the model.

In this chapter, a site-based model based on the formulation reported by Rezaiean and Der Kiureghian [112, 115] is proposed that stochastically simulates two-component horizontal accelerograms compatible with any seismic scenario defined by an earthquake of magnitude $4 < M_w < 6.5$, distance-to-site $10 < R_{epi} < 100$ km and different types of soil (rock, stiff and soft soil). The model is based on a set of predictive equations for parameters that govern a fully non-stationary stochastic process that is

used to simulate earthquake accelerograms. The predictive equations are calibrated using regression analysis on a dataset of accelerograms recorded in the tectonic region to which the UK belongs. The simulation of accelerograms is entirely made in the time domain, it essentially involves the generation of random variables and uses a few input data readily available in structural engineering practice. This model is the first of its kind for the general region of NW Europe including the UK.

3.2 Target geographical region

The predictive model proposed is based on the assumption that the nature of accelerograms (intensity, frequency content and time duration) of strong magnitude earthquakes in the British Isles would be similar to those strong earthquakes occurred in the same SCR to which the UK belongs, namely NW Europe. This assumption avoids (i) the use of small-magnitude records to predict moderate-to-large accelerograms, and (ii) the inclusion of earthquakes from other SCRs or other intraplate regions. A systematic description of the boundaries of NW Europe was needed. Various definitions have been reported in the literature, for example, Goes et al. [258] defined it as a relatively small area excluding the UK and the Scandinavian peninsula, whereas Ambraseys [259] defined it as a more expanded area including the UK and most of Norway and Sweden. The approach used to define boundaries for NW Europe, was the Flinn-Engdhal (F-E) regionalisation scheme [260], comprising the countries and areas shown in Figure 3-1. Such a definition of NW Europe is within the limits of the European SCR defined by Johnston et al. [27]. Hence, it can be considered as a subset of the SCR of interest, possessing relatively uniform tectonic features.

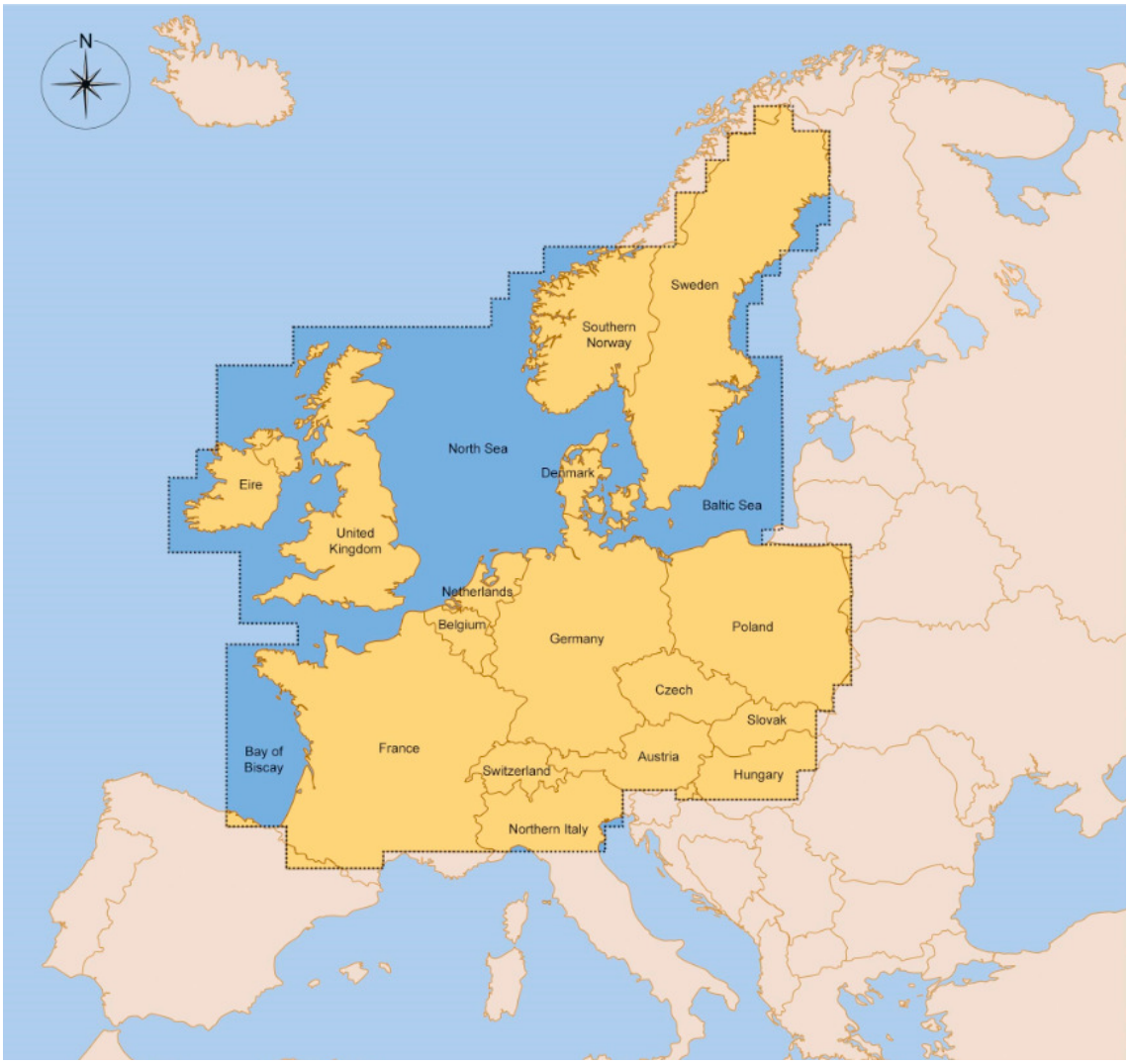

Figure 3-1. Map of the NW Europe F-E region [260]

3.3 Dataset and model parameters

A suitable pan-European on-line database in the public domain providing accelerograms from the countries/areas in Figure 3-1, was the Internet Site for European Strong-Motion Data (ISESD) [261]. It is acknowledged that the existence of the most recent pan-European strong-motion databank [262] that unifies all European databases of accelerograms. However, such a database could not be used as it was not yet available in the public domain at the time of writing. For the region of interest, the related accelerograms obtained from the ISESD database were selected considering the following parameters:

- *Earthquake magnitude* defined by the moment magnitude scale (M_w), considering magnitudes M_w 4 and 6.5 as the lower and upper bounds.
- *Earthquake distance metric* defined by the epicentral distance (R_{epi}), considering distances R_{epi} > 10 km as the lower limit in order to not include near-fault records. The largest R_{epi} found for the region of interest was 193 km, although very few records were available for distances > 100 km.
- *Type of soil* defined qualitatively by directly specifying the class site: rock, stiff soil and soft soil. These categories are based on the Boore et al. [263] criteria: very soft soil: V_{S30} < 180 m/s; soft soil: 180 < V_{S30} < 360 m/s; stiff soil: 360 < V_{S30} < 750 m/s; rock: V_{S30} > 750 m/s).
- *Faulting mechanism* was not possible to include as such information was not available in its entirety for the region of interest.

Additionally, only accelerograms recorded in free-field conditions were included. All those recorded in buildings or other types of structure were discarded. Aftershocks were also included as the separation between mainshocks and aftershocks in European earthquakes has an unclear effect [264]. The vertical component of earthquakes was not included in the model presented. This is for simplicity purposes only; hence, it is acknowledged that such a component needs addressing for actual nuclear and structural engineering applications. The total number of accelerograms retrieved was 220 records (110 pairs of horizontal accelerograms) obtained from 43 earthquakes. In terms of the type of soil, the dataset used in this work includes 42 pairs of accelerograms recorded in rock, 52 in stiff soil and 16 in soft soil. Figure 3-2 provides a graphical summary of the dataset. Complete information about the earthquakes used to define the dataset can be found in Appendix B.

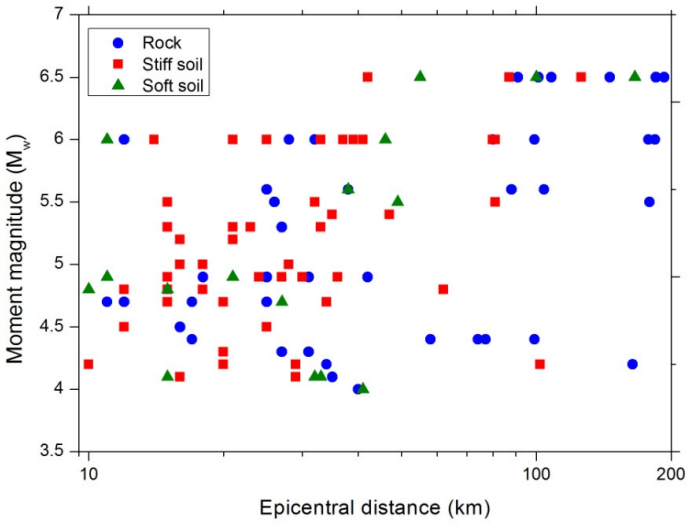

Figure 3-2. Distribution of magnitudes and distances for the dataset used in this work

3.4 Stochastic process and model calibration

As mentioned in Section 3.1, the model presented in this chapter has taken advantage of the stochastic process reported by Rezaeian and Der Kiureghian [112], as it presents particular features that ease its calibration and use for structural engineering purposes. The main features are: (i) temporal and spectral non-stationarities are totally decoupled; this eases the selection of functional parameters governing both non-stationarities to be fitted to real accelerograms, (ii) the model works exclusively in the time domain; hence Fourier analysis or other analyses in the frequency domain are not required, and (iii) the simulation of accelerograms essentially involves the generation of random variables, avoiding the use of more complex numerical analysis. In this section, the functional parameters of the stochastic process that characterise temporal and spectral non-stationarities are fitted to the dataset of accelerograms. Such functional parameters are then regressed against the three variables defined in Section 3.3, namely, earthquake magnitude, distance-to-site and type of soil. This enables a set of predictive equations for the functional parameters to be obtained allowing the simulation of sets of two-component horizontal accelerograms.

3.4.1 Mathematical formulation

The stochastic model is based on a time-modulated filtered white-noise process with the filter having time-varying properties. It requires a time-modulating function to achieve temporal nonstationarity, and a filter function with time-varying properties to achieve spectral nonstationarity. The fully nonstationary stochastic model, $x(t)$, in its continuous form, is defined as follows:

$$x(t) = q(t,\underline{\alpha})\left[\frac{1}{\sigma_f(t)}\int_{-\infty}^{t} h[t-\tau,\underline{\lambda}(\tau)]\,w(\tau)\,d\tau\right] \tag{3-1}$$

where $q(t,\underline{\alpha})$ is the time-modulating function in which $\underline{\alpha}$ is a vector of parameters that control the shape and intensity of the function; $h[t-\tau,\underline{\lambda}(\tau)]$ is the linear filter with time-varying parameters $\underline{\lambda}(\tau)$; $w(\tau)$ is a white-noise (Gaussian zero-mean) process; and $\sigma_f^2(t) = \int_{-\infty}^{t} h^2[t-\tau,\underline{\lambda}(\tau)]d\tau$ is the variance of the process defined by the integral in Equation 3-1. In this work, $q(t,\underline{\alpha})$ is presented as a piece-wise modulating function to model the temporal non-stationarity:

$$q(t,\underline{\alpha}) = \begin{cases} 0 & if\ t \le T_0 \\ \alpha_1\left(\dfrac{t-T_0}{T_1-T_0}\right)^2 & if\ T_0 < t \le T_1 \\ \alpha_1 & if\ T_1 < t \le T_2 \\ \alpha_1 \cdot e^{-\alpha_2 (t-T_2)^{\alpha_3}} & if\ t > T_2 \end{cases} \tag{3-2}$$

Although other functions are available (e.g. gamma-type functions), the time-modulating function defined in Equation 3-2 was chosen to give flexibility to the definition of the starting time and duration of the strong-shaking phase of accelerograms. This function has six parameters: $\underline{\alpha} = (\alpha_1,\alpha_2,\alpha_3,T_0,T_1,T_2)$ in which α_1

controls the maximum intensity, α_2 and α_3 are shape controllers of the decaying intensity, T_0 is the beginning of the process, and finally, T_1 and T_2 represent the start and end time of the strong shaking phase of an accelerogram. The time-varying linear filter proposed by Rezaeian and Der Kiureghian [112, 115] was used in this work:

$$h[t-\tau,\underline{\lambda}(t)]=\begin{cases}\dfrac{\omega_f(t)}{\sqrt{1-\xi_f^2(t)}}e^{[-\xi_f(\tau)\omega_f(\tau)(t-\tau)]}\sin\left[\omega_f(\tau)\sqrt{1-\xi_f^2(\tau)}(t-\tau)\right]; & \tau\le t\\ 0; \quad otherwise\end{cases} \tag{3-3}$$

This filter represents the pseudo-acceleration response of a single-degree-of-freedom linear oscillator subjected to a unit impulse, in which τ is the time of the pulse. In Equation 3-3, the vector of parameters of the linear filter is $\underline{\lambda}(\tau)=[\omega_f(\tau),\xi_f(\tau)]$, in which $\omega_f(\tau)$ is the frequency function defining the distribution of the predominant frequency within the accelerogram, and $\xi_f(\tau)$ is the damping function controlling the bandwidth of the process. As it is expected that the predominant frequencies decay with time [113], a simple and reasonable model to consider for the frequency function is a linear decaying model:

$$\omega_f(\tau)=\omega_0-(\omega_0-\omega_n)\frac{\tau}{t_n} \tag{3-4}$$

where ω_0 and ω_n are the frequencies at the beginning and end of the accelerogram, and t_n is the total duration of the record. Although the bandwidth of accelerograms is expected to increase with time [113], as a first approximation, this variation in bandwidth can be considered to be fairly insignificant [112]. Therefore, a constant damping function is used in this work; i.e.

$$\xi_f(\tau) = \xi_f \tag{3-5}$$

Consequently, the fully non-stationary stochastic filtered white-noise process can be completely defined by nine parameters $(\alpha_1, \alpha_2, \alpha_3, T_0, T_1, T_2, \omega_0, \omega_n, \xi_f)$. Such parameters can be calibrated for a single recorded accelerogram and then be used to generate as many stochastic simulations as required which are compatible with the real record. In any case, synthetic accelerograms are likely to lead to overestimates of structural response at long structural periods [114]. In order to correct this issue, a high-pass filter is required to adjust the low-frequency content of the stochastic simulations. The high-pass filter used in this work is the second-order critically damped oscillator [113]:

$$\ddot{z}(t) + 2\omega_c \dot{z}(t) + \omega_c^2 z(t) = \hat{x}(t) \tag{3-6}$$

In Equation 3-6, $\ddot{z}(t)$ is the simulated (corrected) stochastic accelerogram and ω_c is the so-called "corner frequency" whose value depends upon the earthquake magnitude, the faulting geometry and the shear wave velocity [40]. The procedure to calibrate the nine parameters against the dataset of accelerograms selected is described in detail in Appendix B.

3.4.2 Model calibration

The two horizontal components of simulated ground motion accelerograms have to be orientated consistently in terms of their energy content to allow the structural engineer to make reasonable estimations of nonlinear structural responses. A minor setback of the dataset of accelerograms described in Section 3.3 is that their orientations are arbitrary and depend on the orientation of the recording instruments. Therefore, the

dataset needs to be standardised to make reliable simulations. In this work, the dataset's standardisation was undertaken by orientating the two horizontal components into their principal axes, in which case they are not statistically correlated [265]; hence, their covariance is zero [266]. In general, the major principal component points to the earthquake epicentre, the intermediate principal component is perpendicular to the major component, and the minor principal component is vertical (not included). In this work, the major and intermediate components for each of the selected 110 pairs of accelerograms are estimated. Then, the nine parameters of the stochastic process are fitted to each rotated accelerogram. As an example, Figure 3-3 shows the normalised histograms for each parameter of the stochastic process for the major component of the accelerogram dataset.

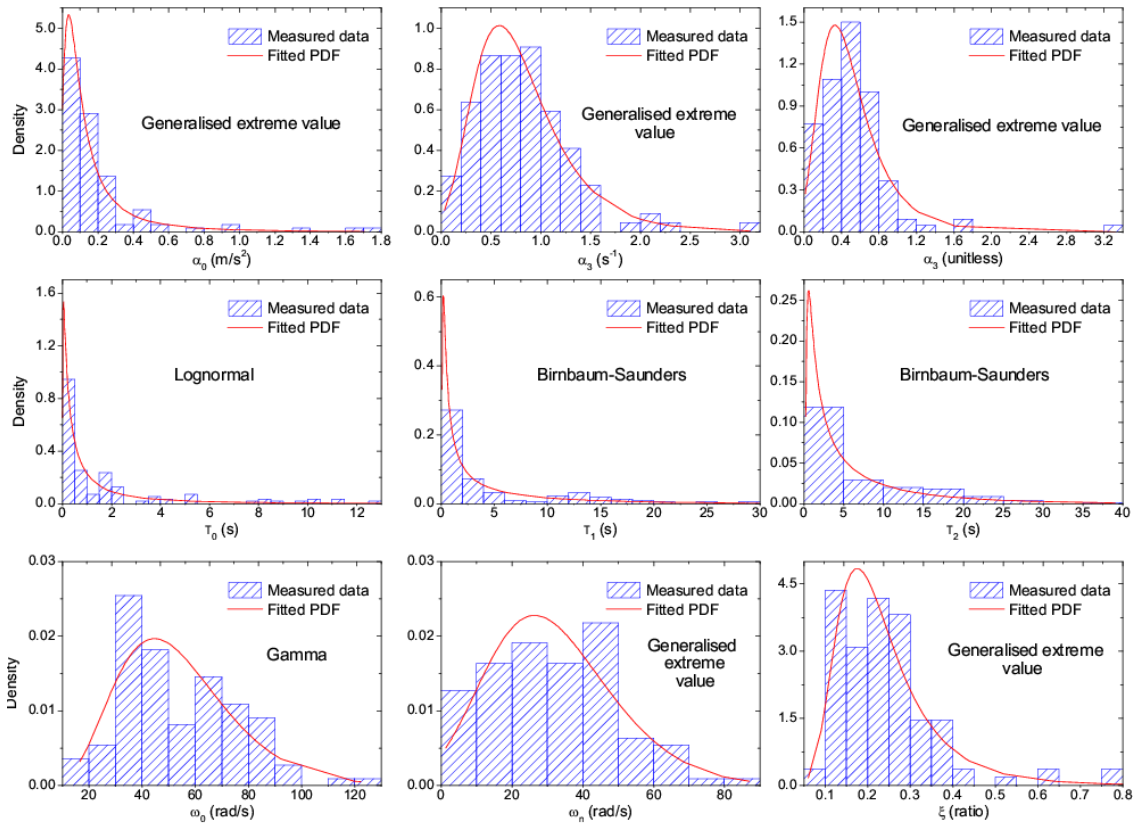

Figure 3-3. Normalised histograms for each parameter of the stochastic process and their fitted marginal distributions for the major components of the accelerogram dataset.

After generalising the statistical behaviour of the nine parameters of the stochastic process, empirical predictive equations are proposed for each of them. These predictive equations were obtained by means of regression analysis and a functional form is proposed to predict the statistical behaviour of each parameter (dependent variable) as a function of earthquake moment magnitude (M_w), epicentral distance (R_{epi}) and type of soil (independent variables). However, when assessing the significance of the regressions, the errors are assumed to be normally distributed for the functional form to be statistically meaningful. This statement implies that the dependent variables are also normally distributed [267]. However, as can be seen from Figure 3-3, the dependent variables exhibit a non-normal statistical behaviour. Therefore, a transformation to the normal domain is required. The following change of variables was used [115]:

$$v_i = \Phi^{-1}\left[F_{\theta i}(\theta_i)\right] \quad i = 1,\ldots,9 \tag{3-7}$$

In Equation 3-7, v_i is the i-th transformed standard normal random variable; Φ^{-1} is the inverse standard normal cumulative distribution; θ_i is i-th parameter that defines the stochastic process, and $F_{\theta i}(\theta_i)$ is the marginal cumulative distribution function fitted for each θ_i. Once the nine dependent variables were transformed into normal distributions, empirical predictive equations were fitted to the measured data by means of regression analysis. As all data points of the dataset cannot be considered statistically independent observations, the random-effects regression technique by means of the algorithm proposed by Abrahamson and Youngs [268] was used to account for such an effect. The final functional form of the model was obtained using the forward stepwise method [267]. The main objective was to keep the number of explanatory variables as low as possible with the highest possible statistical significance, using only one functional

form for all dependent variables. The functional form proposed for all parameters is given in Equation 3-8, with the regression coefficients presented in Table 3-1.

$$v_i = \beta_{i,0} + \beta_{i,1} \cdot M_w + \beta_{i,2} \cdot \sqrt{R_{epi}} + \beta_{i,3} \cdot \ln\left(M_w \cdot R_{epi}\right) + \beta_{i,4} \cdot D_1 + \beta_{i,5} \cdot D_2 + n_i + \varepsilon_i \quad i = 1,\ldots,9 \tag{3-8}$$

Table 3-1. Regression coefficients and standard deviations for the error random variables

	Major component								
	β_0	β_1	β_2	β_3	β_4	β_5	τ	σ	p-value
v_1 (α_1)	0.7814	1.0668	0.2751	-1.6070	0.4110	0.0175	0.4852	0.5323	0.0000
v_2 (α_2)	4.1555	-0.2059	0.1435	-0.7665	-0.1218	0.2462	0.3564	0.8328	0.0008
v_3 (α_3)	0.9996	-0.0814	-0.0848	0.0069	0.0245	-0.6082	0.0781	0.9301	0.0215
v_4 (T_0)	-4.6028	-0.3342	-0.5952	1.9832	-0.2727	-0.1397	0.5740	0.7547	0.0075
v_5 (T_1)	-2.5345	-0.4945	-0.3979	1.4768	-0.0901	-0.0583	0.6754	0.7045	0.0231
v_6 (T_2)	-4.2075	-0.3931	-0.4153	1.7161	0.0544	0.0253	0.6779	0.6803	0.0114
v_7 (ω_0)	-0.7748	-0.8501	-0.4613	1.6332	-0.5170	-0.3077	0.1836	0.8411	0.0000
v_8 (ω_n)	-5.0464	-0.3083	-0.4932	1.9619	-0.6393	-0.2972	0.0141	0.8893	0.0001
v_9 (ξ)	-4.7793	-0.3850	-0.6217	2.1016	-0.2991	0.1322	0.1497	0.9501	0.0094
	Intermediate component								
	β_0	β_1	β_2	β_3	β_4	β_5	τ	σ	p-value
v_1 (α_1)	0.5402	1.1438	0.3179	-1.6877	0.3794	-0.0083	0.4614	0.5215	0.0000
v_2 (α_2)	4.2933	-0.2351	0.2155	-0.8684	0.0720	0.1836	0.2663	1.0900	0.0081
v_3 (α_3)	1.7895	0.1881	0.0324	-0.5290	-0.3243	-0.6067	0.0374	0.9414	0.0353
v_4 (T_0)	-3.2093	-0.3599	-0.4034	1.5237	-0.4577	-0.0341	0.4960	0.8228	0.0255
v_5 (T_1)	-1.3461	-0.4227	-0.2670	1.0069	0.0036	-0.0502	0.8223	0.5098	0.0407
v_6 (T_2)	-4.7822	-0.4157	-0.5005	1.9481	0.0585	0.0649	0.7318	0.6281	0.0058
v_7 (ω_0)	0.1198	-0.7409	-0.3740	1.2472	-0.5771	-0.4125	0.2953	0.7965	0.0000
v_8 (ω_n)	-5.4575	-0.4664	-0.5289	2.2222	-0.4059	-0.2255	0.1628	1.0345	0.0000
v_9 (ξ)	-1.8771	-0.5859	-0.3816	1.4128	0.0405	0.3150	0.0640	0.9628	0.0194

In Equation 3-8, M_w and R_{epi} are the moment magnitude and epicentral distance (in km) for the seismic scenario to be simulated. The type of soil is modelled through two dummy variables D_1 and D_2: $D_1 = D_2 = 0$ for rock; $D_1 = 1$ and $D_2 = 0$ for stiff soil; and $D_1 = 0$ and $D_2 = 1$ for soft soil. Finally, n_i and ε_i are two normal random variables with zero mean and variances τ_i^2 and σ_i^2 that represent the residuals of the regressions

for inter-event (random effect among different earthquakes) and intra-event (random effect among different accelerograms for the same earthquake) respectively. The total error of the model is then a normal random variable with zero mean and variance τ_i^2 + σ_i^2. Table 5 also provides the standard deviations τ_i and σ_i. P-values in Table 3-1 are addressed in the following section.

3.4.3 Statistical significance of the model

In this section, the significance of the regressions are assessed for both the overall model adequacy and the coefficients obtained. Initially, the overall significance of the regression was assessed. For this case, the p-values for the f-test for the null hypothesis $H_0 : \beta_1 = \cdots = \beta_5 = 0$ are reported in Table 3-2. As all p-values are smaller than the standard 5% significance level, all null hypotheses are rejected. Also, the residual analysis was performed, and the total residuals were plotted against the model variables to check for deviations from normality. As an example, Figure 3-4 shows scatter plots of the total residuals for the nine dependent variables against M_w. From this set of plots it is possible to observe that there are no apparent deviations from normality.

Tests on the significance of individual regression coefficients were also performed. P-values for the t-test for the null hypothesis $H_0 : \beta_i = 0$ are reported in Table 3-2 (β_0's are not included in this analysis as constants were not scrutinised). Some p-values are higher than the standard 0.05 significance level, which means that the corresponding null hypothesis fails to be rejected. In such a case, the regression coefficients are of little value in explaining the variation of the corresponding dependent variable. However, as the functional form, in its entirety, is still able to represent the variation of the nine

dependent variables (see p-values in Table 3-1), the regression coefficients of Table 3-1 were considered valid for simulations.

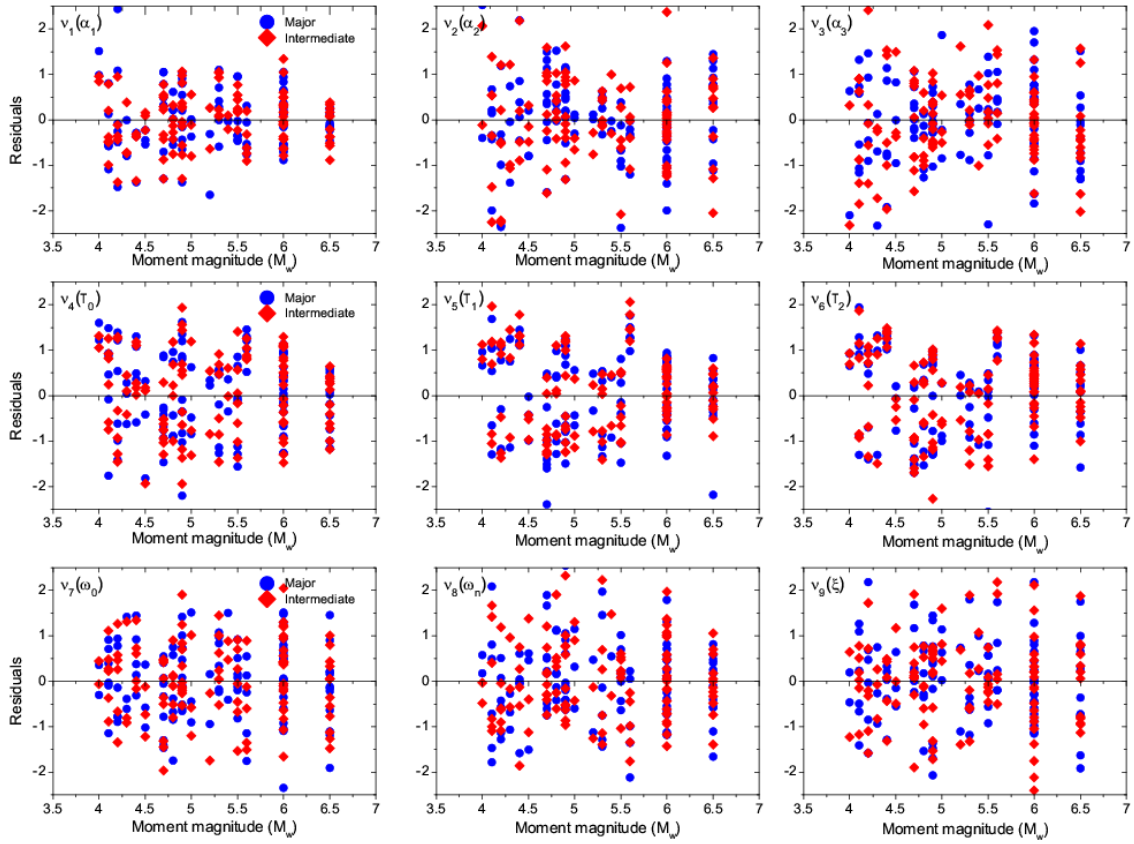

Figure 3-4. Scatter plots of residuals against moment magnitude for the nine normalised variables

Table 3-2. P-values for the t-test for the null hypothesis H_0: $\beta_0 = 0$

	Major component					Intermediate component				
	β_1	β_2	β_3	β_4	β_5	β_1	β_2	β_3	β_4	β_5
ν_1 (α_1)	0.000	0.031	0.000	0.014	0.936	0.000	0.010	0.000	0.019	0.969
ν_2 (α_2)	0.202	0.367	0.167	0.558	0.370	0.239	0.275	0.206	0.780	0.589
ν_3 (α_3)	0.623	0.605	0.990	0.909	0.033	0.262	0.845	0.358	0.136	0.035
ν_4 (T_0)	0.049	0.001	0.001	0.212	0.626	0.037	0.018	0.010	0.040	0.907
ν_5 (T_1)	0.005	0.022	0.014	0.688	0.843	0.015	0.118	0.090	0.987	0.864
ν_6 (T_2)	0.023	0.015	0.004	0.805	0.931	0.017	0.004	0.001	0.792	0.824
ν_7 (ω_0)	0.000	0.003	0.002	0.010	0.239	0.000	0.013	0.018	0.004	0.110
ν_8 (ω_n)	0.053	0.002	0.000	0.002	0.270	0.013	0.005	0.001	0.094	0.477
ν_9 (ξ)	0.026	0.000	0.001	0.177	0.650	0.001	0.026	0.018	0.855	0.282

3.4.4 Correlations within principal axes

The variables v_i (either for the major or intermediate component) are correlated as they were derived using the same dataset, i.e. they are jointly normal random variables. Therefore, for consistency, such a correlation must be preserved when simulating accelerograms using the stochastic model and the predictive equations obtained from the regressions. This correlation can be estimated as the correlation coefficient between the inter-event η_i and the intra-event ε_i components of the total residual of regressions [115]. Table 3-3 shows the matrices of correlation coefficients for variables v_i for the major and intermediate components.

Table 3-3. Correlation coefficients matrices for variables v_i for the major and intermediate component

	Major component								
	v1	v2	v3	v4	v5	v6	v7	v8	v9
v1	1								
v2	0.4049	1							
v3	0.1551	-0.4909	1					Sym	
v4	-0.095	-0.0811	0.2381	1					
v5	-0.1872	-0.1506	0.2655	0.7648	1				
v6	-0.3815	-0.1849	0.1728	0.6766	0.883	1			
v7	0.081	-0.0557	0.0935	0.415	0.3592	0.2766	1		
v8	0.1741	-0.0108	0.0755	-0.1476	-0.1823	-0.2478	0.0998	1	
v9	-0.1388	-0.1155	0.0657	0.0959	-0.0167	-0.0003	-0.2352	-0.1544	1
	Intermediate component								
	v1	v2	v3	v4	v5	v6	v7	v8	v9
v1	1								
v2	0.479	1							
v3	0.095	-0.549	1						
v4	-0.093	-0.117	0.176	1				Sym	
v5	-0.235	-0.160	0.200	0.734	1				
v6	-0.379	-0.226	0.095	0.625	0.892	1			
v7	0.185	-0.048	0.258	0.405	0.366	0.308	1		
v8	0.195	0.091	0.050	-0.164	-0.180	-0.185	0.218	1	
v9	-0.252	-0.038	-0.068	0.097	0.013	0.021	-0.312	-0.337	1

3.5 Simulation of accelerograms and model validation

As an example of simulated accelerograms using the proposed model, Figure 3-5 and Figure 3-6 show the time-histories of acceleration, velocity and displacement corresponding to two events taken from the dataset used and three stochastic simulations for each event. The selected events are: (1) M_w 6, R_{epi} = 32 km, rock (ISESD ID: 140) and (2) M_w 4, R_{epi} = 40 km, stiff soil (ISESD ID: 1338). These figures show that for a single seismic scenario, a great variability in terms of intensity, frequency content and duration of the strong shaking phase is present in the simulated accelerograms. Such variability is likely to have a significant effect when assessing the seismic risk of civil structures for seismic scenarios of interest that dictate the seismic hazard of the selected site.

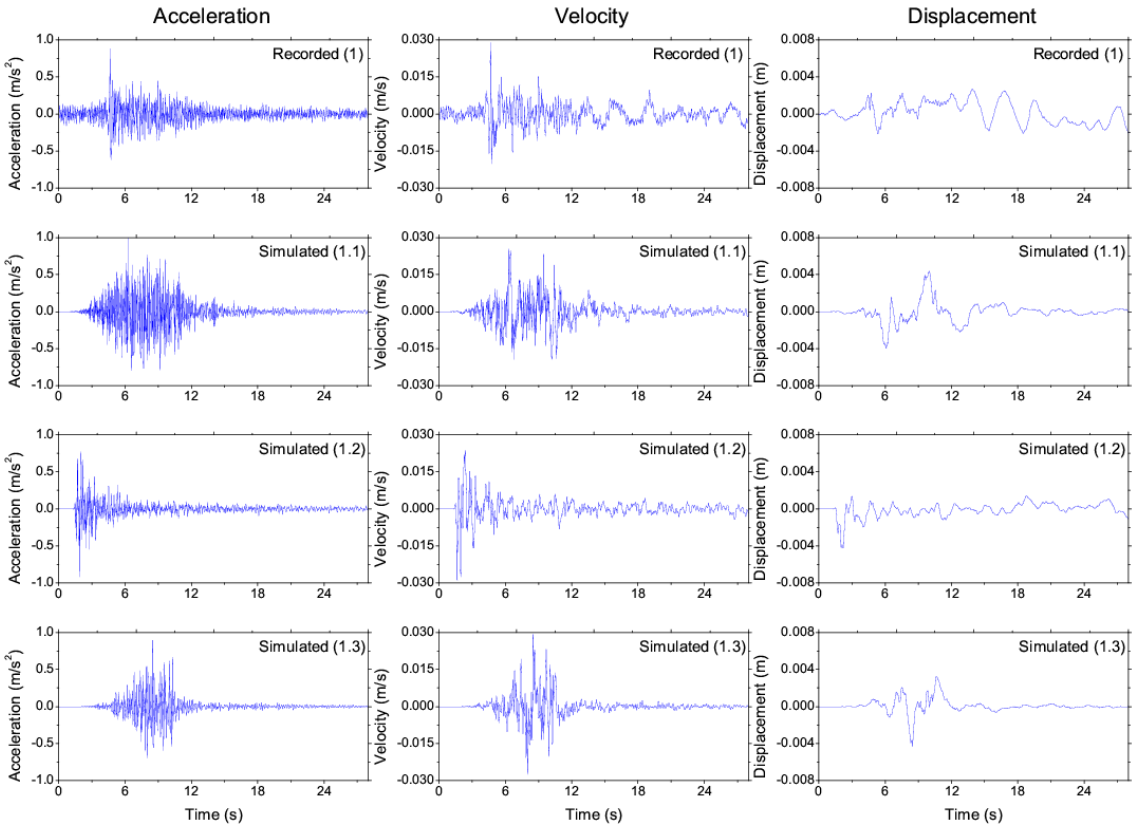

Figure 3-5. Recorded (first row) and simulated traces (last three rows) of acceleration, velocity and displacement recorded in rock conditions. M_w 6, R_{epi} = 32 km, rock

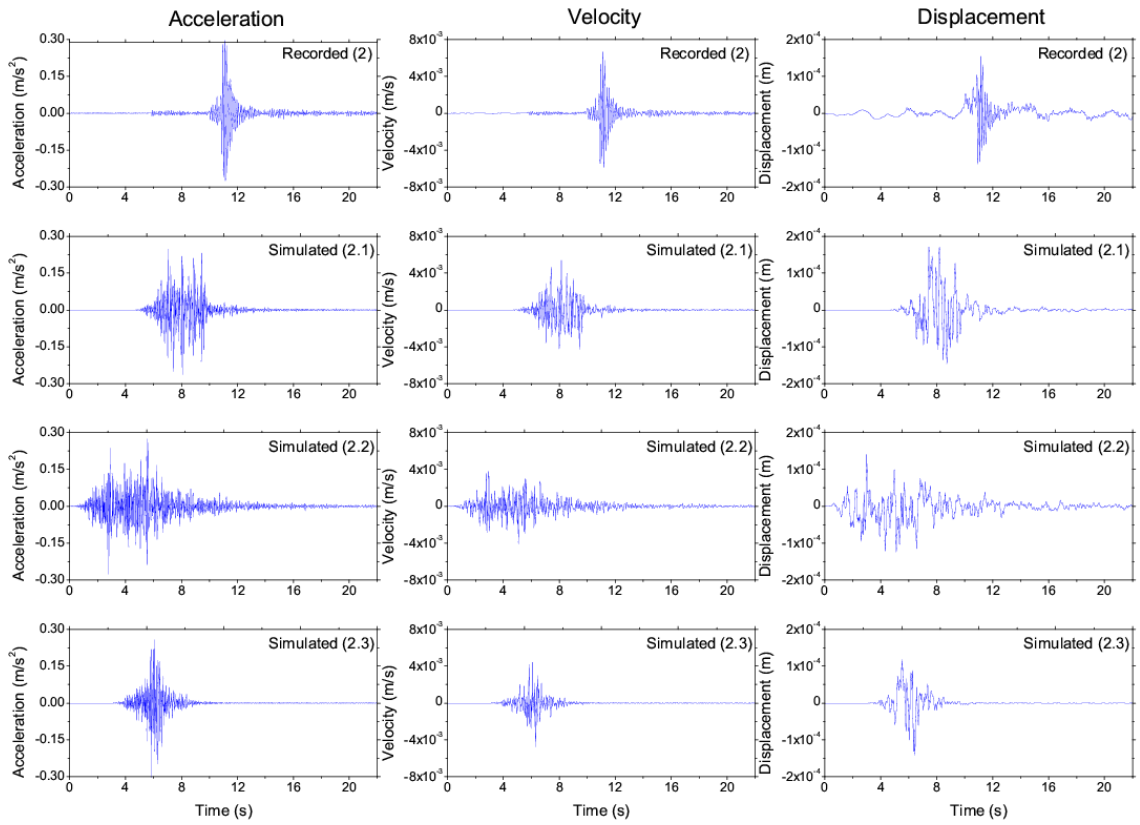

Figure 3-6. Recorded (first row) and simulated traces (last three rows) of acceleration, velocity and displacement recorded in rock conditions M_w 4, R_{epi} = 40 km, stiff soil

Additionally, Figure 3-7 shows the 5% damped acceleration response spectra for 30 simulations for the major component associated to the two events defined above plus the response spectra for the major components of the real records. It is observed that real accelerograms can be considered as only one record likely to be generated under the seismic scenario analysed. The variability present in the response spectra can be regarded as the natural variability associated with the earthquake generation phenomenon. Such variability should be properly accounted for when defining the seismic input for seismic probabilistic risk analysis. For NW European earthquakes, the proposed model seems to characterise reasonably well the natural variability of earthquakes for different scenarios defined by magnitudes, distances and types of soil.

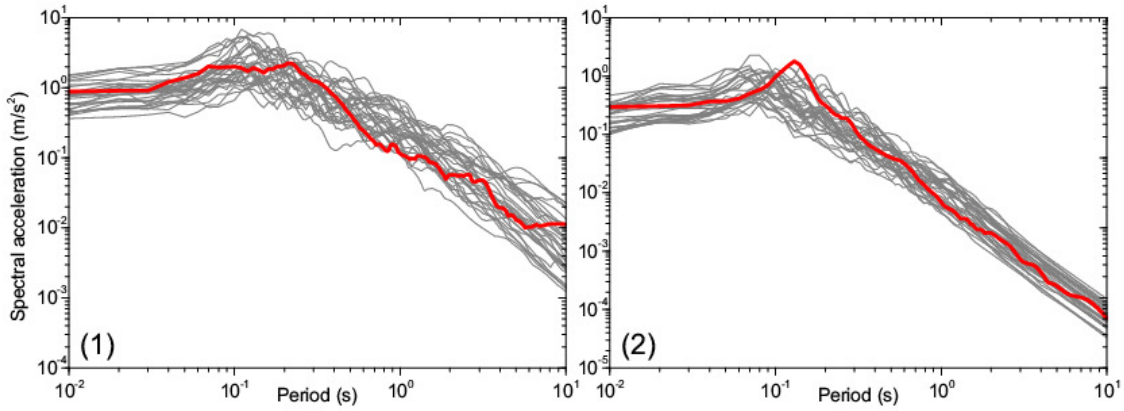

Figure 3-7. 5% damped acceleration response spectra for 30 simulations and real accelerograms (thick red line) for four real records

A complete validation of the model in terms of PGA, PGV, and 5% damped spectral acceleration can be found in Appendix B. Such a validation was made using 15 GMPEs grouped in three different geographical regions: (i) the UK, (ii) Europe and the Middle East, and (iii) other SCRs. As an example, Figure 3-8 shows the validation made in terms of PGA for two magnitudes M_w 5 and M_w 6, epicentral distances 10 km < R_{epi} < 100 km, in rock conditions (UK and Europe & Middle East) and hard rock conditions (SCRs). The GMPEs selected to make comparisons are described in details as follows:

- For the UK: the models PML [71] and PML [72] are of particular relevance as they have been extensively used for seismic hazard assessments of high-risk civil structures in the UK, including nuclear facilities [87]. Despite their widespread use, many concerns have been raised on the suitability of such predictive equations, calibrated about 30 years ago, and the necessity of upgrading earthquake estimation in the UK [25]. Other models included that are intended for UK use were Musson [269] and Rietbrock et al. [29], which is the most recent GMPE specifically calibrated for the UK at the time of writing. The latter study calibrated two models based on the dependency/independency with

magnitude of the stress parameter that defines the expected Fourier spectra of British earthquakes.

- For Europe and the Middle East: It was of interest to compare the proposed model with other models developed for the region of NW Europe. An early attempt was the model developed by Ambraseys [259] although the attenuation was modelled using the Medvedev-Sponheuer-Karnik (MSK) intensity scale. No PGA attenuation model is found in literature that has been calibrated with information exclusively taken from this region. Consequently, the closest models suitable for comparisons with the proposed model could be models calibrated using data from the wider region of Europe and the Middle East. In particular, the models reported by Akkar and Bommer [270], Ambraseys at al. [271], Bommer et al. [272] and Dahle et al. [273] are models that have widely been used in Europe. Additionally, the model of Akkar et al. [46] is part of the new generation of attenuation relations recently developed for Europe and the Middle. This GMPE was randomly selected as representative from the five models that belong to the same project. Comprehensive comparisons among such five models can be found in Douglas et al. [70].
- For other SCRs: There is no total agreement in the literature as to what extent different SCRs can be considered equivalent in terms of their seismicity features. Johnston [27] defined nine major SCRs worldwide and the comparison presented focuses on five of them: Eastern North America (ENA), Australia, India, Western China and NW Europe. In particular, the models of Toro et al. [274] and Campbell [45] are intended for use in ENA; the models of Liang et al. [275] and Kennedy et al. [276] are intended for use in Australia; the model of Raghu Kanth and Iyengar [277] is intended for use in India, the model of Chen

[278] is intended for use in Western China; and finally, the model proposed that is intended for use in NW Europe. In addition, the model of Rietbrock et al. [29] was included to observe differences in attenuation between the UK and other SCRs.

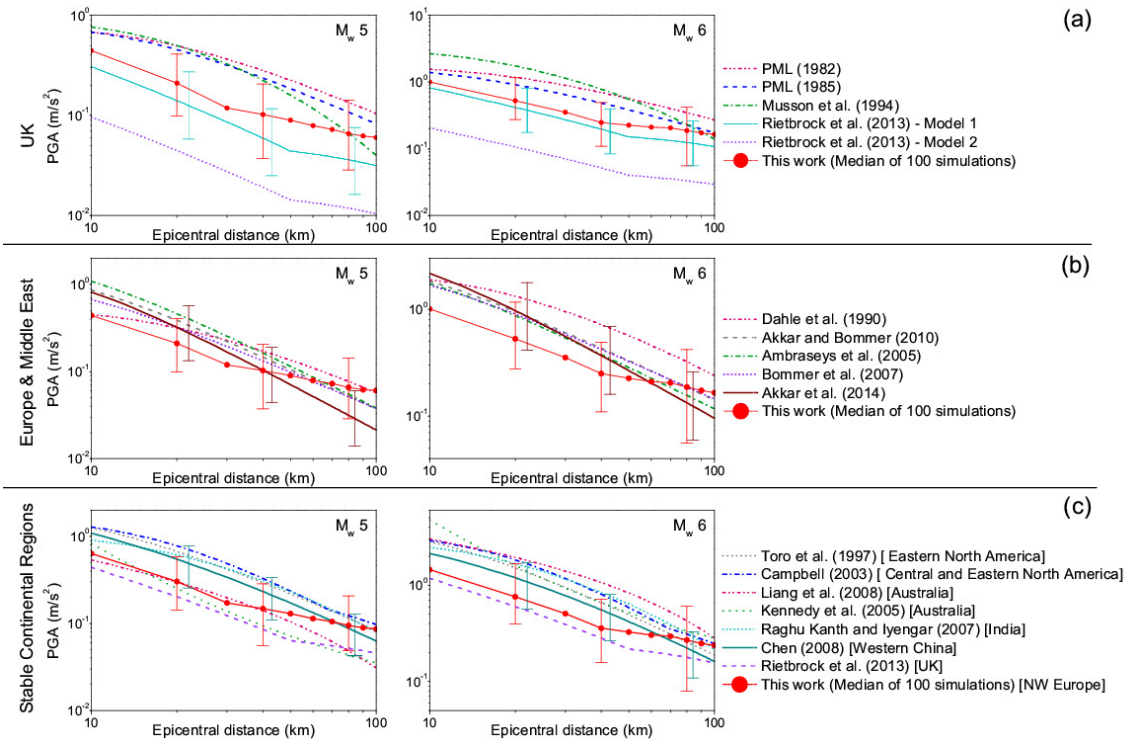

Figure 3-8. PGA estimation for two earthquake magnitudes M_w 5 and 6, epicentral distances of 10 km < R_{epi} < 100 km for (a) the UK in rock, (b) Europe and the Middle East in rock and (c) SCRs in hard rock. See Appendix B for details on adjustments

For the case of the UK, in Figure 3-8a, it is possible to see that the proposed model agree reasonably well with the magnitude-dependent stress parameter model reported by Rietbrock et al. [29]. In general, the models of PML [71-72] and Musson et al. [269] predicted higher values of PGAs, especially for epicentral distances shorter than 60-70 km. The constant stress parameter model of Rietbrock et al. [29] predicted systematically lower values of PGAs compared to the estimations made using the proposed model. The fact that the models of PML [71-72] estimated greater values of

PGAs in the whole range of distances, compared to the proposed model, is a somewhat expected outcome. Such prediction equations were calibrated using datasets that comprised earthquakes from sites such as Central America, Greece, New Zealand and California. These zones belong to different tectonic regimes than those in Britain, and in general, they are more seismically active zones. This fact has raised many concerns on the validity of the PML equations and their current use in the British nuclear industry [25]. It is also likely that the use of PML equations may have led to an over-estimation of seismic hazard analyses for nuclear sites in the UK. For the case of Europe and the Middle East, in Figure 3-8b, it can be observed that the PGAs estimated by the proposed model, in general, fall below the predictions made by the selected GMPEs, especially for epicentral distances < 60-70 km. For greater distances (up to 100 km), the predictions are in the same region. The proposed model, in general, tends to predict lower PGAs compared to GMPEs developed for Europe and intraplate regions, and this an expected outcome. The studies selected have broader target geographical regions, and therefore, they have been subjected to different and more active tectonic processes compared to NW Europe. For the case of other SCRs, Figure 3-8c shows that there is a rather wide range of PGA intensities and attenuation rates among these SCRs. An explanation supporting this statement can be found in Johnston et al. [27]. All nine major SCRs share the same primary crustal features, but there are still differences between them as each continent has experienced its own particular geological/tectonic development. Nevertheless, from a broad point of view, it seems that ENA, Australia and India exhibit a rather similar behaviour; Western China can be considered to have an average behaviour whereas NW Europe has smaller intensities compared to other SCRs. These results are in reasonably good agreement with findings reported by Bakun and McGarr [279]. Although in their analysis the attenuation is modelled using the

Modified Mercalli Intensity (MMI) scale, they suggested that ENA and NW Europe could be considered as the upper and lower limits of intensity attenuation among SCRs, and the rest (a common SCR) might be somewhere in between.

3.6 Discussion

- *On the definition of NW Europe:* Though different definitions of NW Europe have been used in the literature, it is acknowledged that the F-E regionalisation scheme [260] is only intended to set clear boundaries among different regions of the Earth and not necessarily based on their tectonic features. However, the NW European area defined by the F-E scheme is contained within the borders of the European SCR defined by Johnston [27]; hence, a relatively similar tectonic behaviour may be expected within this constrained area. It may be argued that the F-E definition of NW Europe includes areas of high seismic activity (in relative terms), such as the Alps and the Pyrenees. However, this was deemed suitable as it was necessary to include areas that possessed recorded accelerograms from strong earthquake magnitudes, say M_w 6-6.5. In this light, the model proposed would be calibrated using data from strong earthquakes (for NW European standards) that were recorded in areas that could be assumed to be comparable due to geographical proximity. This would avoid the use of accelerograms from such high earthquake magnitudes recorded in areas that possess more available information (e.g. active crustal regions) but whose characteristics may not be directly applied in NW Europe.

- *Underlying assumption of the model proposed:* The database of British earthquakes is mainly composed of small magnitude events whose features are unsuitable for predicting the characteristics of moderate-to-large earthquake accelerograms. For this

reason, it is assumed that the inherent features of accelerograms (intensity, frequency content and time duration), caused by moderate-to-strong earthquakes in Britain, would be similar to those in the Stable Continental Region to which the UK belongs, namely NW Europe. In terms of PGA, estimations made with the proposed model closely follow predictions made with the latest GMPEs calibrated for the UK in the range of magnitudes and distances of interest in probabilistic seismic hazard analysis in Britain. Also, estimations made with the proposed model confirm a result that has been earlier reported in the literature: i.e. NW Europe has associated smaller PGA intensities than other SCRs covered in earthquake engineering research. When compared with GMPEs calibrated for the wider region of Europe, it is expected that lower PGA estimations are obtained with the proposed model, as the European region comprises more seismically active zones than NW Europe. In general, this result is confirmed from the validation analyses performed.

- *Comparison with a model for active crustal regions:* The stochastic accelerogram model reported by Rezaeian and Der Kiureghian [112, 115] calibrated for active crustal regions is used for a general comparison with the proposed model. Table 3-4 shows a detailed comparison in terms of the dataset, mathematical formulation, variable selection and marginal distributions, and regression analysis between the two models. Although both share the same mathematical model, Table 3-4 shows several differences between their developments. The various modifications introduced in this work were necessary to adopt in order to define a suitable model for NW European accelerograms' features.

Table 3-4. Comparison between an NGA accelerogram model and this work

	Rezaeian and Der Kiureghian [112, 115]	**This work**
Target geographical region	Active crustal regions	Northwest Europe
Dataset		
Database	NGA	ISESD
Number of accelerograms	203	220
Magnitudes (M_w)	6.1-7.7	4-6.5
Distances	$10 < R_{rup} < 100$ km	$10 < R_{epi} < 100$ km
Type of soil	$V_{s30} > 600$ m/s	Rock, stiff and soft soil
Style of faulting	Strike-slip, reverse	Not included
Mathematical formulation		
Mathematical model	Rezaeian and Der Kiureghian [112]	Rezaeian and Der Kiureghian [112]
Time-modulating function	Gamma type (3 parameters)	Piece-wise type (6 parameters)
Linear filter	PSA SDOF (3 parameters)	PSA SDOF (3 parameters)
Variable selection		
Time-modulating function	1. Arias intensity, $\mathbf{I_a}$ 2. Effective duration, $\mathbf{D_{5\text{-}95}}$ 3. Middle time of the strong-shaking phase, $\mathbf{t_{mid}}$	1. Maximum intensity, $\boldsymbol{\alpha_1}$ 2, 3. Controllers of decaying intensity, $\boldsymbol{\alpha_2}$, $\boldsymbol{\alpha_3}$ 4. Start time, $\mathbf{T_0}$ 5, 6. Start and end time of strong-shaking phase, $\mathbf{T_1}$, $\mathbf{T_2}$
Filter parameter	1. Frequency at t_{mid}, $\boldsymbol{\omega_{mid}}$ 2. Rate of frequency change, $\boldsymbol{\omega'}$ 3. Damping ratio, $\boldsymbol{\xi_f}$	1. Frequency at beginning, $\boldsymbol{\omega_0}$ 2. Frequency at end, $\boldsymbol{\omega_f}$ 3. Damping ratio, $\boldsymbol{\xi_f}$
Matching procedure for parameters of dataset's accelerograms	Nonlinear optimisation	Monte Carlo simulation
Marginal distributions of variables		
Time-modulating function	$\mathbf{I_a}$: Normal $\mathbf{D_{5\text{-}95}}$: Beta $\mathbf{t_{mid}}$: Beta	$\boldsymbol{\alpha_1}$, $\boldsymbol{\alpha_2}$, $\boldsymbol{\alpha_3}$: Generalised extreme value (GEV) $\mathbf{T_0}$: Lognormal $\mathbf{T_1}$, $\mathbf{T_0}$: Birnbaum-Saunders
Filter parameter	$\boldsymbol{\omega_{mid}}$: Gamma $\boldsymbol{\omega'}$: Two-sided exponential $\boldsymbol{\xi_f}$: Beta	$\boldsymbol{\omega_0}$: Gamma $\boldsymbol{\omega_f}$: GEV $\boldsymbol{\xi_f}$: GEV
Regression analysis		
Modelling of random-effects regression	Rezaeian and Der Kiureghian's [115] algorithm	Abrahamson and Youngs's [268] algorithm
Type of functional form	Linear	Nonlinear
Explanatory variables of functional form	**F** = type of faulting **M** = moment magnitude **R** = distance-to-site $\mathbf{V_{s30}}$ = shear-wave velocity (type of soil is modelled **quantitatively**)	**M** = moment magnitude **R** = epicentral distance $\mathbf{D_1}$ and $\mathbf{D_2}$ = dummy variables (type of soil is modelled **qualitatively**)

- *Limitations*: One of the limitations of the model proposed that could be envisaged *a priori* is related to the lack of information of the dataset for accelerograms recorded at epicentral distances longer than 100 km. The model proposed was not able to appropriately capture the attenuation rate of PGAs, PGVs and spectral accelerations when simulating seismic scenarios for such distances. For this reason, the applicability of the model was set to a maximum epicentral distance of 100 km. In this light, it is acknowledged that the model presented possesses a rather high epistemic uncertainty. The epistemic uncertainty of this model can only be reduced by adding more accelerograms to the dataset; therefore, the model should be subjected to revisions/updates when more data are available.

- *GMPEs vs Stochastic Accelerogram Models:* As GMPEs do not primarily aim to provide ground motion accelerograms, nonlinear time-history analysis in the context of SPRA, could not be rationally performed based solely on such predictive models. For seismic assessment of critical structures, such as nuclear power stations, comprehensive sets of accelerograms compatible with the local seismicity are required. In this sense, the main objective of the model proposed is to establish a mathematical model able to simulate any number of accelerograms for any seismic scenarios (magnitude, distance, type of soil) within NW Europe. However, as GMPEs are widely used and recognised by practitioners/researchers, they can also be used as a validation framework of the model presented in this work.

3.7 Conclusions

The work presented in this chapter has led to the following conclusions:

- The definition of the boundaries for a NW European region that possesses uniform tectonic behaviour, which in turn could be considered representative for UK standards, seems to be a matter open to discussion as different definitions were found in the literature. The approach used in this work, based on the Flinn-Engdhal regionalisation scheme, was initially found to be a reasonable alternative to define an area of moderate-to-low seismic activity. This area includes recorded accelerogram data from earthquakes of magnitudes and distances relevant for structural engineering purposes in the context of SPRA for NPPs in the UK.

- The predictive equations calibrated by means of the random-effects regression technique are able to account for the sample-dependency of the dataset used. Several functional forms for these predictive equations were tested. For simplicity, only one functional form, with the least possible number of explanatory variables, was chosen for all parameters that govern the stochastic process. This implies that different levels of statistical significance for the predictive equations were obtained. However, all predictive equations proposed were appropriate for explaining the statistical behaviour of the dependent variables at the standard 5% significance level normally used in statistical hypothesis testing.

- The model proposed requires three input variables typically used in structural engineering applications, namely, earthquake magnitude, distance-to-site and type of soil for a design seismic scenario. Once this information is set, the simulation of accelerograms is entirely made in the time domain and essentially involves the generation of random variables. In this light, this model is considered to be straightforward to define seismic inputs for nonlinear time-history analysis of structures.

- The predictive model proposed in this work was found to capture the natural variability of accelerograms produced by different seismic scenarios. Verifications using recorded accelerograms from NW Europe show that a real recording can be considered to be one accelerogram likely to be produced by a specific seismic scenario and the artificial recordings are able to simulate the natural dispersion associated to the earthquake generation phenomenon.

- Regarding PGA estimations obtained with the model proposed, it is found that there is a reasonably good agreement with the latest predictive models calibrated for the UK and Europe, for the magnitudes and distances of interest in seismic hazard and risk analysis. However, when compared with the models used in hazard assessments in the UK [71-72], the proposed model systematically estimates lower PGAs. This may support some concerns reported in the literature on the validity of such equations, especially for their use in the British nuclear industry. Even though further evidence is required to support this statement, it is likely that such models may have led to conservative results for nuclear sites in the UK. Additionally, comparisons made with other SCRs show that PGA intensities and attenuation rates are somewhat different. This may be explained by the fact that each SCR has experienced its own tectonic evolution. Nevertheless, results obtained in this work suggest that, Eastern North America, Australia and India possess a rather similar behaviour and have associated higher PGA intensities. On the other hand, NW Europe can be considered to have associated smaller PGA intensities. Finally, Western China could be regarded as possessing an average behaviour.

- Regarding estimations on spectral acceleration (shown in Appendix B), there is also a reasonably good agreement between the model proposed and predictive models

calibrated for the UK, Europe and other SCRs. This is valid for a wide range of periods for the magnitudes and distances of interest for time-history analyses of structures. Consequently, it can be concluded that the proposed model is suitable to rationally define the loading input in structural engineering analyses for the NW European regions.

Chapter 4

Seismic risk analysis: using stochastically simulated accelerograms

4.1 Introduction

As earlier discussed in Section 2.3.3.2 , the paucity of accelerograms to define seismic inputs for SPRA in areas of medium-to-low seismic activity has led structural engineers to using techniques on selecting, scaling and matching procedures applied to available records. In general, these procedures are intended to match a spectral shape predicted by *ad-hoc* ground motion prediction equations (GMPEs). Currently, GMPEs play a critical role in seismic hazard and risk analysis and much research effort has been placed on the development of such models [38, 70]. However, as the SPRA methodology selected for this work requires the direct specification of sets of accelerograms, the use of GMPEs is actually an unnecessary intermediate step towards this objective [36]. Promising trends in earthquake engineering have been developed as an alternative to GMPEs in seismic

hazard and risk analysis, e.g. [84]. This chapter presents an alternative and straightforward approach that does not make use of GMPEs to conduct SPRA for NPPs in the UK, through an example of application. In this procedure, a large set of accelerograms are generated by direct stochastic simulation by means of the predictive model described in Chapter 3. A hypothetical UK nuclear site was selected as a representative of a high seismic demand area (for British standards) and the risk is assessed using a simplified model of a 1000 MW Pressurised Water Reactor building. For completion, the alternative procedure is compared to the usual GMPE-based procedure to perform SPRA for nuclear facilities, in order to highlight that the risk assessment procedure becomes remarkably more straightforward when using the approach proposed (see Appendix C for a complete version of this Chapter).

4.2 Description of methodologies: current vs. proposed

In the current state-of-the-art approach to perform SPRA for nuclear power plants, described in detail in Section 2.3, three types of assessments are reported: (i) intensity-based, (ii) scenario-based and (iii) time-based assessments. For simplicity, this chapter is focused on scenario-based assessments, although the methodology proposed could also be used for applications in the two other assessments.

When performing scenario-based assessments, it is required to define the seismic input for the single scenario (or all scenarios of interest) that contributes most strongly to the hazard of the nuclear site. Such a scenario can be obtained by means of the deaggregation of the hazard curve of the site [32]. Then, a spectral shape predicted by *ad-hoc* GMPE(s) compatible with such scenario is estimated and few available accelerograms are scaled to match such a spectral shape. The scaled accelerograms are then used to perform nonlinear time-history analysis of a suitable structural model in

order to estimate the damage state of the NPP. However, in order to estimate the probability of unacceptable performance with high statistical confidence, a great number of observations of the damage state are required. This leads to the necessity of sampling the structural response (i.e. the output of nonlinear time-history analysis) normally obtained by means of Monte Carlo-type procedures. For illustration purposes, Figure 4-1 summarises the steps involved to define the seismic input and calculate the structural output in scenario-based SPRA when using the traditional GMPE-based procedure.

The procedure summarised in Figure 4-1 is somewhat cumbersome as a number of intermediate steps are required in order to obtain both suitable accelerograms and a great number of observations of the damage state of the NPP studied. The approach presented in this chapter that makes use of the stochastic accelerogram model described in Chapter 3 is more direct than the traditional procedure. Indeed, once the seismic scenario (or all scenarios of interest) that contributes most strongly to the hazard of the nuclear site is determined, an unlimited number of accelerograms compatible with such a scenario can be simulated. In this light, neither GMPEs nor scaling/matching procedures are necessary. In this approach, the ground motion input is sampled and the damage state is directly calculated rather than sampled. Clearly, no Monte Carlo-type procedures would be required to simulate the structural output. For illustration purposes, Figure 4-2 summarises the steps involved to define the seismic input and calculate the structural output in SPRA when using the proposed procedure.

The following sections are devoted to present a step-by-step comparison of SPRA between the traditional GMPE-based methodology and the proposed approach through a

particular application for NPPs in the UK. For both analyses performed, the seismic hazard curve of the nuclear site was considered to be known.

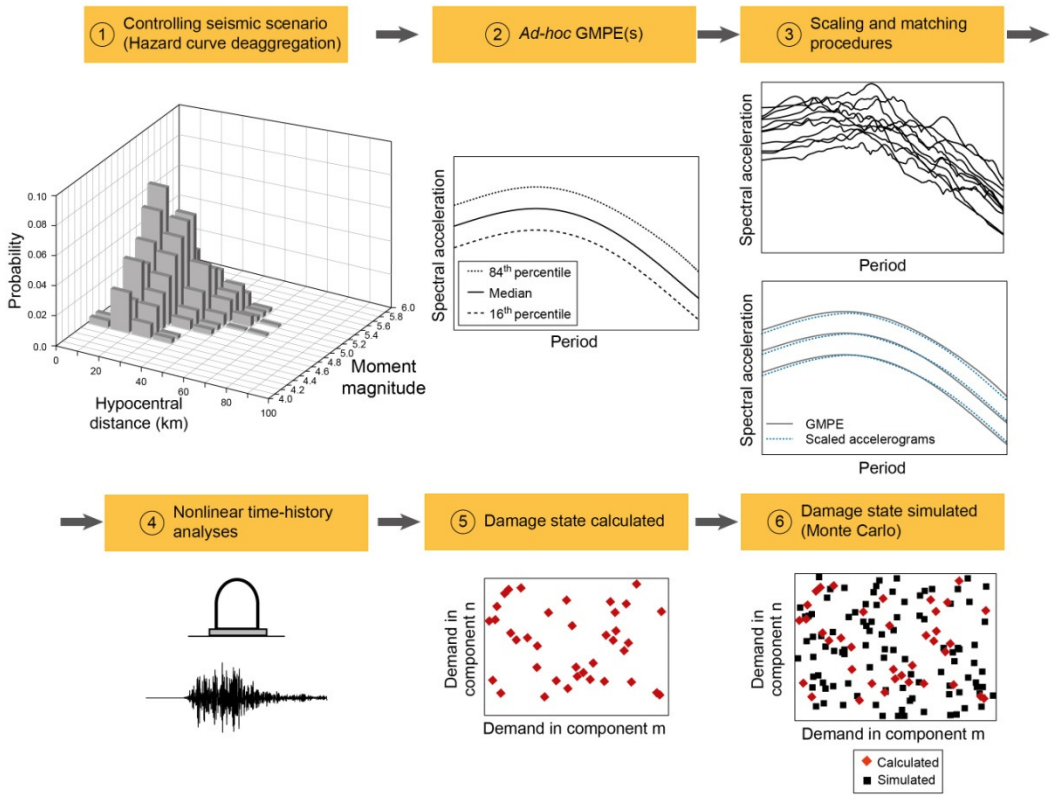

Figure 4-1. Using the GMPE-based approach: steps to define seismic input and calculate structural output in scenario-based SPRA

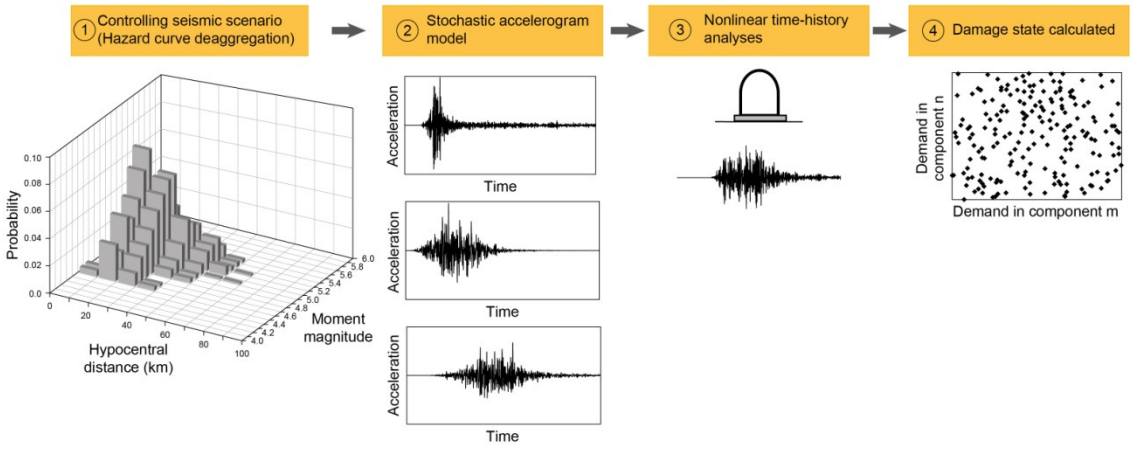

Figure 4-2. Using the proposed approach: steps to define seismic input and calculate structural output in scenario-based SPRA

4.3 Sample nuclear reactor building

Risk assessments conducted hereafter in this PhD thesis were performed considering a sample NPP based on a 1000 MW Pressurised Water Reactor (PWR) shown schematically in Figure 4-3a. This sample nuclear reactor building is composed of two structural units: (i) the containment structure (CS), composed of a post-tensioned concrete cylindrical wall, and (ii) the internal structure (IS), to which the critical key components, equipment and/or machinery of the NPP are attached. These structural units are independent from each other; hence, they are only connected at the foundation level. The height of the CS and IS are 60 and 39 m, respectively, whereas the total weight of the reactor building is approximately 62,000 ton. Figure 4-3b shows the simplified structural model of the sample NPP used in this work to perform time-history analysis. Both the CS and IS are modelled as lumped-mass stick models by means of SAP2000 using beam elements and rigid connections for all elements. Translational and rotational mass of each node, stiffness and geometry properties of each stick element, and material properties were taken from Li et al. [280]. For simplicity, all properties are the same in both horizontal directions. Fundamental periods of vibration of the CS and IS are 0.23 s and 0.18 s, respectively. It is worth mentioning that this type of structural model, although simplified, has been extensively used in nuclear engineering research [281-284].

Risk assessments of NPPs are focused on their critical components supported by the IS as they control the cost of a NPP project in terms of design, analysis, construction, testing and regulatory aspects. As for the CS, it is designed to withstand large internal pressures in order to provide shield against potential radiation release; hence, it is expected to remain within the elastic range during seismic events. The critical

components of the sample NPP, node assignment in the structural model and their location related to the foundation level are summarised in Table 4-1.

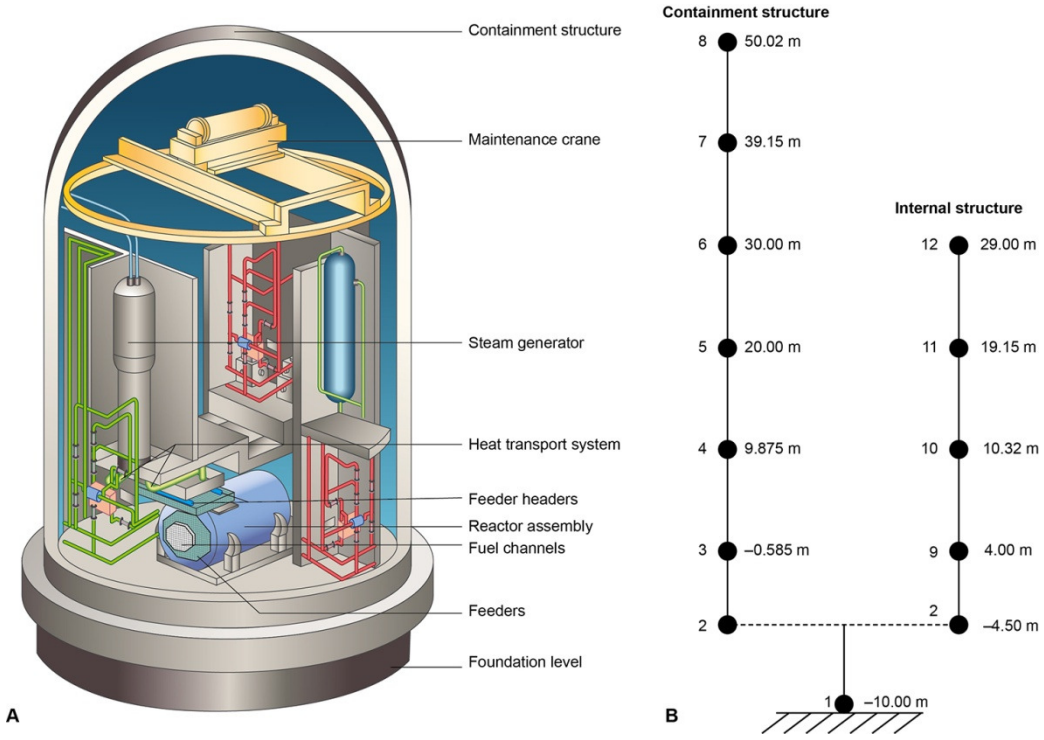

Figure 4-3. Sample NPP reactor building: (a) schematic view; (b) lumped-mass stick model [280]

Table 4-1. Critical components and their location within the sample NPP

Critical component	Node number	Elevation (m)
Reactor assembly and fuel channels	2	-4.50
Feeders and feeder headers	9	4.00
Heat transport system	10	10.32
Steam generator	11	19.15
Maintenance crane	12	29.00

In this work, unacceptable performance of the sample NPP is defined as the failure of any of the critical components indicated in Table 4-1. Consequently, the simplified fault tree used for risk assessments conducted in this work is shown in Figure 4-4. This fault tree possesses one ‘OR’ gate in which the failure of one or more events below it defines the failure of the event above it. Failure of each critical component is expressed by

means of fragility curves. Estimation of such fragility curves are discussed in detail in Section 4.6.

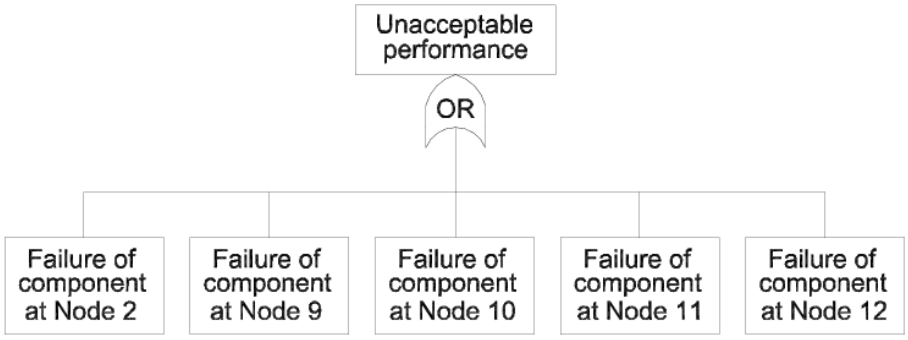

Figure 4-4. Fault tree used for risk assessments conducted in this work

As it will be seen in Section 4.7, nonlinear time-history analyses of the structural model shown in Figure 4-3b were performed. In this work, the inelastic definition for the structural used bilinear shear hinges with 3% post-yield stiffness were assigned to all stick elements of the IS. The yield capacity of each hinge was estimated as $0.5 \cdot \sqrt{f_c^{'}} \cdot A_s$, where $f_c^{'}$ is the compression concrete strength (assumed as 35 N/mm^2) and A_s is the shear area of each stick of the IS as indicated in Li et al. [280].

4.4 Seismic hazard of the nuclear site

A hypothetical UK nuclear site was necessary to select. The level of seismic hazard of nuclear sites in the UK is defined by a seismic event of an annual frequency of exceedance of 10^{-4}, corresponding to a return period of 10,000 years [285]. Therefore, it is of interest to determine the scenario (magnitude, distance) that contributes most strongly to the site's hazard for a 10,000 years return period at the fundamental period of the IS of the sample NPP. The hypothetical nuclear site selected for risk assessments in this work is a typical UK nuclear power plant site with relatively moderate seismicity (Figure 4-5a). The estimation of the dominant seismic scenario was taken from the

deaggregation of the hazard curve for the town selected proposed by Goda et al. [32] for 10,000 years return period at a structural period of 0.2s, shown in Figure 4-5b (for simplicity, the hazard defined for a structural period of 0.2s was assumed to be valid for the fundamental period of the IS = 0.18s). From this figure, it is possible to see that the scenario that contributes most strongly the site's hazard is an earthquake magnitude M_w 5.3 at a hypocentral distance of 15 km (average between 10 and 20 km). Accelerograms compatible with such a scenario will be later required to perform time history analysis of the structural model of the sample NPP.

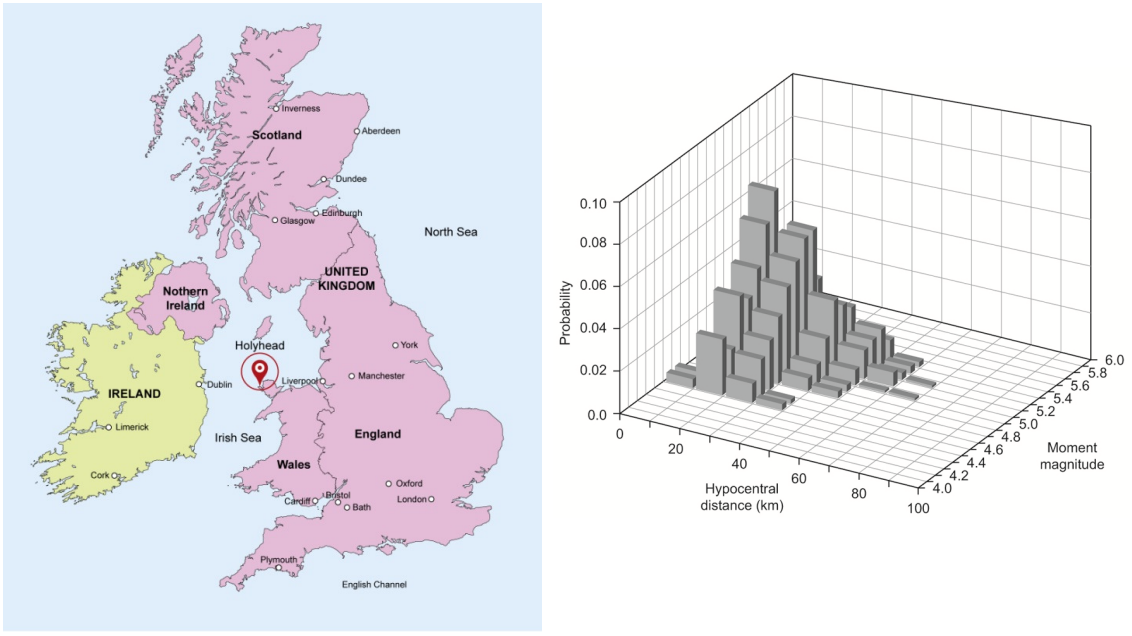

(a) (b)

Figure 4-5. Hypothetical UK nuclear site selected: (a) location; (b) deaggregation of the hazard curve for 10,000 years return period at a structural period of 0.2s (redrawn from Goda et al. [32])

4.5 Definition of seismic inputs: GMPEs vs. stochastic model

4.5.1 Ground motion prediction equations (GMPEs)

The GMPEs selected for this purpose were the same used to define current national seismic hazard maps for the UK in Musson and Sargeant [286], namely, Bommer at el.

[272] and Campbell and Bozorgnia [287]. The underlying basis for the use of the model of Bommer et al. [272] was geographical proximity as it was calibrated using earthquake data from Europe and the Middle East, whereas the model of Campbell and Bozorgnia [287], although calibrated using earthquake data from active crustal zones, was deemed to be suitable for the UK [32]. Additionally, the model of Rietbrock et al. [29] was also included as it is a UK-based model calibrated using weak-motion data from British earthquakes. Table 4-2 shows the GMPEs selected for comparisons and their principal features.

Table 4-2. GMPEs selected for risk assessments in this section

Reference	GMP (1)	HC(2)	M(3)	R(4)	Site classification	Style of faulting
Rietbrock et al. [29]	PGA, PGV, PSA	GM	M_w	R_{JB}	Hard rock	Not included
Bommer et al. [272]	PGA, PSA	GM	M_w	R_{JB}	Rock Stiff soil Soft soil	Normal, strike-slip and reverse
Campbell and Bozorgnia [287]	PGA, PGV,PSA, PGD	GM	M_w	R_{rup}	Rock Stiff soil Soft soil Very soft soil	Normal, strike-slip and reverse

(1): Ground motion parameter predicted: PGA: peak ground acceleration; PGV, peak ground velocity; PGD, peak ground displacement; PSA: pseudospectral acceleration
(2): Definition of the horizontal component: GM: geometric mean
(3): Magnitude scale used
(4): Distance metric used

The following conditions/assumptions were made in order to be consistent in the generation of sets of accelerograms compatible with the seismic scenario defined in Section 4.4.

1. Scale magnitude: The moment magnitude scale (M_w) was used. All GMPEs selected are consistent with such a scale.

2. Distance metric: The epicentral distance (R_{epi}) was used. For simplicity in these calculations, the earthquake rupture was modelled as a point source, the fault was assumed to be vertical, and a very small focal depth was assumed; hence all distance

metrics could be considered approximately equivalent. These assumptions are considered to be conservative.

3. Type of soil: It was assumed rock type conditions. As the model of Rietbrock et al. [29] was calibrated for hard rock conditions, the modification factors proposed by Van Houtte et al. [288] were used to adjust it to rock conditions.

4. Style of faulting: The type of faulting was not considered. However, strike-slip conditions were set to those GMPEs that included style of faulting as this type is the most likely to occur in British earthquakes [31].

5. Component of motion: The larger horizontal (LH) component of motion was used. As the GMPEs selected were calibrated considering the geometric mean (GM) of the two horizontal components, the coefficients proposed by Beyer and Bommer [289] were used to estimate LH.

Following Huang et al. [142-143], 11 accelerograms for each GMPE of Table 4-2 were scaled by means of the Distribution-Scaling Method [221] to match the spectral shape and variability predicted by the corresponding GMPE. For this purpose, it was decided to use recorded accelerograms that were used in the calibration of their corresponding GMPE, where possible, compatible with the scenario of interest. This was done as an attempt to preserve the natural features of frequency content and time duration of real records from the location of interest for the corresponding GMPE. The criterion for selecting accelerograms was to use records from earthquake magnitude $5.2 < M_w < 5.4$, epicentral distance $10 < R_{epi} < 20$km, and rock conditions ($V_s \geq 750$ m/s). For the model of Rietbrock et al. [29], no such accelerograms were available; therefore, the 11

accelerograms were simulated using the stochastic model described in Chapter 3. For the model of Bommer et al. [272], the 11 recorded accelerograms selected are summarised in Table 4-3. For the model of Campbell and Bozorgnia [287], only 3 accelerograms fell into the selection criterion defined. These records are indicated in Table 4-3. The remaining 8 accelerograms were obtained through simulations. As the stochastic model described in Chapter 3 is not suitable to simulate accelerograms from active crustal regions, it was used the computer code "Strong Ground Motion Simulation (SGMS)" [290]. SGMS is based on the Specific Barrier Model [291] which is a complete and self-consistent description of the earthquake faulting process. In this case, the tectonic regime selected to simulate accelerograms with SGMS was "inter-plate" (rather than "intra-plate" or "extensional" regimes) as it is more consistent with the corresponding GMPE. Table 4-3 is a general summary of the 11 accelerograms selected for each GMPE used for risk assessments in this work.

Table 4-3. Summary of the 11 accelerograms associated to each GMPE selected

No	Earthquake name	Location [(1)]	Wave ID[(2)]	Mw	Distance (km)[(3)]
Rietbrock at al. [29]					
1 - 11	Simulated accelerograms using the stochastic model for NW Europe, considering a scenario M_w 5.3, R_{epi} = 15 km and rock conditions.				
Bommer et al. [272]					
1	Friuli	Northern Italy	981	5.4	11
2	Calabria	Southern Italy	169	5.2	10
3	Montenegro	Albania	193	5.4	15
4	Kalamata	Southern Greece	1900	5.3	17
5	Javakheti Highland	Turkey-Georgia-Armenia	487	5.4	20
6	Umbria Marche	Central Italy	765	5.2	11
7	Umbria Marche	Central Italy	826	5.2	14
8	Umbria Marche	Central Italy	791	5.2	18
9	Mt. Hengill Area	Iceland	5085	5.4	15
10	Mt. Hengill Area	Iceland	5086	5.4	15
11	Mt. Hengill Area	Iceland	5078	5.4	18

Table 3 (cont). Summary of the 11 accelerograms associated to each GMPE selected

No	Earthquake name	Location [1]	Wave ID[2]	Mw	Distance (km)[3]
Campbell and Bozorgnia [287]					
1	Lytle Creek	California, USA	43	5.33	16.7
2	Whittier Narrows-02	California, USA	715	5.27	16.5
3	Anza (Horse Canyon)-01	California, USA	225	5.19	12
4 – 11	Simulated accelerograms using the SGMS computer code, considering a scenario M_w 5.3, R_{epi} = 15 km and rock conditions.				

(1): Location for accelerograms used for Bommer et al. [272] is the Flinn-Engdhal region.
(2): Wave ID for accelerograms used for Bommer et al. [272] are given by the ISESD database and Campbell and Bozorgnia [287] are given by the PEER database.
(3): Distance metric for accelerograms used for Bommer et al. [272] is R_{epi} and Campbell and Bozorgnia [287] is R_{JB}.

Figure 4-6a shows the spectral accelerations of the 11 scaled accelerograms for each GMPE whereas Figure 4-6b shows the median, 84th and 16th percentiles for the 11 scaled accelerograms and their corresponding GMPEs.

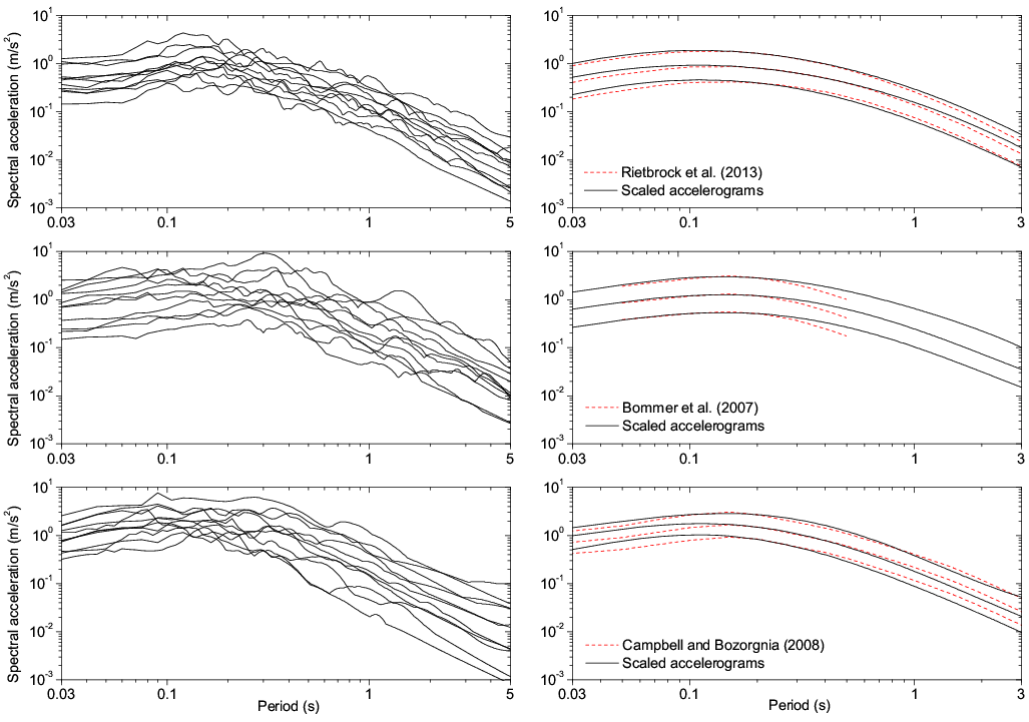

(a) (b)

Figure 4-6. (a) Spectral accelerations of the 11 accelerograms scaled for each GMPE; (b) median, 84th and 16th percentiles of spectral accelerations predicted by each GMPE and their corresponding scaled accelerograms

From Figure 4-6b, it is possible to see that the scaled accelerograms are able to capture reasonably well the spectral shape and variability predicted by the GMPEs selected. Consequently, the scaled accelerograms were considered suitable to perform nonlinear time-history analysis with the structural model of the sample NPP.

4.5.2 Stochastic ground motion accelerogram

For the stochastic model, the generation of accelerograms compatible with the seismic scenario of interest is significantly more straightforward. As the model proposed is an unlimited source of accelerograms compatible with the dominant seismic scenario, there is no need of using intermediate steps towards obtaining suitable records. Selection of GMPE(s) suitable to use in the UK and scaling-matching procedures are not needed when using the stochastic model. For illustration purposes, Figure 4-7a shows five simulated accelerograms and Figure 4-7b shows the spectral acceleration of 50 simulated accelerograms for a scenario M_w 5.3 and epicentral distance R_{epi} = 15 km.

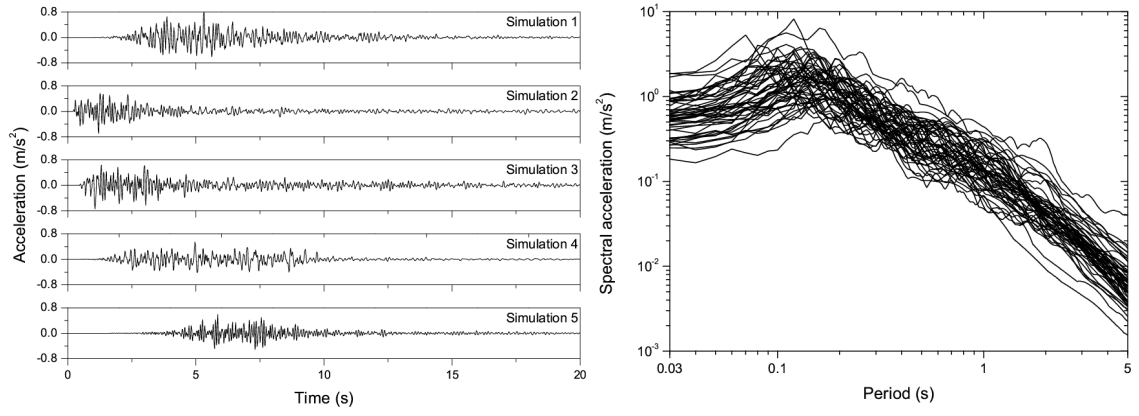

(a) (b)

Figure 4-7. Sample input compatible with a scenario M_w 5.3 and epicentral distance R_{epi} = 15 km: (a) five simulated accelerograms and (b) spectral acceleration of 50 simulated accelerograms.

Before performing nonlinear-time history analysis using the accelerograms defined in this section, it is necessary to define the vulnerability of the sample nuclear reactor building against seismic actions. In the next section, the fragility analysis of the sample NPP is discussed.

4.6 Fragility analysis

The theoretical background to estimate fragility curves for NPPs is thoroughly discussed in Section 2.3.2.2. In this PhD thesis, the fragility parameters a, β_r, β_u (and HCLPF) were estimated following a simplified approach. It is initially defined the seismic demand parameter used to characterise the fragility curves for the critical components of the sample NPP defined in Section 4.3. In this case, the average floor spectral acceleration (AFSA) over a frequency range from 1 to 33 Hz was selected to estimate fragility curves (i.e. the average of 33 floor spectral ordinates at frequencies from 1 to 33 Hz with increments of 1 Hz). The frequency range 1 to 33 Hz to calculate AFSA was selected as most frequencies of NPP components are comprised within such a range (see Pisharady and Basu [162] for a complete summary of typical frequency ranges for NPP components).

The HCLPF capacity for the critical components were estimated by means of linear dynamic analysis of the structural model using a large set of accelerograms compatible with the seismic hazard of the selected nuclear site. The number and nature of input accelerograms, range of earthquake magnitudes and distances, and type of analysis used to determine fragility parameters are all matters open to discussion. Table 4-4 shows some examples reported in the literature showing a wide variety of criteria among researchers. However, it is apparent that the majority of such studies intended to use

accelerograms (either recorded or simulated or a combination of both) that to some extent are representatives of the nuclear site's seismic hazard.

Table 4-4. Examples of the nature of seismic inputs used to determine fragility curves of NPP structures and components

Reference	Application (country)	Number and nature of accelerograms	Range of magnitudes (scale)	Range of distances (km)	Nature of time-history analyses
Cho and Joe [292]	Containment & component cooling water buildings – Standard NPP (Korea)	**87** recorded in southeast Korean peninsula	2.7 - 4.8 (1)	Unspecified	Linear
Choi et al. [281]	CANDU containment structure (Korea)	**30** recorded around the world	5.7 – 7.6 (M_w)	0.10 – 18.3 (R_{rup})	Nonlinear
Huang et al. [144]	Components of a sample NPP (Eastern United States)	**11** simulated compatible with local tectonic regime	5.3 (M_w)	7.5 (2)	Linear
Kennedy et al. [172]	Diablo Canyon NPP (Western United States)	**52** (24 recorded in WUS + 28 simulated from WUS motions)	6.5 – 7.5 (M_w)	0.1 – 25 (2)	Linear
Nakamura et al. [174]	PWR-type building (Japan)	**1** simulated matched with site UHS	Unspecified	Unspecified	Nonlinear
Ozaki et al. [282]	PWR-type building (Japan)	**12** simulated based on local standard motions	Unspecified	Unspecified	Linear and nonlinear
Zentner [163]	Reactor coolant system – Standard NPP (France)	**50** simulated matched with site response spectrum	Unspecified	Unspecified	Nonlinear

(1): Unspecified earthquake magnitude scale
(2): Unspecified distance metric

In this work, an innovative approach to estimate the HCLPF capacity for the critical components was used. As the stochastic model used is an unlimited source of accelerograms compatible with any seismic scenario required by the analyst, a large database of simulated recordings compatible with the site's hazard was used. For simplicity purposes, the seismic hazard of the site selected was characterised by means of its dominant events [293], i.e. the scenarios that are most likely to contribute to the hazard which are directly obtained from the disaggregation of the hazard curve. From

Figure 4-5b, it is possible to see that the dominant events for the nuclear site selected are earthquakes magnitude $4.5 < M_w < 5.5$ at hypocentral distances of $10 < R_{hyp} < 30$km. For simplicity in these calculations, it was assumed a very small focal depth; hence $R_{hyp} \approx R_{epi}$. A large set of scenarios within such ranges (magnitude, distance) was sampled. For each scenario, a single corresponding accelerogram was simulated with the model proposed and a linear time-history analysis of the sample NPP structural model was performed. Then, AFSAs for each node were calculated. This procedure was repeated until convergence on the median value for AFSAs for all nodes was reached. This median value for AFSAs for each node was assigned as their HCLPF capacity level. In the absence of seismic capacity data for the critical components considered in this study, their HCLPF seismic capacity was assumed to be equal to the seismic loading at the component location, represented in this work as the median value for AFSAs. It is acknowledged that this is a conservative assumption but it enables the methodology to be demonstrated in this PhD thesis. Figure 4-8a shows the simulated seismic scenarios and Figure 4-8b shows the convergence of the median value of AFSAs for each node, which is reached after performing approximately 200 simulations.

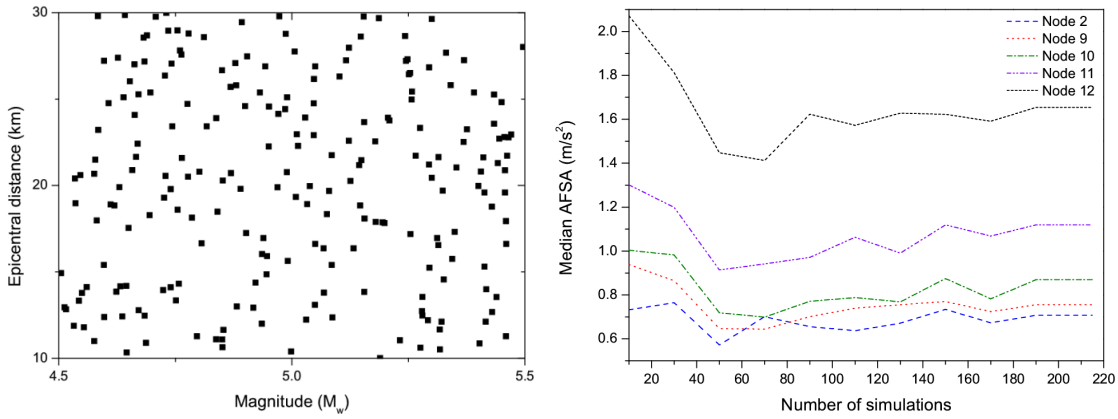

(a) Simulated seismic scenarios (b) Convergence of median AFSAs

Figure 4-8. Estimation of the HCLPF capacity level for the critical components of the sample NPP

From Figure 4-8b, it is obtained that the HCLPF for the critical components are: 0.71, 0.76, 0.87, 1.12 and 1.65 m/s^2 for Nodes 2, 9, 10, 11 and 12, respectively. For the logarithmic standard deviations β_r and β_u, approximate values are possible to obtain from the literature, for example, in the comprehensive review reported by Park et al. [171]. However, in this work, the results proposed by Llambias [294] were used as they were specifically derived for PWRs in the UK. In this case, β_r and β_u were taken as the average considering all the values proposed by Llambias [294] for critical components in UK hard site conditions, i.e., β_r = 0.35 and β_u = 0.41. These values are considered to be on the safe side: the sum of both logarithmic standard deviations should conservatively be (β_r + β_u) ≈ 0.7-0.8 [120, 295]. Therefore, the values for the deterministic estimator for the capacity of the critical components $\hat{a}$ expressed in terms of AFSA between 1-33 Hz are: 2.47, 2.63, 3.03, 3.90 and 5.77 m/s^2 for Nodes 2, 9, 10, 11 and 12 respectively. As an example, Figure 4-9a and Figure 4-9b show families of 11 fragility curves for the critical components at Nodes 2 and 12. These curves were built using Equation 2-2 considering confidence levels Q from 1/22 to 21/22 with increments of 1/11. The median fragility curve (Q=0.5) is shown in the solid bold line. Figure 4-10 shows the median fragility curves for the critical components at all nodes of the IS.

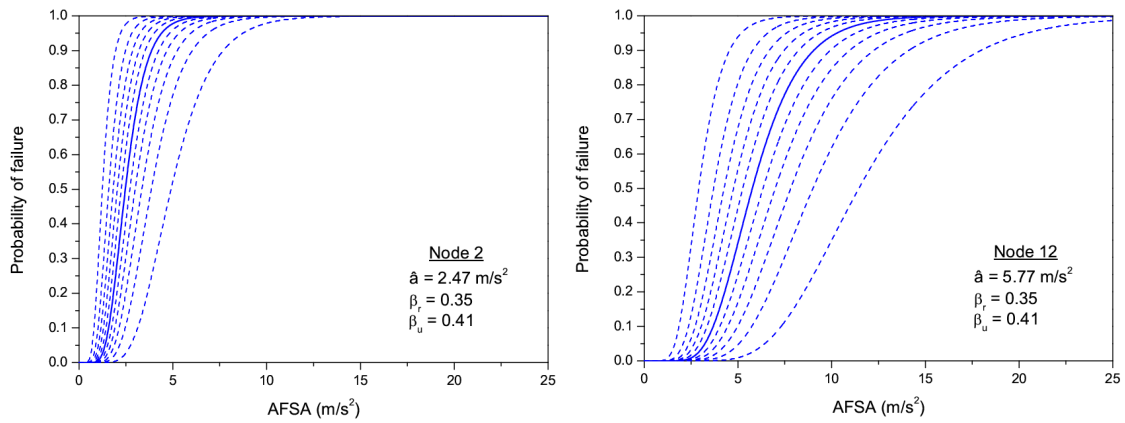

(a) (b)

Figure 4-9. Family of fragility curves for the critical components at (a) Node 2 (reactor assembly); (b) 12 (maintenance crane);

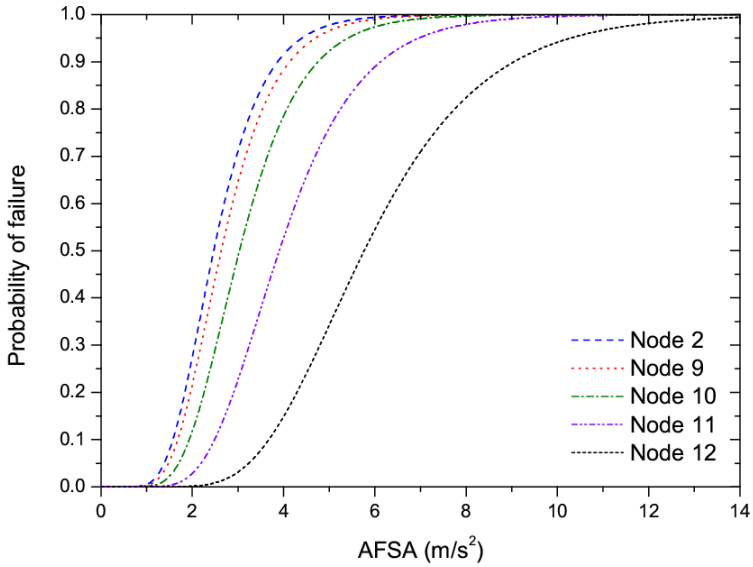

Figure 4-10. Median fragility curves for the critical components at all nodes of the IS.

4.7 Structural response

Nonlinear time-history analyses were performed on the structural model of the sample NPP using the 11 accelerograms selected for each GMPE described in Section 4.5.1. For the stochastic model proposed, a databank of 600 accelerograms were simulated as described in Section 4.5.2 and then used to conduct nonlinear time-history analysis. It is worth mentioning that the size of the databank of 600 nonlinear dynamic analyses and their associated results of the structural response is only intended to have a statistically large collection of data to choose from. This does not mean that 600 nonlinear dynamic analyses are needed to perform to make a statistically significant estimation of the seismic risk as it will be seen in Section 4.8. The structural response of all analyses was calculated in all nodes of the IS in terms of the same demand parameter used to define fragility curves, i.e. AFSA over a frequency range from 1 to 33 Hz. Consequently, for each GMPE a matrix of results of order 11 x 5 (11 accelerograms and 5 nodes) was obtained, whereas for the stochastic model proposed, such matrix of results is of order 600 x 5. As an example of these results, Figure 4-11 shows the median floor spectral

accelerations between 1 and 33 Hz for Node 2 (reactor assembly) and Node 12 (maintenance crane).

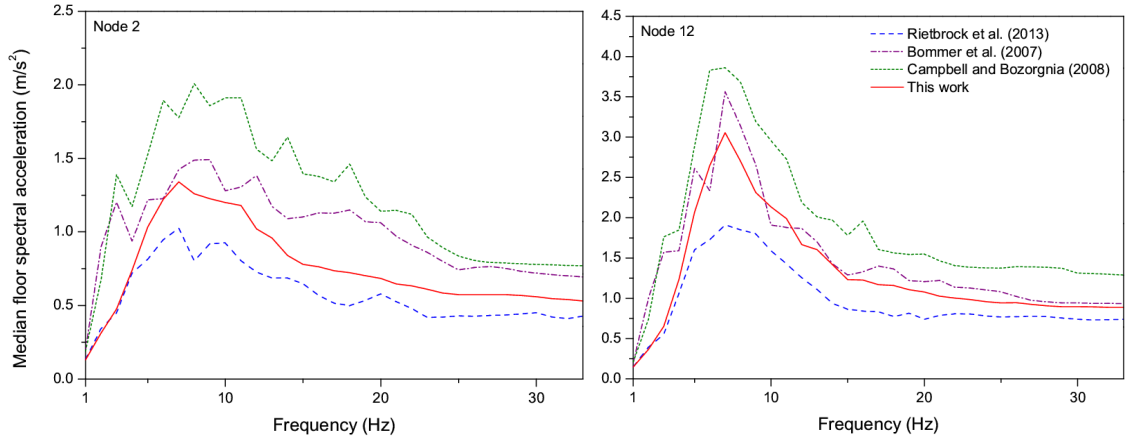

(a) (b)

Figure 4-11. Median floor spectral acceleration at: (a) Node 2 (reactor assembly) and (b) Node 12 (maintenance crane)

As the matrices of results associated to each GMPE are comprised of only 11 rows, it is required to sample the structural response (output) in order to enlarge the number of row vectors to hundreds or thousands to estimate the probability of unacceptable performance of the sample NPP with high confidence. Such simulations of the structural response were performed using the Monte Carlo-based algorithm indicated in Appendix G of FEMA P-58 [145]. This algorithm simulates hundreds of vectors of demands that preserve the original statistical correlation present in the underlying matrix of demands. For comparison, Figure 4-12a-c shows some results obtained from the augmentation of the matrices of results from 11 to 200 rows. This figure shows the vector of demands (AFSAs) for Nodes 2 and 9 for the three GMPEs selected. Additionally, 200 direct results (randomly selected from the databank of 600) obtained from performing time-history analysis using accelerograms simulated with the model proposed are shown in

Figure 4-12d. Certainly, when using the proposed model, no Monte Carlo simulations of the structural response are required to perform.

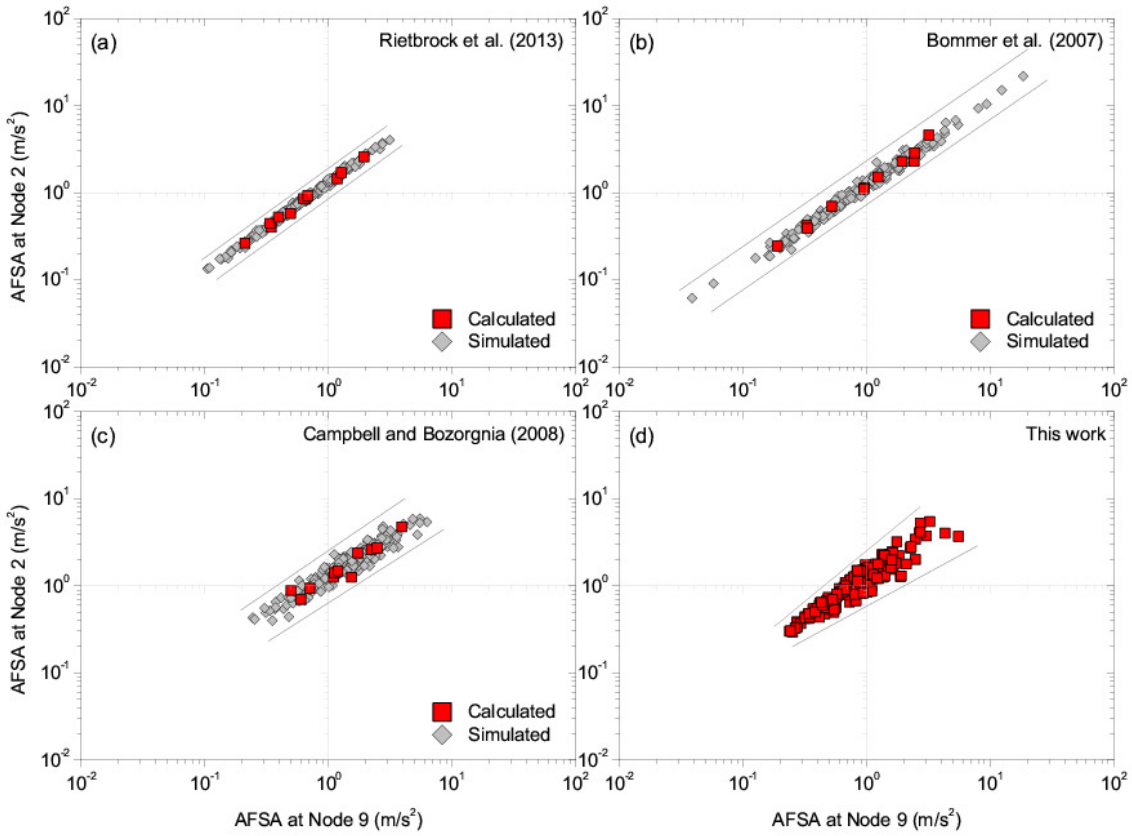

Figure 4-12. Comparison of AFSAs at Nodes 2 vs 9 for the three selected GMPEs and the proposed model

4.8 Risk assessment calculations

Figure 2-12 shows the flowchart that summarises the risk calculations. From this flowchart, it is possible to see that it requires three variables: (i) the number (k) of fragility curves (FC) for each component, (ii) the number (m) of row vectors (RV) in the demand-parameter matrix and, (iii) the number (n) of trials (T) required to estimate the statistical distribution of the probability of unacceptable performance. A sensitivity analysis was carried out in order to obtain the number for each variable that produces a numerically stable value for the probability of unacceptable performance. Table 4-5

summarises this sensitivity analysis. This table informs two benchmark values of the statistical distribution of the probability of unacceptable performance: the mean and median values of such distributions. However, the median value was arbitrarily selected as the final benchmark associated to each distribution.

Table 4-5. Sensitivity analysis for risk assessment calculations

Rietbrock et al. (2013)					Bommer et al. (2007)				
Fragility curves	Row vectors	Trials	Median	Mean	Fragility curves	Row vectors	Trials	Median	Mean
11	200	2000	0.150	0.158	11	200	2000	0.348	0.349
	1000		**0.153**	0.159		1000		0.349	0.350
	2000		0.151	0.159		2000		0.345	0.346
21	200	2000	0.145	0.159	21	200	2000	**0.350**	0.351
101			0.150	0.163	101			0.345	0.353
201			0.145	0.161	201			0.345	0.356
101	1000	2000	0.149	0.163	21	1000	2000	0.344	0.349
		3000	0.150	0.164			3000	0.348	0.353
		4000	0.149	0.163			4000	0.344	0.349
Campbell and Bozorgnia (2008)					This work				
Fragility curves	Row vectors	Trials	Median	Mean	Fragility curves	Row vectors	Trials	Median	Mean
11	200	2000	0.475	0.475	11	200	2000	0.210	0.225
	1000		0.478	0.474		300		0.210	0.224
	2000		0.477	0.476		400		0.210	0.221
21	200	2000	**0.485**	0.482	21	200	2000	0.210	0.229
101			0.475	0.483	101			**0.215**	0.233
201			0.470	0.483	201			0.215	0.235
21	1000	2000	0.475	0.478	101	200	2000	0.215	0.233
		3000	0.477	0.479			3000	0.215	0.232
		4000	0.472	0.475			4000	0.215	0.233

In Table 4-5, the number of FC, RV and T highlighted in yellow are the ones that produced the highest median value, whereas their associated median value has been highlighted in blue. Among the three values highlighted in blue for each GMPE and the model proposed, the highest was selected as the final benchmark (highlighted in bold) for the probability of unacceptable performance for each approach. The results of the sensitivity analysis are as follows: for Rietbrock et al. [29]: 101 FC, 1000 RV and 3000

T; for Bommer et al. [272]: 21 FC, 1000 RV and 3000 T; for Campbell and Bozorgnia [287]: 21 FC; 1000 RV and 3000 T; and for the model proposed in this work: 101 FC, 200 RV (i.e. 200 accelerograms) and 2000 T. Finally, the probabilities of unacceptable performance obtained are: 15.3%, 35,0% and 48.5% when using the GMPEs of Rietbrock et al. [29], Bommer et al. [272] and Campbell and Bozorgnia [287], respectively; whereas a value of 21.5% was obtained when using the model proposed. It is acknowledged that these results may be influenced by the definition of the HCLPF capacity explained in Section 4.6. However, the interest of this work is in the relative values rather than the values themselves. Figure 4-13 shows the corresponding cumulative distribution functions for each approach studied.

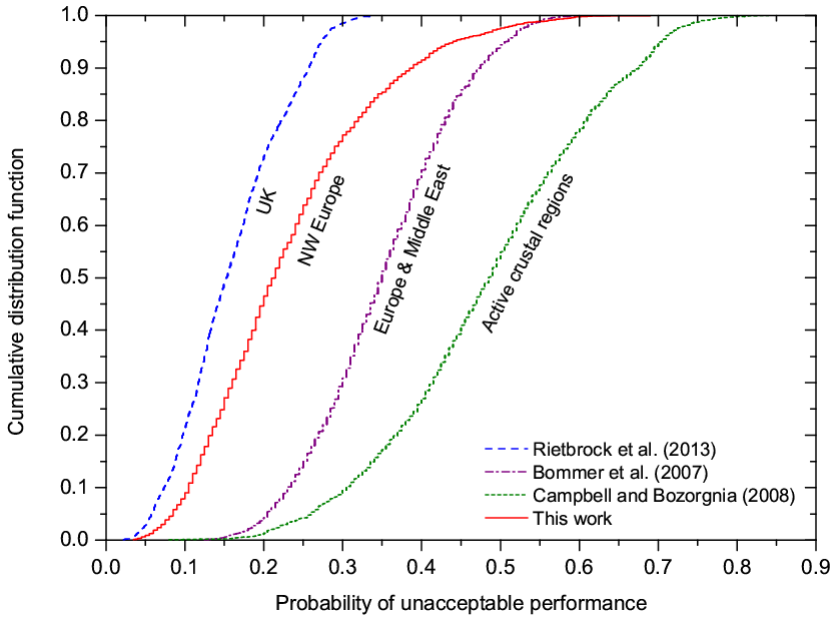

Figure 4-13. Statistical distributions of the probability of unacceptable performance of the sample NPP for the three GMPEs selected and the model proposed

4.9 Discussion

- *Conservatism of using active crustal models for the UK:* When assessing seismic risk of high critical structures in the UK, such as NPPs, it seems that there may be an unnecessarily excessive conservatism if models from active crustal regions are used.

These models have been customarily applied in seismic hazard analysis in the UK [32, 286]. This is mainly due to the naturally high epistemic uncertainty of ground motion models of any nature developed for the UK. Such uncertainty is intended to overcome by using data from areas with a wealth of available data. However, an upper limit imposed by ground motion models calibrated for the broader region of Europe and the Middle East seem to be a more reasonable alternative for hazard and risk assessments in the UK. It is acknowledged that NGA attenuation relations have been described to be suitable to be applied in the Euro-Mediterranean region as there is a generally good fit between both types of models [296-297]. However, as the results reported in Section 4.7 imply, it seems that the intrinsic nature of accelerograms in terms of their content of frequencies and intensities could have a different effect when estimating the damage state of critical components of NPPs. For future applications of nuclear facilities, it seems reasonable to discard the use of active crustal models available in the literature (mainly based on data from California and Taiwan) for estimating their seismic risk in the UK.

- *Comparison with a NPP in Eastern United States:* Huang et al. [144] reported a SPRA of a sample NPP of similar characteristics as the reactor building examined in this work located in Eastern United States, a zone classified as Stable Continental Region as well as NW Europe. The seismic scenario that controlled the hazard of the site selected was an earthquake magnitude M_w 5.3 at distance-to-site of 7.5 km, i.e. a scenario controlled by near-fault conditions. The reported probability of unacceptable performance of such sample NPP was 51%. This higher value can be explained by intrinsic characteristics present in near-fault accelerograms, such as forward directivity and permanent translation causing velocity pulses [298], that can have a significant influence on the content of frequencies and intensities of

accelerograms. These particular features of near-fault accelerograms will have a direct effect when assessing the damage state of critical components of NPPs. In any case, the seismic risk for sample NPPs reported for Eastern United States and the results obtained in this work for the UK, although different in absolute terms, they are of the same order of magnitude. As Huang et al. [144] also showed, the seismic risk for a conventional NPP can be drastically reduced, in the region of 5 orders of magnitude, by the use of seismic isolation devices. A similar outcome could be inferred for a nuclear facility in the UK. The use of seismic protection technology for a NPP in Britain aimed at reducing the seismic risk to values that could be considered negligible for a design event of 10,000 years return period is studied in Chapter 5 for potential future applications.

- *Comparison of assessment methods and outcome*: The seismic risk result obtained with the proposed methodology seems to be well constrained by the GMPEs selected for comparisons. Indeed, the UK model used [29] was calibrated using weak ground motion data from the UK. As it is not clear to what extent data from low magnitude earthquakes can be used to predict features of moderate-to-large earthquakes, the risk may be underestimated when using this model. On the other hand, the model for Europe and the Middle East used for comparisons [272] was calibrated using data from a broader region possessing a wider variety of tectonic regimes compared to data used to calibrate the model used in this work. Therefore, a higher value of risk was expected to obtain with such a model. Another aspect worth mentioning is regarding the artificial enlargement of observations of the damage state by simulation procedures. The Monte Carlo procedure used for this purpose uses a few seed observations to extrapolate them aimed at creating a statistically robust databank of observations. As this is a rather statistics-based treatment of data, it does not

necessarily consider how the nonlinear response of a given structure changes for stronger seismic demands. When using the proposed procedure this effect is included in nature. This effect might be even more important when a NPP is subjected to stronger earthquakes as the nature of accelerograms (intensity, frequency content and time duration) changes considerable for increasing magnitudes. Therefore, it could have a significant influence in the final assessment of risk. This assertion is by no means conclusive and it is therefore left as a matter of further research. Finally, one disadvantage of the proposed approach is that it is computationally more demanding than conventional approaches. The major task contributing to the use of computer resources is the execution of a large number of nonlinear time-history analyses of a structural model of the NPP analysed. However, the exceptionally high relevance of next generation NPPs will require conducting such comprehensive studies.

4.10 Conclusions

The work presented in this chapter has led to the following conclusions:

- The use of the stochastic model calibrated for NW Europe described in Chapter 3 seems to produce reasonable seismic risk results for nuclear applications in the British Isles. It can be inferred that the true value for the seismic risk of the sample NPP analysed here is somewhere in between: (a) the UK model of Rietbrock et al. [29], and (b) the European model of Bommer et al. [272] and/or similar models that have used the same target geographical region (such as the new generation of GMPEs calibrated for Europe [70]). In this light, the model described in Chapter 3 can be considered as a reasonable approach for use in risk assessments of nuclear facilities in the UK. The use of the model for active crustal regions of Campbell and Bozorgnia [287] is likely to produce excessively conservative results for UK seismic

conditions. The use of such a model and similar ones (e.g. the GMPES of the projects NGA [37] and NGA-West2 [38]) to assess the seismic risk of nuclear applications in the UK may not be adequate and may lead to unrealistic results.

- The proposed approach effectively simplifies the methodology for assessing seismic risk which is more rational and more direct to generate sets of accelerograms compatible with the controlling scenario of the seismic hazard at the site. Although not analysed in this article, the stochastic model described in Chapter 3 could also be applied in the framework of probabilistic seismic hazard analysis for NW European sites. The use of such model in the simulation approach of PSHA would also allow the replacement of GMPEs when specifying the seismic hazard of the site selected [36].

- The pattern of the nonlinear structural response obtained with the proposed approach differs in shape compared with those from the conventional procedure performed. When using Monte Carlo procedures to simulate and enlarge the damage state of the NPP, the observations of the structural response seem to be enclosed by parallel lines. On the other hand, when using the proposed approach, the observations of the structural response seem to follow a rather divergent pattern, i.e. the stronger the seismic demand, the greater the incursion in the inelastic structural response; hence, greater scattering of observations. This behaviour seems reasonable from a structural engineering point of view and it can be intuitively expected.

Chapter 5

Seismic risk control: reducing risk using seismic protection technology

5.1 Introduction

As discussed in Section 1.1.3, applications of seismic protection technology in the nuclear industry are scarce: Koeberg NPP in South Africa, with two isolated unit plants, and Cruas NPP in France, with four isolated unit plants. In the UK, the benefits of using seismic protection systems were early recognised as a strategy to increase margins of safety of NPPs. In early 1990s, laboratory tests were carried out on small-scale specimens of low-damping rubber bearings and viscous dampers for applications in Liquid-Metal-Cooled Reactors (LMRs). However, no further analyses were reported and no real applications of seismically protected NPPs were built in the UK. Nowadays, the scenario has significantly changed as several new projects of isolated reactors in medium-to-low seismic areas are currently under way (see Section 2.4.1.3 for a

complete description). All these applications of reactors seismically isolated consider the use of different types of elastomeric-based bearings: JHR and ITER share the same design of devices based on low-damping rubber bearings [299], APR1400 uses lead-rubber bearings [16], and ASTRID and ALFRED will use lead-rubber bearings and/or high-damping rubber bearings [300-301]. Additionally, other approaches to seismically protect reactor buildings without isolating the entire nuclear island have been investigated: e.g. the long-serving Russian *Voda-Vodyanoi Energetichesky Reaktor*, VVER-1000, a 1000 MW Pressurised Water Reactor, has been the subject of studies that propose the use of high performance viscous dampers to protect its critical components in future applications [302]. Following the experience reported elsewhere of seismically protected reactor buildings in zones of medium-to-low seismicity, this chapter analyses the suitability of several SPS that can be used in next generation UK reactors subjected to the seismic conditions of the British Isles.

In this chapter, the sample NPP reactor building described in Section 4.3 equipped with three different types of SPS was analysed: (i) a seismically isolated nuclear island using low-damping rubber bearings plus viscous dampers; (ii) a seismically isolated nuclear island using lead-rubber bearings and/or high-damping rubber bearings, and (iii) a non-seismically isolated nuclear island using only viscous dampers located at the critical components of the NPP. The efficiency of these SPS was assessed to achieve possible risk reduction for both rock and soil sites in comparison with a conventional NPP. The risk was calculated following the methodology for SPRA described in Chapter 4. Using the same hypothetical UK nuclear site described in Section 4.4, the risk was initially assessed for the single scenario that contributes most strongly to the hazard of such a site. However, as the uncertainty in determining the controlling seismic scenario for UK sites is relatively high, the variation of risk is studied for different scenarios, following a

proposed scenario-based incremental dynamic analysis (IDA). Scenario-based IDA, as introduced in this PhD thesis, aims at the generation of surfaces for the unacceptable performance of NPPs in the UK as a function of earthquake magnitude (M_w) and distance-to-site (R_{epi}). Unacceptable performance surfaces can be a substantial contribution to the UK nuclear industry in order to provide insights as how the seismic risk varies when the NPP is subjected to most (or all) dominant scenarios of the selected nuclear site.

5.2 Description of methodology

This chapter has two specific objectives, namely, (a) to determine the most efficient approach of SPS to reduce the seismic risk of NPPs buildings subjected to the UK seismic conditions including the influence of the foundation soil; and (b) once the most effective SPS has been determined, to investigate how the reduction in seismic risk of NPPs buildings changes when considering several or all dominant scenarios for the particular site selected.

All analyses carried out in this work were made considering the structural model based on the 1000 MW Pressurised Water Reactor building described in Section 4.3. Such a structural model was used to define two types of models: (1) a conventional NPP and (2) a seismically protected NPP. The former is intended to model the base case, i.e. a traditionally built fixed-to-the-ground NPP (Model 1 hereafter), whereas the latter comprises three models that use different types of seismic protection devices suitable for NPPs. For the seismically protected NPP, the following devices were analysed: (a) low-damping rubber bearings (LDRB) in combination with linear viscous dampers (LVD) aimed at adding a 10% critical (viscous) damping, referred to as Model 2a hereafter; (b) lead-rubber bearings (LRB) aimed at adding a 20% critical (hysteretic)

damping, referred to as Model 2b hereafter; and finally, (c) linear viscous dampers located at the critical components of the NPP, aimed at adding a 30% critical (viscous) damping, referred to as Model 2c hereafter. Then, for the hypothetical UK nuclear site described in Section 4.4, two types of foundation soil were defined: (i) generic rock site and (ii) generic soil site. The efficiency in reducing the seismic risk of Models 2a, 2b and 2c relative to Model 1 was made using the methodology for SPRA described in Chapter 4. In order to give answer to the first objective of this chapter, the risk was assessed considering the single scenario (moment magnitude, epicentral distance) that contributes most strongly to the hazard of the site selected. Figure 5-1 summarises the tasks performed to comply with Objective (a) of this chapter.

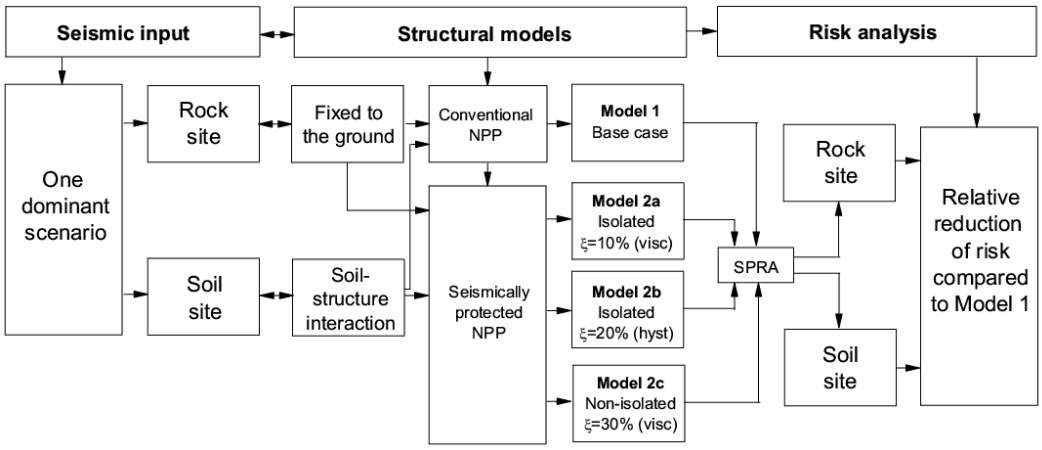

Figure 5-1. Relationships among the tasks performed to comply with Objective (a)

Regarding Objective (b), once the most effective SPS has been determined, the change in seismic risk of the NPP building are assessed considering all dominant scenarios of the particular site selected. For this purposes, it is introduced in this chapter a scenario-based incremental dynamic analysis (IDA) intended to generate surfaces for the probability of unacceptable performance of NPPs as a function of earthquake magnitude and distance-to-site. Such surfaces were generated for two models, conventional NPP and seismically protected NPP, in generic rock site. Then, the relative performance

between those surfaces was studied in order to gain in-depth knowledge about the behaviour for the reduction of risk for all dominant scenarios of the particular site selected. Figure 5-2 summarises the tasks performed to comply with Objective (b) of this chapter.

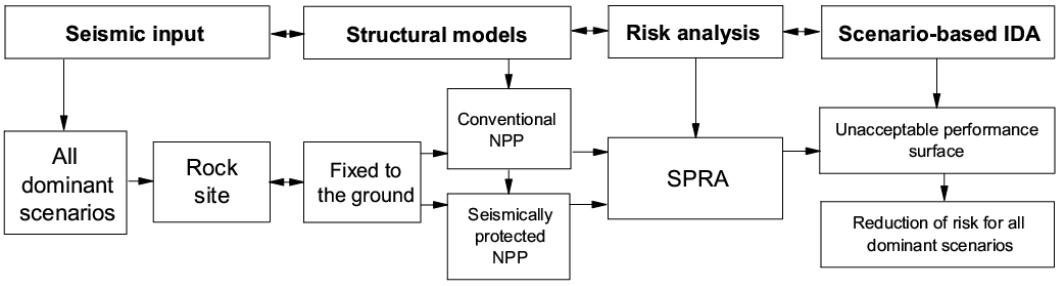

Figure 5-2. Relationships among tasks performed to comply with Objective (b)

5.3 Structural models

5.3.1 Definition and properties of structural models

The properties and particular characteristics of Models 1, 2a, 2b and 2c mentioned in Section 5.2 are defined in detail in this section. It is worth mentioning that Models 2a and 2b are intended to provide seismic isolation to the entire nuclear island, i.e. the CS and IS are supported by a common mat which in turn is separated from the foundation mat by the interface of isolation where the devices are located. Figure 5-3 shows a schematic view of a seismically isolated nuclear island. Certainly, due to the nature of the simplified structural model of the sample NPP used in this work, the seismic isolators modelled for Models 2a and 2b is an assembly of isolators, i.e. the entire isolation system, rather than all individual isolators.

The particular features of each structural model used in this work are summarised in Table 5-1 and described in detail as follows:

- Model 1 is intended to represent the base case, i.e. the NPP building that uses conventional construction without any kind of seismic protection device.

- In model 2a, the LDRB system was modelled as a horizontal linear spring as these devices exhibit a visible linear behaviour in shear with little addition of supplemental damping [303]. The stiffness of the spring was selected in order to obtain a structural period of $\mathbf{T_{obj} = 2\ s}$. Additional external damping was included at the foundation level by considering $\boldsymbol{\xi = 10\%}$ by means of a linear viscous damper. Figure 5-4 shows the general behaviour of LVD: the force-velocity governing equation is linear and the force-deformation hysteresis curve has oval shape.

- In model 2b, the LRB system was modelled using a bilinear constitutive relationship as shown in Figure 5-3. Its properties were calibrated to obtain a structural period of $\mathbf{T_{obj} = 2\ s}$ and to provide supplemental hysteretic damping of $\boldsymbol{\xi = 20\%}$, both features calculated at the maximum displacement design level ($\mathbf{u_d = 25\ cm}$). As models 2a and 2b are seismically isolated, it is appropriate to consider for the internal damping in the structure a lower value than the 5% normally used in seismic analysis of structures. This is due to the fact that in base isolated structures the seismic demand is significantly reduced to such a level that the structure can remain in its linear range experiencing little or no damage. Thus, no energy dissipation through non-structural damage can be expected in these models. Therefore, the internal structural damping in was modelled considering $\xi = 2\%$ for these models as recommended in Chopra [304].

- Model 2c is intended to analyse the effect of using LVD to seismically protect each critical component of the sample NPP without the need of isolating the entire nuclear island. Therefore, five viscous dampers were included in the sample NPP as shown in Figure 5-4. It is acknowledged that such a configuration of dampers may not be possible to materialise in an actual application. Nevertheless, it is considered to be a first

approximation on the use of dampers to protect critical components. The damping constants for each device were calculated using $C_i = 2 \cdot \xi \cdot m_i \cdot \omega_1$, where m_i ($i = 2,9,10,11,12$) is the mass of each node of the IS, ω_1 is the fundamental frequency of vibration of the IS, and ξ is the critical damping ratio of the devices. In this work, a value of $\boldsymbol{\xi = 30\%}$ was used for all devices. As this model does not consider seismic isolation, the internal damping in the structure was modelled considering the traditional $\boldsymbol{\xi = 5\%}$.

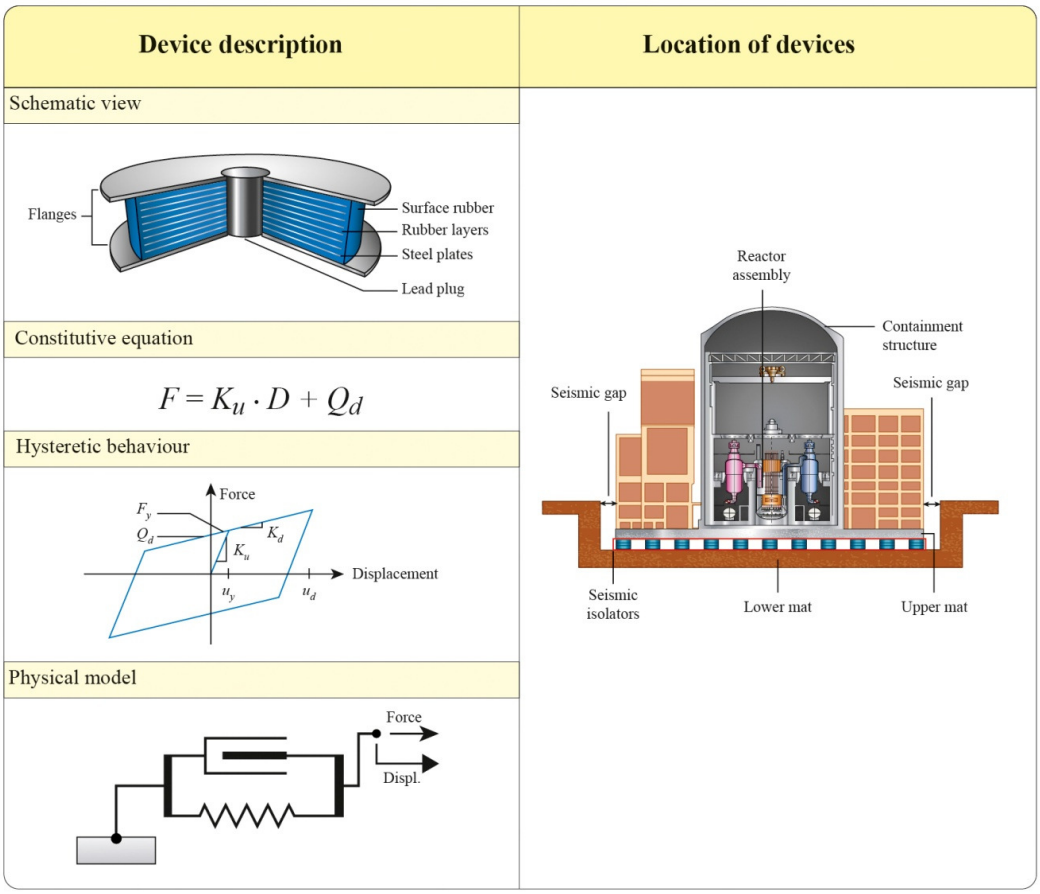

Figure 5-3. Device description and location of devices for Model 2b

Table 5-1. Design features of the structural models used in this work

Model	Seismic Protection System	Description
1	None	Conventional NPP
2a	Low-damping rubber bearings **(LDRB)** + linear viscous dampers **(LVD)**	T_{obj} = **2 s.** $\boldsymbol{\xi}$ **= 10% (viscous)**
2b	Lead-rubber bearings **(LRB)**	T_{obj} = **2 s.** $\boldsymbol{\xi}$ **= 20% (hysteretic)** u_y = 2.5cm; u_d = 25cm; Q_d/W = 0.02
2c	Linear viscous dampers **(LVD)**	T_{obj} = 0.18 s. $\boldsymbol{\xi}$ **= 30% (viscous)** p/device

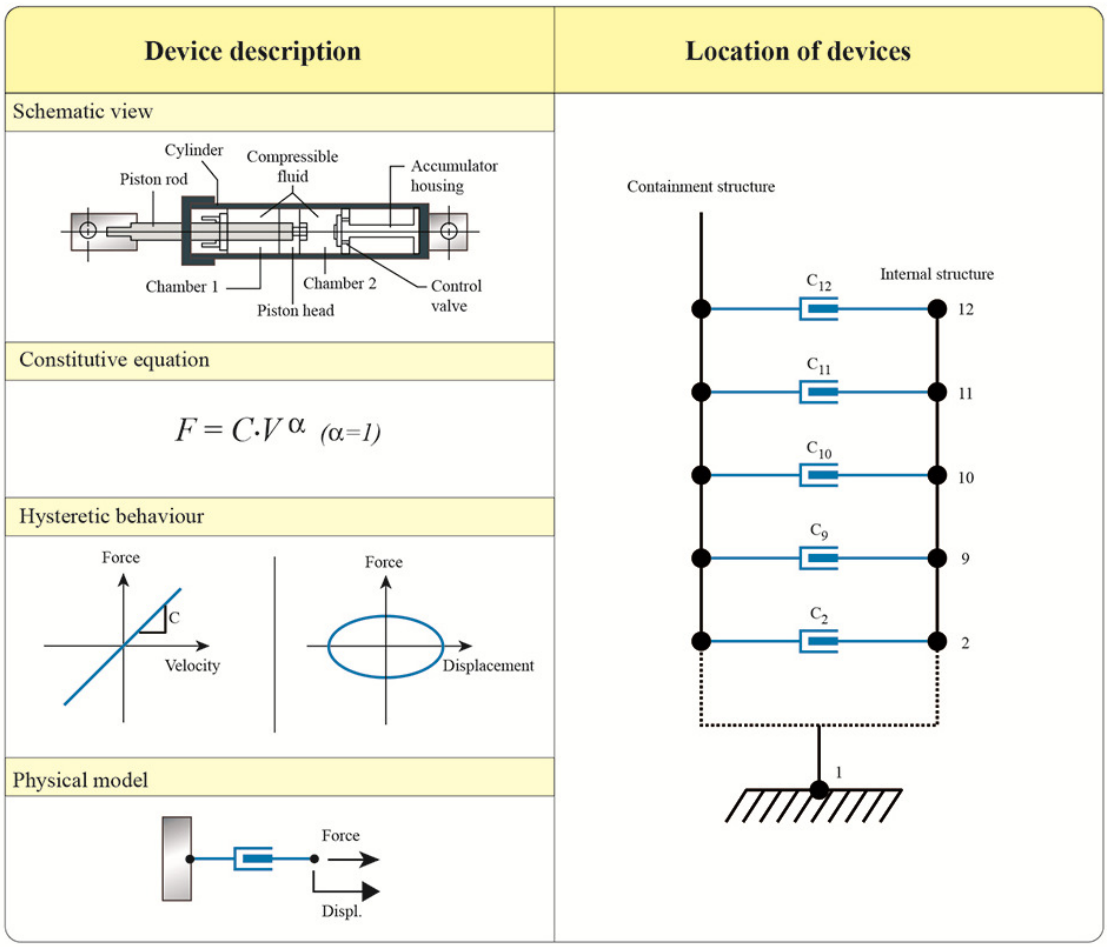

Figure 5-4. Device description and location of devices for Model 2c

5.3.2 Fragility analysis

The estimation of fragility curves for the critical components of the sample NPP used in this work is addressed in detail in Section 4.6. It is worth highlighting that in all risk analyses performed in this chapter, families of 101 fragility curves for each component were used as a result of the sensitivity analysis described in Section 4.8.

5.3.3 Soil-structure interaction

The influence of the type of foundation soil on the seismic behaviour of models 1, 2a, 2b and 2c was studied by analysing their response on both a generic rock and a generic soil site. These sites were characterised by their corresponding shear-wave velocity of the top 30m of the subsurface profile (V_{S30}). The rock site was considered to possess

V_{S30} > 760 m/s, whereas for the soil site, it was considered to possess V_{S30} in the region of 360 m/s which is associated to a soft-to-medium soil profile. These definitions are in line with those made to analyse the influence of the type of soil on the seismic behaviour of other reactor buildings, e.g. the AP1000 nuclear reactor building [305].

For the structural models in the rock site, a fixed base connection to the ground was considered. For the soil site, it is acknowledged that there are currently available thorough soil-structure interaction (SSI) analyses for nuclear reactors [306-309]. However, such approaches are out of the scope of this work as this work is intended to provide a first approximation on the behaviour of NPPs in soil sites in the UK. Therefore, a simple approach to model SSI in the time domain was followed. Despite several methodologies available to model SSI in the time domain [310], a straightforward discrete approach based on soil impedances was implemented in this work. In such a methodology, the interface soil-structure is modelled by soil impedances defined by six frequency-independent elastic springs and dampers associated to the six rigid body degrees of freedom. Such springs and dampers model the dynamic stiffness of the soil located both underneath and adjoining the embedded portion of the building. In nuclear engineering research, such an approach has been used previously [311-312]. In this work, the soil impedances proposed by Llambias et al. [313] and validated in Llambias [314] were directly used as they were proposed for PWR buildings in UK soil sites. Figure 5-5 shows the generic case for modelling SSI using soil impedances and Table 5-2 shows the values for such impedances proposed by Llambias et al. [313].

When modelling SSI as indicated in Figure 5-5 and Table 5-2, the fundamental periods of vibration of the sample NPP changed to 0.33s for the CS and 0.27s for the IS. This

increase in the fundamental periods of vibration of the CS and IS of about 30% in comparison with the fixed base case is in line with the increase obtained for other nuclear reactor buildings and nuclear structures when modelling SSI [308, 312].

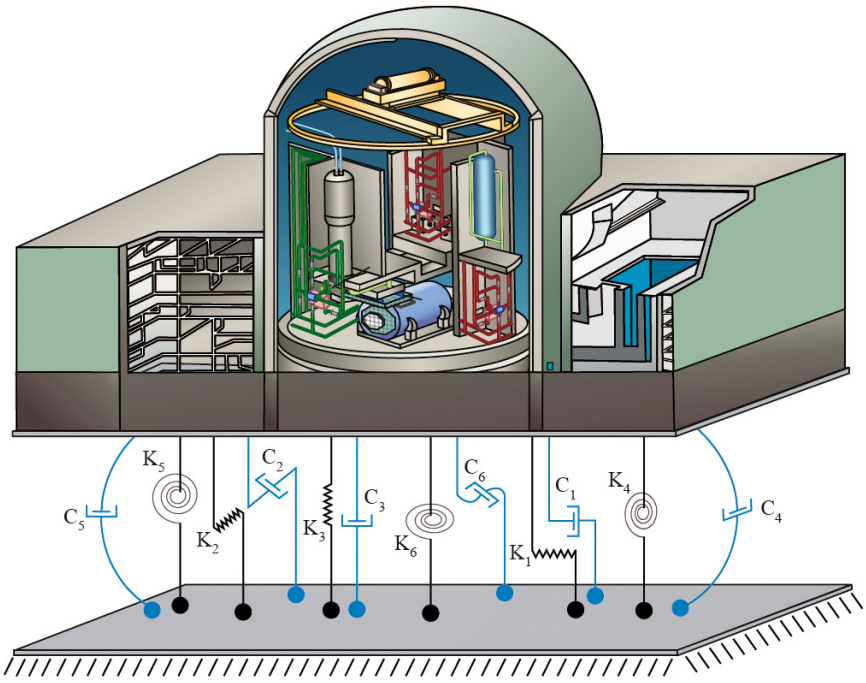

Figure 5-5. Generic case for modelling SSI by means of soil impedances

Table 5-2. Soil impedances proposed by Llambias et al. [313].

Direction	Value
Stiffness terms	
Translational (K_1, K_2) (N/m)	3.87E+10
Vertical (K_3) (N/m)	9.27E+10
Rotational (K_4, K_5) (Nm/rad)	2.64E+13
Torsional (K_6) (Nm/rad)	1.78E+13
Damping terms	
Translational (C_1, C_2) (Ns/m)	1.02E+09
Vertical (C_3) (Ns/m)	3.39E+09
Rotational (C_4, C_5) (Nms/rad)	2.95E+11
Torsional (C_6) (Nms/rad)	1.25E+11

5.4 Input definition

Accelerograms compatible with the controlling seismic scenario of the nuclear site selected (Section 4.4) were simulated using the stochastic model described in Chapter 3. Also, in Section 4.8, it was reported that a suite of 200 accelerograms were sufficient to

estimate the probability of unacceptable performance of NPPs with high statistical confidence. Following this result, two sets of 200 accelerograms each were simulated for both rock and soil sites. For illustration purposes, Figure 5-6 shows a graphical summary of the two bins of 200 accelerograms each for the rock and soil sites that are compatible with the seismic scenario of interest. Figure 5-6a shows a small sample of three simulated accelerograms from each bin. Figure 5-6b shows the 5% damped spectral acceleration of 50 simulated accelerograms from each bin. Figure 5-6c shows the median, 84th and 16th percentiles of the 200 simulated accelerograms from each bin. These statistics are compared with those estimated using two GMPEs that have been deemed to be suitable for use in the UK: Bommer at el. [272] and Campbell and Bozorgnia [287], as earlier explained in Section 4.5.1.

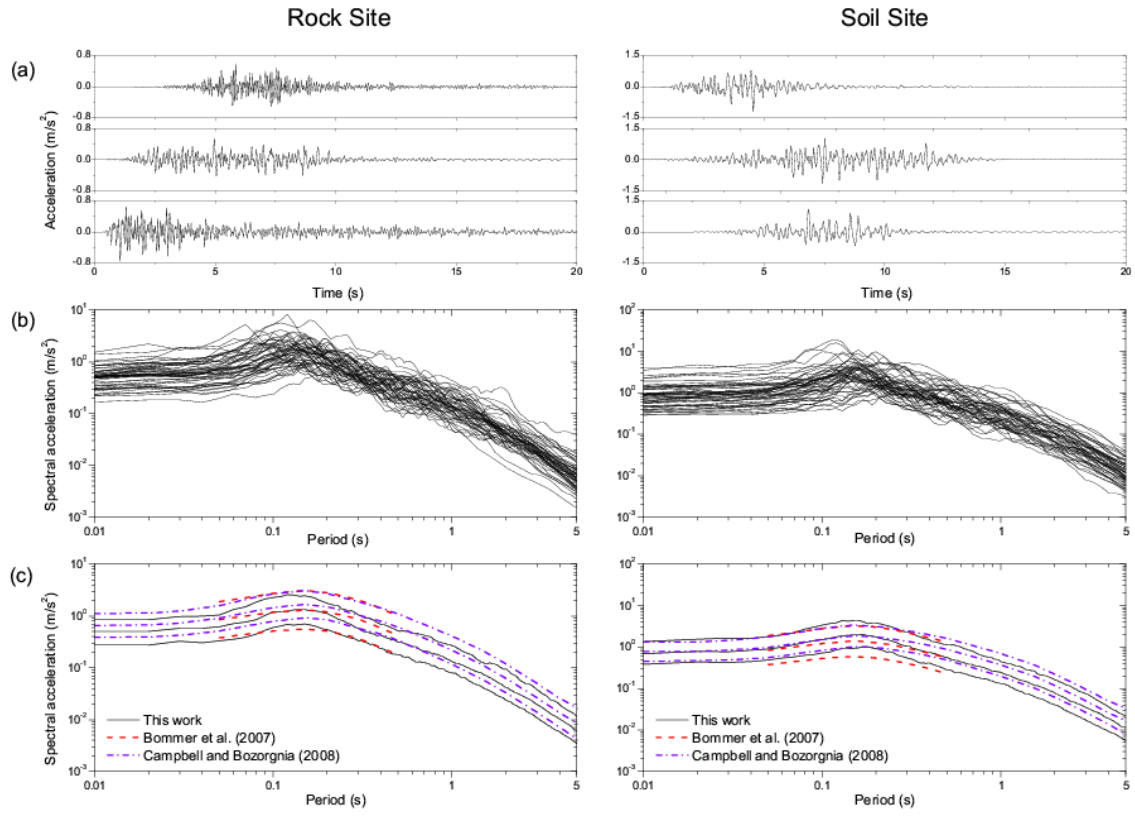

Figure 5-6. Summary of the accelerogram definition compatible with the scenario of interest in rock and soil sites: (a) sample of three simulations; (b) 5% damped spectral acceleration of 50 sample simulations; (c) median, 84th and 16th percentiles of the 200 simulations compared with two GMPEs suitable for UK use.

5.5 Risk assessment calculations

Following the results from the sensitivity analysis reported in Section 4.8, nonlinear time history analysis were conducted for Models 1, 2a, 2b and 2c using the two bins of accelerograms defined in Section 4 for both the rock and soil sites. For illustration purposes, an example of the damage state for all models as scatter plots of AFSAs in Nodes 2 and 9 is shown in Figure 5-7 for the rock site and in Figure 5-8 for the soil site. In these figures, the more dots are located in the top-right quadrant, the higher is the seismic demand, and therefore, the higher is the nonlinear behaviour of the structural model. On the other hand, the more dots are located in the bottom-left quadrant, the lower is the seismic demand, and therefore, only linear behaviour can be expected of the structural model. From Figure 5-7 and Figure 5-8, it is possible to visually recognise that in Models 2a and 2b the seismic demand has been significantly reduced whereas in Model 2c the reduction is less effective when compared with Model 1.

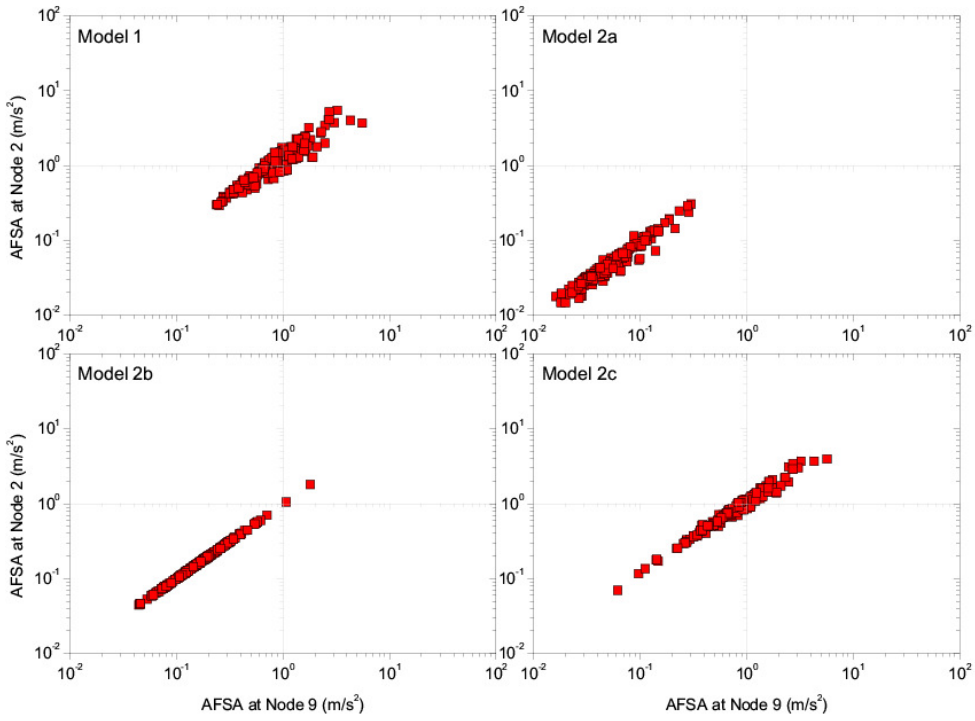

Figure 5-7. Scatter plots of AFSAs at Nodes 2 and 9 for all models in the rock site

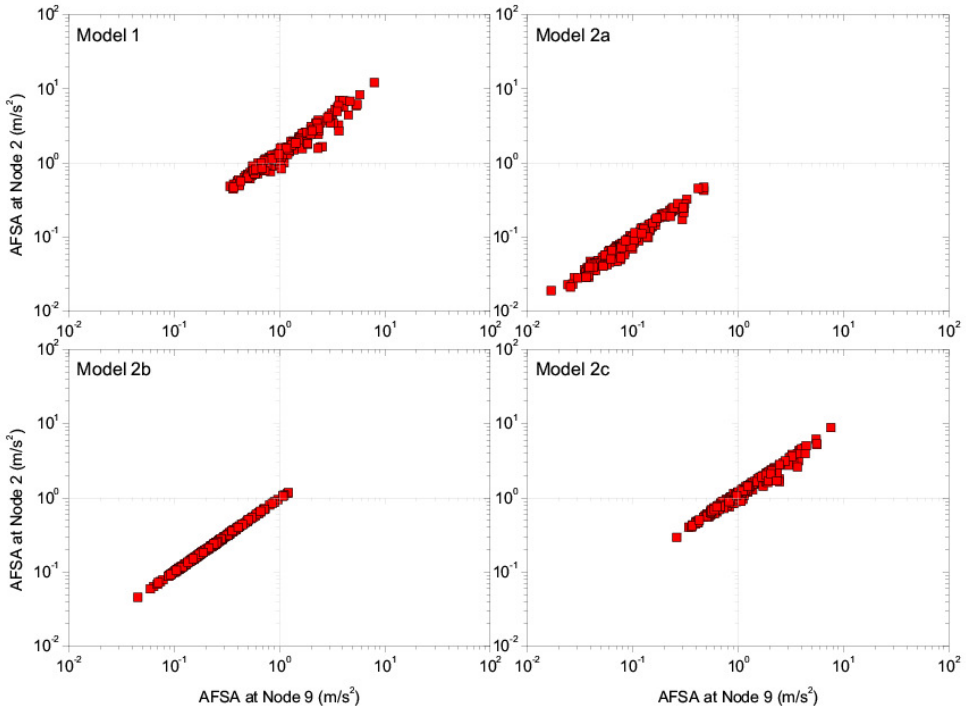

Figure 5-8. Scatter plots of AFSAs at Nodes 2 and 9 for all models in the soil site

Once the damage state for the four models has been calculated, the seismic risk was assessed following the overall procedure described in Section 4. The final cumulative distribution functions for the probability of unacceptable performance for all models are shown in Figure 5-9a for the rock site and Figure 5-9b for the soil site. The mean value for each distribution was taken as the benchmark value for the seismic risk for each model; these final values are indicated in Table 5-3. It is worth mentioning that for Model 2a, it was not possible to obtain a robust estimation of the probability of unacceptable performance. This is due to the fact that the seismic demand was considerably reduced: the probability of unacceptable performance obtained was zero when using 200 observations of the damage state. This does not mean that the probability of unacceptable performance is zero as the seismic demand, although notably low, is greater than zero. This means that the probability of unacceptable performance is an extremely small number that needs a much greater number of observations of the damage state and trials to be captured by the methodology used. In

order to find a first approximation for the probability of unacceptable performance of Model 2a, the number of accelerograms was enlarged to 400, the number of fragility curves was increased to 201 and the number of trials was augmented to 6000, in order to obtain a value for the probability of unacceptable performance greater than zero. The values shown in Figure 5-9 and Table 5-3 associated to Model 2a are only intended to give a rough approximation for the probability of unacceptable performance as different approaches need to be used to make a statistically robust estimation. However, for structural engineering purposes, the values reported for Model 2a are sufficient to establish a remarkable reduction of risk when compared with the base case.

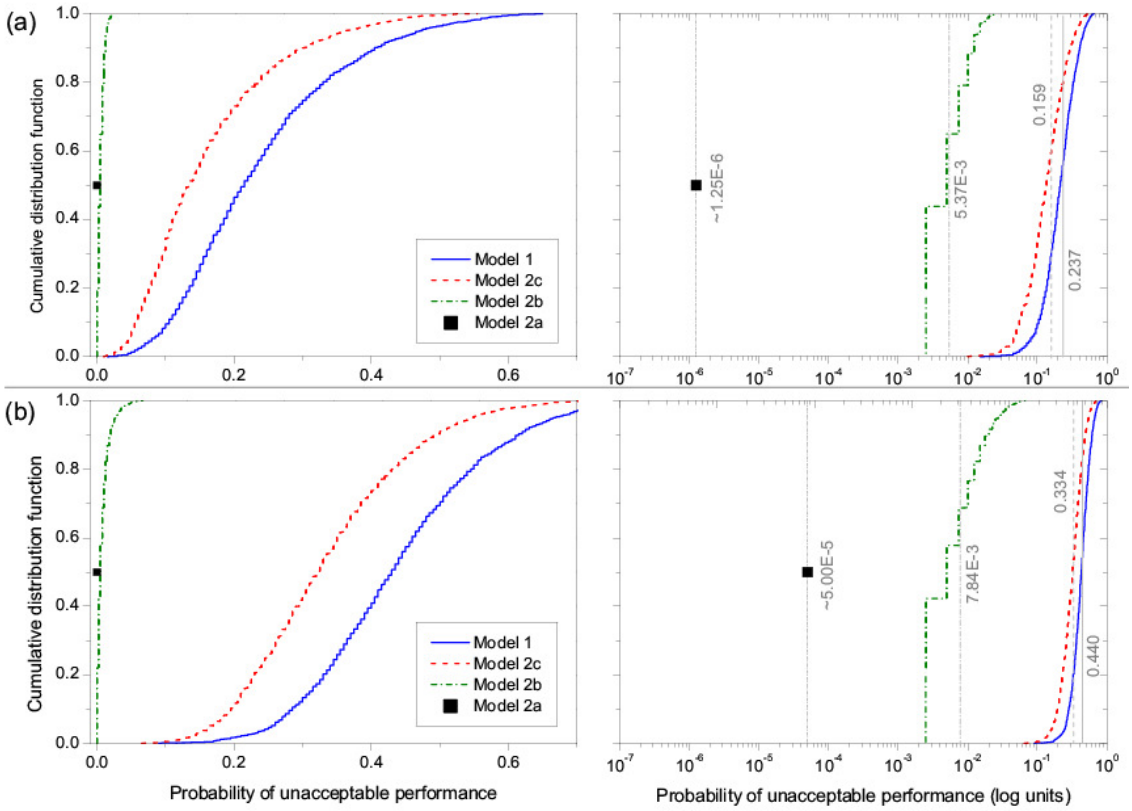

Figure 5-9. Final cumulative distribution functions for the probability of unacceptable performance for all models: (a) rock site; (b) soil site.

Table 5-3. Summary of the seismic risk and reduction achieved for each model

Model	Rock Site		Soil Site	
	Risk	Reduction	Risk	Reduction
1	0.237	-	0.440	-
2a	~1.25E-6	~ 5 orders of magnitude	~5.00E-5	~ 4 orders of magnitude
2b	5.37E-3	~ 2 orders of magnitude	7.84E-3	~ 2 orders of magnitude
2c	0.159	32.9%	0.334	24.1%

From Figure 5-9 and Table 5-3, it is possible to see that Model 2a achieves the largest reduction of seismic risk: the use of low-damping rubber bearings plus viscous dampers that introduce a critical damping of ξ=10% to the sample NPP can reduce the risk of about 4~5 orders of magnitude depending on the type of soil. Model 2b also achieves an important reduction: the use of lead-rubber bearings that introduce a critical damping of ξ=20% can achieve a reduction of about 2 orders of magnitude. In this sense, viscous damping seems to maximise the reduction of risk in comparison with hysteretic damping for UK seismic conditions. Model 2c achieves the least effective reduction: the introduction of linear viscous dampers that introduce ξ=30% to protect the critical components of the sample NPP without seismically isolating it, reduces the risk ranging from 24.1% to 32.9% for soil and rock sites, respectively. From Table 5-3, it is also possible to realise that all strategies of seismic protection systems considered in this work were effective in reducing the risk for UK seismic conditions; however, the efficiency is always greater in rock sites than soil sites.

5.6 Scenario-based IDA and unacceptable performance surfaces

In previous sections of this PhD thesis, all seismic risk assessments were made considering the single scenario that contributed most strongly to the hazard of the site selected, in this case, an earthquake M_w5.3 located at R_{hyp}=15 km. This scenario was obtained as a result of the deaggregation of the seismic hazard curve of the site selected. Nevertheless, the determination of the controlling seismic scenario depends on the

spatial seismicity modelling and ground motion modelling when the seismic hazard assessment of the site is conducted. Goda et al. [32] reported that for the UK, "dominant scenario events identified based on different smoothing approaches vary significantly, which may have important implications for advanced earthquake engineering applications (e.g., response spectral shape and record selection for nonlinear dynamic analysis)". For the particular case of the hypothetical nuclear site selected in this work, Goda et al. [32] showed that controlling scenarios for a structural period of 0.2s may fall into scenarios that approximately comprises magnitudes $4.5 < M_w < 6.5$ and distances $10 < R_{hyp} < 60$ km depending on the spatial seismicity model and the attenuation models used. The modelling of these two effects plays a role particularly important in low-seismicity regions due to a large uncertainty about seismological and tectonic knowledge present in these regions [315]. It is therefore desired to know how the seismic risk of the sample NPP used in this work changes when different controlling scenarios are taken into account. To assess such an effect, it is proposed to use a scenario-based incremental dynamic analysis (IDA) that is a straightforward approach based on the conventional IDA.

5.6.1 Description of scenario-based IDA and definition of bins

Conventional IDA [316-317] is a powerful tool in structural and earthquake engineering used to estimate the dynamic behaviour of a structure that is forced to cover the complete range of structural response, from elastic behaviour to global dynamic instability. IDA establishes a relationship between an intensity measure (IM, e.g. PGA, PGV, 5% damped spectral acceleration at the structure's first-mode period, etc) of a multiply scaled suite of accelerograms and a damage measure (DM) of the structure, i.e. any observable structural output due to a given IM (e.g. peak roof drift, maximum peak inter-storey drift angle, etc.). Although IDA has been widely used in research [318-320],

its main limitation has been regarded as the legitimacy of the rather simple approach to monotonically scale accelerograms to several IMs [321-322]. Careful selection of the seed accelerograms is needed to appropriately represent the changing characteristics of recordings (intensity distribution, frequency content and time duration) for progressively increasing IMs selected. Extensive literature is currently available aimed at the efficient selection of records in order to reduce the bias in the structural response [323]. This has led basis for several variations of IDA, e.g. Progressive IDA [324] that is aimed at the optimal selection of accelerograms reducing the number of recordings needed in comparison with conventional IDA; and Adaptive IDA [325] that adaptively changes the suites of accelerograms at different IM levels to better reflect the variation of accelerograms' properties as to be in agreement with the site's hazard analysis. In this PhD project, it is proposed to use a Scenario-based IDA for risk assessments purposes of NPPs. In this sense, the main difference of philosophies between traditional IDAs and the proposed methodology is that the latter does not seek to estimate the IM that would produce global dynamic instability of the structure; rather, it intends to estimate the IM that would produce a 100% of probability of unacceptable performance which in turn can be defined according to particular performance requirements of the NPP analysed. Certainly, as the seismic performance required for NPPs is more stringent than for conventional civil structures, it is expected that for the IM that produces 100% probability of unacceptable performance, global dynamic instability is still far from being reached.

The proposed procedure is explained by means of an example of application. This example aims at the estimation of the relative reduction of risk between a conventional NPP and its seismically isolated version for different seismic scenarios. As shown in Section 5.5, the use of LDRB in combination with LVD gave the most effective

reduction of risk for the particular scenario analysed. Also, Table 4 demonstrated that for UK conditions, seismic protection systems were more effective in rock compared to soil conditions. Therefore, Models 1 and 2a in rock conditions were used in the subsequent example. The following steps were taken to conduct scenario-based IDA:

(a) Definition of IM: Unlike conventional-type IDAs that normally use only one IM, scenario-based IDA uses two IMs: earthquake magnitude (M_w) and distance-to-site (R_{epi}). In this light, the final product of scenario-based IDA is a surface rather than a curve. For the particular sample NPP used in this work, R_{epi} was increased from 10 km to 60 km in increments of 10 km. Then, for each R_{epi}, the earthquake magnitude M_w was increased from 4.5 to 6.5 in increments of 0.2. Then, for each scenario defined by the pair (M_w, R_{epi}), bins of accelerograms were simulated using the stochastic accelerogram model described in Chapter 3, making a total of 66 bins of 400 accelerograms each, i.e. 26,400 simulated accelerograms (it is worth mentioning that 200 accelerograms of each bin were used for Model 1 whereas the 400 recordings of each bin were used for Model 2a, following the results reported in Section 5). In this sense, instead of progressively scale accelerograms as is done in traditional IDA methodologies, in the proposed methodology an epicentral distance is fixed and the earthquake magnitude is progressively increased to then stochastically simulate accelerograms compatible with that given scenario. This definition of seismic inputs explicitly guarantees that accelerograms' properties are preserved when the IMs are increased requiring no scaling, selection and matching techniques. A small sample of 6 bins of the simulated accelerograms is shown in Figure 5-10. In this figure, two accelerograms plus the 5%-damped spectral acceleration of 50 simulations are shown for the bins of magnitudes M_w 4.5, 5.5 and 6.5 for the epicentral distances R_{epi} 10, 30 and 60 km.

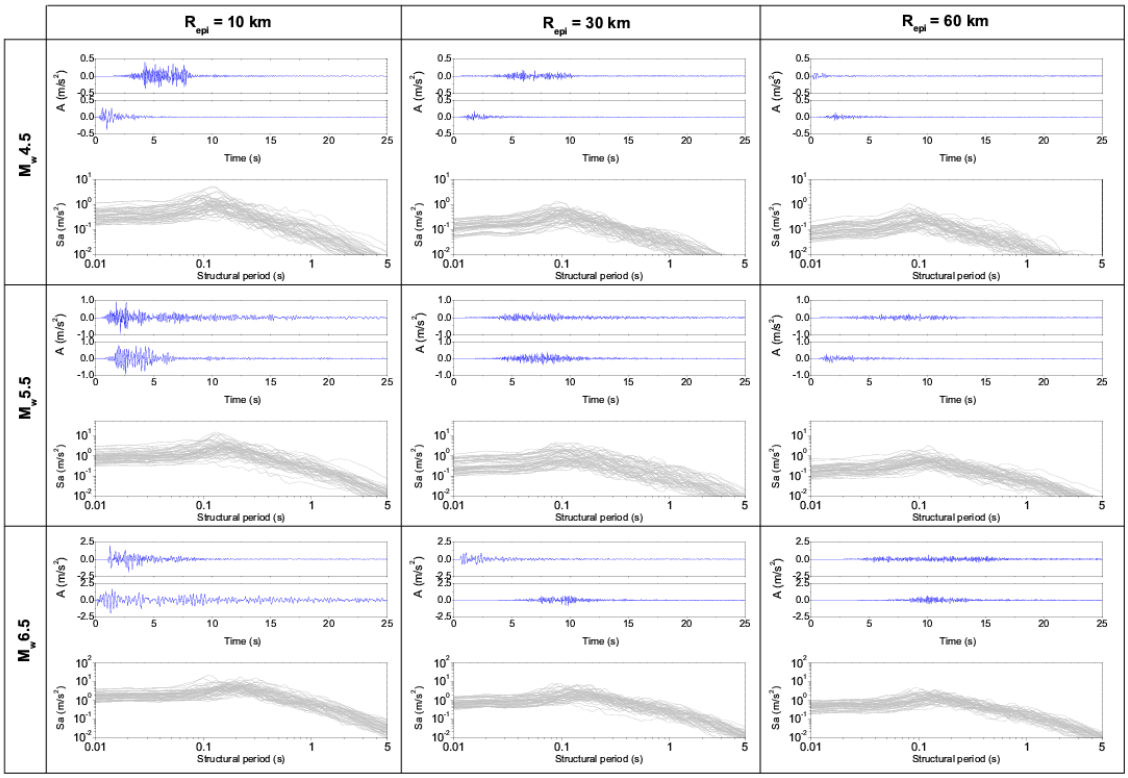

Figure 5-10. Sample of bins of simulated accelerograms: two simulations plus 5%-damped response spectra for 50 simulations for the bins of magnitudes M_w 4.5, 5.5 and 6.5 for the epicentral distances R_{epi} 10, 30 and 60 km.

(b) Definition of DM: As the analysis proposed is intended to use for risk assessments, the DM used in this work was the mean probability of unacceptable performance of the sample NPP as defined in Section . Nevertheless, it is worth mentioning that the underlying measure for the seismic demand used to define the probability of unacceptable performance was the AFSA over a frequency range of 1 to 33 Hz for calculated in all critical components.

(c) Assessment of risk: Once the IM and DM are defined, nonlinear time-history analyses were performed using Models 1 and 2a and the risk was assessed following the overall methodology described in Section 4. For simplicity, the mean value was taken as the benchmark value for the probability of unacceptable performance for both models.

(g) Generation of unacceptable performance surfaces: After the risk is assessed, the post-processing of the results basically involves the generation of surfaces of the unacceptable performance as a function of M_w and R_{epi}. In this example, interpolation of discrete points was made (i) for the earthquake magnitude in units of 0.1 and (ii) for the epicentral distance in units of 5 km; hence, the matrix of results (magnitude, distance) is of size 21 x 11. For Model 1, the colour map surface for the mean for the probability of unacceptable performance is shown in Figure 5-11. From this figure, it is possible to see that the surface has a nonlinear behaviour reaching a maximum of 88.9% for the scenario M_w6.5, R_{epi}10 km.

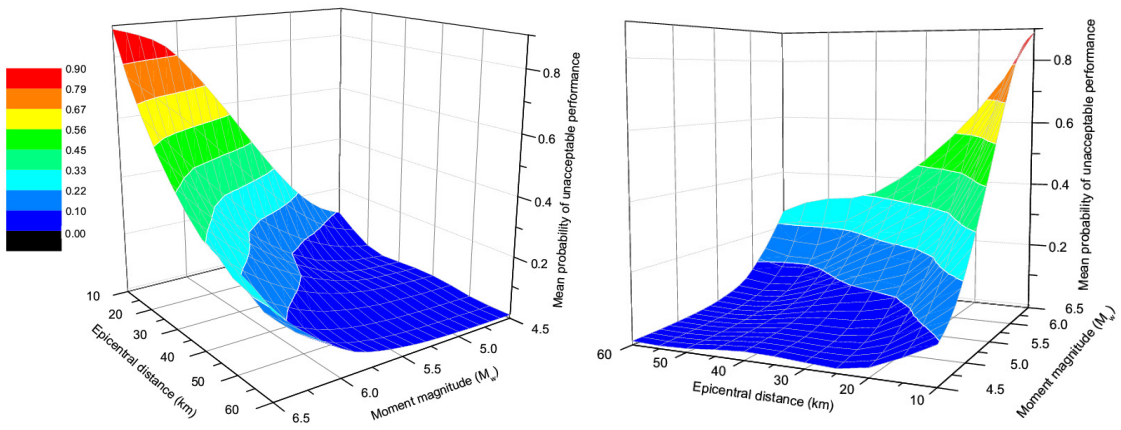

Figure 5-11. Colour map surface for the mean unacceptable performance of Model 1

Similarly, for Model 2a, the colour map surface for the mean probability of unacceptable performance is shown in Figure 5-12. All scenarios analysed in this figure were within the linear range of the structural response, reaching a maximum value of 0.13% for the scenario M_w6.5, R_{epi}10 km. In this example, both Figure 5-11 and Figure 5-12 must not be taken in absolute terms, but rather, in terms of the relative performance between them. In this sense, it is of interest to study the behaviour of the risk reduction for all the scenarios considered.

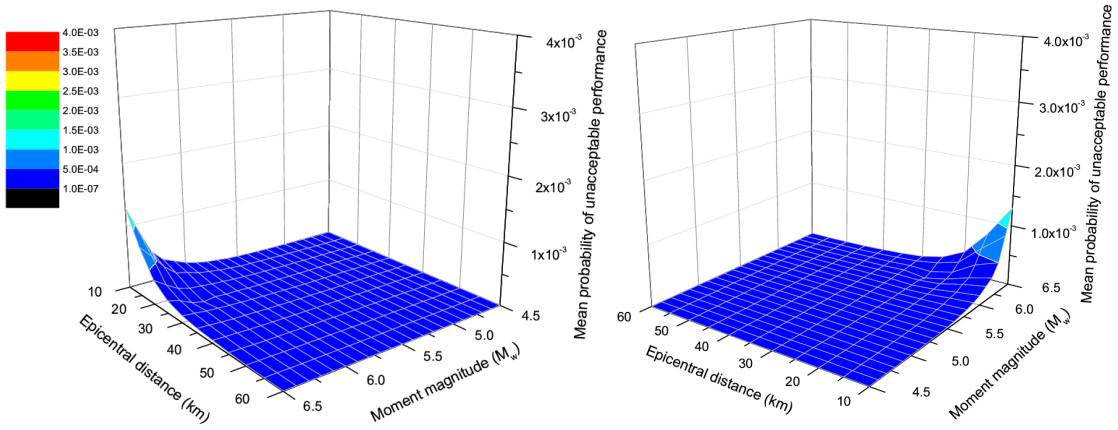

Figure 5-12. Colour map surface for the mean unacceptable performance of Model 2a

5.6.2 Analysis of risk reduction for all controlling scenarios

As seen in the previous section, scenario-based IDA provides valuable information to study how the risk of a given structure changes when different seismic scenarios are taken into account. As it is of interest to study the behaviour of the reduction of risk of the sample NPP for all dominant scenarios, the relative performance shown in Figure 5-11 and Figure 5-12 is analysed in this section. Figure 5-13 shows both surfaces of unacceptable performance of Models 1 and 2a in log units as stacked wire frames. In this figure, it is possible to see that there are several orders of magnitude separating both surfaces suggesting the effectiveness of the isolation system in reducing the risk throughout the set of scenarios considered. In order to gain an in-depth understanding of the reduction of risk, Figure 5-14 shows a spline-smoothed contour plot for the reduction of risk defined as the ratio between Models 1 and 2a. In general, this figure shows that the reduction of risk ranges from 3 to 5 orders of magnitude while for most scenarios the reduction is in the region of 4 orders of magnitude.

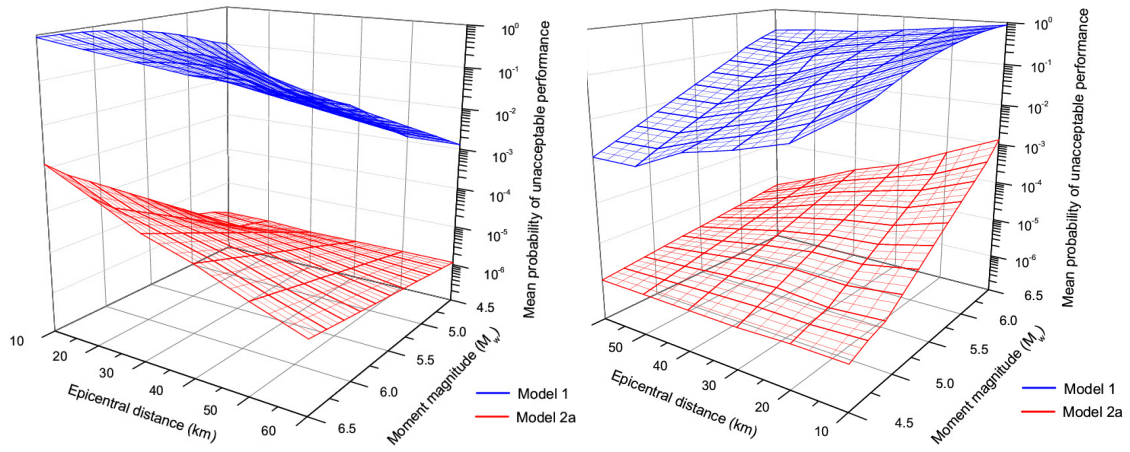

Figure 5-13. Mean unacceptable performance surface (wire frame) for Models 1 and 2a (in log scale)

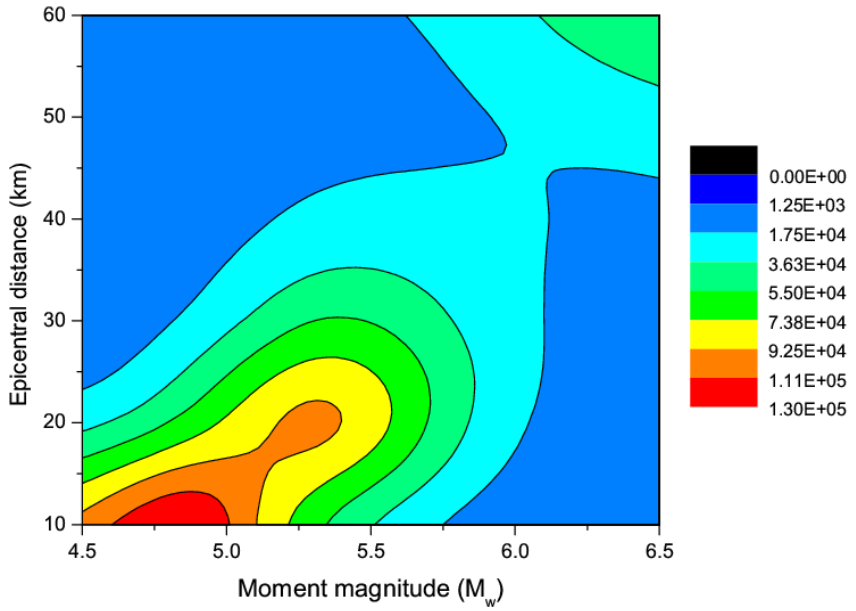

Figure 5-14. Spline-smoothed contour plot for the reduction of risk between Model 1 and Model 2a

5.7 Discussion

- *On the determination of the unacceptable performance for seismically isolated models*: As mentioned in Section 5, the seismic demand on critical components of seismically isolated nuclear reactor buildings (in particular Model 2a in this work) is significantly reduced by the use of isolation devices. This reduction leads to a probability of unacceptable performance that is an extremely small number which

conventional SPRA approaches cannot capture with total accuracy. These events of exceptionally low probability of occurrence fall into the so-called rare events simulation domain for which efficient approaches that can adaptively sample the input are available in the literature. Examples of such procedures are: line sampling [326], horseracing simulation [327], subset simulation [328], etc. Though the values reported in this work for the probability of unacceptable performance of seismically isolated NPPs are considered acceptable for structural engineering purposes, adaptive sampling procedures could be used to improve the accuracy of the values obtained in this work.

- *Recommended approach for using SPS in potential NPPs in UK seismic conditions:* Results obtained in this work suggest that for UK seismic conditions, the use of low-damping rubber bearings and supplemental viscous dampers would be more effective in reducing the seismic risk in comparison with lead-rubber bearings or high-damping rubber bearings. This result is more in agreement with the approach followed by the JHR and ITER reactor buildings in contrast with the devices selected for the APR1400, ASTRID and ALFRED reactor buildings. Also, this result obtained in terms of probabilistic risk assessment confirms the early attempts (although unfruitful) based on small-scale experimental tests to encourage the use LDRB and VD in nuclear reactor buildings in the UK [19]. The devices recommended for potential nuclear deployments in the UK have several advantages. Low-damping rubber bearings are: (i) simple to manufacture as the compounding and bonding process to steel is well understood, (ii) easy to model, and (iii) their mechanical response is unaffected by rate, temperature, history, or ageing [303]. As these devices are able to dissipate little energy, a supplementary damping system based on viscous dampers seems to be an efficient alternative. Viscous dampers are:

(i) activated at low displacements, (ii) require minimal restoring force, (iii) easy to model, and (iv) their mechanical properties are largely frequency- and temperature-independent [329].

- *Use of computer time of scenario-based IDA*: It is acknowledged that the proposed methodology of scenario-based IDA to determine unacceptable performance surfaces of NPPs is computationally demanding. The major task contributing to the use of computer resources is the realisation of a large number of nonlinear time-history analyses of a structural model of the NPP. Minor tasks contributing to the use of computer resources are: (i) the simulation of accelerograms compatible with seismic scenarios of interest and (ii) performing the analysis of risk (SPRA) for each scenario of interest. For real NPP projects, structural models could reach several thousands of degrees of freedom possessing a significant amount of systems, equipment and critical components whose seismic response need to be analysed in detail. Nevertheless, the extremely high criticality of NPPs projects are deemed worthy of investing such resources. Nowadays, powerful computational resources are available to the technical community to perform such extremely demanding tasks, e.g. ARCHER, the UK National Supercomputing Service, a system that possesses 118,080 processor cores enabling it to perform $3x10^{14}$ instructions per second.

5.8 Conclusions

The work presented in this chapter has led to the following conclusions:

- The use of low-damping rubber bearings plus viscous dampers that provide a critical damping (viscous) of ξ=10% seems to be the most suitable approach for UK seismic conditions. This approach was more efficient to reduce the risk than the use of lead

rubber bearings or high-damping rubber bearings that provide a critical damping (hysteretic) of ξ=20%. This is due to the fact that hysteretic damping-based systems need to be subjected to a rather significant demand of displacement in order to develop their full capacity to dissipate energy. A relatively high unused capacity of energy dissipation of these systems is likely to occur if used in the low seismic environment of the British Isles. As viscous damping-based systems are generally activated at low demand of displacements, they are more suitable for the UK seismic conditions. Regarding the foundation soil, the efficiency in reducing such risk was always greater in rock conditions in comparison with soil sites.

- Scenario-based IDA is an intuitive and straightforward methodology to study how the seismic risk of NPPs changes when considering different controlling scenarios. The procedure simplifies the assembly of accelerograms compatible with the seismic scenarios of interest by means of direct stochastic simulation. This methodology avoids the use of procedures normally used in conventional-type IDAs, such as (i) the correct selection of seed accelerograms in order to avoid bias in the structural response, and (ii) the use of scaling procedures in order to match spectral shapes predicted by *ad-hoc* GMPEs. The final product of scenario-based IDA is a surface rather than a curve as obtained in traditional IDAs as it provides the probability of unacceptable performance of NPPs as a function of earthquake magnitude (M_w) and distance-to-site (R_{epi}). The necessity of conducting scenario-based IDA for NPPs lies on the high uncertainty in determining controlling seismic scenarios in areas of medium-to-low seismicity. Therefore, it is vital to study how the seismic risk of NPPs changes by covering the entire range of scenarios likely to occur in the site selected using a rational approach to model the seismic input. The main disadvantage

of scenario-based IDA is that it is very demanding in terms of computer resources. For real NPP projects in which structural models can reach several thousands of degrees of freedom, the performing of a high number of nonlinear dynamic analyses of a structural model is the main barrier that needs to be overcome. Nevertheless, the necessity of making appropriate risk-informed decisions in mission-critical projects such as nuclear power stations justifies the use of such expensive technical resources. Nowadays, the advent of supercomputing systems can ease the performing of such extremely demanding tasks.

- For the example analysed in this work based on a representative UK nuclear site, it was found that: (i) for conventionally constructed NPPs, the seismic risk rapidly increases with a nonlinear behaviour especially for scenarios defined by greater magnitudes and shorter distances; (ii) for seismically isolated NPPs, the seismic risk of the sample NPP is remarkably reduced as the structural response is always in the linear range for all scenarios analysed. In terms of the relative performance of these models, it was found that reduction of risk ranges from 3 to 5 orders of magnitude while for most scenarios the reduction is in the region of 4 orders of magnitude. It can be concluded that the potential use of low-damping rubber bearings and supplemental viscous dampers would be more effective in reducing the seismic risk for the new generation of nuclear reactor buildings in the UK. Certainly, this result is from a purely structural engineering point of view as other important aspects such as through life operational safety and licensing aspects of the seismic protection systems are not considered.

Chapter 6

Conclusions and further work

6.1 Conclusions

A complete framework for seismic probabilistic safety assessment and risk control of nuclear power plants (NPPs) in Northwest Europe, with particular application in the UK, has been presented. It was initially defined a rational mathematical model that allows the stochastic simulation of accelerograms to conduct nonlinear dynamic analyses for safety assessments. Such a model is a function of a few variables customarily known in structural engineering projects and the simulation process is computationally inexpensive. In addition, a methodology to probabilistically assess the risk of NPPs is proposed that is based on stochastically simulated accelerograms. As such, the methodology is more straightforward than conventional approaches as it focuses on the simulation of seismic inputs without the need of using ground motion prediction equations (GMPEs) and selecting/scaling procedures. Furthermore, as the structural response is directly calculated, there is no need of using Monte Carlo-type

procedures to simulate structural outputs, as is done in current practice. Using the proposed methodology for risk assessments, different strategies on the use of seismic protection systems for NPPs were studied in order to control the risk associated to conventionally constructed NPPs. Such strategies were based on the experience reported in other areas of medium-to-low seismic activity of seismically protected nuclear reactor buildings. Further analyses were presented to study how the reduction of risk changes when all controlling scenarios of a site are included in risk analysis. A scenario-based incremental dynamic analysis (IDA) was introduced aimed at the generation of surfaces for unacceptable performance of NPPs as function of earthquake magnitude (M_w) and distance-to-site (R_{epi}). Finally, general guidelines are proposed on the most suitable approach to potentially use seismic protection devices in the development of next generation reactors belonging to the UK New Build Programme. The work conducted in this PhD project has led to the conclusions stated in Sections 6.1.1 to 6.1.3 for each of the three main areas of this work. It is worth remembering that these conclusions are stated from a predominantly structural engineering viewpoint and for a stand-alone seismic risk study.

6.1.1 Seismic input

- Although there is no total agreement in the literature as to how to define a tectonically uniform region for NW Europe, the Flinn-Engdahl regionalisation scheme was found to be a reasonable alternative to define an area of moderate-to-low seismic activity that in turn could be representative for UK standards. Under such a scheme, accelerograms from a wide variety of scenarios comprising magnitudes $4 < M_w < 6.5$, epicentral distances $10 < R_{epi} < 100$ km and different types of soil (rock, stiff soil and soft soil) were found, avoiding the necessity of using earthquake data from other regions that may possess a different tectonic behaviour.

- The dataset of accelerograms used to calibrate the ground motion model proposed in this work was found to be appropriate to conduct regression analysis on the governing parameters of a fully nonstationary stochastic process suitable to simulate accelerograms. Only one functional form for all governing parameters was decided to use for the sake of simplicity, using the least possible number of explanatory variables. Although such a decision implied that the whole model has a relatively high epistemic uncertainty, the predictive equations proposed are statistically significant in modelling the behaviour of the original dataset, and therefore, suitable to stochastically simulate accelerograms compatible with such a dataset. The simulated recordings were found to capture the natural variability of accelerograms produced by different seismic scenarios that have been registered in NW Europe.
- The model proposed is a straightforward mathematical approach to rationally simulate accelerograms compatible for seismic scenarios of interest for design of nuclear structures in the UK and the general region of NW Europe. The simulation process is entirely made in the time domain and only demands numerical analysis customarily used in the structural engineering practice. In terms of PGA, PGV and spectral accelerations, the simulated accelerograms are comprehensively validated by ground motion prediction equations (GMPEs) calibrated for the UK, Europe and the Middle East, and other stable continental regions.

6.1.2 Seismic risk analysis

- The methodology proposed to probabilistically assess the seismic risk of nuclear power plants effectively simplifies traditional approaches when defining seismic inputs for nonlinear dynamic analyses. As the seismic input is directly simulated for the seismic scenarios of interest, it is not necessary to select seed appropriate

accelerograms that will then need to be scaled to match a selected set of GMPEs of interest. Selection of *ad-hoc* GMPEs normally demands extensive research resources, particularly for areas of medium-to-low seismic activity. Therefore, for the particular case of the UK and general region of NW Europe, the methodology proposed is significantly more straightforward to perform such tasks.

- In addition, under the proposed methodology, the structural output is directly calculated; hence, there is also no need of using Monte Carlo algorithms to simulate the structural response to make a robust estimation of the damage state of the NPP. Furthermore, it was found that the pattern of the nonlinear structural response obtained with the proposed approach differs in shape compared with those obtained performing conventional procedures. Monte Carlo algorithms, although extensively used in research, are a rather statistics-based approach to artificially enlarge the number of observations of the damage state. Consequently, they might not necessarily be able to appropriately model the progressive path into the nonlinear response of the structure analysed. This effect might be even more pronounced for stronger earthquakes as the intrinsic nature of accelerograms changes significantly for increasing magnitudes, which ultimately may lead to inaccurate results in risk assessments.
- The main obstacle of the proposed methodology is the need for more demanding computational resources as a relatively large number of nonlinear dynamic analyses are needed to perform. For real applications, structural models could be particularly complex involving several thousands of degrees of freedom to capture critical details of structures, systems, and components. For such cases, supercomputing resources may be needed to use to implement the proposed approach.

- Results of risk obtained with the proposed methodology are well constrained by established approaches that use GMPEs to define seismic inputs. In particular, it was demonstrated that the use of predictive models calibrated for active crustal regions are likely to introduce excessive conservatism for nuclear applications in the UK: their use may not be adequate and may lead to unrealistic results.

6.1.3 Seismic protection systems

- For UK seismic conditions, it was found that the use of devices that provide a relatively low amount of viscous damping, say ~10%, will produce the most efficient approach to reduce the seismic risk. The use of hysteretic-based devices was found to be less efficient as they are normally activated at relatively larger demands of displacement that are highly unlikely to occur in the British Isles. The reduction of risk when using viscous damping is considerably large as it can reach several orders of magnitude when compared to conventionally constructed NPPs.
- It was found that the proposed methodology to conduct Scenario-based IDA is an intuitive and direct methodology to study how the seismic risk of NPPs changes when considering different controlling scenarios. Scenario-based IDA is particularly useful in areas of medium-to-low seismic activity as the determination of controlling scenarios for a given site is normally subjected to a very high uncertainty due to the lack of knowledge about seismological and tectonic process of these areas. In this light, the final product of Scenario-based IDA can help to make risk-informed decisions for a particular project. The main barrier of Scenario-based IDA is that is computationally expensive, requiring performing a very large number of nonlinear dynamic analyses.

6.2 Further work

The topics identified as potential areas for further research for each of the three main areas of this work are stated in Sections 6.2.1 to 6.2.3. These topics are concerned to structural engineering aspects only.

6.2.1 Seismic input

- *Update using new European database of accelerograms*: The stochastic model presented in this work was calibrated using accelerograms taken from the pan-European on-line database ISESD [261] as it was the only suitable source available in the public domain at the moment of conducting this research. Nevertheless, a more updated database, RESORCE [330], that is intended to be a standardised accelerometric databank for Europe, was made available after conducting this work. Such a database represents an improvement in quality and quantity of information compared to previous databases aimed to contribute to the improvement of risk studies all over Europe. As such, it is of interest to include potential new recordings now available that were not included in the model's original dataset and conduct new regression analyses in order to update the model. This process may affect the functional form of the parameters that govern the fully nonstationary stochastic process: its statistical significance (p-values shown in Table 3-1) may decrease, which will reduce the epistemic uncertainty of the model, or increase, in which case new functional forms will need to be tested to provide a better fit to the data.

- *Addition of near-fault accelerograms*: The stochastic model presented in this work deliberately did not include accelerograms recorded at epicentral distances shorter than 10 km, i.e. it is a model valid for far-field conditions. This was to exclude intrinsic features of near-fault records, such as, severe directivity pulses, which can

have a substantial influence on the frequency content of accelerograms [298]. In this light, the stochastic model proposed is not applicable for nuclear sites whose controlling seismic scenarios are shorter than 10 km. Therefore, it is of interest to extend the framework proposed and add an additional model valid for near-fault conditions in order to generalise its applicability. A starting point for such a model could be the complete methodology to simulate near-fault accelerograms for performance-based earthquake engineering recently proposed by Dabaghi and Der Kiureghian [331].

6.2.2 Seismic risk analysis

- *Perform intensity- and time-based assessments*: As all analyses of risk presented in this work are scenario-based, it is of interest to gain broader knowledge of the representative nuclear site selected by conducting intensity- and time-based assessment of risk. For an intensity-based assessment, it will be necessary to define the 10,000-year-return-period uniform hazard/risk spectrum (UHS/URS) of the site and select the specific intensity associated to the fundamental period of the NPP. The definition of stochastically simulated accelerograms associated to such intensity, although different compared to the definition for scenario-based assessments, will not represent a major challenge. One way to characterise a large set of suitable accelerograms for this type of assessment is to define an algorithm such as to: (i) simulate accelerograms compatible with all controlling seismic scenarios of the site for a 10,000-year return period event, (ii) conduct linear dynamic analysis using a single-degree-of-freedom system that possesses the same fundamental period of the NPP, and (iii) select those accelerograms that produce a maximum structural response equal to the intensity obtained from the UHS/URS defined for the site. As time-based assessments are conducted as series of intensity-based assessments, the

definition of sets of accelerograms is essentially the same as described previously. The hazard curve of the site is divided in a finite number of points (normally eight), then for each intensity obtained, the procedure described previously must be conducted repetitively to define their associated bins of accelerograms.

- *Detailed structural models:* It is acknowledged that the structural models used in this work, although valid, are somewhat simplified. As detailed NPP models contain sensitive information, they are not normally available in the literature. However, as all analyses conducted in this PhD thesis were presented in terms of relative performance, the models used in no way limit the framework proposed. In any case, it is of interest to apply the framework for safety assessment and risk control proposed using detailed models for the: (i) reactor building, (ii) fragility analysis, and (iii) soil-structure interaction. An appropriate 3D finite-element-method model containing details of all key components of a modern NPP will allow performing specific performance assessments for major structural components, e.g. primary circuit pipework for the reactor pressure vessel. In addition, innovative approaches for the fragility analysis could be incorporated, e.g. use fragility surfaces instead of fragility curves as it has been reported that the use of two parameters may provide a more accurate description of the failure function of structures and components [176]. Also, an enhanced soil-structure interaction analysis, including effects of slip and separation [306, 308], may provide higher accuracy for the numerical values of risk presented in this work.

6.2.3 Seismic protection systems

- *Beyond-design basis events*: The design philosophy of the UK nuclear regulator [285] is based on the provision of structural robustness and resilience. In this light,

NPPs should be designed in such a way that the structure is able to withstand events without being damaged to an extent disproportionate to the original cause, i.e. to avoid the occurrence of the so-called "cliff-edge" effect. This leads to the demonstration that: (i) the NPP remains fully elastic up to a significant margin beyond the design basis, or (ii) the NPP is able to accommodate the seismic demand through a ductile response beyond the design basis event without any danger of radiation release. As shown in Section 5.6.2, the use of seismic protection systems is an effective technique to control seismic risk for all controlling scenarios of the nuclear site selected considering a 10,000-year-return-period design basis event. Nevertheless, there is currently no clear consensus on the definition of beyond-design basis events and little research has been conducted in this regard for next generation NPPs [332]. Two examples that address beyond-design events are: (i) the American approach [213] that defines such an event as a ground motion equal to 150% of the design-basis event, i.e. it simply involves the scaling of the seismic input used for design; and (ii) the French approach [333] that considers a 20,000-year return period event, i.e. it involves performing a new PSHA to identify the controlling seismic scenarios for the site associated to such a return period and then re-assess the risk. As the UK nuclear regulation is non-prescriptive, the specification of the beyond-design basis event is not specifically addressed. Nevertheless, considering the framework proposed in this work, it seems reasonable to investigate beyond-design basis events under the French approach to gain insights as to how the cliff-edge effect is controlled by both conventional and seismically protected NPPs under UK seismic conditions.

- *Variability in devices' mechanical properties:* All analysis of risk presented in Chapter 5 were made considering fixed mechanical properties for the devices.

Nevertheless, their properties will tend to vary from the values assumed for design for two reasons: (i) there is variability in the basic materials at the time of fabrication, and (ii) during the lifespan of the nuclear structure due to ageing, contamination, ambient temperature, etc. [334]. Consequently, it is of interest to analyse the impact on risk assessments affected by the total variability of the mechanical properties of an assembly of isolators both for design and beyond-design basis events.

References

1. IAEA. *Power Reactor Information System (PRIS)*. http://www.iaea.org/pris 2015; Available from: http://www.iaea.org/pris.
2. Meiswinkel, R., J. Meyer, and J. Schnell, *Design and Construction of Nuclear Power Plants*. Beton Kalender. 2013, Berlin, Germany: Ernst & Sohn.
3. Chapman, N.A., H. Tsuchi, and K. Kitayama, *Tectonic events and nuclear facilities*, in *Volcanic and Tectonic Hazard Assessment for Nuclear Facilities*, C.B. Connor, N.A. Chapman, and L.J. Connor, Editors. 2008, Cambridge University Press. p. 1-23.
4. IAEA, *IAEA Annual Report 2014*. 2014, International Atomic Energy Agency.
5. WNA. *Nuclear Power Plants and Earthquakes*. http://www.world-nuclear.org 2014.
6. USGS. *Search earthquake archives*. http://earthquake.usgs.gov/earthquakes/search/ 2016.
7. Hirano, M., et al., *Insights from review and analysis of the Fukushima Dai-ichi accident.* Journal of Nuclear Science and Technology, 2012. **49**(1): p. 1-17.
8. ENSREG, *EU Stress Tests Specifications*, in *EU Stress Tests*. 2011, European Nuclear Safety Regulators Group: Brussels, Belgium.
9. Hayashi, M. and L. Hughes, *The Fukushima nuclear accident and its effect on global energy security.* Energy Policy, 2013. **59**: p. 102-111.
10. Martelli, A., M. Forni, and P. Clemente. *Recent Worldwide Application of Seismic Isolation and Energy Dissipation and Conditions for Their Correct Use*. in *Proceedings of the 15th World Conference on Earthquake Engineering*. 2012. Lisbon.
11. Martelli, A. and M. Forni, *Seismic isolation and other antiseismic systems: recent applications in Italy and worldwide.* Seismic Isolation and Protection Systems, 2010. **1**(1): p. 75-123.
12. Forni, M., A. Poggianti, and A. Dusi. *Seismic isolation of nuclear power plants*. in *Proceedings of the 15th World Conference on Earthquake Engineering*. 2012.
13. Medel-Vera, C. and T. Ji, *Seismic protection technology for nuclear power plants: a systematic review.* Journal of Nuclear Science and Technology, 2014. **52**(5): p. 607-632.
14. Bignan, G., et al. *The Jules Horowitz Reactor: A New European MTR (Material Testing Reactor) Open to International Collaboration: Update Description and Focus on the Modern Safety Approach*. in *IAEA International Conference on Research Reactors: Safe Operation and Effective Utilization*. 2011. Rabat, Morocco: International Atomic Energy Agency.
15. Syed, M.B., et al., *The challenging requirements of the ITER anti seismic bearings.* Nuclear Engineering and Design, 2014. **269**(0): p. 212-216.
16. Lee, H.-P., et al. *Development of Laminated Rubber Bearings for the APR1400 Nuclear Power Plant*. in *23rd Conference on Structural Mechanics in Reactor Technology (SMiRT 23)*. 2015. Manchester, UK.
17. CEA, *4th Generation Sodium-Cooled Fast Reactors - The ASTRID Technological Demonstrator*. 2012, CEA (Commissariat à l'énergie atomique et aux énergies alternatives) - Nuclear Energy Division: Saclay, France.
18. Alemberti, A., et al., *Lead-cooled Fast Reactor (LFR) Risk and Safety Assessment. White Paper. Revision 8*. 2014, Generation IV International Forum.
19. Austin, N.M., et al., *UK contribution to CEGB・EPRI・CRIEPI program on seismic isolation.* Nuclear Engineering and Design, 1991. **127**(3): p. 253-264.
20. HM_Government, *Report: Nuclear Industrial Strategy - The UK's Nuclear Future*. 2013, HM Government & Nuclear Industry Association: London.
21. NIA, *Capability Report: Capability of the UK Nuclear New Build Supply Chain*. 2012, Nuclear Industry Association: London.
22. Weightman, M., *Japanese earthquake and tsunami: Implications for the UK nuclear industry*. 2011, Office for Nuclear Regulation - HM Chief Inspector of Nuclear Installations: Bootle, Merseyside.
23. Davies, L.P., *Risk assessment in the UK nuclear power industry.* Safety Science, 2002. **40**(1–4): p. 203-230.
24. Musson, R.M.W., *UK seismic hazard assessments for strategic facilities: a short history.* Bollettino di Geofisica Teorica ed Applicata, 2014. **55**(1): p. 165-173.
25. Bommer, J.J., M. Papaspiliou, and W. Price, *Earthquake response spectra for seismic design of nuclear power plants in the UK.* Nuclear Engineering and Design, 2011. **241**(3): p. 968-977.
26. Musson, R.M.W., *The seismicity of the British Isles.* Annals of Geophysics, 1996. **39**(3).
27. Johnston, A.C., et al., *The Earthquakes of Stable Continental Regions*, in *TR-102261*. 1994, Electric Power Research Institute.

28. Musson, R.M.W. *UK Seismic Hazard Assessments for Strategic Facilities: A Short History*. in *30th National GNGTS Conference (Gruppo Nazionale di Geofisica della Terra Solida)*. 2011. Trieste, Italy.
29. Rietbrock, A., F. Strasser, and B. Edwards, *A Stochastic Earthquake Ground-Motion Prediction Model for the United Kingdom.* Bulletin of the Seismological Society of America, 2013. **103**(1): p. 57-77.
30. Musson, R.M.W., *The Case for Large M > 7 Earthquakes Felt in the UK in Historical Times*, in *Historical Seismology*, J. Fréchet, M. Meghraoui, and M. Stucchi, Editors. 2008, Springer Netherlands. p. 187-207.
31. Baptie, B., *Seismogenesis and state of stress in the UK.* Tectonophysics, 2010. **482**(1–4): p. 150-159.
32. Goda, K., W. Aspinall, and C.A. Taylor, *Seismic Hazard Analysis for the U.K.: Sensitivity to Spatial Seismicity Modelling and Ground Motion Prediction Equations.* Seismological Research Letters, 2013. **84**(1): p. 112-129.
33. Douglas, J., *Earthquake ground motion estimation using strong-motion records: a review of equations for the estimation of peak ground acceleration and response spectral ordinates.* Earth-Science Reviews, 2003. **61**(1–2): p. 43-104.
34. Douglas, J. and H. Aochi, *A Survey of Techniques for Predicting Earthquake Ground Motions for Engineering Purposes.* Surveys in Geophysics, 2008. **29**(3): p. 187-220.
35. Boore, D.M. and W.B. Joyner, *The empirical prediction of ground motion.* Bulletin of the Seismological Society of America, 1982. **72**(6B): p. S43-S60.
36. Atkinson, G.M. *Integrating advances in ground-motion and seismic-hazard analysis*. in *15th World Conference on Earthquake Engineering*. 2012. Lisbon, Portugal.
37. Power, M., et al., *An Overview of the NGA Project.* Earthquake Spectra, 2008. **24**(1): p. 3-21.
38. Bozorgnia, Y., et al., *NGA-West2 Research Project.* Earthquake Spectra, 2014. **30**(3): p. 973-987.
39. Hanks, T.C. and R.K. McGuire, *The character of high-frequency strong ground motion.* Bulletin of the Seismological Society of America, 1981. **71**(6): p. 2071-2095.
40. Brune, J.N., *Tectonic stress and the spectra of seismic shear waves from earthquakes.* Journal of Geophysical Research, 1970. **75**(26): p. 4997-5009.
41. Boore, D.M., *Simulation of Ground Motion Using the Stochastic Method.* pure and applied geophysics, 2003. **160**(3-4): p. 635-676.
42. Anbazhagan, P., A. Kumar, and T.G. Sitharam, *Ground motion prediction equation considering combined dataset of recorded and simulated ground motions.* Soil Dynamics and Earthquake Engineering, 2013. **53**: p. 92-108.
43. Star, L.M., J.P. Stewart, and R.W. Graves, *Comparison of Ground Motions from Hybrid Simulations to NGA Prediction Equations.* Earthquake Spectra, 2011. **27**(2): p. 331-350.
44. Burks, L.S. and J.W. Baker, *A predictive model for fling-step in near-fault ground motions based on recordings and simulations.* Soil Dynamics and Earthquake Engineering, 2016. **80**: p. 119-126.
45. Campbell, K.W., *Prediction of Strong Ground Motion Using the Hybrid Empirical Method and Its Use in the Development of Ground-Motion (Attenuation) Relations in Eastern North America.* Bulletin of the Seismological Society of America, 2003. **93**(3): p. 1012-1033.
46. Akkar, S., M.A. Sandıkkaya, and J.J. Bommer, *Empirical ground-motion models for point- and extended-source crustal earthquake scenarios in Europe and the Middle East.* Bulletin of Earthquake Engineering, 2014. **12**(1): p. 359-387.
47. Douglas, J., *Ground-motion prediction equations 1964-2010*, in *Final Report BRGM/RP-59356-FR*. 2011, BRGM.
48. Ibrahim, R., et al., *Long-Period Ground-Motion Prediction Equations for Moment Magnitude Estimation of Large Earthquakes in Japan.* Bulletin of the Seismological Society of America, 2016. **106**(1): p. 54-72.
49. Ghofrani, H. and G.M. Atkinson, *Ground-motion prediction equations for interface earthquakes of M7 to M9 based on empirical data from Japan.* Bulletin of Earthquake Engineering, 2013. **12**(2): p. 549-571.
50. Haendel, A., et al., *Mixtures of ground-motion prediction equations as backbone models for a logic tree: an application to the subduction zone in Northern Chile.* Bulletin of Earthquake Engineering, 2014. **13**(2): p. 483-501.
51. Bradley, B.A., *A New Zealand-Specific Pseudospectral Acceleration Ground-Motion Prediction Equation for Active Shallow Crustal Earthquakes Based on Foreign Models.* Bulletin of the Seismological Society of America, 2013. **103**(3): p. 1801-1822.

52. Rodríguez-Pérez, Q., *Ground-Motion Prediction Equations for Near-Trench Interplate and Normal-Faulting Inslab Subduction Zone Earthquakes in Mexico.* Bulletin of the Seismological Society of America, 2014. **104**(1): p. 427-438.
53. Gülerce, Z., B. Kargıoğlu, and N.A. Abrahamson, *Turkey-Adjusted NGA-W1 Horizontal Ground Motion Prediction Models.* Earthquake Spectra, 2016. **0**(0): p. null.
54. Massa, M., et al., *Empirical Ground-Motion Prediction Equations for Northern Italy Using Weak- and Strong-Motion Amplitudes, Frequency Content, and Duration Parameters.* Bulletin of the Seismological Society of America, 2008. **98**(3): p. 1319-1342.
55. Bindi, D., et al., *Ground motion prediction equations derived from the Italian strong motion database.* Bulletin of Earthquake Engineering, 2011. **9**(6): p. 1899-1920.
56. Bindi, D., et al., *Towards a new reference ground motion prediction equation for Italy: update of the Sabetta–Pugliese (1996).* Bulletin of Earthquake Engineering, 2009. **7**(3): p. 591-608.
57. Lanzano, G., et al., *Ground-Motion Prediction Equations for Region-Specific Probabilistic Seismic-Hazard Analysis.* Bulletin of the Seismological Society of America, 2016. **106**(1): p. 73-92.
58. Villalobos-Escobar, G.P. and R.R. Castro, *Empirical ground-motion relations using moderate earthquakes recorded by Medellín–Aburrá Valley (Colombia) strong-motion networks.* Bulletin of Earthquake Engineering, 2013. **11**(4): p. 863-884.
59. Emolo, A., et al., *Ground-Motion Prediction Equations for South Korea Peninsula.* Bulletin of the Seismological Society of America, 2015. **105**(5): p. 2625-2640.
60. Harbindu, A., S. Gupta, and M.L. Sharma, *Earthquake ground motion predictive equations for Garhwal Himalaya, India.* Soil Dynamics and Earthquake Engineering, 2014. **66**: p. 135-148.
61. Skarlatoudis, A.A., et al., *Ground-Motion Prediction Equations of Intermediate-Depth Earthquakes in the Hellenic Arc, Southern Aegean Subduction Area.* Bulletin of the Seismological Society of America, 2013. **103**(3): p. 1952-1968.
62. Sokolov, V., et al., *Ground-motion prediction equations for the intermediate depth Vrancea (Romania) earthquakes.* Bulletin of Earthquake Engineering, 2008. **6**(3): p. 367-388.
63. Atkinson, G.M., *Ground-Motion Prediction Equations for Hawaii from a Referenced Empirical Approach.* Bulletin of the Seismological Society of America, 2010. **100**(2): p. 751-761.
64. Pasyanos, M., *Validation of Attenuation Models for Ground Motion Applications in Central and Eastern North America.* Earthquake Spectra, 2015. **31**(4): p. 2281-2300.
65. Yenier, E. and G.M. Atkinson, *Regionally Adjustable Generic Ground-Motion Prediction Equation Based on Equivalent Point-Source Simulations: Application to Central and Eastern North America.* Bulletin of the Seismological Society of America, 2015. **105**(4): p. 1989-2009.
66. Pezeshk, S., A. Zandieh, and B. Tavakoli, *Hybrid Empirical Ground-Motion Prediction Equations for Eastern North America Using NGA Models and Updated Seismological Parameters.* Bulletin of the Seismological Society of America, 2011. **101**(4): p. 1859-1870.
67. Atkinson, G.M., *Ground-Motion Prediction Equations for Eastern North America from a Referenced Empirical Approach: Implications for Epistemic Uncertainty.* Bulletin of the Seismological Society of America, 2008. **98**(3): p. 1304-1318.
68. Bora, S.S., et al., *Development of a Response Spectral Ground-Motion Prediction Equation (GMPE) for Seismic-Hazard Analysis from Empirical Fourier Spectral and Duration Models.* Bulletin of the Seismological Society of America, 2015. **105**(4): p. 2192-2218.
69. Graizer, V., E. Kalkan, and K.-W. Lin, *Global Ground Motion Prediction Equation for Shallow Crustal Regions.* Earthquake Spectra, 2013. **29**(3): p. 777-791.
70. Douglas, J., et al., *Comparisons among the five ground-motion models developed using RESORCE for the prediction of response spectral accelerations due to earthquakes in Europe and the Middle East.* Bulletin of Earthquake Engineering, 2014. **12**(1): p. 341-358.
71. PML, *British earthquakes, Technical Report 115/82, Principia Mechanica Ltd., London.* 1982.
72. PML, *Seismological studies for UK hazard analysis, Technical Report 346/85, Principia Mechanica Ltd., London.* 1985.
73. Stewart, J.P., et al., *Selection of Ground Motion Prediction Equations for the Global Earthquake Model.* Earthquake Spectra, 2015. **31**(1): p. 19-45.
74. Cotton, F., et al., *Criteria for Selecting and Adjusting Ground-Motion Models for Specific Target Regions: Application to Central Europe and Rock Sites.* Journal of Seismology, 2006. **10**(2): p. 137-156.
75. Shoushtari, A.V., A.B. Adnan, and M. Zare, *On the selection of ground–motion attenuation relations for seismic hazard assessment of the Peninsular Malaysia region due to distant Sumatran subduction intraslab earthquakes.* Soil Dynamics and Earthquake Engineering, 2016. **82**: p. 123-137.

76. Yaghmaei-Sabegh, S., *A new method for ranking and weighting of earthquake ground-motion prediction models.* Soil Dynamics and Earthquake Engineering, 2012. **39**: p. 78-87.
77. Wang, G., et al., *Design Ground Motion Library: An Interactive Tool for Selecting Earthquake Ground Motions.* Earthquake Spectra, 2015. **31**(2): p. 617-635.
78. Arroyo, D., M. Ordaz, and R. Rueda, *On the Selection of Ground-Motion Prediction Equations for Probabilistic Seismic-Hazard Analysis.* Bulletin of the Seismological Society of America, 2014. **104**(4): p. 1860-1875.
79. Azarbakht, A., S. Rahpeyma, and M. Mousavi, *A New Methodology for Assessment of the Stability of Ground-Motion Prediction Equations.* Bulletin of the Seismological Society of America, 2014. **104**(3): p. 1447-1457.
80. Kale, Ö. and S. Akkar, *A New Procedure for Selecting and Ranking Ground-Motion Prediction Equations (GMPEs): The Euclidean Distance-Based Ranking (EDR) Method.* Bulletin of the Seismological Society of America, 2013. **103**(2A): p. 1069-1084.
81. Anbazhagan, P., et al., *Selection of Ground Motion Prediction Equations for Seismic Hazard Analysis of Peninsular India.* Journal of Earthquake Engineering, 2015: p. 1-39.
82. Mousavi, M., et al., *Selection of Ground Motion Prediction Models for Seismic Hazard Analysis in the Zagros Region, Iran.* Journal of Earthquake Engineering, 2012. **16**(8): p. 1184-1207.
83. Atkinson, G.M. and M. Morrison, *Observations on Regional Variability in Ground-Motion Amplitudes for Small-to-Moderate Earthquakes in North America.* Bulletin of the Seismological Society of America, 2009. **99**(4): p. 2393-2409.
84. Musson, R.M.W., *The use of Monte Carlo simulations for seismic hazard assessment in the U.K.* Annals of Geophysics, 2000. **43**(1).
85. Weatherill, G. and P.W. Burton, *An alternative approach to probabilistic seismic hazard analysis in the Aegean region using Monte Carlo simulation.* Tectonophysics, 2010. **492**(1–4): p. 253-278.
86. Fahjan, Y.M., *Selection and scaling of real earthquake accelerograms to fit the Turkish design spectra.* Teknik Dergi, 2008. **19**(3): p. 4423-444.
87. Lubkowski, Z., et al., *An Evaluation of Attenuation Relationships for Seismic Hazard Assessment in the UK*, in *13th World Conference on Earthquake Engineering*. 2004: Vancouver, Canada. p. Paper 1422.
88. Halldórsson, B., G. Mavroeidis, and A. Papageorgiou, *Near-Fault and Far-Field Strong Ground-Motion Simulation for Earthquake Engineering Applications Using the Specific Barrier Model.* Journal of Structural Engineering, 2011. **137**(3): p. 433-444.
89. Liu, P., R.J. Archuleta, and S.H. Hartzell, *Prediction of Broadband Ground-Motion Time Histories: Hybrid Low/High- Frequency Method with Correlated Random Source Parameters.* Bulletin of the Seismological Society of America, 2006. **96**(6): p. 2118-2130.
90. Lam, N., J. Wilson, and G. Hutchinson, *Generation of synthetic earthquake accelerograms using seismological modelling: a review.* Journal of Earthquake Engineering, 2000. **4**(3): p. 321-354.
91. Mobarakeh, A.A., F.R. Rofooei, and G. Ahmadi, *Simulation of earthquake records using time-varying Arma (2,1) model.* Probabilistic Engineering Mechanics, 2002. **17**(1): p. 15-34.
92. Rofooei, F.R., A. Mobarake, and G. Ahmadi, *Generation of artificial earthquake records with a nonstationary Kanai–Tajimi model.* Engineering Structures, 2001. **23**(7): p. 827-837.
93. Sgobba, S., et al., *An evolutionary stochastic ground-motion model defined by a seismological scenario and local site conditions.* Soil Dynamics and Earthquake Engineering, 2011. **31**(11): p. 1465-1479.
94. Zentner, I., *A procedure for simulating synthetic accelerograms compatible with correlated and conditional probabilistic response spectra.* Soil Dynamics and Earthquake Engineering, 2014. **63**: p. 226-233.
95. Graves, R.W. and A. Pitarka, *Broadband Ground-Motion Simulation Using a Hybrid Approach.* Bulletin of the Seismological Society of America, 2010. **100**(5A): p. 2095-2123.
96. Shahjouei, A. and S. Pezeshk, *Synthetic Seismograms Using a Hybrid Broadband Ground-Motion Simulation Approach: Application to Central and Eastern United States.* Bulletin of the Seismological Society of America, 2015. **105**(2A): p. 686-705.
97. Boore, D.M., *Stochastic simulation of high-frequency ground motions based on seismological models of the radiated spectra.* Bulletin of the Seismological Society of America, 1983. **73**(6A): p. 1865-1894.
98. Zerva, A., *On the spatial variation of seismic ground motions and its effects on lifelines.* Engineering Structures, 1994. **16**(7): p. 534-546.
99. Vetter, C. and A.A. Taflanidis, *Comparison of alternative stochastic ground motion models for seismic risk characterization.* Soil Dynamics and Earthquake Engineering, 2014. **58**: p. 48-65.

100. Zerva, A. and V. Zervas, *Spatial variation of seismic ground motions: An overview.* Applied Mechanics Reviews, 2002. **55**(3): p. 271-297.
101. Sabetta, F. and A. Pugliese, *Estimation of response spectra and simulation of nonstationary earthquake ground motions.* Bulletin of the Seismological Society of America, 1996. **86**(2): p. 337-352.
102. Montaldo, V., et al., *Simulation of the Fourier phase spectrum for the generation of synthetic accelerograms.* Journal of Earthquake Engineering, 2003. **7**(3): p. 427-445.
103. Pousse, G., et al., *Nonstationary Stochastic Simulation of Strong Ground Motion Time Histories Including Natural Variability: Application to the K-Net Japanese Database.* Bulletin of the Seismological Society of America, 2006. **96**(6): p. 2103-2117.
104. Lin, Y.K., *On random pulse train and its evolutionary spectral representation.* Probabilistic Engineering Mechanics, 1986. **1**(4): p. 219-223.
105. Jurkevics, A. and T.J. Ulrych, *Representing and simulating strong ground motion.* Bulletin of the Seismological Society of America, 1978. **68**(3): p. 781-801.
106. Nau, R.F., R.M. Oliver, and K.S. Pister, *Simulating and analyzing artificial nonstationary earthquake ground motions.* Bulletin of the Seismological Society of America, 1982. **72**(2): p. 615-636.
107. Rupakhety, R. and R. Sigbjörnsson, *Spatial variability of strong ground motion: novel system-based technique applying parametric time series modelling.* Bulletin of Earthquake Engineering, 2012. **10**(4): p. 1193-1204.
108. Polhemus, N.W. and A.S. Cakmak, *Simulation of earthquake ground motions using autoregressive moving average (ARMA) models.* Earthquake Engineering & Structural Dynamics, 1981. **9**(4): p. 343-354.
109. Conte, J.P. and B.F. Peng, *Fully Nonstationary Analytical Earthquake Ground-Motion Model.* Journal of Engineering Mechanics, 1997. **123**(1): p. 15-24.
110. Der Kiureghian, A. and J. Crempien, *An evolutionary model for earthquake ground motion.* Structural Safety, 1989. **6**(2–4): p. 235-246.
111. Wen, Y.K. and P. Gu, *Description and Simulation of Nonstationary Processes Based on Hilbert Spectra.* Journal of Engineering Mechanics, 2004. **130**(8): p. 942-951.
112. Rezaeian, S. and A. Der Kiureghian, *A stochastic ground motion model with separable temporal and spectral nonstationarities.* Earthquake Engineering & Structural Dynamics, 2008. **37**(13): p. 1565-1584.
113. Papadimitriou, K., *Stochastic Characterization of Strong Ground Motion and Applications to Structural Response*, in *Earthquake Engineering Research Laboratory*. 1990, California Institute of Technology: Pasadena, California.
114. Liao, S. and A. Zerva, *Physically compliant, conditionally simulated spatially variable seismic ground motions for performance-based design.* Earthquake Engineering & Structural Dynamics, 2006. **35**(7): p. 891-919.
115. Rezaeian, S. and A. Der Kiureghian, *Simulation of synthetic ground motions for specified earthquake and site characteristics.* Earthquake Engineering & Structural Dynamics, 2010. **39**(10): p. 1155-1180.
116. Scawthorn, C., *A Brief History of Seismic Risk Assessment*, in *Risk Assessment, Modeling and Decision Support*, A. Bostrom, S. French, and S. Gottlieb, Editors. 2008, Springer Berlin Heidelberg. p. 5-81.
117. Wang, Z., *Seismic Hazard Assessment: Issues and Alternatives.* pure and applied geophysics, 2011. **168**(1-2): p. 11-25.
118. Chen, J.T., et al., *Procedural and Submittal Guidance for the Individual Plant Examination of External Events (IPEEE) for Severe Accident Vulnerabilities*, in *NUREG-1407*. 1991, US Nucelar Regulatory Commission: Washington, DC, USA.
119. Budnitz, R.J., et al., *An Approach to the Quantification of Seismic Margins in Nuclear Power Plants*, in *NUREG/CR-4334*. 1985, Lawrence Livermore National Laboratory: Livermore, CA, USA.
120. Prassinos, P.G., M.K. Ravindra, and J.B. Savy, *NUREG/CR-4482 - Recommendations to the Nuclear Regulatory Commission on Trial Guidelines for Seismic Margin Reviews of Nuclear Power Plants*. 1986, Lawrence Livermore National Laboratory: Livermore, CA, USA.
121. Reed, J.W., et al., *A Methodology for Assessment of Nuclear Power Plant Seismic Margin (revision 1)*, in *NP-6041-SL*. 1991, Electric Power Research Institute: Palo Alto, California.
122. ASCE_4-98, *Seismic Analysis of Safety-related Nuclear Structures and Commentary*. 2000.

123. USNRC, *PRA Procedures Guide: A Guide to the Performance of Probabilistic Risk Assessments for Nuclear Power Plants*, NUREG/CR-2300, Editor. 1983, US Nuclear Regulatory Commission: Washington, D.C., USA.
124. Garrick, B.J. and R.F. Christie, *Probabilistic risk assessment practices in the USA for nuclear power plants.* Safety Science, 2002. **40**(1–4): p. 177-201.
125. Keller, W. and M. Modarres, *A historical overview of probabilistic risk assessment development and its use in the nuclear power industry: a tribute to the late Professor Norman Carl Rasmussen.* Reliability Engineering & System Safety, 2005. **89**(3): p. 271-285.
126. Niehaus, F., *Use of Probabilistic Safety Assessment (PSA) for nuclear installations☆.* Safety Science, 2002. **40**(1–4): p. 153-176.
127. Kumagai, Y., et al., *PRA-Based SMA: the First Tool toward a Risk-Informed Approach to the Seismic Design of the IRIS.* Journal of Nuclear Science and Technology, 2007. **44**(10): p. 1268-1274.
128. Gjorgiev, B., D. Kančev, and M. Čepin, *Risk-informed decision making in the nuclear industry: Application and effectiveness comparison of different genetic algorithm techniques.* Nuclear Engineering and Design, 2012. **250**: p. 701-712.
129. Kennedy, R.P., *Performance-goal based (risk informed) approach for establishing the SSE site specific response spectrum for future nuclear power plants.* Nuclear Engineering and Design, 2011. **241**(3): p. 648-656.
130. Volkanovski, A. and M. Čepin, *Implication of PSA uncertainties on risk-informed decision making.* Nuclear Engineering and Design, 2011. **241**(4): p. 1108-1113.
131. IAEA, *Defence in depth in nuclear safety*, INSAG-10, Editor. 1996, International Atomic Energy Agency: Vienna, Austria.
132. Shin, L.C., et al., *Defense-in-depth and diversity evaluation to cope with design bases events concurrent with common mode failure in digital plant protection system for KNGR.* Nuclear Engineering and Design, 2001. **207**(1): p. 95-104.
133. Huang, H.-W., et al., *Development and diversity and defense-in-depth application of ABWR feedwater pump and controller model.* Nuclear Engineering and Design, 2009. **239**(6): p. 1136-1147.
134. Favaro, F.M. and J.H. Saleh, *Observability-in-depth: an essential complement to the defense-in-depth safety strategy in the nuclear industry.* Nuclear Engineering and Technology, 2014. **46**(6): p. 803-816.
135. IAEA, *Development and Application of Level 1 Probabilistic Safety Assessment for Nuclear Power Plants*, SSG-3, Editor. 2010, International Atomic Energy Agency: Vienna, Austria.
136. IAEA, *Development and Application of Level 2 Probabilistic Safety Assessment for Nuclear Power Plants*, SSG-4, Editor. 2010, International Atomic Energy Agency: Vienna, Austria.
137. USNRC, *State-of-the-Art Reactor Consequence Analyses (SOARCA) Report*, NUREG-1935, Editor. 2010, United States Nuclear Regulatory Commission: Washington, D.C. USA.
138. Garrick, B.J., *PRA-based risk management: history and perspectives*, in *Nuclear News*, July_2014, Editor. 2014, American Nuclear Society. p. 48-53.
139. Smith, P.D., et al., *Seismic Safety Margins Research Program*, NUREG/CR-2015, Editor. 1981, Lawrence Livermore National Laboratory: Livermore, CA, USA.
140. EPRI, *TR 1002988 - Seismic fragility application guide*. 2002, Electric Power Research Institute: California, USA.
141. Mosleh, A., *PRA: a perspective on strenghts, current limitations, and possible improvements.* Nuclear Engineering and Technology, 2014. **46**(1): p. 1-10.
142. Huang, Y.-N., A.S. Whittaker, and N. Luco, *A probabilistic seismic risk assessment procedure for nuclear power plants: (I) Methodology.* Nuclear Engineering and Design, 2011. **241**(9): p. 3996-4003.
143. Huang, Y.-N., A. Whittaker, and N. Luco, *A probabilistic seismic risk assessment procedure for nuclear power plants: (II) Application.* Nuclear Engineering and Design, 2011. **241**(9): p. 3985-3995.
144. Huang, Y.-N., A.S. Whittaker, and N. Luco, *Seismic performance assessment of base-isolated safety-related nuclear structures.* Earthquake Engineering & Structural Dynamics, 2010. **39**(13): p. 1421-1442.
145. FEMA, *FEMA P-58: Seismic Performance Assessment of Buildings*. 2012: California & Washington DC, USA.
146. Bertero, R.D. and V.V. Bertero, *Performance-based seismic engineering: the need for a reliable conceptual comprehensive approach.* Earthquake Engineering & Structural Dynamics, 2002. **31**(3): p. 627-652.

147. Bozorgnia, Y., et al., *Guidelines for performance-based seismic design of tall buildings*, in *PEER Report 2010/05*. 2010, Pacific Earthquake Engineering Research Center: Berkeley, California, USA.
148. Astrella, M.J. and A. Whittaker, *The performance-based design paradigm*, MCEER-05-0011, Editor. 2005, Multidisciplinary Center for Earthquake Engineering Research: Buffalo, New York, USA.
149. Kaviani, P., F. Zareian, and E. Taciroglu, *Performance-based seismic assessment of skewed bridges*, P. 2014/01, Editor. 2014, Pacific Earthquake Engineering Research Center: California, USA.
150. IAEA, *Defining initiating events for purposes of probabilistic safety assessment*, IAEA-TECDOC-719, Editor. 1993, International Atomic Energy Agency: Vienna, Austria.
151. Khericha, S., et al., *Development of Simplified Probabilistic Risk Assessment Model for Seismic Initiating Event*, INL/CON-11-22248, Editor. 2012, Idaho National Laboratory: Idaho Falls, ID, USA.
152. Bedford, T. and R. Cooke, *Probabilistic risk analysis: foundations and methods*. 2001, Cambridge, UK: Cambridge University Press.
153. Acosta, C. and N. Siu, *Dynamic event trees in accident sequence analysis: application to steam generator tube rupture.* Reliability Engineering & System Safety, 1993. **41**(2): p. 135-154.
154. Siu, N., *Risk assessment for dynamic systems: An overview.* Reliability Engineering & System Safety, 1994. **43**(1): p. 43-73.
155. Karanki, D.R. and V.N. Dang, *Quantification of Dynamic Event Trees – A comparison with event trees for MLOCA scenario.* Reliability Engineering & System Safety, 2016. **147**: p. 19-31.
156. Karanki, D.R., T.-W. Kim, and V.N. Dang, *A dynamic event tree informed approach to probabilistic accident sequence modeling: Dynamics and variabilities in medium LOCA.* Reliability Engineering & System Safety, 2015. **142**: p. 78-91.
157. Zamalieva, D., A. Yilmaz, and T. Aldemir, *A probabilistic model for online scenario labeling in dynamic event tree generation.* Reliability Engineering & System Safety, 2013. **120**: p. 18-26.
158. Kennedy, R.P. and M.K. Ravindra, *Seismic fragilities for nuclear power plant risk studies.* Nuclear Engineering and Design, 1984. **79**(1): p. 47-68.
159. Kennedy, R.P., et al., *Probabilistic seismic safety study of an existing nuclear power plant.* Nuclear Engineering and Design, 1980. **59**(2): p. 315-338.
160. EPRI, *TR-103959 - Methodology for developing seismic fragilities*. 1994, Electric Power Research Institute: California, USA.
161. De Grandis, S., M. Domaneschi, and F. Perotti, *A numerical procedure for computing the fragility of NPP components under random seismic excitation.* Nuclear Engineering and Design, 2009. **239**(11): p. 2491-2499.
162. Pisharady, A.S. and P.C. Basu, *Methods to derive seismic fragility of NPP components: A summary.* Nuclear Engineering and Design, 2010. **240**(11): p. 3878-3887.
163. Zentner, I., *Numerical computation of fragility curves for NPP equipment.* Nuclear Engineering and Design, 2010. **240**(6): p. 1614-1621.
164. Klügel, J.-U., *Comment on "Sigma: Issues, Insights and Challenges" by F. O. Strasser, N. A. Abrahamson, and J. J. Bommer.* Seismological Research Letters, 2009. **80**(3): p. 494-498.
165. Paté-Cornell, M.E., *Uncertainties in risk analysis: Six levels of treatment.* Reliability Engineering & System Safety, 1996. **54**(2–3): p. 95-111.
166. Kennedy, R. *Overview if Methods for Seismic PRA and Margin Analysis Including Recent Innovations*. in *Proceedings of the OECD-NEA Workshop on Seismic Risk*. 1999. Tokyo, Japan.
167. Hora, S.C., *Aleatory and epistemic uncertainty in probability elicitation with an example from hazardous waste management.* Reliability Engineering & System Safety, 1996. **54**(2–3): p. 217-223.
168. Kiureghian, A.D. and O. Ditlevsen, *Aleatory or epistemic? Does it matter?* Structural Safety, 2009. **31**(2): p. 105-112.
169. Hofer, E., *When to separate uncertainties and when not to separate.* Reliability Engineering & System Safety, 1996. **54**(2–3): p. 113-118.
170. Hwang, H. *Determination of HCLPF Value for Seismic Margins Study*. in *SMiRT 10*. 1989. Anaheim, California, USA.
171. Park, Y.J., C.H. Hofmayer, and N.C. Chokshi, *Survey of seismic fragilities used in PRA studies of nuclear power plants.* Reliability Engineering & System Safety, 1998. **62**(3): p. 185-195.
172. Kennedy, R.P., B.E. Sarkar, and L.S. Cluff, *On some aspects of seismic fragility evaluation for Diablo Canyon seismic PRA.* Nuclear Engineering and Design, 1990. **123**(2–3): p. 167-188.

173. Bhargava, K., et al., *Evaluation of seismic fragility of structures—a case study.* Nuclear Engineering and Design, 2002. **212**(1–3): p. 253-272.
174. Nakamura, N., et al., *Study of ultimate seismic response and fragility evaluation of nuclear power building using nonlinear three-dimensional finite element model.* Nuclear Engineering and Design, 2010. **240**(1): p. 166-180.
175. EDF_Energy, *Report: EU Sress Test - Hinkley Point B (Rev 001)*. 2012: London.
176. Kafali, C. and M. Grigoriu, *Seismic fragility analysis: Application to simple linear and nonlinear systems.* Earthquake Engineering & Structural Dynamics, 2007. **36**(13): p. 1885-1900.
177. Seyedi, D.M., et al., *Development of seismic fragility surfaces for reinforced concrete buildings by means of nonlinear time-history analysis.* Earthquake Engineering & Structural Dynamics, 2010. **39**(1): p. 91-108.
178. Kim, J.H., I.-K. Choi, and J.-H. Park, *Uncertainty analysis of system fragility for seismic safety evaluation of NPP.* Nuclear Engineering and Design, 2011. **241**(7): p. 2570-2579.
179. Fernandez Ares, A. and A. Fatehi, *Development of probabilistic seismic hazard analysis for international sites, challenges and guidelines.* Nuclear Engineering and Design, 2013. **259**.
180. Krinitzsky, E.L., *Deterministic versus probabilistic seismic hazard analysis for critical structures.* Engineering Geology, 1995. **40**(1–2): p. 1-7.
181. Mualchin, L., *Development of the Caltrans deterministic fault and earthquake hazard map of California.* Engineering Geology, 1996. **42**(4): p. 217-222.
182. Bommer, J.J., *Deterministic vs. probabilistic seismic hazard assessment: an exaggerated and obstructive dichotomy.* Journal of Earthquake Engineering, 2002. **6**(sup001): p. 43-73.
183. McGuire, R.K., *Deterministic vs. probabilistic earthquake hazards and risks.* Soil Dynamics and Earthquake Engineering, 2001. **21**(5): p. 377-384.
184. Di Maio, F., et al., *Integrated Deterministic and Probabilistic Safety Analysis for Safety Assessment of Nuclear Power Plants.* Science and Technology of Nuclear Installations, 2015. **2015**: p. 2.
185. Orozova, I.M. and P. Suhadolc, *A deterministic–probabilistic approach for seismic hazard assessment.* Tectonophysics, 1999. **312**(2–4): p. 191-202.
186. Romeo, R. and A. Prestininzi, *Probabilistic versus deterministic seismic hazard analysis: an integrated approach for siting problems.* Soil Dynamics and Earthquake Engineering, 2000. **20**(1–4): p. 75-84.
187. Cornell, C.A., *Engineering seismic risk analysis.* Bulletin of the Seismological Society of America, 1968. **58**(5): p. 1583-1606.
188. McGuire, R.K., *Fortran program for seismic risk analysis*. 1976, US Geological Survey Open-File Report 76-67.
189. McGuire, R.K., *Probabilistic seismic hazard analysis: Early history.* Earthquake Engineering & Structural Dynamics, 2008. **37**(3): p. 329-338.
190. McGuire, R.K., *Seismic Hazard and Risk Analysis*. 2004: Earthquake Engineering Research Institute.
191. Sen, T.K., *Probabilistic Seismic Hazard Analysis*, in *Fundamentals of Seismic Loading on Structures*, J.W. Sons, Editor. 2009.
192. Gutenberg, B. and C.F. Richter, *Frequency of earthquakes in California.* Bulletin of the Seismological Society of America, 1944. **34**(4): p. 185-188.
193. Youngs, R.R. and K.J. Coppersmith, *Implications of fault slip rates and earthquake recurrence models to probabilistic seismic hazard estimates.* Bulletin of the Seismological Society of America, 1985. **75**(4): p. 939-964.
194. James, N., et al., *Seismic microzonation of a nuclear power plant site with detailed geothechnical, geophysical and site effect studies.* Natural Hazards, 2014. **71**(1): p. 419-462.
195. Sigbjörnsson, R. and N.N. Ambraseys, *Uncertainty Analysis of Strong-Motion and Seismic Hazard.* Bulletin of Earthquake Engineering, 2003. **1**(3): p. 321-347.
196. Restrepo-Velez, L.F. and J.J. Bommer, *An exploration of the nature of the scatter in ground-motion prediction equations and the implications for seismic hazard assessment.* Journal of Earthquake Engineering, 2003. **7**(sup001): p. 171-199.
197. Kulkarni, R.B., R.R. Youngs, and K.J. Coppersmith. *Assessment of confidence intervals for results of seismic hazard analysis*. in *Proceedings of the 8th World Conference on Earthquake Engineering*. 1984. San Francisco, CA, USA.
198. Bommer, J.J., et al., *On the Use of Logic Trees for Ground-Motion Prediction Equations in Seismic-Hazard Analysis.* Bulletin of the Seismological Society of America, 2005. **95**(2): p. 377-389.

199. Bommer, J.J. and F. Scherbaum, *The Use and Misuse of Logic Trees in Probabilistic Seismic Hazard Analysis.* Earthquake Spectra, 2008. **24**(4): p. 997-1009.
200. Foulser-Piggott, R., *Quantifying the epistemic uncertainty in ground motion models and prediction.* Soil Dynamics and Earthquake Engineering, 2014. **65**: p. 256-268.
201. Sabetta, F., et al., *Sensitivity of PSHA results to ground motion prediction relations and logic-tree weights.* Soil Dynamics and Earthquake Engineering, 2005. **25**(4): p. 317-329.
202. Güllü, H. and R. İyisan, *A Seismic Hazard Study through the Comparison of Ground Motion Prediction Equations Using the Weighting Factor of Logic Tree.* Journal of Earthquake Engineering, 2015: p. 1-24.
203. Coppersmith, K.J. and J.J. Bommer, *Use of the SSHAC methodology within regulated environments: Cost-effective application for seismic characterization at multiple sites.* Nuclear Engineering and Design, 2012. **245**(0): p. 233-240.
204. Bommer, J.J., et al., *A SSHAC Level 3 Probabilistic Seismic Hazard Analysis for a New-Build Nuclear Site in South Africa.* Earthquake Spectra, 2015. **31**(2): p. 661-698.
205. Coppersmith, K.J., J.J. Bommer, and R.W. Bryce, *An application of the SSHAC Level 3 process to the probabilistic seismic hazard analysis for nuclear facilities at the Hanford Site, Eastern Washington, USA*. 2014, US Department of Energy: Germantown, MD.
206. Klügel, J.-U., *Probabilistic Seismic Hazard Analysis for Nuclear Power Plants - Current Practice from A European Perspective.* Nuclear Engineering and Technology, 2009. **41**(10): p. 1243-1254.
207. Choi, I.-K., et al., *Development of the site-specific uniform hazard spectra for Korean nuclear power plant sites.* Nuclear Engineering and Design, 2009. **239**(4): p. 790-799.
208. Nakajima, M., et al., *Evaluation of seismic hazard curves and scenario earthquakes for Korean sites based on probabilistic seismic hazard analysis.* Nuclear Engineering and Design, 2007. **237**(3): p. 277-288.
209. Roshan, A.D. and P.C. Basu, *Application of PSHA in low seismic region: A case study on NPP site in peninsular India.* Nuclear Engineering and Design, 2010. **240**(10): p. 3443-3454.
210. Riera, J. and I. Iturrioz. *Influence of seismic source geometry on PSHA predictions in stable continental regions (SCR).* in *23rd International Conference on Structural Mechanics in Reactor Technology*. 2015. Manchester, UK.
211. Abrahamson, N., et al., *Probabilistic Seismic Hazard Analysis for Swiss Nuclear Power Plants Sites (PEGASOS Project)*, in *Final Report*. 2004, Nationale Genossenschaft fur die Lagerung radioaktiver Abfalle (Nagra): Wettingen, Switzerland.
212. Lapajne, J.K. and P. Fajfar, *Seismic hazard reassessment of an existing NPP in Slovenia.* Nuclear Engineering and Design, 1997. **175**(3): p. 215-226.
213. ASCE/SEI_43-05, *Seismic Desing Criteria for Structures, Systems and Components in Nuclear Facilities*. 2005, American Society of Civil Engineers - Structural Engineering Institute: Reston, Virginia, USA.
214. IAEA, *Seismic Hazards in Site Evaluation for Nuclear Installations*, in *Specific Safety Guide SSG-9*. 2010, International Atomic Energy Agency: Vienna, Austria.
215. Katsanos, E.I., A.G. Sextos, and G.D. Manolis, *Selection of earthquake ground motion records: A state-of-the-art review from a structural engineering perspective.* Soil Dynamics and Earthquake Engineering, 2010. **30**(4): p. 157-169.
216. Kwong, N.S., A.K. Chopra, and R.K. McGuire, *Evaluation of ground motion selection and modification procedures using synthetic ground motions.* Earthquake Engineering & Structural Dynamics, 2015. **44**(11): p. 1841-1861.
217. Jayaram, N., T. Lin, and J.W. Baker, *A Computationally Efficient Ground-Motion Selection Algorithm for Matching a Target Response Spectrum Mean and Variance.* Earthquake Spectra, 2011. **27**(3): p. 797-815.
218. Ay, B.Ö. and S. Akkar, *A procedure on ground motion selection and scaling for nonlinear response of simple structural systems.* Earthquake Engineering & Structural Dynamics, 2012. **41**(12): p. 1693-1707.
219. NIST, *Selecting and Scaling Earthquake Ground Motions for Performing Response-History Analyses.* National Institute of Standards and Technology (NIST), 2012.
220. Baker, J.W., *Conditional Mean Spectrum: Tool for Ground-Motion Selection.* Journal of Structural Engineering, 2011. **137**(3): p. 322-331.
221. Huang, Y.-N., et al., *Scaling Earthquake Ground Motions for Performance-Based Assessment of Buildings.* Journal of Structural Engineering, 2011. **137**(3): p. 311-321.
222. Bradley, B.A., *A ground motion selection algorithm based on the generalized conditional intensity measure approach.* Soil Dynamics and Earthquake Engineering, 2012. **40**: p. 48-61.

223. Luco, N. and P. Bazzurro, *Does amplitude scaling of ground motion records result in biased nonlinear structural drift responses?* Earthquake Engineering & Structural Dynamics, 2007. **36**(13): p. 1813-1835.
224. Grant, D.N. and R. Diaferia, *Assessing adequacy of spectrum-matched ground motions for response history analysis.* Earthquake Engineering & Structural Dynamics, 2013. **42**(9): p. 1265-1280.
225. Hancock, J., J.J. Bommer, and P.J. Stafford, *Numbers of scaled and matched accelerograms required for inelastic dynamic analyses.* Earthquake Engineering & Structural Dynamics, 2008. **37**(14): p. 1585-1607.
226. Harmsen, S., D. Perkins, and A. Frankel, *Deaggregation of probabilistic ground motions in the central and eastern United States.* Bulletin of the Seismological Society of America, 1999. **89**(1): p. 1-13.
227. Olsson, A., G. Sandberg, and O. Dahlblom, *On Latin hypercube sampling for structural reliability analysis.* Structural Safety, 2003. **25**(1): p. 47-68.
228. European_Commision, *Report EUR 16559: Proposal for design guidelines for seismically isolated nuclear plants*. 1995.
229. IAEA, *Verification of analysis methods for predicting the behaviour of seismically isolated nuclear structures*. 2002, International Atomic Energy Agency.
230. Takahashi, K., et al., *A development of three-dimensional seismic isolation for advanced reactor systems in Japan - Part 2.* Transactions of the 18th International Conference on Structural Mechanics in Reactor Technology (SMiRT 18), 2005(Paper K10-2).
231. Kato, A., et al., *A development program of three-dimensional seismic isolation for advanced reactor system in Japan.* Transactions of the 17th International Conference on Structural Mechanics in Reactor Technology (SMiRT 17), 2003(Paper K09-1).
232. Cho, S.G., W.K. Park, and S.M. Yun. *Estimation of stiffness characteristics of LRB bearings by finite element analysis*. in *23rd International Conference on Structural Mechanics and Reactor Technology*. 2015. Manchester, UK.
233. Kim, M.K., J.H. Kim, and I.-K. Choi. *A shaking table test for the evaluation of floor response spectrum of seismic isolated structure*. in *23rd International Conference on Structural Mechanics in Reactor Technology*. 2015. Manchester, UK.
234. Choun, Y.-S., J. Park, and I.-K. Choi, *Effects of mechanical property variability in lead rubber bearings on the response of seismic isolation system for different ground motions.* Nuclear Engineering and Technology, 2014. **46**(5): p. 605-618.
235. Ahmad, K., M.A. Sayed, and D. Kim. *Seismic fragility of base-isolated nuclear power plant structures considering spatially varying ground motions*. in *23rd International Conference on Structural Mechanics in Reactor Technology*. 2015. Manchester, UK.
236. Kumar, M., A.S. Whittaker, and M.C. Constantinou, *Experimental investigation of cavitation in elastomeric seismic isolation bearings.* Engineering Structures, 2015. **101**: p. 290-305.
237. Huang, Y.-N., et al., *Response of base-isolated nuclear structures for design and beyond-design basis earthquake shaking.* Earthquake Engineering & Structural Dynamics, 2013. **42**(3): p. 339-356.
238. Whittaker, A.S. and M. Kumar, *Seismic isolation of nuclear power plants.* Nuclear Engineering and Technology, 2014. **46**(5): p. 569-580.
239. Cho, S.G., G. So, and D. Kim. *Comparative analysis of seismic response of different base isolated systems by shaking table test*. in *23rd International Conference on Structural Mechanics in Reactor Technology*. 2015. Manchester, UK.
240. Kumar, M., A.S. Whittaker, and M.C. Constantinou, *Seismic isolation of nuclear power plants using elastomeric bearings*, in *MCEER-15-0008*. 2015, Multidisciplinary Center for Earthquake Engineering Research (MCEER): Buffalo, New York, USA.
241. Kumar, M. and A. Whittaker. *On the calculation of the clearance to the hard stop for seismically isolated nuclear power plants*. in *23rd International Conference on Structural Mechanics in Reactor Technology*. 2015. Manchester, UK.
242. Minagawa, K., S. Fujita, and Y. Hase. *Seismic response analysis of isolated building considering position and nonlinearity of rubber bearings*. in *23rd International Conference on Structural Mechanics and Reactor Technology*. 2015. Manchester, UK.
243. Wang, Y. and L. Ibarra. *Seismically optimization of modified base-isolated systems for next generation nuclear structures*. in *23rd International Conference on Stuctural Mechanics in Reactor Technology*. 2015. Manchester, UK.
244. Shimizu, H., et al. *Development of evaluation method for seismic isolation systems of nuclear power facilities - Proposal for a base-isolated design, methodology to install NPP's facilities*. in

23rd International Conference on Structural Mechanics in Reactor Technology. 2015. Manchester, UK.

245. Mori, T., et al. *Development of evaluation method for seismic isolation systems of nuclear power facilities - Break test of full scale lead rubber bearings for nuclear facilities, Part 3 Finite element analysis model for break test*. in *23rd International Conference on Structural Mechanics in Reactor Technology*. 2015. Manchester, UK.
246. Watanabe, H., et al. *Development of evaluation method for seismic isolation systems of nuclear power facilities - Experimental study on structural characteristics of base isolated foundation coupled with seismic isolator*. in *23rd International Conference on Structural Mechanics in Reactor Technology*. 2015. Manchester, UK.
247. Kanazawa, K., et al. *Development of evaluation method for seismic isolation systems of nuclear power facilities - Break test of full scale lead rubber bearings for nuclear facilities, Part 4 Break boundary criteria of real-size isolator specimens*. in *23rd International Conference on Structural Mechanics in Reactor Technology*. 2015. Manchester, UK.
248. Imaoka, T., et al. *Development of evaluation method for seismic isolation systems of nuclear power facilities - Break test of full scale lead rubber bearings for nuclear facilities, Part 1 Outline of break test of LRB of 1.6m in diameter*. in *23rd International Conference on Structural Mechanics in Reactor Technology*. 2015. Manchester, UK.
249. Nakayama, T., et al. *Development of evaluation method for seismic isolation systems of nuclear power facilities - Break test of full-scale lead rubber bearings for nuclear facilities, Part 2 Ultimate properties of LRB based on break tests*. in *23rd International Conference on Structural Mechanics in Reactor Technology*. 2015. Manchester, UK.
250. Chen, J., et al., *Seismic analysis and evaluation of the base isolation system in AP1000 NI under SSE loading.* Nuclear Engineering and Design, 2014. **278**: p. 117-133.
251. Jung, J.-W., H. Jang, and J.-W. Hong. *Floor response spectrum analysis of base isolated nuclear power plant and simplified model*. in *23rd International Conference on Structural Mechanics in Reactor Technology*. 2015. Manchester, UK.
252. Kubo, T., et al., *A seismic design of nuclear reactor building structures applying seismic isolation system in a high seismicity region - a feasibility case study in Japan.* Nuclear Engineering and Technology, 2014. **46**(5): p. 581-594.
253. Forni, M., et al., *Seismic isolation of lead-cooled reactors: the European Project SILER.* Nuclear Engineering and Technology, 2014. **46**(5): p. 595-604.
254. Chataigner, J., et al. *Preliminary design and optimization of an energy dissipation device for high energy dropped loads*. in *23rd International Conference on Structural Mechanics in Reactor Technology*. 2015. Manchester, UK.
255. Nawrotzki, P. and D. Siepe. *Seismic protection of machinery, buildings and equipment of nuclear power plants by using 3-D base control systems*. in *23rd International Conference on Structural Mechanics in Reactor Technology*. 2015. Manchester, UK.
256. Kurmann, D., G. Attanasi, and D. Proske. *A base-isolated system for severe acceident-management at Beznau NPP*. in *23rd International Conference on Structural Mechanics in Reactor Technology*. 2015. Manchester, UK.
257. Medel-Vera, C. and T. Ji, *A stochastic ground motion accelerogram model for Northwest Europe.* Soil Dynamics and Earthquake Engineering, 2016. **82**: p. 170-195.
258. Goes, S., et al., *The effect of plate stresses and shallow mantle temperatures on tectonics of northwestern Europe.* Global and Planetary Change, 2000. **27**(1–4): p. 23-38.
259. Ambraseys, N.N., *Intensity-attenuation and magnitude-intensity relationships for northwest european earthquakes.* Earthquake Engineering & Structural Dynamics, 1985. **13**(6): p. 733-778.
260. Young, J.B., et al., *The Flinn-Engdahl Regionalisation Scheme: The 1995 revision.* Physics of the Earth and Planetary Interiors, 1996. **96**(4): p. 223-297.
261. Ambraseys, N.N., et al., *Internet site for European strong-motion data.* Bolletino di Geofisica Teorica ed Applicata, 2004. **45**(3): p. 113-129.
262. Douglas, J., *Preface of special issue: A new generation of ground-motion models for Europe and the Middle East.* Bulletin of Earthquake Engineering, 2014. **12**(1): p. 307-310.
263. Boore, D.M., W.B. Joyner, and T.E. Fumal, *Estimation of Response Spectra and Peak Accelerations from Western North American Earthquakes: An Interim Report*. 1993, USGS.
264. Douglas, J. and B. Halldórsson. *On the use of aftershocks when deriving ground-motion prediction equations*. in *9th U.S. National and 10th Canadian Conference on Earthquake Engineering*. 2010. Toronto, Ontario, Canada.
265. Penzien, J. and M. Watabe, *Characteristics of 3-dimensional earthquake ground motions.* Earthquake Engineering & Structural Dynamics, 1975. **3**(4): p. 365-373.

266. Kubo, T. and J. Penzien, *Time and frequency domain analyses of three dimensional ground motions San Fernando Earthquake*. 1976, Earthquake Engineering Research Center.
267. Rawlings, J.O., S.G. Pantula, and D.A. Dickey, *Applied Regression Analysis: A Research Tool*. Springer Texts in Statistics. 1998: Springer.
268. Abrahamson, N. and R. Youngs, *A stable algorithm for regression analyses using the random effects model.* Bulletin of the Seismological Society of America, 1992. **82**(1): p. 505-510.
269. Musson, R.M.W., P.C. Marrow, and P.W. Winter, *Attenuation of earthquake ground motion in the UK, Report AEA/CS/16422000/ZJ745/004, AEA Technology Consultancy Services, 30 pp.* 1994.
270. Akkar, S. and J.J. Bommer, *Empirical Equations for the Prediction of PGA, PGV, and Spectral Accelerations in Europe, the Mediterranean Region, and the Middle East.* Seismological Research Letters, 2010. **81**(2): p. 195-206.
271. Ambraseys, N.N., et al., *Equations for the Estimation of Strong Ground Motions from Shallow Crustal Earthquakes Using Data from Europe and the Middle East: Horizontal Peak Ground Acceleration and Spectral Acceleration.* Bulletin of Earthquake Engineering, 2005. **3**(1): p. 1-53.
272. Bommer, J.J., et al., *The Influence of Magnitude Range on Empirical Ground-Motion Prediction.* Bulletin of the Seismological Society of America, 2007. **97**(6): p. 2152-2170.
273. Dahle, A., H. Bungum, and L.B. Kvamme, *Attenuation models inferred from intraplate earthquake recordings.* Earthquake Engineering & Structural Dynamics, 1990. **19**(8): p. 1125-1141.
274. Toro, G.R., N.A. Abrahamson, and J.F. Schneider, *Model of Strong Ground Motions from Earthquakes in Central and Eastern North America: Best Estimates and Uncertainties.* Seismological Research Letters, 1997. **68**(1): p. 41-57.
275. Liang, J.Z., et al., *Estimation of Strong Ground Motions in Southwest Western Australia with a Combined Green's Function and Stochastic Approach.* Journal of Earthquake Engineering, 2008. **12**(3): p. 382-405.
276. Kennedy, J., H. Hao, and B. Gaull, *Earthquake ground motion attenuation relations for SWWA*, in *Earthquake Engineering in Australia*. 2005: Albury, New South Wales, Australia. p. Paper 15.
277. Raghu Kanth, S.T.G. and R.N. Iyengar, *Estimation of seismic spectral acceleration in Peninsular India.* Journal of Earth System Science, 2007. **116**(3): p. 199-214.
278. Chen, L., *Ground motion attenuation relationships based on Chinese and Japanese strong ground motion data*, in *European School for Advanced Studies in Reduction of Seismic Risk*. 2008, ROSE School: Pavia, Italy.
279. Bakun, W.H. and A. McGarr, *Differences in attenuation among the stable continental regions.* Geophysical Research Letters, 2002. **29**(23): p. 2121.
280. Li, Z.X., Z.C. Li, and W.X. Shen, *Sensitivity Analysis for Floor Response Spectra of Nuclear Reactor Buildings (in Chinese).* Nuclear Power Engineering, 2005. **26**(1).
281. Choi, I.-K., et al., *Probabilistic seismic risk analysis of CANDU containment structure for near-fault earthquakes.* Nuclear Engineering and Design, 2008. **238**(6): p. 1382-1391.
282. Ozaki, M., et al., *Improved response factor methods for seismic fragility of reactor building.* Nuclear Engineering and Design, 1998. **185**(2–3): p. 277-291.
283. Yoo, B., et al., *Seismic base isolation technologies for Korea advanced liquid metal reactor.* Nuclear Engineering and Design, 2000. **199**(1–2): p. 125-142.
284. Huang, Y.-N., et al., *Seismic demands on secondary systems in base-isolated nuclear power plants.* Earthquake Engineering & Structural Dynamics, 2007. **36**(12): p. 1741-1761.
285. HSE, *Health and Safety Executive - Office for Nuclear Regulation. T/AST/013 - Issue 4: Technical Assessment Guide - External Hazards*. 2011.
286. Musson, R.M.W. and S. Sargeant, *Eurocode 8 seismic hazard zoning maps for the UK.* British Geological Survey, 2007. **Technical Report, CR/07/125N**.
287. Campbell, K.W. and Y. Bozorgnia, *NGA Ground Motion Model for the Geometric Mean Horizontal Component of PGA, PGV, PGD and 5% Damped Linear Elastic Response Spectra for Periods Ranging from 0.01 to 10* Earthquake Spectra, 2008. **24**(1): p. 139-171.
288. Van Houtte, C., S. Drouet, and F. Cotton, *Analysis of the Origins of κ (Kappa) to Compute Hard Rock to Rock Adjustment Factors for GMPEs.* Bulletin of the Seismological Society of America, 2011. **101**(6): p. 2926-2941.
289. Beyer, K. and J.J. Bommer, *Relationships between Median Values and between Aleatory Variabilities for Different Definitions of the Horizontal Component of Motion.* Bulletin of the Seismological Society of America, 2006. **96**(4A): p. 1512-1522.
290. Halldórsson, B. <*http://civil.eng.buffalo.edu/engseislab/products.htm*>. 2004.
291. Halldorsson, B. and A.S. Papageorgiou, *Calibration of the Specific Barrier Model to Earthquakes of Different Tectonic Regions.* Bulletin of the Seismological Society of America, 2005. **95**(4): p. 1276-1300.

292. Cho, S.G. and Y.H. Joe, *Seismic fragility analyses of nuclear power plant structures based on the recorded earthquake data in Korea.* Nuclear Engineering and Design, 2005. **235**(17–19): p. 1867-1874.
293. Dehghani, M. and R. Tremblay. *Standard Dynamic Loading Protocols for Seismic Qualification of BRBFs in Eastern and Western Canada*. in *15th World Conference on Earthquake Engineering*. 2012. Lisbon, Portugal.
294. Llambias, J.M., *The use of the uniform risk spectra in the seismic PSA for a PWR power station.* Nuclear Engineering and Design, 1995. **154**(2): p. 193-201.
295. Ellingwood, B., *NUREG/GR-0008 - Validation of seismic probabilistic risk assessments of nuclear power plants*. 1994, US Nuclear Regulatory Commission: Washington, DC.
296. Stafford, P., F. Strasser, and J. Bommer, *An evaluation of the applicability of the NGA models to ground-motion prediction in the Euro-Mediterranean region.* Bulletin of Earthquake Engineering, 2008. **6**(2): p. 149-177.
297. Campbell, K. and Y. Bozorgnia, *Next Generation Attenuation (NGA) empirical ground motion models: can they be used in Europe?*, in *First European Conference on Earthquake Engineering and Seismology*. 2006: Geneva, Switzerland.
298. Mavroeidis, G.P. and A.S. Papageorgiou, *A Mathematical Representation of Near-Fault Ground Motions.* Bulletin of the Seismological Society of America, 2003. **93**(3): p. 1099-1131.
299. Sollogoub, P. *Seismic Isolation of Nuclear Installations in France*. in *SILER International Educational Workshop*. 2014. Rome, Italy.
300. Forni, M., *SILER Report Summary*, in *Final Report Summary - SILER (Seismic-Initiated events risk mitigation in LEad-cooled Reactors)*. 2015, European Union: Bologna, Italy.
301. Moretti, G. and U. Pasquali. *Seismic Isolation of LFR Reactor Buildings*. in *SILER International Educational Workshop*. 2013. Rome, Italy.
302. Kostarev, V.V., A.V. Petrenko, and P.S. Vasilyev, *A new method for essential reduction of seismic and external loads on NPP's structures, systems and components.* Transactions of the 17th International Conference on Structural Mechanics in Reactor Technology (SMiRT 17), 2003(Paper K13-1).
303. Naeim, F. and J.M. Kelly, *Design of seismic isolated structures. From theory to practice*. 1999: Wiley.
304. Chopra, A., *Dynamics of Structures. Theory and Applications to Earthquake Engineering*. 1995, New Jersey: Prentice Hall.
305. Tuñón-Sanjur, L., et al., *Finite element modeling of the AP1000 nuclear island for seismic analyses at generic soil and rock sites.* Nuclear Engineering and Design, 2007. **237**(12–13): p. 1474-1485.
306. Saxena, N. and D.K. Paul, *Effects of embedment including slip and separation on seismic SSI response of a nuclear reactor building.* Nuclear Engineering and Design, 2012(0).
307. Ostadan, F. and R. Kennedy, *Consistent site-response/soil-structure interaction analysis and evaluation.* Nuclear Engineering and Design, 2014. **269**(0): p. 72-77.
308. Saxena, N., D.K. Paul, and R. Kumar, *Effects of slip and separation on seismic SSI response of nuclear reactor building.* Nuclear Engineering and Design, 2011. **241**(1): p. 12-17.
309. Elkhoraibi, T., A. Hashemi, and F. Ostadan, *Probabilistic and deterministic soil structure interaction analysis including ground motion incoherency effects.* Nuclear Engineering and Design, 2014. **269**(0): p. 250-255.
310. Wolf, J.P., *Soil-structure-interaction analysis in time domain.* Nuclear Engineering and Design, 1989. **111**(3): p. 381-393.
311. Wagenknecht, E., *Response of a NPP reactor building under seismic action with regard to different soil properties.* Nuclear Engineering and Design, 1987. **104**(2): p. 187-195.
312. Bhaumik, L. and P. Raychowdhury, *Seismic response analysis of a nuclear reactor structure considering nonlinear soil-structure interaction.* Nuclear Engineering and Design, 2013. **265**(0): p. 1078-1090.
313. Llambias, J.M., D.J. Shepherd, and M.D. Rodwell, *Sensitivity of seismic structural response to interpretation of soils data.* Soil Dynamics and Earthquake Engineering, 1993. **12**(6): p. 337-342.
314. Llambias, J.M. *Validation of Seismic Soil Structure Interaction (SSI) Methodology for a UK PWR Nuclear Power Station*. in *12th International Conference on on Structural Mechanics in Reactor Technology (SMiRT 12)*. 1993. Stuttgart, Germany.
315. Atkinson, G.M. and K. Goda, *Effects of Seismicity Models and New Ground-Motion Prediction Equations on Seismic Hazard Assessment for Four Canadian Cities.* Bulletin of the Seismological Society of America, 2011. **101**(1): p. 176-189.

316. Vamvatsikos, D. and C.A. Cornell, *Applied Incremental Dynamic Analysis.* Earthquake Spectra, 2004. **20**(2): p. 523-553.
317. Vamvatsikos, D. and C.A. Cornell, *Incremental dynamic analysis.* Earthquake Engineering & Structural Dynamics, 2002. **31**(3): p. 491-514.
318. Zareian, F. and H. Krawinkler, *Assessment of probability of collapse and design for collapse safety.* Earthquake Engineering & Structural Dynamics, 2007. **36**(13): p. 1901-1914.
319. Liao, K.-W., Y.-K. Wen, and D.A. Foutch, *Evaluation of 3D Steel Moment Frames under Earthquake Excitations. I: Modeling.* Journal of Structural Engineering, 2007. **133**(3): p. 462-470.
320. Tagawa, H., G. MacRae, and L. Lowes, *Probabilistic evaluation of seismic performance of 3-story 3D one- and two-way steel moment-frame structures.* Earthquake Engineering & Structural Dynamics, 2008. **37**(5): p. 681-696.
321. Bradley, B.A., *A critical examination of seismic response uncertainty analysis in earthquake engineering.* Earthquake Engineering & Structural Dynamics, 2013. **42**(11): p. 1717-1729.
322. Kiani, J. and M. Khanmohammadi, *New Approach for Selection of Real Input Ground Motion Records for Incremental Dynamic Analysis (IDA).* Journal of Earthquake Engineering, 2015. **19**(4): p. 592-623.
323. Haselton, C., et al., *Evaluation of ground motion selection and modification methods: predicting median interstory drift response of buildings*, in *PEER Report 2009/01*. 2009, Pacific Earthquake Engineering Research Center: California, Berkeley.
324. Azarbakht, A. and M. Dolšek, *Progressive Incremental Dynamic Analysis for First-Mode Dominated Structures.* Journal of Structural Engineering, 2011. **137**(3): p. 445-455.
325. Lin, T. and J. Baker, *Introducing Adaptive Incremental Analysis: A New Tool for Linking Ground Motion Selection and Structural Response Assessment*, in *11th International Conference on Structural Safety & Reliability*. 2013: New York.
326. Schuëller, G.I., H.J. Pradlwarter, and P.S. Koutsourelakis, *A critical appraisal of reliability estimation procedures for high dimensions.* Probabilistic Engineering Mechanics, 2004. **19**(4): p. 463-474.
327. Zuev, K.M. and L.S. Katafygiotis, *The Horseracing Simulation algorithm for evaluation of small failure probabilities.* Probabilistic Engineering Mechanics, 2011. **26**(2): p. 157-164.
328. Au, S.-K. and J.L. Beck, *Estimation of small failure probabilities in high dimensions by subset simulation.* Probabilistic Engineering Mechanics, 2001. **16**(4): p. 263-277.
329. Symans, M., et al., *Energy Dissipation Systems for Seismic Applications: Current Practice and Recent Developments.* Journal of Structural Engineering, 2008. **134**(1): p. 3-21.
330. Akkar, S., et al., *Reference database for seismic ground-motion in Europe (RESORCE).* Bulletin of Earthquake Engineering, 2014. **12**(1): p. 311-339.
331. Dabaghi, M. and A. Der Kiureghian, *Stochastic modeling and simulation of near-fault ground motions for performance-based earthquake engineering*, in *PEER Report 2014/20*. 2014, Pacific Earthquake Engineering Research Center: Berkeley, California, USA.
332. Gürpinar, A., A. Godoy, and J.J. Johnson. *Considerations for beyond design basis external hazards in NPP safety analysis*. in *23rd International Conference on Structural Mechanics in Reactor Technology*. 2015. Manchester, UK.
333. Niel, J.-C., *French approach to European stress test: International perspective on lessons learnt from Fukushima*, ASN_(French_nuclear_regulatory_body), Editor. 2014, US Nuclear Regulatory Commission.
334. Huang, Y.-N., et al., *Assessment of base-isolated nuclear structures for design and beyond-design basis earthquake shaking*, in *MCEER-09-0008*. 2009, Multidisciplinary Center for Earthquake Engineering Research (MCEER): Buffalo, New York, USA.

Appendix A

Seismic protection technology for nuclear power plants: a systematic review

Journal of Nuclear Science and Technology, 2015
Vol. 52, No. 5, 607–632, http://dx.doi.org/10.1080/00223131.2014.980347

Taylor & Francis
Taylor & Francis Group

REVIEW

Seismic protection technology for nuclear power plants: a systematic review

Carlos Medel-Vera* and Tianjian Ji

School of Mechanical, Aerospace and Civil Engineering, The University of Manchester, M13 9PL, Manchester, United Kingdom

(*Received 22 July 2014; accepted final version for publication 20 October 2014*)

Seismic protection systems (SPS) have been developed and used successfully in conventional structures, but their applications in nuclear power plants (NPPs) are scarce. However, valuable research has been conducted worldwide to include SPS in nuclear engineering design. This study aims to provide a state-of-the-art review of SPS in nuclear engineering and to answer four significant research questions: (1) why are SPS not adopted in the nuclear industry and what issues have prevented their deployment? (2) what types of SPS are being considered in nuclear engineering research? (3) what are the strategies for location of SPS within NPPs? and (4) how may SPS provide improved structural performance and safety of NPPs under seismic actions? This review is conducted following the procedures of systematic reviews, where possible. The issues concerning the use of SPS in NPPs are identified: cost, safety, licensing and scarcity of applications. NPPs demand full structural integrity and reactor's safe shutdown during earthquake actions. Therefore, horizontal isolation may be insufficient in active seismic zones and isolation in the vertical direction may be required. Based on the results in this review, it is likely that next generation reactors in seismic zones will include state-of-the-art SPS to achieve full standardised design.

Keywords: nuclear power plant; nuclear reactor; safety; seismic protection technology/system; seismic isolation; energy dissipation; vibration control

Downloaded by [The University of Manchester Library] at 08:36 21 June 2016

1. Introduction

Seismic protection systems (SPS) are currently considered to be part of a proven and mature technology for mitigating the effects of seismic actions in a wide range of civil structures [1,2]. However, there are currently only two nuclear power plants (NPPs) equipped with such technology, and these were designed about 40 years ago [3]. There is a clear difference between developments in two areas: on the one hand, the development of SPS and their successful application in controlling seismic effects in a broad variety of civil structures; on the other hand, the growing nuclear engineering industry, whose evolution has not included SPS to provide increased seismic safety in its structures. Despite the fact that no NPP has been built equipped with SPS in the last 40 years, extensive research has been conducted in different countries in order to include seismic protection technologies in nuclear engineering design. The first review of seismic isolation for nuclear structures was published 35 years ago [4]. The last peered literature review on this topic was published over 20 years ago [5]. This work aims to provide an update review and includes publications from 1980s to 2010s and answer four specific review questions.

This review is conducted following the procedure of a systematic review [6], where possible. This methodology is often used in health care and medical research [7,8], and is normally used to assess a wider range of experiments, interventions or trials. A systematic review can be seen as a process, in which a group of protocols, checklists or procedures are followed during a literature review in order to answer specific questions. As it is systematic, a similar outcome can be reached by other researchers following the same or similar procedures. At the end of the process, a sound body of evidence has been assembled based on the best information available. This should allow the original questions to be answered and provide a foundation for a critical analysis of the existing research.

All of the general procedures of a systematic review are followed, except the realisation of meta-analysis, as it is not applicable in this qualitative research. The modified methodology consists of five steps.

*Corresponding author. Email: carlos.medelvera@postgrad.manchester.ac.uk

© 2014 Atomic Energy Society of Japan. All rights reserved.

Downloaded by [The University of Manchester Library] at 08:36 21 June 2016

Table 1. Key words and descriptors used to define the search strategy.

(1) Nuclear power plants/reactors
(2) Seismic protection technologies/systems
(3) Seismic isolation
(4) Energy dissipation
(5) Vibration control

1.1. Step 1: review questions

Establishing clear questions is a fundamental requirement for defining the framework of the review. In this light, four key questions have been identified and used in the present work: (1) why are SPS not used in the nuclear industry and what issues have prevented their deployment in NPPs? (2) what sort of seismic protection devices are being considered in nuclear engineering research? (3) what are the strategies for the location of SPS within NPPs? and (4) how may SPS help to improve structural performance and safety of NPPs under seismic actions? This work aims to answer the four questions and identify areas for further research through providing a literature review of SPS in nuclear engineering research.

1.2. Step 2: search strategy

A search strategy needs to be defined, comprising keywords/descriptors and sources of information. For this work, the keywords used for the initial search are listed in Table 1.

The sources of information used for this work are the international peer-reviewed journals listed in Table 2 and the recent conference proceedings on nuclear/earthquake engineering shown in Table 3. The proceedings of the latest conferences on Structural Mechanics in Reactor Technology (SMiRT) held in 2011 (New Delhi, India) and 2013 (San Francisco, CA, USA) were not available for public domain at the moment of submission of this work. The search provides more than 350 papers. In addition, four books about core subjects for this work (both nuclear energy and seismic protection technologies) were consulted and three books about systematic reviews were also included.

Table 2. Journals examined in the search.

Journal	Publisher
(1) *Journal of Nuclear Science and Technology*	Taylor & Francis
(2) *Nuclear Engineering and Design*	Elsevier
(3) *Earthquake Engineering and Structural Dynamics*	Wiley
(4) *Engineering Structures*	Elsevier
(5) *Earthquake Spectra*	EERI

Table 3. Conference proceedings examined in the search

Conference	Year
(1) 15th World Conference on Earthquake Engineering	2012
(2) 20th SMiRT (Structural Mechanics in Reactor Technology)	2009
(3) 19th SMiRT (Structural Mechanics in Reactor Technology)	2007
(4) 18th SMiRT (Structural Mechanics in Reactor Technology)	2005
(5) 17th SMiRT (Structural Mechanics in Reactor Technology)	2003
(6) 16th SMiRT (Structural Mechanics in Reactor Technology)	2001

1.3. Step 3: selection criteria

The abstracts and conclusions of the selected papers were carefully read and their body scanned and read to different degrees. Selection criteria were set to discard those studies which were not directly related to any of the four review questions. The outcome of this step resulted in 80 relevant papers. With the seven books this gave a total of 87 references selected for this work.

1.4. Step 4: individual findings

Each reference was analysed, its contribution was extracted and presented in standardised tables. In this way, a body of information was constructed aiming to ease the interpretation of results in the next stage. Tables 6 and 7 are the outcome of this step.

1.5. Step 5: analysis and interpretation

Based on the reviewers' judgement, all the evidence/information during the process are gathered and analysed in such a way that the review questions can be appropriately answered. This step forms the main body of this review and is presented in five sections:

- Section 2 is aimed at identifying links between the areas of seismic protection technologies and the nuclear industry and examining how these aspects affect the low acceptance of SPS in NPPs. This section attempts to answer the first review question.
- Section 3 aims to characterise the devices in SPS for use in nuclear facilities. This characterisation is made in terms of physical (e.g. geometry, material, etc.) and mechanical (e.g. stiffness, damping, etc.) properties, identifying similarities and differences in comparison with those considered in conventional structures. This section contributes to answering the second review question.
- The purpose of Section 4 is to establish the spatial configuration (e.g. two-dimensional (2D), three-dimensional (3D), plan and height distribution, etc.) of how the seismic protection is considered

for nuclear facilities, recognising similarities and differences in comparison to approaches used in traditional civil structures. This section is intended to answer the third review question.

- As most of the research conducted relates to the safety-related parts of a nuclear facility, Section 5 aims to complement the answers presented in the last two sections by addressing SPS for non-safety-related equipment of NPPs.
- Section 6 has two objectives. First, the establishment of how the devices (Section 3) and spatial configurations (Section 4) may provide a substantial increment in seismic safety for NPPs. This part attempts to answer the fourth review question. Second, this section covers future research and identifies new research questions on this topic.

Downloaded by [The University of Manchester Library] at 08:36 21 June 2016

2. Key issues for seismic protection systems of nuclear power plants

2.1. *Development of SPS for NPPs*

The deployment of SPS, and particularly seismic isolation in NPPs, started in the 1970s with two facilities: Koeberg NPP in South Africa, which had two isolated unit plants; and Cruas NPP in France, which had four isolated unit plants [3,9]. After this promising start, various countries with a wide range of seismic activities reported research on the applicability of SPS in future nuclear power stations. During the 1980s in Japan, a joint commercial industry project began long-term research on the feasibility of the use of seismic isolation in combination with energy dissipation devices for light water reactors (LWRs) [10,11]. This is currently the most common nuclear reactor in the world, comprising 80% of the units worldwide [12]. Also during the 1980s, a joint government, industry and academia project in the USA started to develop a comprehensive Research and development (R&D) programme on the applicability of seismic isolation into NPPs [13]. By the end of 1980s, research efforts were focused on developing the first seismically protected American nuclear reactor, the Advanced Liquid Metal Reactor (ALMR), supported by high-damping rubber bearings (HDRB). This project aimed to develop a standardised reactor building in order to make it seismically safe and economically competitive [14]. At the same time, similar efforts were made in Italy for the development of innovative nuclear reactors, called RSP/I by their Italian initials, which would provide high levels of seismic safety by the addition of HDRB. Again, the main objective of this initiative was the standardisation of their design in order to reach not only rigorous safety levels, but also economic competitiveness [15]. Even countries with low to medium seismicity reported investigations with the same objectives. In the early 1990s, the United Kingdom was part of a tripartite agreement of power industries, alongside the USA and Japan, contributing through experimental research on the behaviour of laminated rubber bearings and viscous dampers applicable to liquid-metal-cooled reactors (LMR) [16]. Similarly, by the mid-1990s, a long-term R&D project was developed in South Korea intending to determine the effectiveness of different types of laminated rubber bearings for the nuclear industry, focused on their applicability to the Korea Advanced Liquid Metal Reactor (KALIMER) [17]. During mid-1980s, the local experience in New Zealand on seismic isolation was reported based on lead–rubber bearings (LRBs) and their potential application to nuclear reactors [18].

A common feature of the earlier work and many subsequent research projects was the standardised seismic design of the so-called 'nuclear island'. This is formed by the containment vessel and internal safety-related components, including the reactor vessel, all of them supported by a common foundation structure [19,20]. A standardised seismic design using SPS is aimed at the possibility that a NPP would become site-independent of the local seismicity of the construction location. This may promote the deployment of the same NPP design in any geographical region, regardless of how severe their seismicity levels are. The potential benefits of a standardised seismic design provided by the use of SPS have a direct impact on the following issues: (1) reducing costs, both in the amount of structure needed and the seismic equipment qualification, be it analytical and/or experimental proof of the adequacy of safety-related equipment to withstand seismic loads; (2) a substantial increment in safety margins including the assurance of full structural integrity after a severe earthquake; and (3) an improvement of economic competitiveness in comparison with other sources of energy and simplification of licensing procedures [5,15,16,19,21–23]. However, it seems that the limited number of real applications of seismically protected NPPs and the lack of specific codes and standards to design SPS for nuclear structures are the key reasons in preventing their deployment [3,23].

The nuclear industry is developing safer and more efficient nuclear reactors, but the systems become increasingly sensitive to seismic loads. Coladant [9] and Gantenbein and Buland [24] pointed out that fast breeder reactors (FBRs), belonging to the so-called Generation III/III+, were more sensitive to seismic loads than pressurised water reactors (PWRs) belonging to the Generation II. Lo Frano and Forasassi [25,26] pointed out that the primary coolant in a lead-cooled fast reactor (LFR, in the category of *Generation IV*) is a high-mass-density fluid and additional inertia forces (sloshing) should be taken into account to ensure an adequate seismic response of the reactor. In addition, Austin et al. [16], Kato et al. [27] and Okamura et al. [28] pointed out that modern reactors were increasingly subjected to larger thermal loads in comparison with previous versions. One way to reduce this thermal stress intensity could be achieved by using thinner structural elements, which in turn may lead to an unsatisfactory performance of

the nuclear island under seismic loads. In this light, SPS provide a solution, compromising between the thinner elements and better seismic mitigation features, in comparison with the design of previous generation rectors. It is likely that the next generation of reactors in development, Generations III and IV, will be more demanding in terms of their serviceability requirements under seismic actions. Consequently, SPS may play a major role in assuring this functionality requirement in NPPs.

The following subsections describe the four issues identified by the seismic protection field and the nuclear industry and how they relate to each other.

2.2. *Cost*

Due to the limited real applications of seismic isolated NPPs, it is difficult to provide sound remarks about cost. Nevertheless, some insightful considerations have been reported in the literature. It was early suggested that, in terms of total project costs, no major differences can be expected between a seismically isolated NPP and the non-protected version of the same facility [29–31]. More recently, Malushte and Whittaker [23] reported concerns about the exceptionally high construction costs of next generation NPPs, and the use of SPS would reduce the overall schedule due to a standardised seismic design. For a seismically protected NPP, it is necessary to consider the costs of the SPS plus the elements required to fit the external devices and the seismic gap elements required to accommodate displacements with adjacent non-isolated structures. However, there is also the reduction of costs related to the lower seismic design loads, which would lead to a reduction in the size of the main structural elements and the seismic qualification of safety-related equipment [18,19]. It is acknowledged that seismic loads may not control the design of NPPs, which is more likely to be controlled by radiation shielding and/or loss of coolant accident. However, this does not necessarily apply for many safety-related equipment [23].

The cost of a generic SPS depends on the level of protection required, and therefore, its complexity. However, it is necessary to consider the addition of certain sub-structures, for example, an upper raft acting as a support for the entire nuclear island. This is required in order to decouple the nuclear island from the ground, considering the presence of the SPS between the upper raft and the lower raft (foundation). Some results for non-nuclear applications reported that a seismic isolation system may be around 2%–4% of the overall cost of the building [29]. Similar figures were reported by Staudacher [31] who pointed out a cost of about 5%–10% of raw construction, which in turn is roughly one-third of the total building cost. As the equipment inside a nuclear facility is expected to account for most of the total cost of the facility, lower relative percentages are to be expected than for non-nuclear buildings. Skinner et al. [32] estimated that the cost of generic SPS was less than 2% of the overall cost of an NPP.

Reduction of construction costs is directly related to the consumption of concrete and steel reinforcement. Kato et al. [10] reported savings between 5% and 10% in a seismically isolated boiling water reactor (BWR) building in comparison with the non-isolated version. For a non-nuclear application, Buckle [18] reported similar figures, reaching savings of 10% in material costs. It is acknowledged that the discussion above is based on the promising early steps of nuclear engineering research. No updated information about costs has been found in the literature for this review. However, a related scenario is on non-nuclear applications. De la Llera et al. [33] reported that two seismically isolated high-critical hospitals had costs in the same range of conventional designs.

Another aspect that should not be overlooked is related to the engineering fees. Eidinger and Kelly [21] stated that it was possible to reach savings between 40% and 60% for this item in the design of a standardised NPP in contrast with a non-standardised nuclear facility, considering equal power capacity. These savings were related not only to the significant simplification of the design of the primary earthquake-resistant elements, but also, perhaps even more importantly, to the design of connections/fixings of safety systems, equipment, pipes and components of the nuclear island [23].

A further aspect regarding costs issues, which seems not to be covered in literature, is related to the costs of re-launching the NPP after the occurrence of a relevant earthquake. It will be seen in Section 2.2, using SPS is the most reliable way of assuring full structural integrity and reactor's safe shutdown after a seismic action of medium to large intensity. As traditional designs may not be able to provide the structural reliability required for a nuclear facility, both structural and non-structural damages may be expected under seismic actions. Of course, the latter is related to a certain economic loss to the nuclear facility itself, but the concern is the possible occurrence of a nuclear accident. At this point, further aspects should be taken into account, such as the impact of stopping the NPP as an energy supplier and, certainly, the potential danger towards the environment. It is important to note that in realistic cost analysis, not only the direct cost of the SPS itself should be considered, but also the difference in the structural reliability provided by a seismically protected nuclear facility that is able to ensure full structural integrity after medium and severe earthquakes.

2.3. *Safety*

NPPs and energy supply facilities require higher levels of safety than conventionally designed buildings as they play a strategic role after the occurrence of a severe seismic event [31]. In this light, seismic protection technologies offer a feasible method of reaching a higher level of protection by adding special devices within the structure. These technologies are designed to take most of the inelastic deformations imposed by earthquakes,

Downloaded by [The University of Manchester Library] at 08:36 21 June 2016

Downloaded by [The University of Manchester Library] at 08:36 21 June 2016

allowing the superstructure to remain essentially in its elastic range [18, 34-35] as its seismic demand could be reduced 6–8 times when compared to a conventional structure [17]. Therefore, SPS improve the overall safety and reliability of the building, contributing to ensuring full structural integrity and operability after relevant seismic events [36]. It is important to realise that for conventional seismic design the situation is different. In such a case, structures dissipate energy through inelastic deformation located at plastic hinge zones, and therefore, structural and non-structural damages are allowed to a certain extent as long as the condition of life safety is ensured. However, for NPPs this would lead to unacceptable seismic performance.

It should be noted that the addition of SPS to confine the inelastic deformation of a structure has a beneficial spin-off in terms of engineering modelling and design. For a conventional structure, the study of its inelastic dynamic response is based on assumptions about the non-linear behaviour of its structural elements. Such a situation becomes more complex for NPPs as additional non-linear constraints may affect critical components due to severe thermal loads [27,32]. On the other hand, in a seismically isolated building, the location where the non-linear behaviour will take place is known – the SPS – and therefore, the inelastic response of the structure will also be known. In fact, this may be explained due to the sum of two effects: (1) the possibility of having devices fully tested in the laboratory and hence, knowing their hysteresis curves; and/or (2) the modification of the dynamics of the structure imposed by the SPS which moves the structure to a condition where seismic loads are smaller, and therefore, ensuring the response of the superstructure is in its elastic range [18,34,35]. This fact was early recognised for the particular example of horizontal isolation provided by laminated rubber bearings (e.g. [19,31]). These devices provided an interface of very low stiffness between the superstructure and the foundation, whilst being able to withstand most of the displacement imposed by earthquakes. Consequently, the superstructure is subjected to a reduced seismic input and behaves essentially as a rigid body [26,37]. This is also advantageous for making simpler structural models in preliminary or feasibility analyses.

In general terms, the seismic behaviour of a building with SPS can be better predicted by structural models than that without SPS [5]. It must be noted that uncertainties of the seismic input are still present in both cases. Nevertheless, this aspect should not be overlooked as it will benefit the levels of accuracy of structural modelling and seismic design, and consequently, the overall safety and reliability of NPPs under seismic loads [22].

2.4. *Applications*

The particularly small number of real nuclear applications may have prevented the general acceptance of SPS in the development of nuclear structures. Even in the early stages of seismic isolation technology, the concept itself was questioned. Hadjian and Tseng [38] pointed out that the few field experiences of isolated applications subjected to design conditions were not enough to validate its use. Hence, the transference of the applicability of seismic isolation into nuclear industry would need further and stronger evidence. Nevertheless, in more recent developments of seismic protection, Forni et al. [3] and Martelli [2] reported a different scenario: a general consensus was reached among the technical community, in which seismic protection techniques had become a mature and reliable technology in mitigating seismic effects over a wide variety of civil structures. They pointed out the existence of about 10,000 applications of seismically protected structures in countries such as Japan, USA, Italy, China, Russia and Chile, ranging from areas of high seismic activity to countries of moderate and low seismicity. Some of these applications have already been subjected to severe seismic motions, achieving acceptable structural performances and providing the condition of full structural integrity. Furthermore, it is important to highlight that a key contribution to real nuclear applications equipped with SPS will be made in the near future. Two reactors, although for experimental and research purposes, are currently under construction equipped with seismic isolators in Cadarache, France, an area with moderate seismic activity. The Jules Horowitz Reactor (JHR), aimed at research in nuclear medicine, and the International Thermonuclear Experimental Reactor (ITER), intended for experimental activities in fusion energy, are the new real nuclear applications seismically protected after Koeberg NPP and Cruas NPP [3].

Although the number of NPPs seismically protected is still small, significant research efforts have been recently made in order to broaden the number of applications of NPPs equipped with SPS. There are two significant examples: (1) Takahashi et al. [39] reported that the Japanese government sponsored a large scale R&D project on 3D seismic isolation systems for FBRs between 2000 and 2005, in an attempt to enhance and generalise the concept of seismic protection; (2) Forni and De Grandis [40] summarised comprehensive research conducted in the framework of the SILER Project (Seismic-Initiated Events Risk Mitigation in Lead-Cooled Reactors) that is aimed at implementing seismic isolation on Generation IV heavy metal reactors. These initiatives, among others, will also provide the opportunity to deploy nuclear power in more areas, such as developing countries and other nations with increasingly higher demands for energy.

2.5. *Licensing*

Major licensing hurdles have made it difficult to fully deploy SPS in the nuclear industry. Such hurdles may be explained mainly due to the lack of specific codes and standards on seismically protected NPPs [3].

Downloaded by [The University of Manchester Library] at 08:36 21 June 2016

Additionally, it seems there is a general tendency for nuclear industry practitioners to keep the traditional approach in the seismic design of NPPs and/or an apparent lack of sound knowledge amongst the practitioners concerning the latest seismic protection technologies [23]. These facts could have discouraged the realisation of projects of seismically protected nuclear stations, and consequently, led owners to take traditional design approaches in order to not jeopardise entire projects.

There are several encouraging initiatives towards the development of codes and standards for design of NPPs equipped with SPS. The following examples can be cited: (1) in Japan, the code JEAG 4614-2000 Technical Guideline on Seismic Base Isolated System for Structural Safety and Design of Nuclear Power Plants is the only standard that specifically addressed the seismic isolation of NPPs [3]; (2) in the USA, the standard ASCE 4-98 Seismic Analysis of Safety-Related Nuclear Structures includes a section addressing requirements for design of isolated nuclear structures, although it has not yet endorsed by the American nuclear regulatory authority [23]; (3) in Europe, the report EUR 16559 Proposal for Design Guidelines for Seismically Isolated Nuclear Plants [41]; and (4) the International Atomic Energy Agency's report IAEA-TECDOC-1288 Verification of Analysis Methods for Predicting the Behaviour of Seismically Isolated Nuclear Structures [34].

Recent seismic probabilistic risk analyses have demonstrated that the use of SPS drastically reduces the seismic risk of NPPs [42]. This fact should encourage the reduction and simplification of licensing procedures. Certainly, the initial acceptance of seismic protection itself is a major issue for the established nuclear industry [30]. However, this licensing hurdle may be considered only as an initial barrier, as once the first licence is awarded, it is expected that the process of obtaining the following ones will be easier and faster [21]. This will also increase the economic competitiveness of nuclear energy generation compared with other sources of energy [15]. Considering the fact that SPS have made important progress in technical and non-technical aspects in recent years, it seems that the nuclear engineering industry should be dedicated to address all industry/regulatory issues pending in order to reach the first new generation of NPPs equipped with state-of-the-art SPS [23].

3. Devices in seismic protection systems for nuclear power plants

3.1. *Development of devices in SPS for NPP*

Seismic protection can be provided through three approaches: (1) passive, (2) semi-active and (3) active. Passive systems are the devices located within a structure aimed to increase the inherent energy dissipation capacity of the structure. These systems do not have the ability to change their dynamic properties during seismic excitations and they do not generate active control forces to the structure. A semi-active system is able to change its dynamic properties during a seismic excitation based on feedback provided by the monitored response of the structure, but they do not generate control forces to the structural system. Active systems have the ability to adjust their dynamic properties, provided by the feedback of the real-time response of the structure, and to apply active control forces to the structure, through mechanical or hydraulic actuators. These systems need a well-defined control strategy and use the dynamic response of the structure to determine appropriate control signals to be sent to the actuators [43]. For nuclear engineering, it is noticeable that the majority of research, both theoretical and experimental, is aimed at the use of passive systems, because it is more practical than the active or semi-active control mechanisms. A few cases of active systems have been reported only at a preliminary level whereas little attention has been paid to semi-active systems. **Table 4** gives examples of devices for each approach [44].

Table 4. Example of devices for different protection approaches.

Passive systems	Semi-active systems	Active systems
Elastomeric bearings	Magneto-rheological dampers	Active bracing dampers
Lead–rubber bearings	Electro-rheological dampers	Active mass dampers
Friction pendulum systems		
Viscous and steel dampers		
Tuned-mass dampers		
Air and steel springs		

The devices listed in Table 4 are suitable for deployment over all ranges of seismicity levels for either a non-critical building or a high-risk civil structure. Therefore, their governing principles and design process remain essentially unchanged. Nevertheless, NPPs have distinctive requirements that make them different from conventional structures. Consequently, the goals of seismic protection between both types of structures are different [45]. The key differences are indicated in **Table 5**.

It is inferred from Table 5 that there are two issues related to using SPS in nuclear facilities to match their required seismic performance. (1) Redundancy: SPS for a conventional building normally rely on one group of traditional devices (e.g. elastomeric bearings); for NPPs, it may be necessary to use two or more groups of traditional devices (e.g. elastomeric bearings plus viscous fluid dampers) and/or the inclusion of a fail-safe system against a beyond-design basis event. (2) Spatial configuration: SPS for non-critical buildings do not normally

Table 5. Key differences in seismic design of SPS: NPPs vs. conventional structures.

	NPPs	Conventional structures
Target performance for design basis event	Full structural integrity and reactor's safe shutdown	Damage allowed provided life safety
Target performance for beyond-design basis	SPS must remain functional (fail-safe system required)	No collapse
Isolation of vertical direction	Desired in order to reach full standardised seismic design	Not normally required

Downloaded by [The University of Manchester Library] at 08:36 21 June 2016

incorporate isolation in the vertical direction; new devices able to deal with the vertical vibration may need to be considered, as well as their location within the structure. The following subsections provide brief details of the devices for seismic protection suitable for nuclear engineering. **Table 6** summarises the research on SPS to protect the entire nuclear island. In this table, column 1 gives the source of information; column 2 provides the type of devices considered and their spatial configuration, aiming to provide either horizontal isolation (2D) or full isolation (3D) (to be discussed in the next section); column 3 indicates the application of NPP considered and their potential country of deployment (if applicable) and column 4 highlights the main achievements.

3.2. *Passive devices*

3.2.1. *Elastomeric bearings*

Elastomeric-based bearings, also known generically as seismic isolators or laminated rubber bearings, are composed of layers of either natural rubber or neoprene with alternated steel plates bonded by vulcanisation. These devices have been widely used in seismic protection of non-critical buildings, and comprehensive research has been conducted on their application in the nuclear industry. Depending on the kind of elastomer used, they can be identified as low-damping rubber bearings (LDRB) or HDRB [66]. **Figure 1**(a) shows a schematic view of an elastomeric bearing and Figure 1(b) gives a typical hysteretic curve of an HDRB device. General features reported for these devices for potential nuclear applications can be seen in **Table 7**.

3.2.2. *Lead–rubber bearings*

LRBs are also elastomeric-based devices, normally made using low-damping natural rubber. The difference between basic elastomeric bearings and LRBs is the addition of a lead plug or cylinder which in turn enhances the damping capacity of the bearing [18,62,66]. These devices, initially devised in New Zealand, have also been widely used in the seismic protection of conventional buildings. Their application to nuclear facilities has also been considered by researchers. **Figure 2**(a) shows a schematic view of an LRB device and Figure 2(b) gives a typical hysteretic loop. The latter can be well represented by a bilinear model [18] providing the mechanical behaviour of the lead plug (elasto-plastic) and the lateral response of the natural rubber (linear). General features reported for these devices for potential nuclear applications can be seen in Table 7.

It is worth mentioning that more than 75% of the articles referenced in Table 6 considered the use of elastomeric and LRBs. Therefore, it is highly likely that such devices will be used in new-generation nuclear deployments.

3.2.3. *Steel springs*

Steel springs are intended to isolate the vertical direction of a structure, and also need (1) to withstand the weight of the structure and to provide a long period of vibration in the vertical direction, (2) to be stiff in the other degrees of freedom and (3) to have a non-brittle failure mode [51]. In line with this, research efforts in nuclear engineering have been placed on three types of devices: coned disk springs, metallic bellows and helical springs. These devices have been considered at experimental level for nuclear deployment.

Coned disk springs are made of high-tensile steel of springs, and single disks can be stacked in different arrangements in series and parallel in order to reach different strokes and energy dissipation levels, representing a versatile alternative for vertical isolation of NPP. Hysteresis is generated by friction between single disks stacked in parallel and between groups of disks stacked in series and the stiff centre guide, which in turn restrains the other degrees of freedom of the device. The efficient friction of these devices becomes critical in order to reach high levels of energy dissipation required [52]. Their potential deployment in the nuclear engineering industry has been recently investigated in Japan, specifically for their application in FBRs [28,51–53,61]. **Figure 3**(a) shows a schematic view of an arrangement of coned disk springs considered for vertical isolation of FBRs and Figure 3(b) shows the hysteretic behaviour obtained for a particular arrangement of disks considered at experimental level for potential nuclear applications.

Metallic bellows are composed of multiple thin layers of steel and a certain number of convolutions which determine the vertical displacement capacity of the device. The device comprises one main bellow and one auxiliary bellow subject to high internal pressure.

Table 6. Summary of research on SPS for nuclear islands.

Researcher(s)	Type of devices	Application	Achievements/remarks
Syed et al. [35]	Low-damping rubber bearings (2D)	ITER (France)	Comprehensive summary of the qualification and test programme of isolators for the latest nuclear application
Domaneschi et al. [46]	High-damping rubber bearings (2D)	IRIS (International)	(1) Rocking component has almost no effect in terms of relative displacements and absolute accelerations (2) Rocking component leads significant variations on vertical load which influences isolators' design
Lee and Cho [47]	Lead–rubber bearings (2D)	APR1400 (Korea)	Accelerations are reduced about 60% relative to input
Lo Frano and Forasassi [26]	Elastomeric bearings (2D)	ELSY – LFRs (Europe)	(1) Maximum horizontal accelerations are reduced about 50% (preliminary) (2) Isolators are efficient in controlling sloshing effects produced by high-mass-density coolant (lead)
Wang et al. [48]	(a) High-damping rubber bearings + viscous dampers (2D) (b) High-damping thick rubber bearings + viscous dampers (3D)	Generic NPP (China)	(1) Horizontal accelerations are reduced about 50% with both SPS studied (2) 3D SPS has limited applicability as it may amplify vertical accelerations
Okamura et al. [49]	Low-damping thick rubber bearings + oil dampers (3D)	SFRs (Japan)	Preliminary feasibility in incorporating thick rubber bearings as a 3D SPS
Lo Frano and Forasassi [36]	Generic SPS	IRIS (International)	(1) Effectiveness on introducing flexibility and damping in reduction of NPP's dynamic response (2) Maximum horizontal accelerations are reduced about 50% (preliminary)
Radeva [43]	Active actuators (2D)	Kozloduy & Belene NPPs (Bulgaria)	Preliminary feasibility on incorporating an active SPS into two NPP cases
Sato et al. [50]	Lead–rubber bearings (2D)	ABWRs (Japan)	(1) Lateral deformation of isolators is increased 30% for bidirectional input (2) Lateral deformation of isolators is increased 10% when including temperature rise of lead plug
Okamura et al. [28]	Coned disk springs + steel dampers (2D + V)	FBRs (Japan)	(1) Technical feasibility on design and construction of coned disk springs and steel dampers for NPPs (2) Experimental validation of system disk springs + steel dampers as vertical isolation system
Morishita et al. [51]	Coned disk springs + steel dampers (2D + V)	FBRs (Japan)	Theoretical validation of system disk springs + steel dampers as vertical isolation system
Kitamura et al. [52]	Coned disk springs (2D + V)	FBRs (Japan)	Experimental validation (fabricability and applicability) of coned disk springs as vertical isolation system
Kitamura and Morishita [53]	Coned disk springs (2D + V)	FBRs (Japan)	Determination of optimum properties (frequency and damping) for vertical isolation system

Downloaded by [The University of Manchester Library] at 08:36 21 June 2016

Table 6. (*Continue*).

Researcher/year	Type of devices	Application	Achievements/remarks
Soda and Komatsu [54]	Sliding system (polyethylene + grinded concrete) + oil and friction dampers (2D)	FBRs (Japan)	(1) Experimental and theoretical validation of polyethylene + grinded concrete as feasible sliding surface for horizontal isolation of NPPs (2) Accelerations may increase at the top of the NPP
Shimada et al. [55]	Lead–rubber bearings + rolling seal air spring + rocking suppression system (3D)	FBRs (Japan)	(1) Experimental validation of air and hydraulic rocking suppression devices as vertical isolation system (2) Almost no interaction between horizontal and vertical responses
Suhara et al. [56]	Rolling seal air spring (3D)	FBRs (Japan)	Verification on the workability of air springs
Micheli et al. [57]	High-damping rubber bearings (2D)	ADS (Italy)	(1) Theoretical feasibility in horizontal base isolation system based on HDRB for a NPP case (2) Response spectra peak are reduced 10–15 times
Kageyama et al. [58]	Cable reinforcing air springs + viscous dampers + rocking prevention devices (3D)	FBRs (Japan)	(1) Verification of workability and integrity of air springs under high pressures by seismic loads (2) Experimental validation of cable reinforcing air springs as a single unit of isolation
Kashiwazaki et al. [59]	Elastomeric bearings + hydraulic accumulator units + rocking suppression system (3D)	FBRs (Japan)	(1) Experimental validation of hydraulic accumulators as vertical isolators (2) Critical damping ratio achieved: about 20% in vertical direction (3) Vertical accelerations are reduced by around 2/3
Kostarev et al. [20]	High-damping rubber bearings (2D)	VVER-1000 (Russia)	(1) Theoretical validation of an approach to reduce floor response spectra (2) Maximum spectral floor is reduced about two times
Ogiso et al. [60]	Lead-rubber bearings + metallic bellows (3D)	FBRs (Japan)	(1) Verification of stability and reliability of bellows and validation under fatigue loads (2) Critical damping ratio achieved: about 10% in vertical direction (3) Almost no interaction between horizontal and vertical responses
Somaki et al. [61]	Elastomeric bearings + coned disk springs (3D)	FBRs (Japan)	Preliminary validation of disk springs as suitable vertical isolation system in a 3D SPS
Yoo et al. [17]	(a) High-damping rubber bearings (2D) (b) Lead–rubber bearings (2D) (c) 3D-Laminated rubber bearings (3D)	KALIMER (Korea)	(1) Theoretical and experimental validation of rubber bearings for horizontal isolation for an NPP case (2) Maximum peak accelerations are reduced at least 6–8 times (3) Vertical response may be amplified by horizontal isolation (4) Earthquakes with very low-frequency components may be tuned with isolated structure

Downloaded by [The University of Manchester Library] at 08:36 21 June 2016

Table 6. (*Continue*).

Researcher/year	Type of devices	Application	Achievements/remarks
Austin et al. [16]	Low-damping rubber bearings + viscous dampers (2D)	LMR (UK-USA-Japan)	(1) Experimental determination of behaviour of devices (individually and globally) (2) Combined devices act independently: stiffness provided by isolators and damping by dampers
Fujita [62]	(a) Low-damping rubber bearings (2D) (b) High-damping rubber bearings (2D) (c) Lead–rubber bearings (2D)	FBRs (Japan)	Experimental validation of performance and reliability of rubber bearings under extreme loads
Gantenbein and Buland [24]	Sliding pads + helicoidal springs + viscous dampers (3D)	PWRs – FBRs (France)	Fluid–structure and soil–structure interactions in isolated NPPs were addressed
Gluekler et al. [14]	High-damping rubber bearings (2D)	ALMR (USA)	Programme of development
Kato et al. [10]	(a) Low-damping rubber bearings + steel dampers (2D) (b) Low-damping rubber bearings + viscous dampers (2D)	LWRs (Japan)	(1) Preliminary validation of rubber bearings, steel and viscous dampers as SPS for an NPP case (2) Establishment of potential problems in implementing base isolation into LWRs
Matsumura et al. [11]	(a) High-damping rubber bearings + oil dampers (2D) (b) Elastomeric bearings + viscous dampers (2D) (c) Low-damping rubber bearings + steel dampers (2D) (d) Elastomeric bearings + steel rod dampers (2D) (e) Sliding-elastomer + horizontal springs (2D)	Five non-nuclear structures (Japan)	Accelerations in superstructure are reduced between (1) 1/3–1/2 for small-size earthquakes (2) 1/6–1/5 for medium-size earthquakes
Martelli et al. [15]	High-damping rubber bearings (2D)	RSP/I (Italy)	Programme of development
Shiojiri [63]	(a) Low-damping rubber bearings (2D) (b) Lead-rubber bearings (2D) (c) High-damping rubber bearings (2D)	FBRs (Japan)	(1) Validation of horizontal isolation as the most feasible concept for FBRs at that time (2) Response of isolated reactor building is correlated to peak ground velocity rather than peak ground acceleration
Tajirian et al. [5]	(a) High-damping rubber bearings (2D) (b) High-damping rubber bearings (3D) (c) Low-damping rubber bearings (3D)	PRISM and SAFR (USA)	(1) Theoretical validation of the efficiency of elastomeric-based bearings in horizontal direction (2) Isolation in the vertical direction is limited and acceleration amplifications are possible
Guéraud et al. [19]	Sliding-elastomer bearing pads (low-damping) (2D)	Generic NPP	(1) Preliminary validation of sliding-elastomer pads for horizontal isolation (2) Definition of basic considerations design of seismically isolated NPPs
Hüffmann [29]	Steel helical springs + viscous dampers (3D)	Potential application into NPPs	Preliminary feasibility of devices as 3D SPS. No experimental results reported.

Downloaded by [The University of Manchester Library] at 08:36 21 June 2016

Table 6. (*Continue*).

Researcher/year	Type of devices	Application	Achievements/remarks
Ikonomou [30]	Low-damping rubber bearings + sliding pot bearings (2D)	Generic NPP	(1) Theoretical validation of the proposed SPS regarding reliability, licensing, efficiency and cost (2) Base shears are reduced at least 25 times
Staudacher [31]	Low-damping rubber bearings + mechanical stabilisers (3D)	Generic NPP	Preliminary experimental feasibility of the proposed SPS and its application into the nuclear industry
Wolf and Madden [64]	Active actuators (2D)	Generic NPP	Theoretical validation of active control as SPS considering different controllers and control laws
Varpasuo et al. [65]	Elastomeric bearings + sliding and friction plates (2D)	Generic NPP	Theoretical validation of a trilinear isolation concept for moderate earthquakes
Skinner et al. [32]	Elastomeric bearings + hysteretic dampers (2D)	BWRs	Preliminary validation of the applicability of seismic isolation concept into BWRs

Downloaded by [The University of Manchester Library] at 08:36 21 June 2016

Bellows are wrapped in reinforcement rings in order to provide stability to the whole system, while constraining the other degrees of freedom of the device. Therefore, they can be used as vertical isolation devices as they can work as a low-frequency air spring. They have been considered preliminarily for application for FBRs in Japan [60]. **Figure 4**(a) shows a schematic view of an experimental isolator based on metallic bellows to isolate the vertical direction and Figure 4(b) shows a load vs. displacement relationship in the vertical direction obtained experimentally in a 1/5 scaled model.

Vertical isolation using steel springs was investigated based on traditional-shaped *helical springs*. Gantenbein and Buland [24] reported experimental and analytical studies on their potential application in PWRs and FBRs. Incorporating helical steel springs for vertical isolation in critical facilities was also studied in Mexico (NPP) and Germany (chemical plant) [29], although for mitigating the effects of subsidence of soil and not directly for mitigating seismic effects.

3.2.4. *Air springs*

Air springs have also been considered recently for deployment in nuclear engineering, particularly for FBRs in Japan. Two types of air springs were experimentally studied: (1) vertical air spring [55,56] and (2) 3D air spring [58]. The former was intended to isolate in the vertical direction of the structure whereas the latter comprises horizontal and vertical isolations in one single device, defining a highly innovative device considered as SPS.

Vertical air spring or rolling seal type air spring is composed of an air compartment sealed by rolling rubber which provides the ability to withstand vertical deformations. As air springs have very little or null hysteresis capacity, they need to work together with levelling devices and rocking suppression devices in order to maintain a constant height of the structure at all times [56]. **Figure 5**(a) shows a schematic view of an experimental isolator based on vertical air springs to isolate in the vertical direction and Figure 5(b) shows a

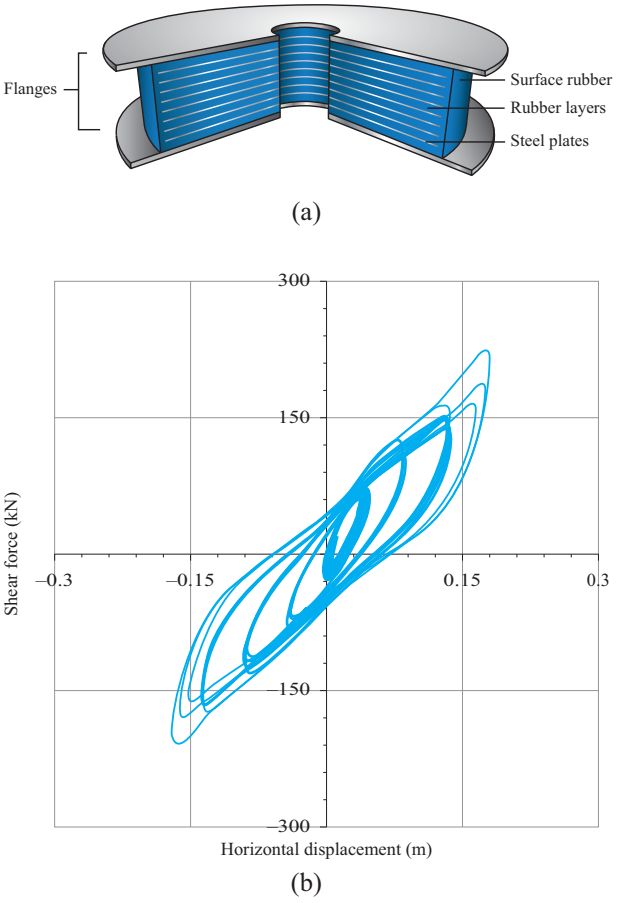

Figure 1. Sketch and mechanical behaviour of elastomeric bearings [62]: (a) schematic view; (b) hysteretic behaviour.

Table 7. Summary of general mechanical and geometric features of devices.

Types of devices	Damping level (*)	Deformation capacity	Dimensions	General remarks
Low-damping rubber bearings	2%–10%	~120% at design level (+)	*D*: 90–160 cm	Very high vertical stiffness Inherent good restoring or self-centring capacity Long-term workability of 60 years
High-damping rubber bearings	10%–20%	300%–500% at rupture level (+)	*D*/*H*: var	
Lead–rubber bearings	20%–30%			Highly ductile lead plug (lead–rubber bearings only)
Coned disk springs	10%	30 cm (±15 cm) (#)	*D*: 100 cm *H*: 100–200 cm	Properties depend on geometry and arrangement of single units
Metallic bellows	10%	80 cm (±40 cm) (#)	*D*: 250 cm *H*: 400 cm	Non-brittle failure. No evidence reported on long-term behaviour
Vertical air spring	Very low	40 cm (±20 cm) (#)	*D*: 300 cm *H*: 140 cm	The ability to withstand high internal pressures is critical for the workability of air springs in general
3D air spring	Very low	50 cm (±100 cm) [H]; 25 cm (±50 cm) [V]	*D*: 800 cm *H*: 350 cm	
Viscous dampers	10%–30%	High range of capacities and dimensions		Damping depends on velocities imposed by earthquakes
Steel hysteretic dampers	10%– 20%	High range of capacities and dimensions		Damping depends on displacements imposed by earthquakes

Notes: (*): critical damping ratio; (+): shear strain capacity; (#): stroke; [H], [V]: horizontal, vertical; *D*, *H*: diameter; height.

Downloaded by [The University of Manchester Library] at 08:36 21 June 2016

hysteresis curve obtained experimentally in a 1/7 scaled model. Little hysteresis is observed in Figure 5(b) as a result of friction on contact parts indicated in Figure 5(a).

Another type of air spring considered for nuclear deployment, specifically for FBR, is the *3D air spring*. They provide horizontal and vertical isolation in one single device based on compressed air and are composed of a rubber sheet between two steel cylinders, reinforcing fabric and reinforcing cables. The gap between the inner and outer cylinders provides the horizontal stroke. The gap between the top of the inner cylinder and the upper structure provides the allowable vertical stroke of the device. Theoretically, this air spring does not have any restoring behaviour; it needs to be used together with a rocking suppression system and supplemental damping in the vertical direction [58]. **Figure 6** shows a schematic view of the experimental 3D air spring. Although some experimental response curves were reported, no experimental behaviour curve was found for this device.

3.2.5. *Viscous dampers*

Viscous fluid dampers, having the same principle as ordinary automotive shock absorbers, are devices that dissipate energy through the conversion of mechanical energy into heat as a piston deforms a highly viscous substance, e.g. silicone gel, oil, etc., inside of a damper housing or container [16,44]. These dampers have been widely used as supplemental energy dissipation devices in conventional civil structures [1], and research has been carried out in nuclear engineering in order to consider them in conjunction with other passive devices to meet the higher requirements of NPPs. Table 6 shows the latest applications of viscous dampers intended for nuclear applications (e.g., [48,49,58]). The main features of viscous dampers are as follows:

- Viscous fluid dampers can be classified into two types: (1) open containers and (2) closed containers. The first one, with cylindrical pot fluid dampers and viscous damping walls, dissipates energy by the relative motion of cylinders or plates inside the fluid in an open container. The second one, with orificed fluid dampers and pre-loaded fluid devices, dissipates energy by forcing the fluid to pass through orifices inside of the device. In general, open container dampers have a relatively lower energy dissipation capacity than the closed container dampers. Nevertheless, the latter require the most sophisticated internal design in contrast with the rather simpler open-container-based devices [44]. Experimental results for open container devices showed a high energy dissipation capacity: Austin et al. [16] reported 8%–10% critical damping ratio, whereas Hüffmann [29] showed a range of 20%–30% achievable with this type of device.
- For open container viscous dampers for potential nuclear applications, Austin et al. [16] reported that viscous fluids were both frequency and temperature dependent. In general, the damping coefficient diminishes with higher frequencies until it becomes stable over a certain number of cycles of loading. On the other hand, temperature should be analysed under two aspects: (1) fluid local temperature and (2) ambient temperature. When the internal temperature of the fluid increases after few loading cycles, the viscosity decreases and,

Downloaded by [The University of Manchester Library] at 08:36 21 June 2016

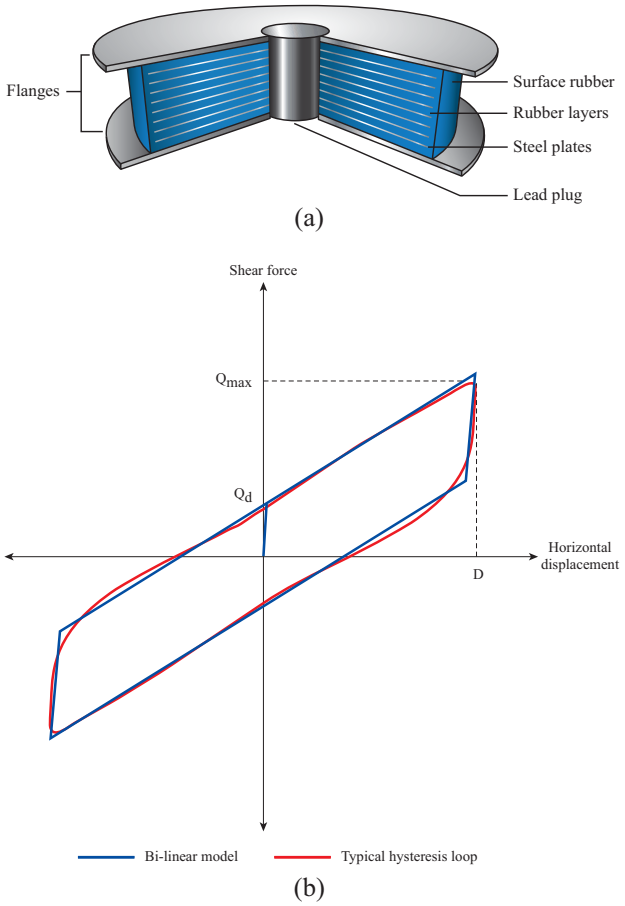

Figure 2. Sketch and mechanical behaviour of lead–rubber bearings [18,62]: (a) schematic view; (b) hysteretic behaviour.

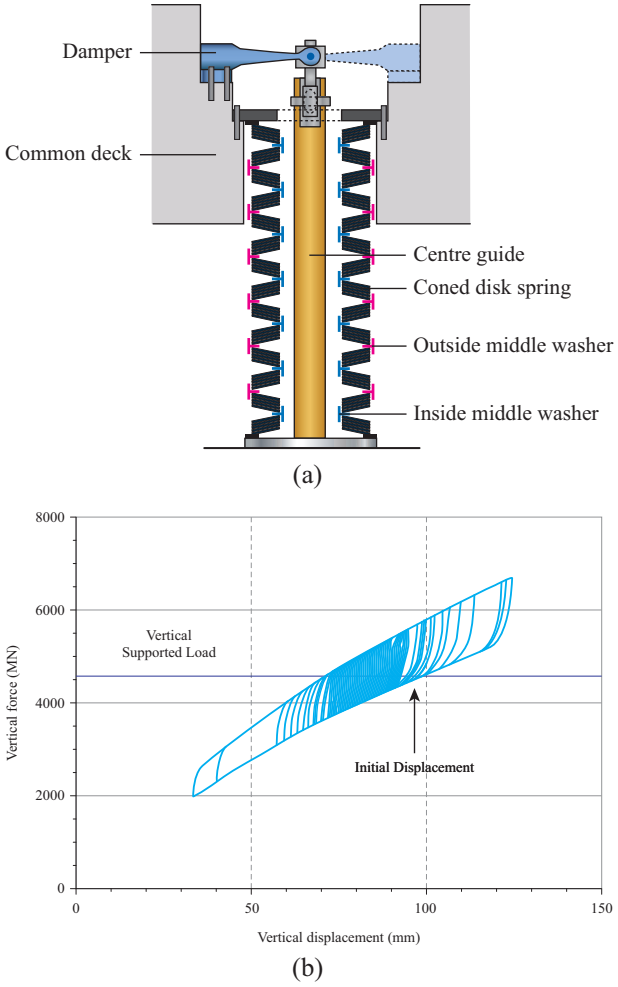

Figure 3. Sketch and mechanical behaviour of coned disk springs [61]: (a) schematic view; (b) hysteretic behaviour.

therefore, a reduction in the energy dissipation capacity is expected. The same negative effect is produced by ambient temperature, as they stated a loss in the energy dissipation capacity of about 50% with an increase in 15 °C in ambient temperature. A controlled working environment is a strong constraint to be considered with open container devices.

- For closed container dampers, the hysteretic behaviour depends on the device's internal geometry as well as the fluid's parameters. However, it is certain that a high level of energy dissipation can be achieved with these devices. The internal geometry can be designed and tested in order to optimise their dissipation capacity. Kato et al. [10] and Matsumura et al. [11] reported experimental attempts both in laboratory tests and in non-nuclear real structures, to deploy viscous oil dampers in LWR applications, confirming an appropriate performance for nuclear applications.

3.2.6. *Steel hysteretic dampers*

Steel hysteretic dampers are devices whose energy dissipation mechanism is based on the inelastic deformation of a metal, normally mild steel or any highly ductile alloy [44]. As well as viscous dampers, steel dampers have been extensively used as SPS in traditional buildings using a wide variety of metallic materials, shapes and sizes [1], all of them using the same principle to dissipate energy. Table 6 shows the latest applications of steel hysteretic dampers intended for nuclear applications (e.g. [28,51,52]).

Theories of plasticity and viscoplasticity are used to model the behaviour of steel hysteretic dampers. Temperature is not a relevant agent affecting the devices' behaviour, even though during a severe earthquake an important portion of the energy is dissipated as heat, raising the temperature of the surrounding material. However, that increment of temperature does not affect the mechanical properties of the device. The exception to this behaviour is for lead-based devices as lead is more sensitive to temperature changes. Additionally, fatigue analysis is critical in order to determine the durability of the device [44]. In the nuclear engineering industry, early attempts were reported by Kato et al. [10] and Matsumura et al. [11] to consider hysteretic dampers

Downloaded by [The University of Manchester Library] at 08:36 21 June 2016

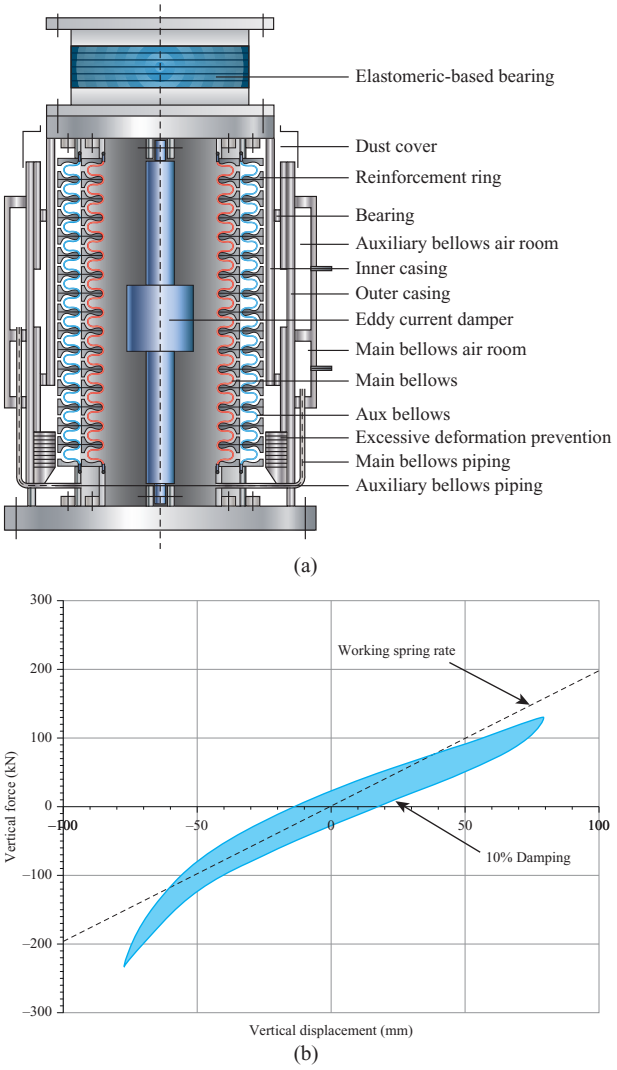

Figure 4. Sketch and mechanical behaviour of metallic bellows [60]: (a) schematic view; (b) hysteretic behaviour.

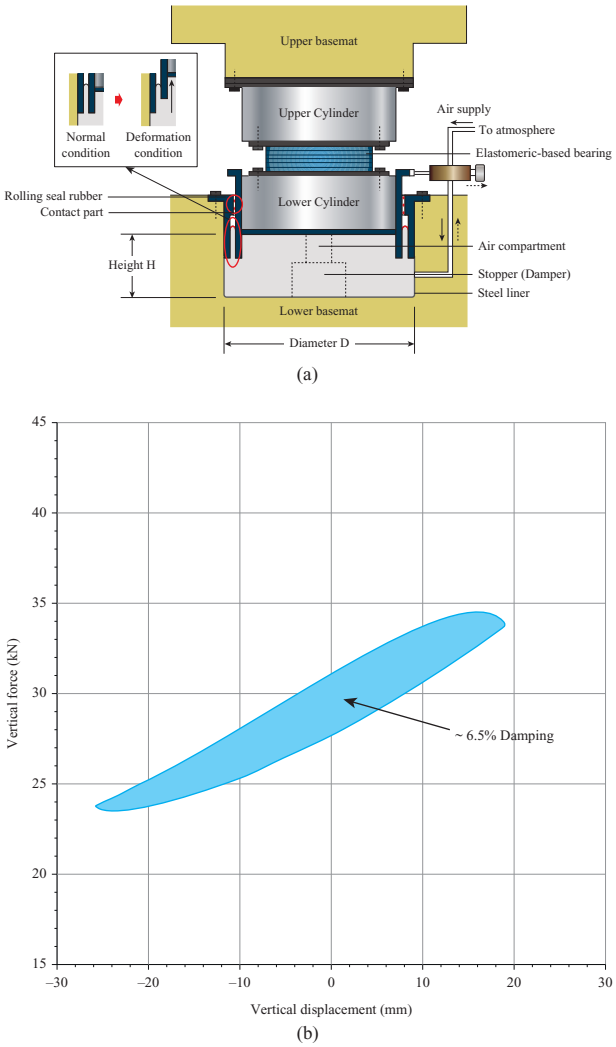

Figure 5. Sketch and mechanical behaviour of vertical air spring [55,56]: (a) schematic view; (b) hysteretic behaviour.

by means of steel rods or bars as SPS, alongside laminated rubber bearings, for deployment in LWRs.

Sections 3.2.1–3.2.6 provided an overview of the devices reported for potential nuclear applications. Some of their general features are summarised in Table 7. Although all values given in Table 7 were reported in literature, they must be taken as a reference only. Column 1 indicates types of devices; column 2 provides an estimation of the damping level possible to attain, measured in terms of critical damping ratio; column 3 gives estimations of the deformation capacity, measured in terms of shear strain capacity for rubber bearings and strokes for steel and air springs; column 4 indicates rough geometric dimensions; and finally, column 5 provides some general remarks.

3.3. *Semi-active and active devices*

The use of semi-active devices as SPS in the nuclear industry has not been investigated yet, as neither theoretical nor experimental results have been reported. Nevertheless, research on the use of semi-active devices has been considered in recent years. A number of applications in traditional civil structures have been successfully deployed. A comprehensive review of semi-active control systems for seismic protection of structures was reported by Symans and Constantinou [67]. The use of this type of protection for nuclear deployment should not be discarded, as this technology has increasingly gained acceptance within seismic protection technologies.

Only a few attempts to deploy active protection in the nuclear industry have been considered. On a theoretical basis, Wolf and Madden [64] reported the benefits of using active control systems for protecting the reactor vessel in NPPs. Later, Izumi [68] reported the existence of the first application in Japan of a low-risk building equipped with an active control system, although with a limited capacity to control the dynamic response of the structure under severe seismic loads. By then, the applicability of active control to NPPs seemed restricted as no

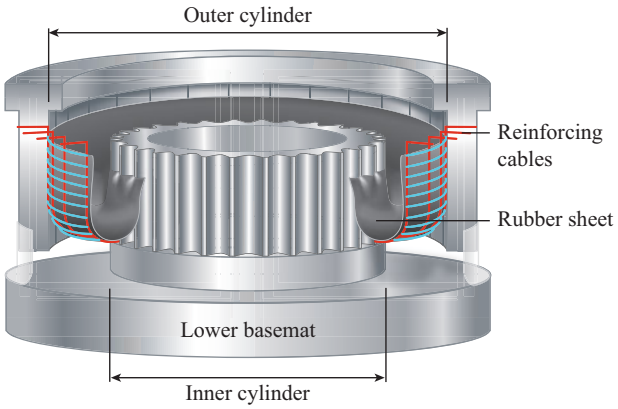

Figure 6. Sketch of 3D air spring [58].

Downloaded by [The University of Manchester Library] at 08:36 21 June 2016

remarkable research and development had been carried out at that time. More recently, Radeva [43] proposed an active control system for two NPPs in Bulgaria and provided some experimental evidence on its performance. These systems were based on hydraulic actuators distributed within the structure whose active control forces were determined in real time by sensors monitoring the dynamic response of the structure. In simple terms, the system was able to reconfigure its properties in real time in order to ensure the best possible structural protection available within the control strategy defined. The use of these systems, totally or partially in conjunction with passive devices, may have potential for nuclear applications.

4. Spatial configuration of seismic protection systems for nuclear power plants

4.1. General consideration

The devices described in the last section are arranged in different configurations within the structure in order to provide different types and levels of protection for NPPs. In this regard, three different types of spatial configuration of devices have been identified: (1) two-dimensional systems with horizontal isolation provided in one single interface (2D), (2) three-dimensional systems with horizontal and vertical isolation provided in one single interface (3D) and (3) three-dimensional systems with horizontal and vertical isolation provided in two interfaces [2D + V]. Conventional civil structures have been traditionally equipped with 2D systems, whereas the use of 3D systems is not normally considered. For the case of high-risk facilities, no 3D systems have been reported to mitigate the effects of severe earthquakes. Nevertheless, for the case of NPPs, extensive research has been carried out with this objective for reaching a full generalisation of the seismic protection concept. **Figure 7** shows schematically the concepts for providing seismic protection to NPPs.

Isolation in the vertical direction to set up 3D systems has not been widely used mainly due to two hurdles: (1) the SPS, being flexible in the vertical direction, must be able to withstand the total weight of the structure, and (2) the SPS must be able to control rocking modes, which arise as a natural consequence of a fully isolated structure [55,57,63]. For nuclear applications, it is critical to consider the effect of the vertical component of seismic loads as serious problems related to malfunction of internal components and/or structural integrity, such as uplift of fuel assemblies, reactivity change and buckling of the reactor vessel may arise [28,51]. The necessity of incorporating 3D SPS into nuclear facilities was reported by Hadjian and Tseng [38] and Seidensticker [69]. Without addressing the isolation of vertical and rocking modes, seismic design cannot be considered fully standardised, remaining site-dependent. Early attempts of developing 3D SPS for potential nuclear applications were reported by Coladant [9], Gantenbein and Bulant [24], Hüffmann [29] and Tajirian et al. [5]. For a long time, a number of 3D systems for nuclear deployment have been studied, reaching no applicable results [23,59].

As mentioned in Section 3.2.1, traditional seismic isolation based on laminated rubber bearings acts as stiff as a traditional foundation system in the vertical direction, thus, the seismic vertical component is transmitted in its entirety to the structure [51]. Accordingly, seismically isolated structures based solely on elastomeric bearings are almost not affected by rocking inputs/modes, even though a high variation on the vertical load may be expected and must be taken into account during the isolators' design process [46]. Furthermore, Kageyama et al. [58], Somaki et al. [61] and Yoo et al. [17] pointed out that the vertical response of internal equipment in horizontally isolated structures tended to be amplified in comparison with the non-isolated version of the building. Hadjian and Tseng [38] also suggested that the seismic design of internal equipment in the vertical direction should be the same as that for the horizontal direction.

It is also worth mentioning the selection of an appropriate plan distribution/layout of the devices as SPS.

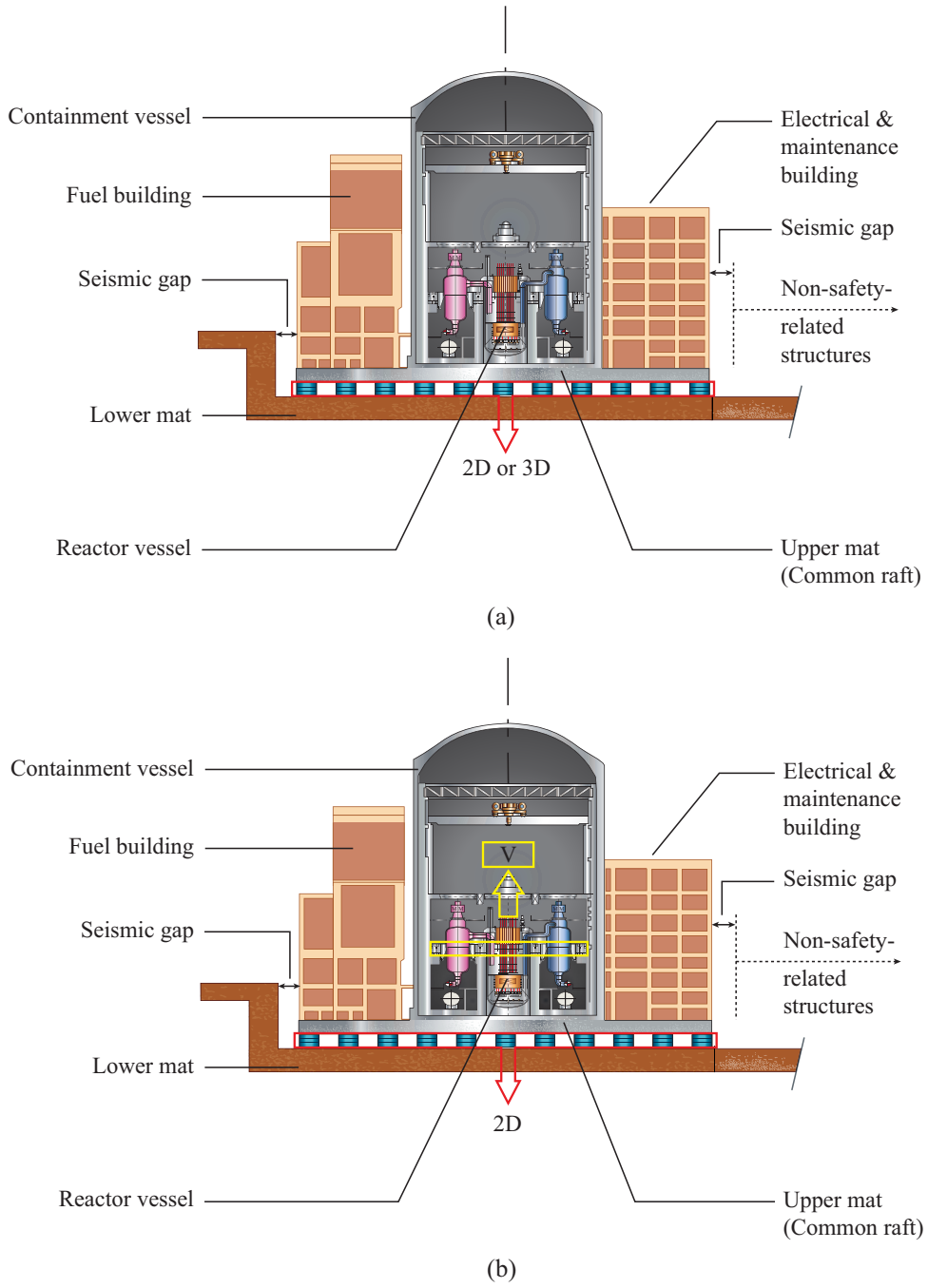

Figure 7. Schematic approaches to provide SPS in NPP [19,27]: (a) one interface (2D or 3D systems); (b) two interfaces (2D + V systems).

They should be located uniformly under the nuclear island and closer to each other under stress concentration and/or critical zones, e.g. under main walls and/or under the reactor vessel. This is done in order to have a permanent load distribution as uniform as possible acting on the devices [35]. Additionally, it is desirable to minimise the global torsion mode of the nuclear island. In this way, lateral displacements of the nuclear island are likely to be uniform, which would ease the design of adjacent structures and flexible connections running through them. Furthermore, as all SPS need to be periodically inspected, they should be installed with enough room in order to perform any maintenance or replacement work [57].

4.2. 2D systems

Horizontal isolation, or 2D systems, is the most common approach to isolate a structure against earthquake actions and it has been widely used in conventional civil structures. Significant research has been conducted for potential deployment in the nuclear industry.

Downloaded by [The University of Manchester Library] at 08:36 21 June 2016

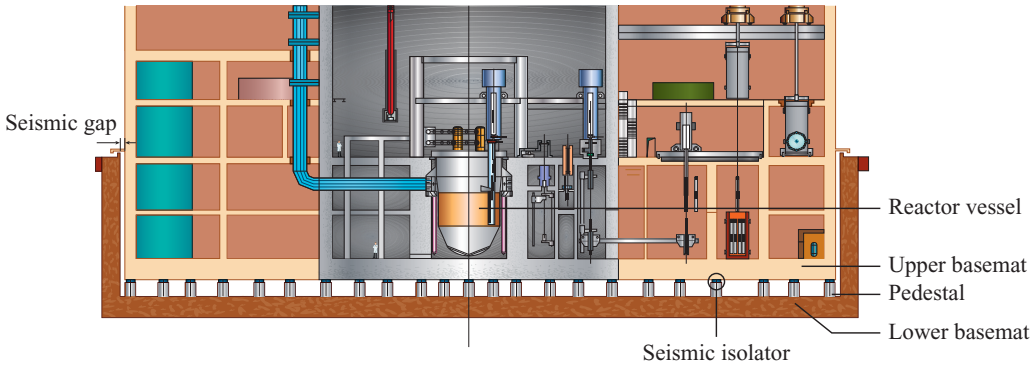

Figure 8. Schematic view of 2D SPS based on elastomeric bearings [57].

Downloaded by [The University of Manchester Library] at 08:36 21 June 2016

In fact, the only NPP equipped with SPS, although using the outdated technology, is based on these systems. Koeberg NPP (South Africa) and Cruas NPP (France) possessed seismically isolated reactor units based on square-sliding elastomer pads and squared elastomer pads, respectively.

The approach used to isolate NPPs in the horizontal direction is by providing an extensive common raft or diaphragm above the devices, supporting the entire nuclear island. The provision of a common mat to isolate the entire nuclear island has two main objectives: (1) to minimise relative displacements between different units of equipment; hence, to reduce the complexity of piping/flexible couplings between them, and (2) to standardise the relative displacements between the nuclear island and the non-isolated parts of the nuclear facility which need to be connected to each other. The latter condition implies that the connecting elements must be able to overcome the seismic gap between the facilities through the design of flexible expansion joints [23]. **Figure 8** shows a schematic view of a 2D system based on elastomeric bearings. In this figure, it is possible to observe the isolators located on pedestals in order to provide enough room for maintenance/inspection. In general, they are placed uniformly under the main walls and closer to each other under the reactor vessel.

As mentioned in Section 3, horizontal isolation for NPPs is based on the same principles as for conventional structures. Nevertheless, a combination of two or more types of devices may be required in order to reach higher performance levels under seismic actions. Horizontal isolation may not be enough to provide full seismic protection to a nuclear facility. Consequently, full standardised seismic design is not achievable with this approach. A mixture of 2D systems with a vertical isolation system, in order to configure either a 3D or a 2D + V system, seems to be the most likely approach for a successful deployment in the next generation of NPPs.

4.3. 3D systems

The approach most often considered by researchers, in order to provide 3D seismic isolation to NPPs, is to provide horizontal and vertical isolations in one single interface, thus protecting the entire nuclear island (see Table 6). The basic principle in most of these systems is that the horizontal isolation device is connected in series with the vertical isolation device. Two problems arise with this approach: (1) as each unit can work separately, the assurance of simultaneous performance is critical for the expected behaviour of the system, and (2) the optimal arrangement of the devices in order to make the SPS simple and efficient [56]. Additionally, as the rocking modes arise as a natural consequence of a fully isolated structure, an efficient rocking suppression system should be provided as an integrated part of the SPS. It is relevant to mention that all of the 3D SPS described below are currently considered at experimental level, as no real high-risk structure (and certainly no NPP) has been equipped with this kind of technology.

Shimada et al. [55] and Suhara et al. [56] reported a 3D SPS based on LRBs connected in series with vertical air springs, as shown in Figure 5. Experimental results on 1/7 and 1/10 small-scaled models confirmed the independency of performance of horizontal and vertical devices. This is a convenient feature for design as the dynamic properties of each device individually remain unchanged in the presence of other devices. For air springs to perform properly, it requires an air supply, air tanks and levelling systems in order to maintain a constant horizontal level of the structure.

Another 3D SPS for potential deployment in NPPs was reported by Ogiso et al. [60], which was based on LRBs in series with metallic bellows subjected to high internal pressures, as shown in Figure 4. Certainly, in order to work properly, this composite device needs a gas supply system, gas tanks and compressors. Experimental results obtained on a 1/5 small-scaled model confirmed that load–displacement behaviour under simultaneous vertical and horizontal loads was the same under single loads. These results confirmed that the response of each device was not affected by the presence of the other. Regarding their reliability, the author pointed out that bellows, well known as piping expansion joints, had many real applications, being effective in reducing large displacements.

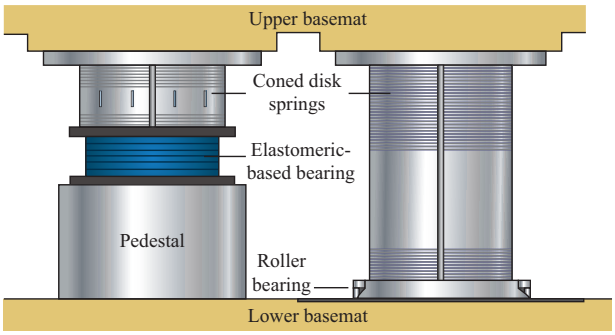

Figure 9. Sketch of a 3D SPS based on lead–rubber bearings in series and parallel with coned disk springs [61].

At a preliminary level, Somaki et al. [61] reported a 3D SPS based on elastomeric-based bearings in series and parallel with coned disk springs as shown in **Figure 9**. As mentioned in previous sections, coned disk springs provide a versatile alternative for the vertical isolation of structures, and their application to nuclear engineering has been widely investigated. Nevertheless, for this particular case, no comprehensive tests have been reported in order to determine the combined behaviour of this device under simultaneous vertical and horizontal loadings.

A more complex 3D SPS was reported by Kashiwazaki et al. [59]. This system was based on elastomeric-based bearings in series with hydraulic load-carrying cylinders connected to accumulator units containing compressed gas, acting as vertical isolators, as shown in **Figure 10**. During a vertical seismic load, the seismic force is converted by the load-carrying cylinders into pressure fluctuations in the fluid. The accumulator unit, which generates the vertical restoring force to be applied to the structure, is composed of two types of tank, a first-stage (variable volume) and a second-stage (constant volume). They are connected to each other through a pipe which in turn possesses an orifice. The size of the orifice can provide different levels of vertical damping forces. Experimental results performed in a small-scaled model intended to provide seismic protection for FBR, stated remarkable features of energy dissipation: a critical damping ratio in the vertical direction of about 20% and a reduction of vertical accelerations by around 2/3. Despite these results, hydraulic devices should be examined carefully for nuclear applications. Eidinger and Kelly [21] commented that hydraulic devices were poor in terms of maintenance and, therefore, they might not be considered fully suitable in the nuclear industry. More and comprehensive laboratory work should be performed in order to determine and to confirm the feasibility of hydraulic devices for nuclear deployment.

An exception to the composite devices described above, which is based on the connection in series and/or parallel of two types of devices, was reported by Kageyama et al. [58], who considered the provision of horizontal and vertical isolations in one single device through a 3D air spring (see Figure 6). Experimental results performed in a 1/4 small-scaled model, confirmed that the response in one direction does not affect the response in the other direction, showing independence of responses.

It is important to highlight that all of the devices described in this section need to be combined with a rocking suppression system aimed to generate restoring forces to control vertical displacements under horizontal seismic loads. A few experimental attempts have been reported in the literature in this regard. Successful re-

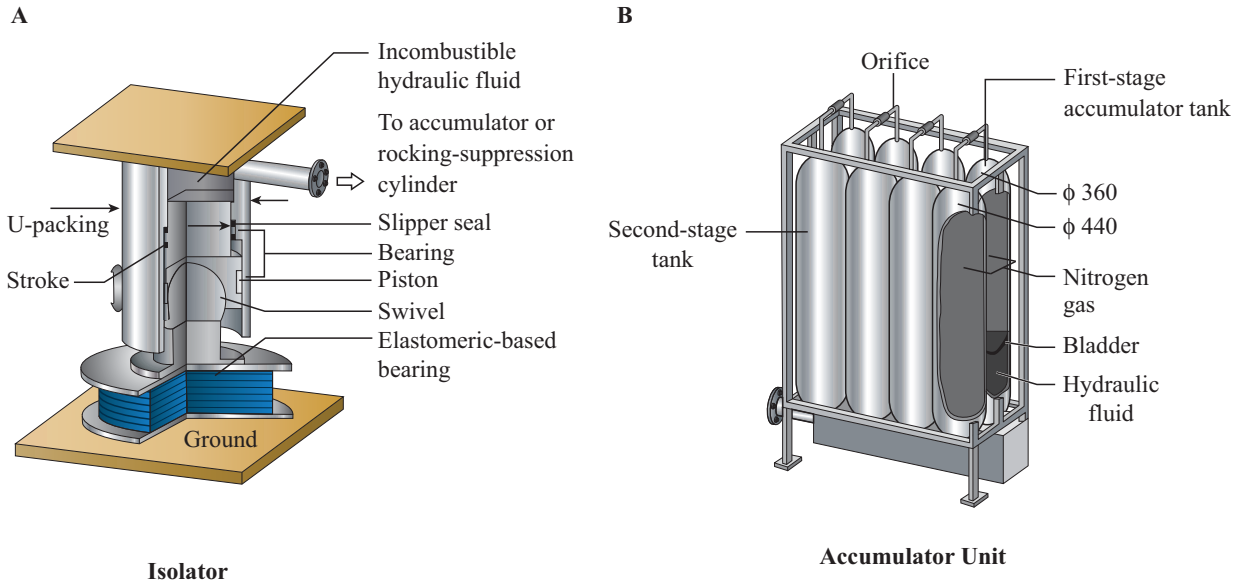

Figure 10. Sketch of a 3D SPS based on elastomeric bearings in series with vertical hydraulic isolators [59].

Downloaded by [The University of Manchester Library] at 08:36 21 June 2016

Downloaded by [The University of Manchester Library] at 08:36 21 June 2016

sults have been reported by Kashiwazaki et al. [59] and Shimada et al. [55], who tested rocking suppression systems based on hydraulic devices and accumulator units; Kageyama et al. [58] reported results considering a rocking prevention system based on wire cables and pulleys. More theoretical and experimental work should be carried out in order to minimise the effects of rocking modes in the seismic performance of NPPs.

Up to this point, all of the devices described can be considered as the latest attempts for reaching a suitable 3D SPS for nuclear deployment. Nevertheless, early attempts to reach the same objective were reported in the literature. Coladant [9] reported a potential 3D SPS based on elastomeric-based bearings, dampers and helical steel springs; Hüffmann [29] reported a full base isolation system based on steel helical springs and viscous dampers; and Staudacher [31] proposed a 3D SPS based on elastomeric-based bearings in combination with stiff brittle elements, called mechanical stabilisers acting as mechanical fuses under severe seismic loads. None of these systems seem to provide the level of seismic protection required for modern NPPs as no further attempts have been reported in terms of possible deployment in the nuclear industry with any of these systems.

It is also worth mentioning that recent research has reported attempts to reach 3D SPS based on elastomeric bearings formed by thick layers of rubber, for potential NPPs in China [48] and Japan [49,70,71]. However, its applicability seems limited as experimental results showed that vertical accelerations may be even amplified when the seismic ground motion contains long-period components.

4.4. *2D + V systems*

A different approach to provide 3D seismic isolation is to consider a mixture of a conventional 2D system at the foundation level plus vertical isolation of the safety-related components at an upper level [28,51–53]. Vertical isolation is limited only to the area in which the reactor vessel and the primary coolant system are located. They are suspended using a large slab structure which in turn is vertically isolated. The provision of the slab avoids considering vertical isolation individually for each piece of equipment, jeopardising the coolant piping system that goes through them [28,51]. The main advantage of this approach is that the rocking motion is considerably reduced in comparison with the systems described in Section 4.3. The reduction is due to the reduced distance between the centre of gravity of the internal components and the position of the bearings. The main drawback of using this proposal is that the internal layout of the plant needs to be changed as additional space is required to accommodate the deck and its supports [51].

Figure 11(a) shows a schematic view of the location of this approach within the nuclear island. Horizontal isolation is provided at the foundation level by means of elastomeric-based bearings. Vertical isolation is provided only to the reactor vessel and the primary coolant system by means of coned disk springs with steel hysteretic dampers. Figure 11(b) shows a schematic view of the vertically isolated common deck. Vertical isolation devices, shown in Figure 3(a), are distributed around the circumference of the reactor vessel and around the perimeter of the deck. For application in FBRs, Okamura et al. [28] suggested a thickness for the deck of 2 m in order to act as a rigid diaphragm, with approximately rectangular dimensions of 32 $\times$ 12 m and supported by 20 vertical isolation devices, whose unloaded height is 2.5 m.

Another system, proposed by Kostarev et al. [20], used an upper raft and was intended to work only in the horizontal direction. In this system, the common deck was also connected to the containment vessel rigidly in the vertical direction. Horizontal degrees of freedom were released in order to connect high-damping viscous dampers between the common deck and the containment vessel, in order to reduce floor horizontal accelerations.

The concept described in Figure 11 appears to be appealing for potential nuclear applications for the following reasons:

- The provision of horizontal isolation at the foundation level has been widely used in conventional structures proving high reliability. On the other hand, the provision of vertical isolation, only limited to the critical parts of the nuclear island, seems to be less cumbersome than providing vertical isolation at the foundation level. Nevertheless, the reliability of vertical isolation devices may be still a pending issue.
- The arrangement of the vertical isolation devices is rather simple, having no interaction with the horizontal isolation system. Independency between isolation systems may be useful for maintenance, inspection and replacement work.
- Apparently, no complex rocking suppression system is required as the rocking movement may be suppressed by its nature.

5. SPS for non-safety-related elements in nuclear power plants

Non-safety-related elements are those parts of a nuclear facility which do not belong to the NPPs' safe shutdown equipment list. Therefore, they do not normally deal with any radioactive material and/or do not perform any primary safety function [72]. Nevertheless, they still play an important role within a nuclear facility as their damage may initiate secondary hazards, loss of structural integrity and functionality and/or related economic losses. Consequently, they could jeopardise the continuous operation of the whole NPP after a severe seismic event. In this light, some research has been con-

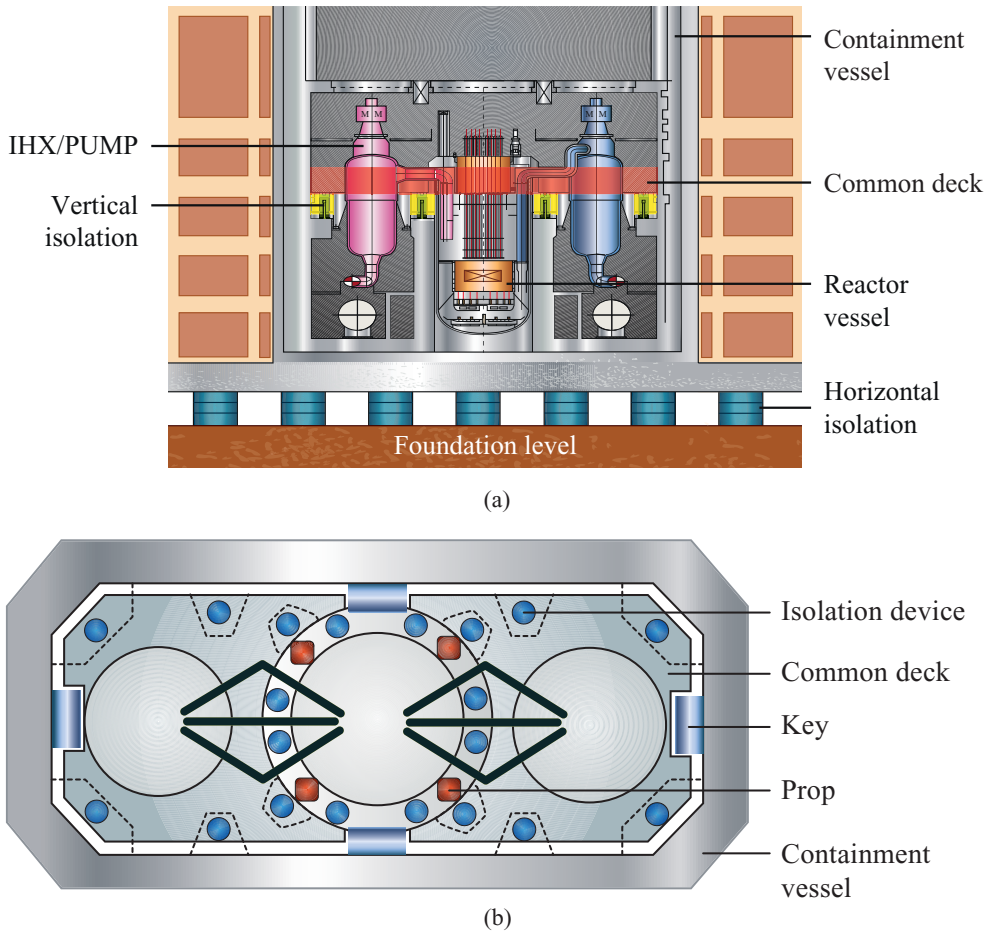

Figure 11. Schematic view of the 2D + V system [28]: (a) location of devices; (b) common deck.

Downloaded by [The University of Manchester Library] at 08:36 21 June 2016

ducted regarding the deployment of SPS for non-critical equipment of nuclear facilities.

The types of equipment and their main features may be summarised as follows:

- *Liquid storage tanks*. They may contain corrosive substances, flammable materials, hazardous chemicals or even water as part of the cooling system. They also play a passive safety function as cooling water and the tank's concrete walls are used as radiological barriers. It is important to ensure the structural integrity and leak-tightness of these elements under the effects of severe seismic loads. The main failures reported in this type of tank are buckling of the tank wall, failure of piping system, uplift of the anchorage system and overturning of tanks. It is relevant to note that the difficulty in dealing with these structures is due to their variable weight as the storage liquid level varies continuously. Therefore, fluid–structure interaction must be considered in the design of the structure and its potential SPS. Some adverse effects may arise when using seismic isolation for protecting liquid storage tanks: increase in the fluid sloshing height and/or damages to the water circulation system due to excessive relative displacements. However, when these effects are considered correctly in the design, seismic isolation can guarantee structural integrity and continuous operation after severe earthquakes [73–75]. Finally, an optimisation of seismic isolation for these elements was reported by Park et al. [76], who proposed a method to estimate the cost effectiveness of seismically isolated pool structures, including fluid–structure interaction effects.
- *Turbines and their housing building*. In general, a turbine does not belong to the safety-related equipment list. Nevertheless, it is an extremely expensive element, very difficult to manufacture, to test, to maintain and to operate. In some NPPs, turbines may be considered as part of the auxiliary heat removal safety system. In such a case, the criticality of turbines becomes clearer. Additionally, they can also be considered as a potential source of projectiles, which could happen during severe earthquakes. These projectiles may impact safety-related elements and could be the trigger of major accidents. In addition, the turbine house should be able to provide appropriate seismic safety to its equipment inside. Even though special protection

against earthquakes is not normally required for these elements, the provision of SPS may be critical when higher seismic performances are required [72,77].

- *Emergency transformers and generators*. Emergency equipment, such as transformers and generators, may have a superior importance within non-safety-related elements. This equipment is seismically fragile and, therefore, its continuous operation as emergency equipment must be ensured during severe earthquakes. Research reported for this type of equipment has considered the deployment of 3D SPS, highlighting the necessity to protect these elements against vertical and horizontal seismic actions [78–80].
- *Steam generators*. In general, the main failure of reported steam generators is corrosion cracking in their pipelines. The cracks may affect generators' performance under seismic actions. For these large and slender elements, a combination of isolators at the foundation level and energy dissipators distributed along their height could be considered to provide seismic protection [81].

The equipment listed above may not be the only items which need to be seismically protected in order to reduce the overall seismic risk of NPPs. Ebisawa and Uga [82] proposed a methodology to select appropriate equipment in order to judiciously apply base isolation. The base isolation can be complemented with the methodology reported by Huang et al. [83], determining correct seismic demands on non-safety-related components in NPPs equipped with seismic protection technologies. In general terms, seismic safety of these elements should not be overlooked as they also define the seismic vulnerability of NPPs in their entirety.

In terms of the devices considered for seismic protection of non-safety-related equipment, the majority of studies have considered the provision of SPS through passive systems. Only one study, at a theoretical level, reported the inclusion of active seismic control to equipment of NPPs [84], whereas no semi-active approaches have been considered. In general, this trend is similar to that obtained for seismic protection of the nuclear island. Passive devices reported for seismic protection of non-critical equipment are the same for the nuclear island, with one exception: the consideration of variable-friction pendulum-based devices, specifically for protection of liquid storage tanks. These devices are based on the concept of friction pendulum system, but instead of having spherical sliding surfaces, they have elliptical ones. Therefore, the oscillation frequency strongly decreases with increasing sliding displacement. Variable frequency pendulum isolators (VFPI) possess one sliding surface, whereas the double variable frequency pendulum isolator (DVFPI) has two; thus, having twice the displacement capacity in comparison with VFPI. Theoretical results reported by Panchal and Jangid [73] and Soni et al. [75] have demonstrated their effectiveness in providing high seismic performance to the system fluid–structure isolation system. Nevertheless, it is necessary to conduct experimental tests in order to completely validate these SPS.

6. Summary, conclusions and further research

6.1. Summary

This review of the current state-of-the-art SPS in NPPs has provided the answers to the four review questions, which have been dealt with in previous sections. The answers are summarised as follows:

(1) *Why does SPS remain as an excluded subject in the nuclear industry and which issues have prevented their complete deployment in NPPs?* SPS remain as an excluded subject in the nuclear industry mainly due to a lack of both experiences in real applications and specific standards and codes to design SPS for NPPs. Despite the fact that some devices have been successfully used in traditional structures (e.g. elastomeric bearings and viscous/steel hysteretic dampers), only a few devices have been deployed in high-risk structures. In addition, the experience with vertical isolation devices is very limited even for conventional structures. As a consequence, nuclear regulatory entities are not encouraged to promote/approve projects with such technology. In such a case, licences are likely to be delayed or even rejected. On the other hand, cost and safety are the factors encouraging the deployment of SPS in the nuclear industry. The cost of SPS is negligible compared to the cost of the total project and an offset is likely to be reached. Safety is indeed increased as SPS are able to ensure full structural integrity and reactor's safe shutdown after severe earthquakes.

(2) *What sorts of seismic protection devices are being considered in nuclear engineering research?* Seismic protection devices considered in nuclear engineering research are mainly intended to provide passive protection. As the concepts behind seismic protection are the same for NPPs and for conventional structures, most devices can be used in both types of structures. However, as NPPs have higher requirements for seismic performance, including isolation of the vertical direction, new devices have been designed and tested experimentally. Important research has been conducted to find vertical isolators suitable for NPPs.

(3) *What are the strategies of location of SPS within NPPs?* Spatial configuration of SPS in NPPs needs to be different compared to conventional

Downloaded by [The University of Manchester Library] at 08:36 21 June 2016

structures. Horizontal isolation provided at the foundation level may not be enough to reach acceptable seismic performances in NPPs. As the inclusion of vertical isolation is desired to reach full standardised seismic design, two approaches have been reported to accommodate vertical isolation devices into NPPs. In any case, space requirements may have important influence on the NPP's layout as vertical isolators reported in the literature can occupy significant geometric dimensions.

(4) *How may SPS help, if possible, to improve structural performance and safety of NPPs under seismic actions?* There is no straightforward answer for this review question. Evidence obtained from conventional structures indicates that the use of SPS has improved structural performance and seismic safety of structures. The same outcome can be inferred in nuclear applications. The safety requirements for NPPs are more demanding than for conventional structures; therefore, the establishment of optimal strategies on seismic protection can be a critical point for potential new NPPs.

6.2. *Conclusions*

The review of the current state-of-the-art SPS in NPPs has led to the following conclusions:

(1) Seismic protection technologies are mature in civil engineering to mitigate the effects of earthquake actions. The significant number of seismically protected structures around the world and their satisfactory performance confirm their value for civil structures. Although few high-risk structures equipped with SPS have been deployed so far, it is highly likely that they can be used in the nuclear engineering industry with fully standardised seismic design.

(2) In order to reach full standardisation of NPPs' seismic design, the traditional design philosophy of seismic protection for non-critical structures must be modified. The revised philosophy should have a direct impact on two aspects: (1) redundancy, as NPPs possess higher safety requirements and seismic performance; and (2) spatial configuration, as NPPs may require the concept of seismic protection to be considered both in the horizontal and vertical directions.

(3) The critical requirement for deployment of SPS in NPPs is the provision of vertical isolation, and consequently, the materialisation of 3D SPS. As this is not normally provided for traditional civil structures, there is a lack of experience which has acted as a drawback for its deployment in NPPs. Nevertheless, extensive and valuable research has been carried out in recent years in order to reach feasible devices able to deal with the isolation in the vertical direction and to be suitable for nuclear applications.

(4) For NPPs, it is more effective to provide SPS to the entire island of safety-related components by means of a common isolation raft, rather than the provision of isolation to individual components. By doing this, the relative displacements between safety-related equipment are minimised and the displacements between the nuclear island and the non-isolated parts of NPPs are standardised.

(5) The majority of devices reported for potential use in nuclear applications are intended to provide passive isolation, for protection to both the nuclear island and non-safety-related elements individually. In general, no semi-active devices have been reported for nuclear applications and only a few attempts have considered active control techniques. Passive devices are, in general, the same as those considered for traditional civil structures, having in mind the necessity to develop new types in order to deal with the requirements stated in the design philosophy stated in point 2.

(6) Two approaches have been reported to provide 3D seismic isolation for the nuclear island: considering either one interface or two interfaces. The majority of the research reported has considered the provision of 3D isolation in one interface, i.e. the deployment of horizontal and vertical isolations in the same interface at the foundation level. However, another approach is based on the provision of horizontal isolation at the foundation level plus vertical isolation only to the reactor vessel and primary coolant system (2D + V). It seems likely that approaches that considered only horizontal isolation (2D) may not be totally suitable for NPPs in zones of moderate-to-high seismic activity, due to requirements of safety-related equipment and the impossibility of reaching full standardisation of seismic design.

(7) Some research has been conducted regarding seismic protection for non-safety-related equipment of NPPs. Even though non-safety-related elements are not directly related to radioactive material or they are not part of primary safety systems, it seems recommendable to provide some extent of seismic protection in order to reduce the overall seismic risk of a complete nuclear facility.

6.3. *Further research*

The potential topics for further research in this field are suggested as follows:

Downloaded by [The University of Manchester Library] at 08:36 21 June 2016

Downloaded by [The University of Manchester Library] at 08:36 21 June 2016

(1) *Development of possible active/semi-active applications in conjunction with passive devices in order to increase the seismic safety of NPPs*. A combination of these approaches may be more efficient than only using passive devices in enhancing the seismic performance of the nuclear island. These combinations can be complementary, i.e. both types of seismic protection acting together as a primary SPS; or supplementary, i.e. only passive protection acting as a primary SPS and active/semi-active control acting as a back-up system focused only on the reactor vessel and the primary coolant system. The definition of a strategy of optimal combination of these concepts of seismic protection should be developed for future design guidelines.

(2) *Assessment of the optimal spatial configuration for 3D isolation approaches, either with one or two interfaces*. It is critical to determine the efficiency of the number of interfaces used, for example, by means of seismic probabilistic risk assessment (SPRA) suitable for NPPs. In this case, failure of structural and non-structural components can be better estimated through structural response parameters (e.g. floor spectral acceleration or story drifts) rather than ground-motion parameters. Therefore, fragility curves for key safety-related elements need to be estimated using such parameters. A starting point for this assessment may be, for example, the work reported by Huang et al. [42]. They proposed a SPRA for NPPs isolated in the horizontal direction using fragility curves for key secondary systems as a function of the average floor spectral acceleration. Selection of adequate demand parameters to estimate fragility curves is critical to correctly assess the seismic vulnerability of NPPs. Certainly, evaluation on the efficiency of 3D seismic protection approaches can make a substantial contribution for future design guidelines. It seems suitable to focus those studies on advanced nuclear reactors for deployment in the following decades. Examples of advanced reactors are the IRIS (International Reactor Innovative and Safety) reactor, the Westinghouse AP1000^{TM} reactor and the ELSY (European Lead-Cooled System) reactor, among others. The IRIS is under development by joint industry and academia bodies, including 20 institutions from nine countries [85]. Similarly, the Westinghouse AP1000^{TM} is a good example of successful development of new generation of reactors with design certification from the American nuclear regulatory institution [86]. Also, the ELSY is aimed at developing a competitive medium-size fast reactor for deployment in the EU region [87]. The first two reactors are Generation III+, whereas the last one is Generation IV. Therefore, they possess the latest technology known by the nuclear industry. Consequently, they offer appealing alternatives to attempt to reach full standardisation of NPPs' seismic design.

(3) *More experimental work should be carried out for those devices intended to be deployed in nuclear industry*. It seems clear that some devices, such as elastomeric-based isolators and steel/viscous dampers, have demonstrated their effectiveness as seismic protection technologies as shown by many real applications. However, those devices which have been designed to deal with isolation in the vertical direction may need more evidence regarding their mechanical behaviour prior to their first deployment.

(4) *Examination of the influence of non-safety-related elements in the overall seismic risk of nuclear facilities*. Despite the fact that these elements do not play any primary safety functions, their importance should not be overlooked. Failure, or unacceptable performances, may jeopardise the assurance of continuous operation to the entire facility.

Acknowledgements

The authors would like to thank Dr Brian Ellis, Ellis Consultant, for his constructive comments on the manuscript.

Nomenclature

ABWR	Advanced boiling water reactor(s)
ADS	Accelerator-driven system
ALMR	Advanced Liquid Metal Reactor(s)
APR1400	Advanced Power Reactor 1400
BWR	Boiling water reactor(s)
ELSY	European Lead-Cooled System
FBR	Fast breeder reactor(s)
HDRB	High-damping rubber bearing(s)
IRIS	International Reactor Innovative and Secure
ITER	International Thermonuclear Experimental Reactor
JHR	Jules Horowitz Reactor
KALIMER	Korea Advanced Liquid Metal Reactor
LDRB	Low-damping rubber bearing(s)
LFR	Lead-cooled fast reactor(s)
LMR	Liquid metal-cooled reactor(s)
LRB	Lead–rubber bearing(s)
LWR	Light water reactor(s)
NPP	Nuclear power plant
PRISM	Power Reactor Inherently Safe Module
PWR	Pressurised water reactor(s)
RSP/I	Reattori ad Elevato Contenuto di Sicurezza Passiva e/o Intrinseca
SAFR	Sodium advanced fast reactor

SFR	Sodium-cooled fast reactor
SPS	Seismic protection system(s)
VVER-1000	Water-Water Energy Reactor 1000

References

[1] Martelli A. State-of-the-art on the development and application of seismic vibration control techniques and some innovatives strengthening methods for civil and industrial structures. Proceedings of International Conference on Structural Mechanics in Reactor Technology (SMiRT 17); 2003 Aug 17–22; Prague (Czech Republic).

[2] Martelli A, Forni M, Clemente P. Recent worldwide application of seismic isolation and energy dissipation and conditions for their correct use. Proceedings of 15th World Conference on Earthquake Engineering; 2012 Sep 24–28; Lisbon (Portugal).

[3] Forni M, Poggianti A, Dusi A. Seismic isolation of nuclear power plants. Proceedings of 15th World Conference on Earthquake Engineering; 2012 Sep 24–28; Lisbon (Portugal).

[4] Kunar RR, Maini T. Review of seismic isolation for nuclear structures. London: Electric Power Research Institute; 1979. (Report: EPRI-NP-1220-SR).

[5] Tajirian FF, Kelly JM, Aiken ID. Seismic isolation for advanced nuclear power stations. Earthquake Spectra. 1990;6(2):371–401.

[6] Higgins JPT, Green S. Cochrane handbook for systematic reviews of interventions. Chichester: Wiley-Blackwell; 2008.

[7] Glasziou P, Irwig L, Bain C, Colditz G. Systematic reviews in health care: a practical guide. Cambridge: Cambridge University Press; 2001.

[8] Egger M, Smith GD, Altman DG. Systematic reviews in health care: meta-analysis in context. London: BMJ Books; 2001.

[9] Coladant C. Seismic isolation of nuclear power plants – EDF's philosophy. Nucl Eng Des. 1991;127(3):243–251.

[10] Kato M, Sato S, Shimomura I. Utilities/industries joint study on seismic isolation systems for LWRs: Part I. Experimental and analytical studies on seismic isolation systems. Nucl Eng Des. 1991;127(3):303–312.

[11] Matsumura T, Sato S, Kato M. Utilities/industries joint study on seismic isolation systems for LWRs: Part II. Observed behaviors of base-isolated general buildings under real earthquakes. Nucl Eng Des. 1991;127(3):313–328.

[12] Suppes GJ, Storvick T. Sustainable nuclear power. Elsevier; 2007. Chapter 12, Nuclear power plant design; p. 319–351.

[13] Eggenberger AJ. Commentary on US R&D programs for seismic base isolation. Nucl Eng Des. 1991;127(3):239–241.

[14] Gluekler EL, Bigelow CC, DeVita V, Kelly JM, Seidensticker RW, Tajirian FF. Seismic isolation development for the US advanced liquid-metal reactor program. Nucl Eng Des. 1991;127(3):295–301.

[15] Martelli A, Masoni P, Forni M, Indirli M, Spadoni B, Pasquale Gd, Lucarelli V, Sano T, Bonacina G, Castoldi A. ENEA activities on seismic isolation of nuclear and non-nuclear structures. Nucl Eng Des. 1991;127(3):265–272.

[16] Austin NM, Hattori S, Rodwell E, Womack GJ. UK contribution to CEGB-EPRI-CRIEPI program on seismic isolation. Nucl Eng Des. 1991;127(3):253–264.

[17] Yoo B, Lee J-H, Koo G-H, Lee H-Y, Kim J-B. Seismic base isolation technologies for Korea advanced liquid metal reactor. Nucl Eng Des. 2000;199(1–2):125–142.

[18] Buckle IG. New Zealand seismic base isolation concepts and their application to nuclear engineering. Nucl Eng Des. 1985;84(3):313–326.

[19] Guéraud R, Noël-Leroux JP, Livolant M, Michalopoulos AP. Seismic isolation using sliding-elastomer bearing pads. Nucl Eng Des. 1985;84(3):363–377.

[20] Kostarev VV, Petrenko AV, Vasilyev PS. A new method for essential reduction of seismic and external loads on NPP's structures, systems and components. Proceedings of 17th International Conference on Structural Mechanics in Reactor Technology (SMiRT 17); 2003 Aug 17–22; Prague (Czech Republic).

[21] Eidinger JM, Kelly JM. Seismic isolation for nuclear power plants: technical and non-technical aspects in decision making. Nucl. Eng. Des. 1985; 84(3):383–409.

[22] Chang Y-W, Kuroda T, Martelli A. Overview and summary of the first international seminar on seismic base isolation of nuclear power facilities. Nucl Eng Des. 1991;127(3):233–237.

[23] Malushte S, Whittaker AS. Survey of past base isolation applications in nuclear power plants and challenges to industry/regulatory acceptance. Proceedings of 18th International Conference on Structural Mechanics in Reactor Technology (SMiRT 18); 2005 Aug 7–12; Beijing (China).

[24] Gantenbein F, Buland P. DEMT experimental and analytical studies on seismic isolation. Nucl Eng Des. 1991;127(3):409–418.

[25] Lo Frano R, Forasassi G. Preliminary analysis of the structural effects due to dynamic loads of the isolated next generation lead cooled reactor. Proceedings of 20th International Conference on Structural Mechanics in Reactor Technology (SMiRT 20); 2009 Aug 9–14; Espoo (Finland).

[26] Lo Frano R, Forasassi G. Preliminary evaluation of the seismic response of the ELSY LFR. Nuc Eng Des. 2012;242(0):361–368.

[27] Kato A, Moro S, Morishita M, Fujita T, Midorikawa S. A development program of three-dimensional seismic isolation for advanced reactor system in Japan. Proceedings of 17th International Conference on Structural Mechanics in Reactor Technology (SMiRT 17); 2003 Aug 17–22; Prague (Czech Republic).

[28] Okamura S, Kitamura S, Takahashi K, Somaki T. Experimental study on vertical component isolation system. Proceedings of 18th International Conference on Structural Mechanics in Reactor Technology (SMiRT 18); 2005 Aug 7–12; Beijing (China).

[29] Hüffmann GK. Full base isolation for earthquake protection by helical springs and viscodampers. Nucl Eng Des. 1985;84(3):331–338.

[30] Ikonomou AS. Alexisismon isolation engineering for nuclear power plants. Nucl Eng Des. 1985;85(2):201–216.

[31] Staudacher K. Protection for structures in extreme earthquakes: full base isolation (3-D) by the Swiss seismafloat system. Nucl Eng Des. 1985;84(3):343–357.

[32] Skinner RI, Bycroft GN, McVerry GH. A practical system for isolating nuclear power plants from earthquake attack. Nucl Eng Des. 1976;36(2):287–297.

[33] De la Llera JC, Lüders C, Leigh P, Sady H. Analysis, testing, and implementation of seismic isolation of buildings in Chile. Earthquake Eng Struct Dyn. 2004;33(5):543–574.

[34] International Atomic Energy Agency. Verification of analysis methods for predicting the behaviour of seismically isolated nuclear structures. Vienna: IAEA; 2002. (Report IAEA-TECDOC-1288).

Downloaded by [The University of Manchester Library] at 08:36 21 June 2016

Downloaded by [The University of Manchester Library] at 08:36 21 June 2016

[35] Syed MB, Patisson L, Curtido M, Slee B, Diaz S. The challenging requirements of the ITER anti seismic bearings. Nucl Eng Des. 2014;269(0):212–216.
[36] Lo Frano R, Forasassi G. Isolation systems influence in the seismic loading propagation analysis applied to an innovative near term reactor. Nucl Eng Des. 2010;240(10):3539–3549.
[37] Perotti F, Corradi dell'Acqua L, Domaneschi M, Forni M, Poggianti A, Bianchi F, Forasassi G, Lo Frano R, Pugliese G, Carelli MD, Ahmed M, Maioli A. Seismic isolation of the IRIS NSSS building. Proceedings of 20th International Conference on Structural Mechanics in Reactor Technology (SMiRT 20); 2009 Aug 9–14; Espoo (Finland).
[38] Hadjian AH, Tseng WS. Issues in seismic isolation of nuclear power plants. Nucl Eng Des. 1985;84(3):433–438.
[39] Takahashi K, Inoue K, Kato A, Morishita M, Fujita T. A development of three-dimensional seismic isolation for advanced reactor systems in Japan – part 2. Proceedings of 18th International Conference on Structural Mechanics in Reactor Technology (SMiRT 18); 2005 Aug 7–12; Beijing (China).
[40] Forni M, De Grandis S. Seismic-initiated events risk mitigation in lead-cooled reactors: the SILER project. Proceedings of 15th World Conference on Earthquake Engineering; 2012 Sep 24–28; Lisbon (Portugal).
[41] European Commission. Proposal for design guidelines for seismically isolated nuclear plants. Luxembourg: European Commission; 1995. (Report EUR 16559).
[42] Huang Y-N, Whittaker AS, Luco N. Seismic performance assessment of base-isolated safety-related nuclear structures. Earthquake Eng Struct Dyn. 2010;39(13):1421–1442.
[43] Radeva S. Multiple-model structural control for seismic protection of nuclear power plant. Nucl Eng Des. 2010;240(4):891–898.
[44] Soong TT, Dargush GF. Passive energy dissipation systems in structural engineering. Chichester: Wiley; 1997.
[45] Lee H-P, Cho M-S, Park J-Y. Developing lead rubber bearings for seismic isolation of nuclear power plants. Proceedings of 15th World Conference on Earthquake Engineering; 2012 Sep 24–28; Lisbon (Portugal).
[46] Domaneschi M, Martinelli L, Perotti F. The effect of rocking excitation on the dynamic behaviour of a nuclear power plant reactor building with base isolation. Proceedings of 15th World Conference on Earthquake Engineering; 2012 Sep 24–28; Lisbon (Portugal).
[47] Lee H-P, Cho M-S. A study on the reduction effect for seismic isolation system of nuclear power plants. Proceedings of 15th World Conference on Earthquake Engineering; 2012 Sep 24–28; Lisbon (Portugal).
[48] Wang F, Wang T, Ding L. Numerical and experimental study on seismic behavior of base-isolated nuclear power plant. Proceedings of 15th World Conference on Earthquake Engineering; 2012 Sep 24–28; Lisbon (Portugal).
[49] Okamura S, Kamishima Y, Negishi K, Sakamoto Y, Kitamura S, Kotake S. Seismic isolation design for JSFR. J Nucl Sci Technol. 2011;48(4):688–692.
[50] Sato N, Furukawa S, Kuno M, Shimamoto R, Takenaka Y, Nakayama T, Kondo A. Heat–mechanics interaction behavior of lead rubber bearings for seismic base isolation under large and cyclic lateral deformation. Part 2: seismic response analysis of base isolated reactor building subjected to horizontal bi-directional earthquake motions. Proceedings of 20th International Conference on Structural Mechanics in Reactor Technology (SMiRT 20); 2009 Aug 9–14; Espoo (Finland).
[51] Morishita M, Kitamura S, Kamishima Y. Structure of 3-dimensional seismic isolated FBR plant with vertical component isolation system. Proceedings of 17th International Conference on Structural Mechanics in Reactor Technology (SMiRT 17); 2003 Aug 17–22; Prague (Czech Republic).
[52] Kitamura S, Nakatogawa T, Miyamoto A, Somaki T. Experimental study on coned disk springs for vertical seismic isolation system. Proceedings of 17th International Conference on Structural Mechanics in Reactor Technology (SMiRT 17); 2003 Aug 17–22; Prague (Czech Republic).
[53] Kitamura S, Morishita M. Design method of vertical component isolation system. Proceedings of 16th International Conference on Structural Mechanics in Reactor Technology (SMiRT 16); 2001 Aug 12–17; Washington, DC.
[54] Soda S, Komatsu Y. Hybrid response control system for nuclear power station. Proceedings of 19th International Conference on Structural Mechanics in Reactor Technology (SMiRT 19); 2007 Aug 12–17; Toronto (Canada)
[55] Shimada T, Suhara J, Takahashi K. Study on 3-dimensional base isolation system applying to new type power plant reactor. Part 2 (Hydraulic 3-dimensional base-isolation system). Proceedings of 18th International Conference on Structural Mechanics in Reactor Technology (SMiRT 18); 2005 Aug 7–12; Beijing (China).
[56] Suhara J, Tamura T, Ohta K, Okada Y, Moro S. Research on 3-D base isolation system applied to new power reactor 3-D seismic isolation device with rolling seal type air spring. Part 1. Proceedings of 17th International Conference on Structural Mechanics in Reactor Technology (SMiRT 17); 2003 Aug 17–22; Prague (Czech Republic).
[57] Micheli I, Cardini S, Colaiuda A, Turroni P. Investigation upon the dynamic structural response of a nuclear plant on aseismic isolating devices. Nucl Eng Des. 2004;228(1–3):319–343.
[58] Kageyama M, Iba T, Umeki K, Somaki T, Moro S. Development of three-dimensional base isolation system with cable reinforcing air spring. Proceedings of 17th International Conference on Structural Mechanics in Reactor Technology (SMiRT 17); 2003 Aug 17–22; Prague (Czech Republic).
[59] Kashiwazaki A, Shimada T, Fujiwaka T, Moro S. Study on 3-dimensional base isolation system applying to new type power plant reactor (hydraulic 3-dimensional base isolation system: no. 1). Proceedings of 17th International Conference on Structural Mechanics in Reactor Technology (SMiRT 17); 2003 Aug 17–22; Prague (Czech Republic).
[60] Ogiso S, Nakamura K, Suzuki M, Moro S. Development of 3D seismic isolator using metallic bellows. Proceedings of 17th International Conference on Structural Mechanics in Reactor Technology (SMiRT 17); 2003 Aug 17–22; Prague (Czech Republic).
[61] Somaki T, Nakatogawa T, Miyamoto A, Sugiyama K, Oyobe Y, Tamachi K. Development of 3-dimensional base isolation system for nuclear power plants. Proceedings of 16th International Conference on Structural Mechanics in Reactor Technology (SMiRT 16); 2001 Aug 12–17; Washington, DC.
[62] Fujita T. Seismic isolation rubber bearings for nuclear facilities. Nucl Eng Des. 1991;127(3):379–391.
[63] Shiojiri H. CRIEPI test program for seismic isolation of the FBR. Nucl Eng Des. 1991;127(3):393–407.
[64] Wolf JP, Madden PA. An assessment of the application of active control to reduce the seismic response of nuclear power plants. Nucl Eng Des. 1981;66(3):383–397.

[65] Varpasuo P, Räty K, Kenttälä J. A trilinear base-isolator concept for nuclear power plants. Nucl Eng Des. 1980;58(3):437–448.
[66] Naeim F, Kelly JM. Design of seismic isolated structures: from theory to practice. New York, NY: Wiley; 1999.
[67] Symans MD, Constantinou MC. Semi-active control systems for seismic protection of structures: a state-of-the-art review. Eng Struct. 1999;21(6):469–487.
[68] Izumi M. Recent progress and development of building vibration-control systems in Japan. Nucl Eng Des. 1991;127(3):273–280.
[69] Seidensticker RW. Applicability of base-isolation R&D in non-reactor facilities to a nuclear reactor plant. Nucl Eng Des. 1991;127(3):291–293.
[70] Aoto K, Uto N, Sakamoto Y, Ito T, Toda M, Kotake S. Design study and R&D progress on Japan sodium-cooled fast reactor. J Nucl Sci Technol. 2011;48(4):463–471.
[71] Kubo S, Shimakawa Y, Yamano H, Kotake S. Safety design requirements for safety systems and components of JSFR. J Nucl Sci Technol. 2011;48(4):547–555.
[72] Kostarev VV, Petrenko AV, Vasilyev PS. An advanced seismic analysis of an NPP powerful turbogenerator on an isolation pedestal. Nucl Eng Des. 2007;237(12–13):1315–1324.
[73] Panchal VR, Jangid RS. Variable friction pendulum system for seismic isolation of liquid storage tanks. Nucl Eng Des. 2008;238(6):1304–1315.
[74] Park J-H, Moo Koh H, Kwan Kim J. Seismic isolation of pool-type tanks for the storage of nuclear spent fuel assemblies. Nucl Eng Des. 2000;199(1–2):143–154.
[75] Soni DP, Mistry BB, Panchal VR. Double variable frequency pendulum isolator for seismic isolation of liquid storage tanks. Nucl Eng Des. 2011;241(3):700–713.
[76] Park K-S, Koh H-M, Song J. Cost-effectiveness analysis of seismically isolated pool structures for the storage of nuclear spent-fuel assemblies. Nucl Eng Des. 2004;231(3):259–270.
[77] Danisch R, Labes M. Aseismic design of turbine houses for nuclear power plants. Nucl Eng Des. 1976;38(3):495–501.
[78] Choun Y-S, Kim MK, Seo J-M. Seismic and vibration isolation of an emergency diesel generator by using a spring-viscous damper system. Proceedings of 19th International Conference on Structural Mechanics in Reactor Technology (SMiRT 19); 2007 Aug 12–17; Toronto (Canada).
[79] Choun Y-S, Kim MK, Ohtori Y. The use of a base isolation system for an emergency diesel generator to reduce the core damage frequency caused by a seismic event. Proceedings of 19th International Conference on Structural Mechanics in Reactor Technology (SMiRT 19); 2007 Aug 12–17; Toronto (Canada).
[80] Ebisawa K, Ando K, Shibata K. Progress of a research program on seismic base isolation of nuclear components. Nucl Eng Des. 2000;198(1–2):61–74.
[81] Bhatti MA, Ciampi V, Kelly JM, Pister KS. An earthquake isolation system for steam generators in nuclear power plants. Nucl Eng Des. 1982;73(3):229–252.
[82] Ebisawa K, Uga T. Evaluation methodology for seismic base isolation of nuclear equipments. Nucl Eng Des. 1993;142(2–3):319–326.
[83] Huang Y-N, Whittaker AS, Constantinou MC, Malushte S. Seismic demands on secondary systems in base-isolated nuclear power plants. Earthquake Eng Struct Dyn. 2007;36(12):1741–1761.
[84] Kobori T, Kanayama H, Kamagata S. Active seismic response control systems for nuclear power plant equipment facilities. Nucl Eng Des. 1989;111(3):351–356. [85] Carelli MD, Conway LE, Oriani L, Petrović B, Lombardi CV, Ricotti ME, Barroso ACO, Collado JM, Cinotti L, Todreas NE, Grgić D, Moraes MM, Boroughs RD, Ninokata H, Ingersoll DT, Oriolo F. The design and safety features of the IRIS reactor. Nucl Eng Des. 2004;230(1–3):151–167.
[86] Schulz TL. Westinghouse AP1000 advanced passive plant. Nucl Eng Des. 2006;236(14–16):1547–1557.
[87] Alemberti A, Carlsson J, Malambu E, Orden A, Struwe D, Agostini P, Monti S. European lead fast reactor – ELSY. Nucl Eng Des. 2011;241(9):3470–3480.

Downloaded by [The University of Manchester Library] at 08:36 21 June 2016

Appendix B

A stochastic ground motion accelerogram model for Northwest Europe

Soil Dynamics and Earthquake Engineering 82 (2016) 170–195

Contents lists available at ScienceDirect

Soil Dynamics and Earthquake Engineering

journal homepage: www.elsevier.com/locate/soildyn

A stochastic ground motion accelerogram model for Northwest Europe

Carlos Medel-Vera *, Tianjian Ji [1]

School of Mechanical, Aerospace and Civil Engineering, Pariser Building, Sackville Street, The University of Manchester, Manchester M13 9PL, UK

ARTICLE INFO

Article history:
Received 1 September 2015
Received in revised form
22 October 2015
Accepted 17 December 2015

Keywords:
Accelerograms
Stochastic models
Synthetic records
Earthquake ground motions
Northwest Europe
United Kingdom

ABSTRACT

This article presents a stochastic ground-motion accelerogram model for Northwest Europe which simulates accelerograms compatible with seismic scenarios defined by earthquake magnitudes $4 < M_w < 6.5$, distance-to-site 10 km $< R_{epi} <$ 100 km and different types of soil (rock, stiff and soft soil). This model is developed based on Rezaeian and Der Kiureghian (2008, 2010) [1,2] and is a set of predictive equations that define a time-modulated filtered white-noise process. Such predictive equations were calibrated by means of the random-effects regression technique using a subset of the European database of accelerograms. The model is validated in terms of PGA, PGV and spectral accelerations using GMPEs for the UK, Europe and Middle East, and other Stable Continental Regions. This model is the first of its kind for NW Europe.

© 2015 Elsevier Ltd. All rights reserved.

1. Introduction

In order to conduct seismic probabilistic risk analysis (SPRA), it is necessary to perform non-linear time history (NLTH) analysis of a structural model. Ultimately, this will lead to an estimation of the probability of unacceptable performance of the structure for the defined seismic hazard [3–5]. The main obstacle for conducting NLTH analysis of structures is the scarcity of accelerograms able to realistically represent the frequency content, intensity distribution and the strong shaking phase duration of recordings compatible with the scenarios that contribute most strongly to the hazard of the site selected [2]. This is an even more remarkable problem for areas of medium-to-low seismicity because: (i) strong earthquakes rarely occur, and (ii) those areas have limited monitoring networks [6]. For the United Kingdom (UK), which is a zone of relatively low seismicity, seismic hazard cannot be disregarded as strong earthquakes can still occur and may jeopardise the structural integrity of high-risk structures [7]. The paucity of accelerograms has led structural engineers to using techniques based on selecting, scaling and matching procedures applied to available records [8–10]. Even though the legitimacy and applicability of these procedures have been the subject of ample discussion in the literature [11–13], they are widely accepted and used by researchers and practitioners [14–16]. In general, these procedures are intended to match a spectral shape predicted by ad-hoc ground motion prediction equations (GMPEs). Currently, GMPEs play a critical role in seismic hazard and risk analysis and much research effort has been placed on the development of such models. Examples of state-of-the-art GMPEs are: the NGA-West2 Research Project [17], a major long-term project that developed attenuation models for active tectonic regions; and similarly for Europe and the Middle East, a new generation of GMPEs developed using the most recent pan-European strong-motion databank [18]. However, as SPRA requires the direct specification of sets of accelerograms, the use of GMPEs is actually an unnecessary intermediate step towards this objective [19]. Promising trends in earthquake engineering have been developed aiming at the replacement of GMPEs in seismic hazard and risk analysis for more rational approaches [20–22], as the one proposed in this work.

Stochastic generation of artificial accelerograms can be used to overcome the scarcity of ground-motion records. Currently, there are three techniques used to generate artificial accelerograms [23]: (i) mathematical or source-based models based on physical/seismological principles (e.g. Halldórsson et al. [24]; Liu et al. [25]); (ii) experimental or site-based models using measured/experimental data (e.g. Mobarakeh et al. [26]; Rofooei et al. [27]; Sgobba et al. [28]); and (iii) hybrid models that combine both approaches (e.g. Graves and Pitarka [29]). As pointed out by Boore [30], source-based models are mostly developed by seismologists in an attempt to explain the physics behind earthquake generation (e.g. source mechanism and propagation path). On the other hand, experimental models are mainly developed by engineers to obtain accelerograms using fitting techniques. From a structural engineering point of view, the main setback in using source-based

E-mail addresses: carlos.medelvera@postgrad.manchester.ac.uk (C. Medel-Vera), tianjian.ji@manchester.ac.uk (T. Ji).
* Corresponding author. Tel.: +44 161 306 2361; fax: +44 161 306 4646.
[1] Tel.: +44 161 306 4604; fax: +44 161 306 4646.

http://dx.doi.org/10.1016/j.soildyn.2015.12.012
0267-7261/© 2015 Elsevier Ltd. All rights reserved.

models is that a profound knowledge of the governing seismological features of the site of interest is needed.

For the UK, the underlying tectonic mechanism that causes earthquakes is not yet fully understood [31] and there is little correlation between the pattern of earthquake occurrence and the structural geology of Britain [32]. Additionally, the database of British earthquakes is mainly composed of accelerograms recorded from small magnitude earthquakes, M_w 2–4.5 [33]. Consequently, the nature of accelerograms (in terms of intensity, frequency content and time duration) is still unknown for stronger earthquakes, say M_w 6, that may occur in the UK [34]. This situation is critical for the British nuclear industry, as such a magnitude is in the order of earthquakes that need to be included in seismic risk analyses, when considering a design basis event of 10,000 years return period [35]. In order to help fill this gap, a site-based model based on Rezaiean and Der Kiureghian [1,2] is proposed that stochastically simulates two-component horizontal accelerograms compatible with any seismic scenario defined by an earthquake of magnitude $4 < M_w < 6.5$, distance-to-site $10 < R_{epi} < 100$ km and different types of soil (rock, stiff and soft soil). These accelerograms can be used to perform SPRA on high-risk structures in the UK and NW Europe. The model is based on a set of predictive equations for parameters that govern a fully non-stationary stochastic process that is used to simulate earthquake accelerograms. The predictive equations are calibrated using regression analysis on a dataset of accelerograms recorded in the tectonic region to which the UK belongs. The simulation of accelerograms is entirely made in the time domain, it essentially involves the generation of random variables and uses a few input data readily available in structural engineering practice. This model is the first of its kind for the general region of NW Europe including the UK. The model is validated through a comparison of estimated peak ground accelerations (PGA), peak ground velocity (PGV) and spectral accelerations with those produced by GMPEs for similar target geographical regions.

This article is organised as follows: Section 2 gives a full description of the target geographical region of interest and defines the dataset of accelerograms selected for this work. The explanatory variables selected to perform regression analyses for the predictive equations are also discussed in this section. Section 3 provides the stochastic process to simulate accelerograms and gives an example of simulation using a single record from NW Europe as the target accelerogram. This section also reports predictive equations for the parameters that govern the stochastic process and their regression coefficients, as a function of earthquake magnitude, distance-to-site and type of soil. Section 4 provides the procedure to simulate accelerograms and validates such simulations against recorded accelerograms from NW Europe and GMPEs. Such attenuation models are from three main regions: the UK, Europe and the Middle East, and other Stable Continental Regions (SCRs) whose tectonic behaviour is expected to be similar to NW Europe's. Section 5 discusses further aspects regarding the calibration and use of the model proposed, its validity, its limitations and its constraints imposed by traditional attenuation relations. Finally, the conclusions from this work are summarised in Section 6.

2. Target geographical region and model parameters

The United Kingdom (UK) is considered to be an intraplate region with moderate-to-low seismicity levels [32]. In seismological terms, it is part of one of several Stable Continental Regions (SCRs), possessing unique tectonic features. These features are mostly linked to the timing and nature of crustal deformation. Johnston et al. [36] reported a comprehensive study on the tectonic character and seismicity of SCRs worldwide. They defined nine major and some minor SCRs that cover approximately 2/3 of all continental crust (and 1/4 of all crust: continental, oceanic and transitional); however, they are only responsible for 0.22% of the global seismic moment release rate. This reflects the relatively low seismicity levels in SCRs (such as the UK) compared to tectonically active zones (such as California and Japan). In spite of this fact, seismic hazard in the UK is non-negligible, as strong ground motions capable of compromising the structural integrity of strategic facilities can still occur [7]. In terms of magnitudes, two of the most significant known earthquakes which occurred in the UK were in 1382 and 1580 in the Dover Straits area. Both events were of magnitude approximately M_L 5.75 [32]. This magnitude is close to the largest known earthquake occurred in the UK: an event M_w 5.8 occurred in the English Caledonides region of the North Sea in 1931 [37]. Additionally, in a study by Musson [38], it was suggested that a major earthquake M_w 7 could have occurred offshore in recent geological times in the NW European passive margin near Britain. Examples of the latest moderate earthquakes which have occurred in the UK are: (i) a M_L 4.7 event in September 2002 in Dudley, West Midlands [39] (ii) a M_w 4 event in April 2007 in Folkestone, Kent [40], and (iii) a M_L 5.2 event in February 2008 near Market Rasen, Lincolnshire [41]. The current state-of-the-art knowledge on the seismicity and seismic hazard zoning of the UK is reported in Musson and Sargeant [42].

Several problems arise when developing predictive models in zones that are not tectonically active. The database of British earthquakes is mainly composed of accelerograms recorded from a few small magnitude earthquakes. The use of such information, in the prediction of accelerograms of moderate-to-strong earthquakes, can produce unreliable and unrealistic results [42]. It is also not entirely consistent to make predictions based on accelerograms recorded in different SCRs from the region of interest. Even though all SCRs share the same fundamental crustal features, there is no overall agreement whether such regions are similar in terms of their earthquake generation and attenuation mechanisms [34]. Therefore, the predictive model proposed in this work is based on the assumption that the nature of accelerograms (intensity, frequency content and time duration) of strong magnitude earthquakes in Britain would be similar to those strong earthquakes occurred in the same SCR to which the UK belongs, namely NW Europe. This assumption effectively avoids both the use of small-magnitude records to predict moderate-to-large accelerograms and the inclusion of earthquakes from other SCRs or other intraplate regions.

2.1. Definition of Northwest Europe

A systematic description of the boundaries of NW Europe was needed. Various definitions have been reported in the literature, for example, Goes et al. [43] defined it as a relatively small area excluding the UK and the Scandinavian peninsula, whereas Ambraseys [44] defined it as a more expanded area including the UK and most of Norway and Sweden. The approach used in this work to define boundaries for NW Europe, was the Flinn–Engdhal (F–E) regionalisation scheme [45], comprising the countries and areas indicated in Table 1 and shown in Fig. 1. Such a definition of NW Europe is within the limits of the European SCR defined by Johnston et al. [36]. Hence, it can be considered as a subset of the SCR of interest, possessing relatively uniform tectonic features.

Regarding the size of the dataset, it is acknowledged that current databases of accelerograms have experienced a particularly rapid expansion in recent years to reach several thousands of available earthquake recordings [17,46]. Such an expansion has led a fast development of GMPEs: Douglas [47] showed that more

Table 1
Countries/areas that comprise the NW Europe F–E region [45].

Eire	Belgium
United Kingdom	Denmark
North Sea	Germany
Southern Norway	Switzerland
Sweden	Northern Italy
Baltic Sea	Austria
France	Czech and Slovak Republics
Bay of Biscay	Poland
The Netherlands	Hungary

than 15 new of these models are published every year. These models normally combine seismic events from different regions in order to calibrate them using datasets composed of a few thousands of recordings. One advantage of using stochastic accelerogram models is that it is possible to obtain similar results as those predicted by GMPEs but using smaller datasets. For example, Rezaeian and Der Kiureghian [1] showed that using a small subset of 206 accelerograms of the NGA database, a particularly good agreement was obtained with four GMPEs of the NGA Project, which in turn were calibrated using a large number of recordings ranging from 1574 to 2754. In this light, a small dataset of

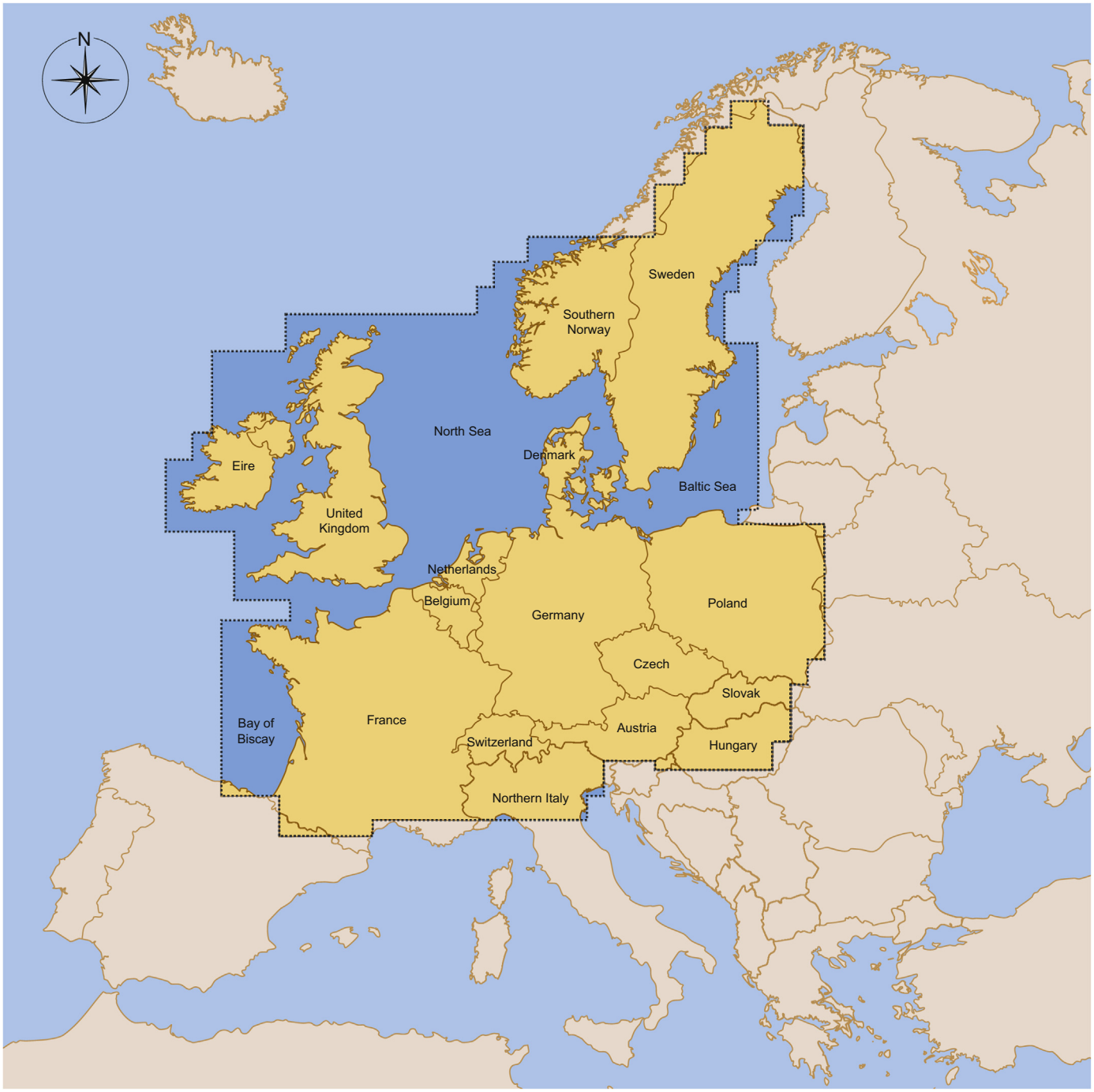

Fig. 1. Map of the NW Europe F–E region [45].

recordings from the European database was used in this work, yet a good agreement was expected to obtain with predictions made with European GMPEs.

A suitable pan-European on-line database in the public domain providing accelerograms from the countries/areas in Table 1, was the Internet Site for European Strong-Motion Data (ISESD) [33]. It is acknowledged that the existence of the most recent pan-European strong-motion databank [18] unifies all European databases of accelerograms. However, such a database was unavailable in the public domain at the time of writing. The variables considered for the model proposed in this work are: (i) earthquake magnitude, (ii) earthquake distance-to-site and (iii) type of soil. These variables are described in detail in the following sections. It is not possible to include the style of faulting in the present model, but a discussion on this topic is provided in Section 2.5.

2.2. Earthquake magnitude: scale and bounds

For this work, the moment magnitude scale (M_w) is used in calibrating the prediction model. Several earthquake magnitudes in the ISESD database are reported in different scales, namely, the surface-wave magnitude (M_s), the body-wave magnitude (m_b) and the local magnitude (M_L). Hence, their equivalent magnitudes in M_w need to be estimated. Conversion scale formulae, based on regression analysis, have been reported in literature [48]. However, the conversion formulae reported by Johnston [49] are used in this work as they were calibrated for SCRs only. Regardless of the conversion formulae used, it is acknowledged that their use can increase the uncertainty of the model [50]. Nevertheless, the use of conversion formulae is unavoidable when dealing with moderate-to-low seismic areas as the calculation of M_w for relatively small earthquakes is rarely undertaken.

For the lower bound magnitude in the dataset, M_w 4 was selected. This value is in line with lower bounds used for seismic hazard assessments in the UK [20]. It is acknowledged that some GMPEs intended for use in the UK [6,37] used a minimum magnitude of M_w 3. However, it is considered that such small earthquakes have little, or no, significance for structural engineering purposes. For the upper bound magnitude, M_w 6.5 was used. This magnitude has also been considered as the maximum value in seismic hazard assessments in Britain [42]. This value is also the maximum earthquake magnitude found in the ISESD database for the F–E region indicated in Table 1.

2.3. Earthquake distance: metric and bounds

Several distance metrics have been used in earthquake engineering: epicentral distance (R_{epi}), hypocentral distance (R_{hyp}), rupture distance (R_{rup}) and the Joyner–Boore distance (R_{JB}) [51]. R_{epi} and R_{hyp} are metrics that consider the earthquake rupture as a point source. These metrics are suitable for low-to-moderate magnitudes, but inappropriate for moderate-to-large earthquakes as the source comprises an extended area. In such scenarios, R_{rup} and R_{JB} are more appropriate. For the information source for this work, the ISESD database reports two distance metrics: R_{epi} and R_{JB}, although the latter is only reported for earthquake magnitudes greater than 6. As the completeness of R_{JB} is sparse, R_{epi} is used in this work. It is worth mentioning that R_{epi} and R_{JB} are closely related to each other, as both are defined along the surface of the Earth. The underlying assumption of using R_{epi} is that the variability of focal depths was not considered in the calibration of the prediction model proposed. British earthquakes, on average, can be considered to be shallow crustal. Small magnitude events have focal depths $\sim$10 km; for stronger events, the depth increases up to $\sim$25 km [52].

For this work, accelerograms recorded at R_{epi} less than 10 km were discarded. This is to exclude some intrinsic features of near-fault records that would need to be addressed in a separate model, e.g. severe directivity pulses [53], which can have a significant influence on the frequency content of accelerograms. The largest R_{epi} found in the ISESD database for the F–E region in Table 1 was 193 km. Certainly, the model proposed does not apply when dominant scenarios are controlled by near-fault conditions. However, some potential nuclear sites in the UK are controlled by seismic scenarios whose distances are $\geq$10 km [20,35,54], in which case the model proposed is fully applicable.

2.4. Type of soil

For the case of GMPEs calibrated for use in Western United States, the type of soil has been included quantitatively, through the average shear wave velocity in the upper 30 m (V_{S30}) [55]. However, for Europe and the Middle East, the type of soil was traditionally included qualitatively by directly specifying the class site (e.g. 'rock', 'stiff soil', etc.) (e.g [56,50]), although the most recent models have been calibrated by direct specification of V_{S30} [57]. For the specific case of UK models, the site classification has been considered qualitatively or it has not been included [37]. For NW Europe, the ISESD database reports both V_{S30} and types of soil based on the Boore et al. [58] criteria: very soft soil: $V_{S30} < 180$ m/s; soft soil: $180 < V_{S30} < 360$ m/s; stiff soil: $360 < V_{S30} < 750$ m/s; rock: $V_{S30} > 750$ m/s. For earthquakes from the F–E region in Table 1, the information for V_{S30} is not complete, but qualitative site classification is provided. Therefore, three types of soil are included: (i) rock, (ii) stiff soil and (iii) soft soil. Very soft soil is discarded as it is unlikely that any major civil structure would be built on such soil.

2.5. Faulting mechanism

For the case of GMPEs, the style of faulting is normally included qualitatively (e.g. 'strike-slip', 'normal', 'reverse') [17,57]. For the UK, the style of faulting is not normally included [37]. This is possibly due to the fact mentioned in Section 1 that the underlying tectonic mechanism causing earthquakes in the UK is not yet fully understood. Baptie [31] reported that the style of faulting related to British earthquakes is mostly strike-slip, but may be reverse and, at a lesser extent, normal. The ISESD database does report the style of faulting, but the information is not complete for the F–E region indicated in Table 1. Therefore, for this work, the faulting mechanism could not be included in the prediction model.

2.6. Summary of the dataset

Only accelerograms recorded in free-field conditions are included. All those recorded in buildings or other types of structure are discarded. Also, aftershocks are included in the dataset used in this work as the separation between mainshocks and aftershocks in European earthquakes has an unclear effect [59]. In summary, the dataset (last accessed 02.09.2013) considered for this work included free-field two-component horizontal accelerograms from earthquakes magnitude M_w 4–6.5, recorded at epicentral distances between 10 and 193 km, considering three generic types of soil: rock, stiff soil and soft soil. The total number of accelerograms obtained for the F–E region (Table 1) was 220 records (110 pairs of horizontal accelerograms) obtained from 43 earthquakes. In terms of the type of soil, the dataset used in this work includes 42 pairs of horizontal

accelerograms recorded in rock, 52 in stiff soil and 16 in soft soil. Fig. 2 provides a graphical summary of this dataset. Table 2 provides information of the earthquakes in this dataset.

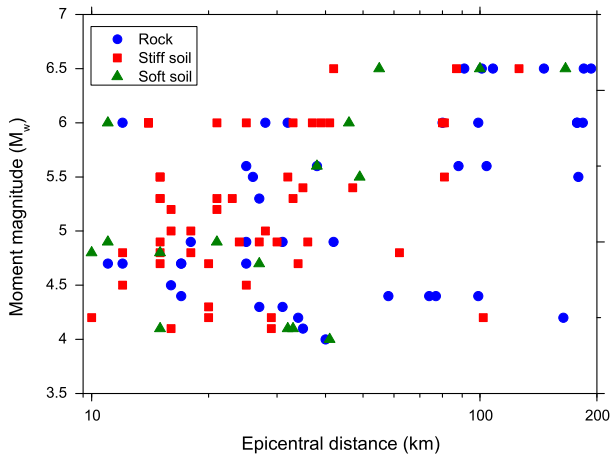

Fig. 2. Distribution of magnitudes and distances for the dataset used in this work.

3. Stochastic process and model calibration

As mentioned in Section 1, site-based or experimental models make simulations based on measured data of recorded earthquakes using mathematical fitting techniques. For the simulation of accelerograms, the majority of such models consist of the modulation in time of a filtered white-noise process. The key issue for these models is their ability to account for non-stationarity in the time and frequency domains. Examples of site-based models can be found in Mobarakeh et al. [26], Rofooei et al. [27], Sgobba et al. [28]. The work presented in this article has taken advantage of the stochastic process reported by Rezaeian and Der Kiureghian [2], as it presents particular features that ease its calibration and use for structural engineering purposes. The main features are: (i) temporal and spectral non-stationarities are totally decoupled; this eases the selection of functional parameters governing both non-stationarities to be fitted to real accelerograms, (ii) the model works exclusively in the time domain; hence Fourier analysis or other analyses in the frequency domain are not required, and (iii) the simulation of accelerograms essentially involves the generation of random variables, avoiding the use of more complex numerical analysis. In this section, the functional parameters of the stochastic process that characterise temporal and spectral

Table 2
Selected earthquakes for the dataset used in this work.

EQ No.	EQ ID[a]	F–E Region	EQ Name	EQ Country	M_w [b]	No. of records	Date	Time (UTC)
1	1406	United Kingdom	Penzance	UK	4.1*	2	10.11.1996	09:28:00
2	346	France	Epagny	France	4.2	4	15.07.1996	00:13:30
3	329	France	Grenoble	France	4.4*	10	11.01.1999	03:36:38
4	480	Switzerland	Domodossola	Italy	4	4	14.06.1993	12:28:37
5	438	Austria	Ebreichsdorf	Austria	4.1*	6	09.01.1996	01:07:22
6	1596	Austria	Bovec	Slovenia	4.3	2	06.05.1998	02:53:00
7	2144	Hungary	Varpalota	Hungary	4.7*	2	12.09.1995	22:14:04
8	34	Northern Italy	Friuli (mainshock)	Italy	6.5	24	06.05.1976	20:00:13
9	38	Northern Italy	Friuli	Italy	5.3*	2	09.05.1976	00:53:44
10	39	Northern Italy	Friuli	Italy	4.8	2	10.05.1976	04:35:54
11	40	Northern Italy	Friuli	Italy	4.9	2	11.05.1976	22:44:01
12	41	Northern Italy	Friuli	Italy	4.5*	2	13.05.1976	13:04:51
13	42	Northern Italy	Friuli	Italy	4.5*	2	15.05.1976	04:26:16
14	45	Northern Italy	Friuli	Italy	4.5*	2	18.05.1976	02:39:39
15	46	Northern Italy	Friuli	Italy	4.3*	2	01.06.1976	04:33:47
16	47	Northern Italy	Friuli	Italy	4.8*	2	01.06.1976	17:21:09
17	48	Northern Italy	Friuli	Italy	4.2	2	08.06.1976	12:14:38
18	50	Northern Italy	Friuli	Italy	4.2*	2	10.06.1976	13:04:23
19	52	Northern Italy	Friuli	Italy	5.2	4	17.06.1976	14:25:51
20	54	Northern Italy	Friuli	Italy	4.7*	4	14.07.1976	05:39:34
21	55	Northern Italy	Friuli	Italy	4.7*	2	15.07.1976	12:58:51
22	57	Northern Italy	San Gregorio	Italy	4.1	2	22.08.1976	02:49:15
23	60	Northern Italy	Friuli	Italy	5.3	10	11.09.1976	16:31:11
24	61	Northern Italy	Friuli	Italy	5.5	14	11.09.1976	16:35:03
25	62	Northern Italy	Friuli	Italy	4.8	4	13.09.1976	18:54:47
26	63	Northern Italy	Friuli	Italy	6	16	15.09.1976	03:15:19
27	64	Northern Italy	Friuli	Italy	4.9	10	15.09.1976	04:38:54
28	1205	Northern Italy	Friuli	Italy	4.7*	2	15.09.1976	04:58:42
29	65	Northern Italy	Friuli	Italy	6	28	15.09.1976	09:21:19
30	66	Northern Italy	Friuli	Italy	4.1	2	15.09.1976	09:45:54
31	72	Northern Italy	Friuli	Italy	5.4	4	16.09.1977	23:48:08
32	1823	Northern Italy	NE Gemona del Friuli	Italy	5*	4	18.04.1979	15:19:20
33	374	Northern Italy	Giaveno	Italy	4.8*	2	05.01.1980	14:32:26
34	124	Northern Italy	Toscana	Italy	4.7*	4	07.06.1980	18:35:01
35	402	Northern Italy	S of Parma	Italy	5	2	09.11.1983	16:29:52
36	403	Northern Italy	Arpiola	Italy	4.2*	2	22.03.1984	00:16:24
37	407	Northern Italy	Garfagnana	Italy	4.7*	4	23.01.1985	10:10:18
38	415	Northern Italy	NE Reggio nell'Emilia	Italy	4.9*	2	02.05.1987	20:43:54
39	477	Northern Italy	Valpelline	Italy	4.2	2	31.03.1996	06:08:02
40	1387	Northern Italy	Bovec	Slovenia	5.6	10	12.04.1998	10:55:33
41	1597	Northern Italy	Trasaghis-Friuli	Italy	4.3*	2	28.05.1998	09:39:19
42	989	Northern Italy	Cresta di Reit	Switzerland	4.9	8	29.12.1999	20:42:34
43	2169	Northern Italy	Meran	Italy	4.8	2	17.07.2001	15:06:12

[a] EQ ID is the earthquake identification used by the ISESD database.
[b] Earthquake magnitudes labelled with an asterisk have been estimated according to Section 2.2.

non-stationarities are fitted to the dataset of accelerograms. Such functional parameters are then regressed against few variables of interest for SPRA, namely, earthquake magnitude, distance-to-site and type of soil. This enables a set of predictive equations for the functional parameters to be obtained. The proposed predictive equations can be used to simulate sets of two-component horizontal accelerograms for SPRA of structures.

3.1. Mathematical formulation

Complete details of the mathematical formulation of the fully non-stationary stochastic process used in this work can be found in Rezaeian and Der Kiureghian [2]. This section provides a summary of the model and an example of its application. Rezaeian and Der Kiureghian [1] used the stochastic model proposed earlier to fit parameters to a dataset of accelerograms from Western United States. This paper is referenced, although several changes are considered in this work.

The stochastic model is based on a time-modulated filtered white-noise process with the filter having time-varying properties. It requires a time-modulating function to achieve temporal non-stationarity, and a filter function with time-varying properties to achieve spectral non-stationarity. The fully non-stationary stochastic model, $x(t)$, in its continuous form, is defined as follows:

$$x(t) = q(t,\underline{\alpha})\left[\frac{1}{\sigma_f(t)}\int_{-\infty}^{t} h[t-\tau,\underline{\lambda}(\tau)]\, w(\tau)\, d\tau\right] \tag{1}$$

where $q(t,\underline{\alpha})$ is the time-modulating function in which $\underline{\alpha}$ is a vector of parameters that control the shape and intensity of the function; $h[t-\tau,\underline{\lambda}(\tau)]$ is the linear filter with time-varying parameters $\underline{\lambda}(\tau)$; $w(\tau)$ is a white-noise (Gaussian zero-mean) process; and $\sigma_f^2(t) = \int_{-\infty}^{t} h^2[t-\tau,\underline{\lambda}(\tau)]d\tau$ is the variance of the process defined by the integral in Eq. (1). In this work, $q(t,\underline{\alpha})$ is presented as a piece-wise modulating function to model the temporal non-stationarity:

$$q(t,\underline{\alpha}) = \begin{cases} 0 & \text{if } t \le T_0 \\ \alpha_1\left(\frac{t-T_0}{T_1-T_0}\right)^2 & \text{if } T_0 < t \le T_1 \\ \alpha_1 & \text{if } T_1 < t \le T_2 \\ \alpha_1 \cdot e^{-\alpha_2(t-T_2)^{\alpha_3}} & \text{if } t > T_2 \end{cases} \tag{2}$$

Although other functions are available (e.g. gamma-type functions), the time-modulating function defined in Eq. (2) was chosen to give flexibility to the definition of the starting time and duration of the strong-shaking phase of accelerograms. This function has six parameters: $\underline{\alpha} = (\alpha_1, \alpha_2, \alpha_3, T_0, T_1, T_2)$ in which α_1 controls the maximum intensity, α_2 and α_3 are shape controllers of the decaying intensity, T_0 is the beginning of the process, and finally, T_1 and T_2 represent the start and end time of the strong shaking phase of an accelerogram. The time-varying linear filter proposed by Rezaeian and Der Kiureghian [1,2] is used in this work:

$$h[t-\tau,\underline{\lambda}(t)] = \begin{cases} \frac{\omega_f(t)}{\sqrt{1-\xi_f^2(t)}} e^{[-\xi_f(\tau)\omega_f(\tau)(t-\tau)]} \sin\left[\omega_f(\tau)\sqrt{1-\xi_f^2(\tau)}(t-\tau)\right]; & \tau \le t \\ 0; \quad \text{otherwise} \end{cases} \tag{3}$$

This filter represents the pseudo-acceleration response of a single-degree-of-freedom linear oscillator subjected to a unit impulse, in which $\tau$is the time of the pulse. In Eq. (3), the vector of parameters of the linear filter is $\underline{\lambda}(\tau) = [\omega_f(\tau), \xi_f(\tau)]$, in which $\omega_f(\tau)$ is the frequency function defining the distribution of the predominant frequency within the accelerogram, and $\xi_f(\tau)$ is the damping function controlling the bandwidth of the process. As it is expected that the predominant frequencies decay with time [60], a simple and reasonable model to consider for the frequency function is a linear decaying model:

$$\omega_f(\tau) = \omega_0 - (\omega_0 - \omega_n)\frac{\tau}{t_n} \tag{4}$$

where ω_0 and ω_n are the frequencies at the beginning and end of the accelerogram, and t_n is the total duration of the record. Although the bandwidth of accelerograms is expected to increase with time [60], as a first approximation, this variation in bandwidth can be considered to be fairly insignificant [2]. Therefore, a constant damping function is used in this work; i.e.

$$\xi_f(\tau) = \xi_f \tag{5}$$

Consequently, the fully non-stationary stochastic filtered white-noise process can be completely defined by nine parameters $(\alpha_1, \alpha_2, \alpha_3, T_0, T_1, T_2, \omega_0, \omega_n, \xi_f)$. Such parameters can be calibrated for a single recorded accelerogram and then be used to generate as many stochastic simulations as required which are compatible with the real record. In any case, artificially simulated accelerograms are likely to lead to overestimates of structural response at long structural periods [61]. In order to correct this issue, a high-pass filter is required to adjust the low-frequency content of the stochastic simulations. The high-pass filter used in this work is the second-order critically damped oscillator [60]:

$$\ddot{z}(t) + 2\omega_c\dot{z}(t) + \omega_c^2 z(t) = \ddot{x}(t) \tag{6}$$

In Eq. (6), $\ddot{z}(t)$ is the simulated (corrected) stochastic accelerogram and ω_c is the so-called "corner frequency" whose value depends upon the earthquake magnitude, the faulting geometry and the shear wave velocity [62]. The procedure to calibrate the nine parameters is briefly described through an example in the next section.

3.2. Example of simulation of accelerograms

The target accelerogram selected for this example is the North-South component of the Friuli earthquake, Northern Italy, which occurred on 06.05.1976, with a magnitude M_w 6.5, recorded in stiff soil at the Codroipo station with an epicentral distance of 42 km. The target accelerogram is shown in Fig. 3a.

- Time-modulating function parameters

The parameters $\underline{\alpha} = (\alpha_1, \alpha_2, \alpha_3, T_0, T_1, T_2)$ are determined by matching the cumulative energy of the target accelerogram, $E_a(t) = \int_0^{t_n} a^2(\tau)\, d\tau$, with the expected cumulative energy of the time-modulating function, $E_x(t) = \int_0^{t_n} q^2(\tau,\underline{\alpha})\, d\tau$. This was done through a Monte Carlo simulation approach. The parameters obtained for the target accelerogram are: $\alpha_1 = 0.232$ m/s^2, $\alpha_2 = 0.797$ s^{-1}, $\alpha_3 = 0.247$, $T_0 = 0.114$ s, $T_1 = 5.07$ s and $T_2 = 16.3$ s. Fig. 3a shows the target accelerogram and the time modulating function obtained using these parameters. Fig. 3b shows the cumulative energy for both functions and how closely they are matched. The error ε_q, in the approximation is obtained by calculating $\varepsilon_q = \int_0^{t_n} |E_x(t) - E_a(t)|dt / \int_0^{t_n} E_a(t)dt$. The error obtained for the sample accelerogram is$\varepsilon_q = 2.27\%$.

- Time-varying linear filter parameters

The iterative approach proposed by Rezaeian and Der Kiureghian [2] to obtain $\omega_f(\tau)$ and $\xi_f(\tau)$ is used. Such a procedure makes use of the *cumulative count of zero-level up-crossings* (Fig. 4a) and the *cumulative count of positive minima and negative maxima* (Fig. 4b) as surrogates of the predominant frequency and bandwidth, respectively. This procedure was done through a Monte Carlo simulation approach. Five damping ratios are considered for this example: $\xi_f = 0.25$, 0.30, 0.35, 0.40 and 0.45. The matching errors between the target and stochastic processes, both

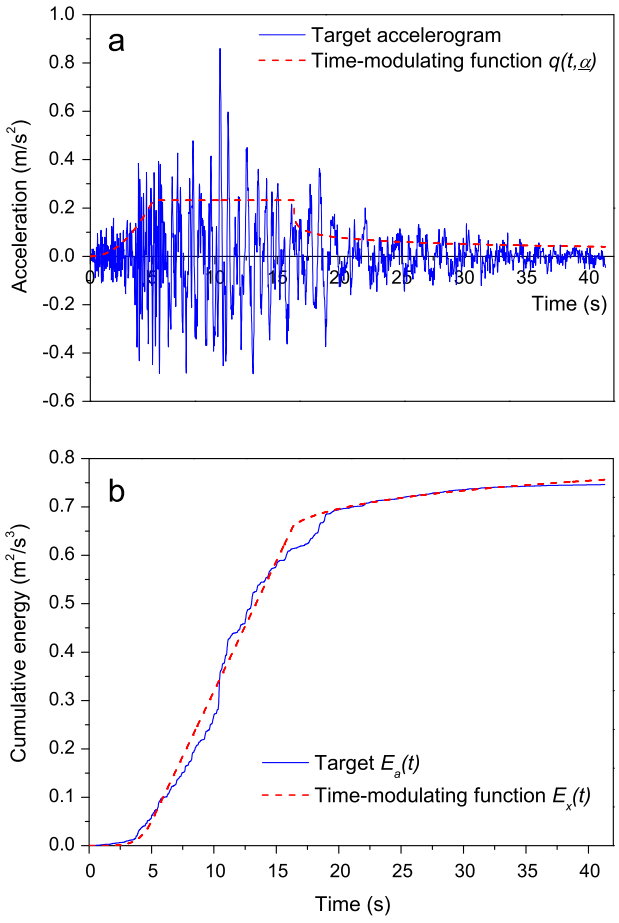

Fig. 3. Time-modulating function fitting process. (a) Target accelerogram and time-modulating function. (b) Cumulative energy for the target accelerogram and time-modulating function.

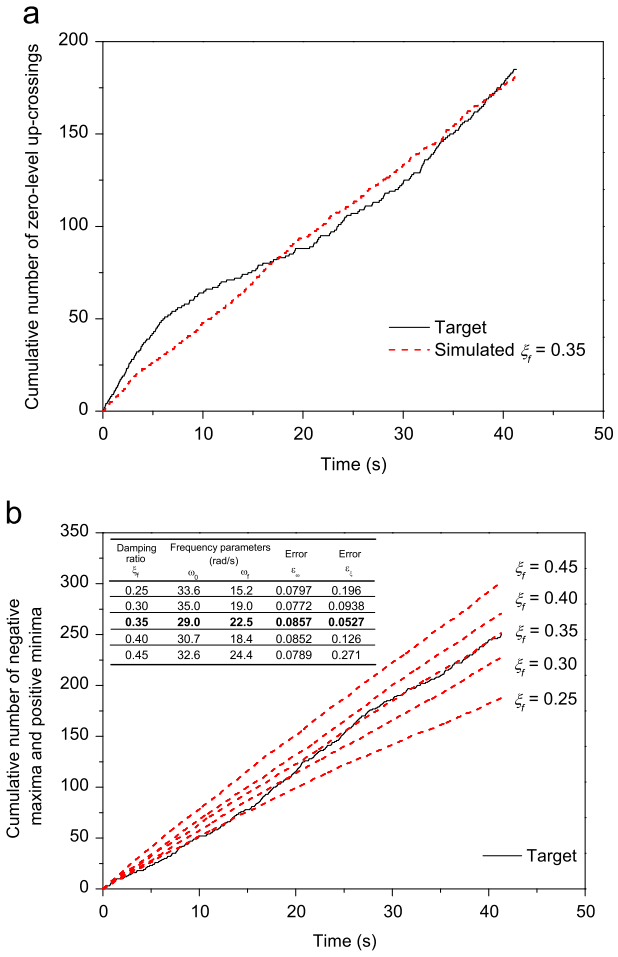

Fig. 4. Time-varying linear filter fitting process. (a) Cumulative number of zero-level up-crossings. (b) Cumulative number of negative maxima and positive minima.

in the cumulative number of zero-level up-crossings, ε_ω, and the cumulative count of positive minima and negative maxima, ε_ξ, can be obtained by minimising the difference between the curves normalised by the target curve. These errors are summarised in Fig. 4b for each damping ratio. The controlling error ε_ξ is minimised for the following filter parameters: frequency function parameters of $\omega_0 = 29.0$ rad/s,$\omega_f = 22.5$ rad/s with a damping ratio of $\xi_f = 0.35$.

Using the nine parameters determined above, it is possible to obtain as many accelerogram simulations as desired, which are compatible with the features of the target accelerogram. Each simulation is based on a different random white-noise process that gives a stochastic character to the model. Fig. 5 shows two simulations obtained and the target accelerogram.

Fig. 6a shows a comparison of 5% damped spectral acceleration for 10 simulated ground-motions and the recorded accelerogram. From this figure, it is possible to observe that at long periods, the simulated accelerograms are systematically above the target response spectrum. The high-pass filter defined in Eq. (6) with a corner frequency of $\omega_c = \pi$ (rad/s) is used to adjust the low-frequency content of the stochastic simulations. From Fig. 6b it can be seen that the post processing reduces the fitting error between the simulations and the target accelerogram in the long-period range without affecting the short/medium-period ranges.

In the next section, the nine functional parameters that define the stochastic process will be obtained for each of the accelerograms in the dataset defined in Section 2.

3.3. Model calibration

The two horizontal components of simulated ground motion accelerograms have to be orientated consistently in terms of their energy content to allow the structural engineer to make reasonable estimations of nonlinear structural responses. A minor setback of the dataset of accelerograms described in Section 2 is that their orientations are arbitrary and depend on the orientation of the recording instruments. Therefore, the dataset needs to be standardised to make reliable simulations. In this work, the dataset's standardisation was undertaken by orientating the two horizontal components into their *principal axes*. In such a scenario, the two components are uncorrelated, facilitating the simulation of suitable components of horizontal accelerograms for structural engineering purposes.

3.3.1. Principal axes

Earthquake ground motions could be orthogonally rotated along their principal axes, in which their intensities are maximum, intermediate and minimum with zero covariances [63]. Consequently, simulated earthquake accelerograms did not need to be statistically correlated when their components were orientated in their principal axes [64]. In general, the major principal component points to the earthquake epicentre, the intermediate principal component is perpendicular to the major component, and the minor principal component is vertical. In this work, the major and intermediate components for each of the selected 110 pairs of

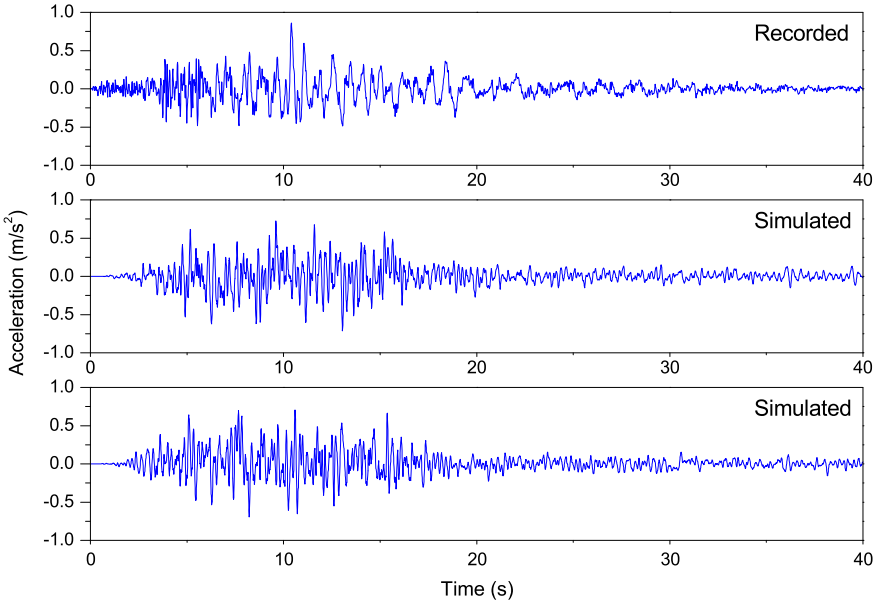

Fig. 5. Target accelerogram and two simulations using the stochastic model.

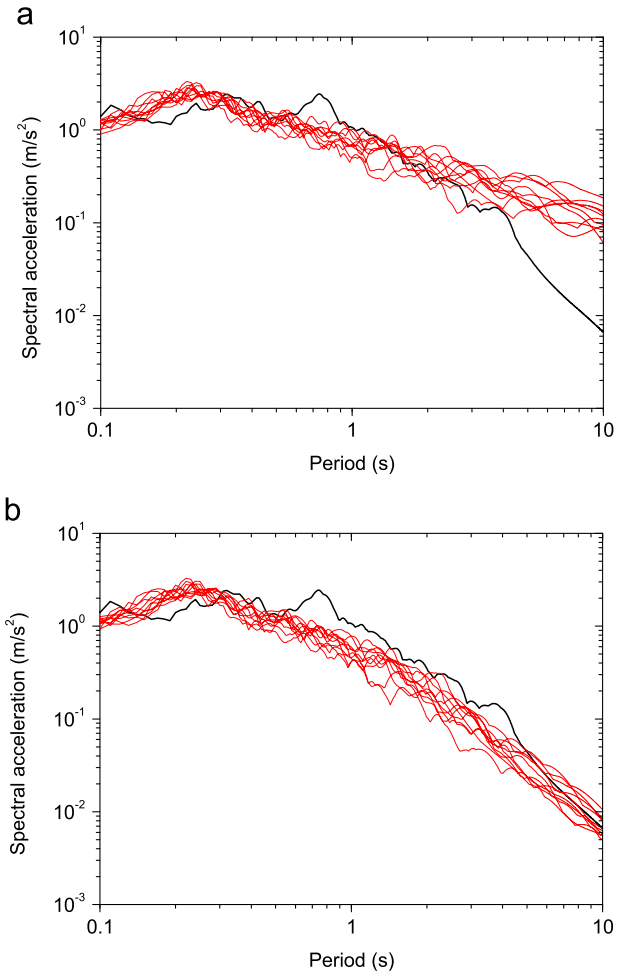

Fig. 6. Acceleration response spectra of the target accelerogram (the thick black line) and 10 simulations (the thin red lines). (a) Before high-pass filtering. (b) After high-pass filtering (For interpretation of the references to color in this figure legend, the reader is referred to the web version of this article.).

accelerograms are estimated. Then, the nine parameters of the stochastic process are fitted to each rotated accelerogram. In this light, such parameter values are associated to two uncorrelated horizontal ground motion components, i.e. the major and intermediate components. The vertical component is not included, although it could be incorporated in future models. When two horizontal ground motion components, $a_i(t)$ and $a_j(t)$, are orientated along their principal axes, their correlation coefficient, ρ_{ij}, is zero [65]. A qualitative measurement used to discriminate between the maximum and intermediate component is the Arias intensity [63], which is a measure of the total energy contained in an accelerogram. Naturally, the major component has the larger Arias intensity and the intermediate component has the smaller Arias intensity. Consequently, each of the 110 pairs of accelerograms was orthogonally rotated until the correlation coefficient reached a zero value (or a numerically small number). In this way, all pairs of accelerograms of the dataset were orientated in their major and intermediate principal components, using the Arias intensity as the discerning criterion. After rotation, the nine parameters of the stochastic process were calibrated for each accelerogram following the procedure discussed in Section 3.2. Table 3 gives a statistical summary of the nine parameters for both principal components.

In order to test the appropriateness of the numerical values for the parameters selected to simulate the major and intermediate components of accelerograms, four recorded bi-axial accelerograms from the dataset were selected to compare them against simulated records. Such accelerograms are identified using the unique waveform ID given by the ISESD database. They correspond to the following events: (1) M_w 6, R_{epi}=32 km (ID: 140); (2) M_w 4, R_{epi}=40 km (ID: 1338); (3) M_w 6.5, R_{epi}=42 km (ID: 49); and (4) M_w 4.7, R_{epi}=15 km (ID: 259). Accelerograms (1) and (2) were recorded in rock conditions whereas (3) and (4) were recorded in stiff soil conditions. Fig. 7 shows the major and intermediate components of the recorded accelerograms and corresponding stochastic simulations using the procedure summarised in Section 3.2.

3.3.2. *Distribution fitting*

For simplicity, some results presented in this section are for the major principal component only; however, when necessary for the completeness of the model, results for the intermediate component are included. To assign one statistical distribution for each parameter

of the stochastic process, their corresponding histograms were obtained. Then, trial marginal distributions were fitted to the corresponding histograms using the maximum likelihood estimation technique. To select the marginal distribution that best fits the corresponding histogram, the Kolmogorov–Smirnov goodness-of-fit test and the standard p-value used in statistical hypothesis testing were calculated for decision-making. All marginal distributions tested and selected were taken from the MATLAB's statistical toolbox. Fig. 8 shows the normalised histograms for each parameter of the stochastic process for the major component of the accelerogram dataset. Table 4 summarises the governing parameters obtained for the fitted marginal distributions and their p-values. From this table it can be seen that all marginal distributions selected are accepted (or more precisely, all null hypotheses stating that the experimental data for each parameter following the assigned marginal distribution fail to be rejected) at the standard 0.05 significance level. Furthermore, the remarkably high p-values confirm the high likelihood that the measured data actually come from the selected marginal distributions.

Table 3
Summary of parameters of the stochastic process for the major and intermediate components for the 220 accelerograms.

Major Component					
Parameter	Minimum	Maximum	Mean	Standard deviation	Coefficient of variation
α_1 (m/s^2)	0.000235	1.70	0.201	0.344	1.71
α_2 (s^{-1})	0.0353	3.10	0.818	0.491	0.600
α_3 (unitless)	0.0128	3.32	0.522	0.405	0.776
T_0 (s)	0.00440	13.0	1.87	2.87	1.53
T_1 (s)	0.0890	30.0	4.73	6.37	1.34
T_2 (s)	0.219	39.0	6.81	7.52	1.10
ω_0 (rad/s)	16.6	122.2	53.6	21.9	0.409
ω_n (rad/s)	1.35	87.0	31.7	18.3	0.576
ξ (ratio)	0.0600	0.800	0.242	0.126	0.519
Intermediate component					
α_1 (m/s^2)	0.000218	2.35	0.188	0.281	1.50
α_2 (s^{-1})	0.0703	2.28	0.788	0.438	0.556
α_3 (unitless)	0.0177	1.35	0.516	0.271	0.525
T_0 (s)	0.00400	12.9	1.80	2.65	1.47
T_1 (s)	0.0959	32.0	4.81	6.63	1.38
T_2 (s)	0.247	35.6	6.76	7.51	1.11
ω_0 (rad/s)	13.6	116.2	53.9	22.2	0.411
ω_n (rad/s)	1.22	80.8	32.4	19.4	0.598
ξ (ratio)	0.0600	0.800	0.248	0.147	0.592

3.3.3. *Regression analysis*

In this section, empirical predictive equations are proposed for each of the nine parameters. These predictive equations were obtained by means of regression analysis and a functional form is proposed to explain the statistical behaviour of each parameter (dependent variable) as a function of earthquake moment magnitude (M_w), epicentral distance (R_{epi}) and type of soil (independent variables). However, when assessing the significance of the regressions, the errors are assumed to be normally distributed for the functional form to be statistically meaningful. This statement implies that the dependent variables are also normally distributed

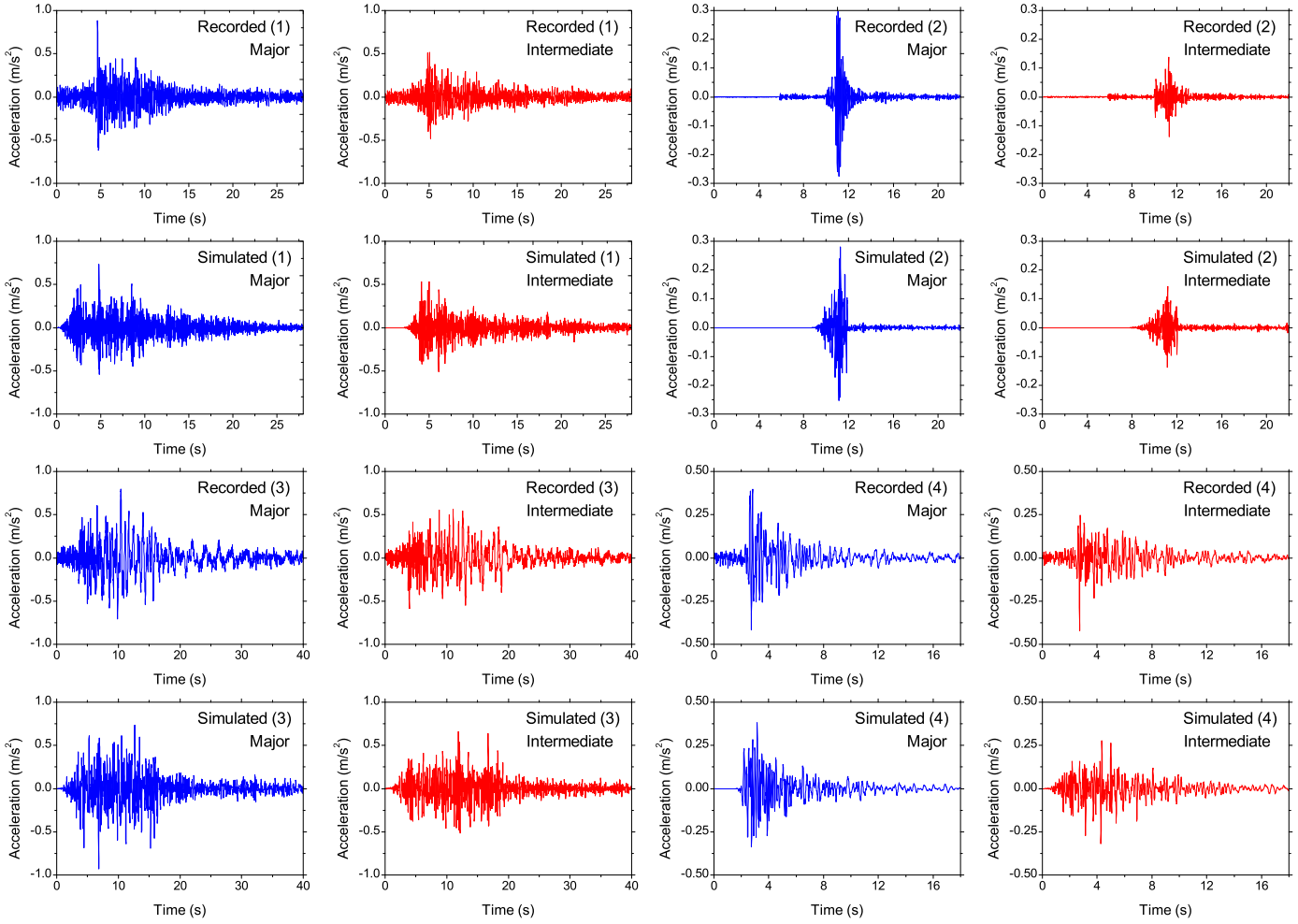

Fig. 7. Four recorded accelerograms (first and third rows) and corresponding simulations (second and fourth rows) for both principal components.

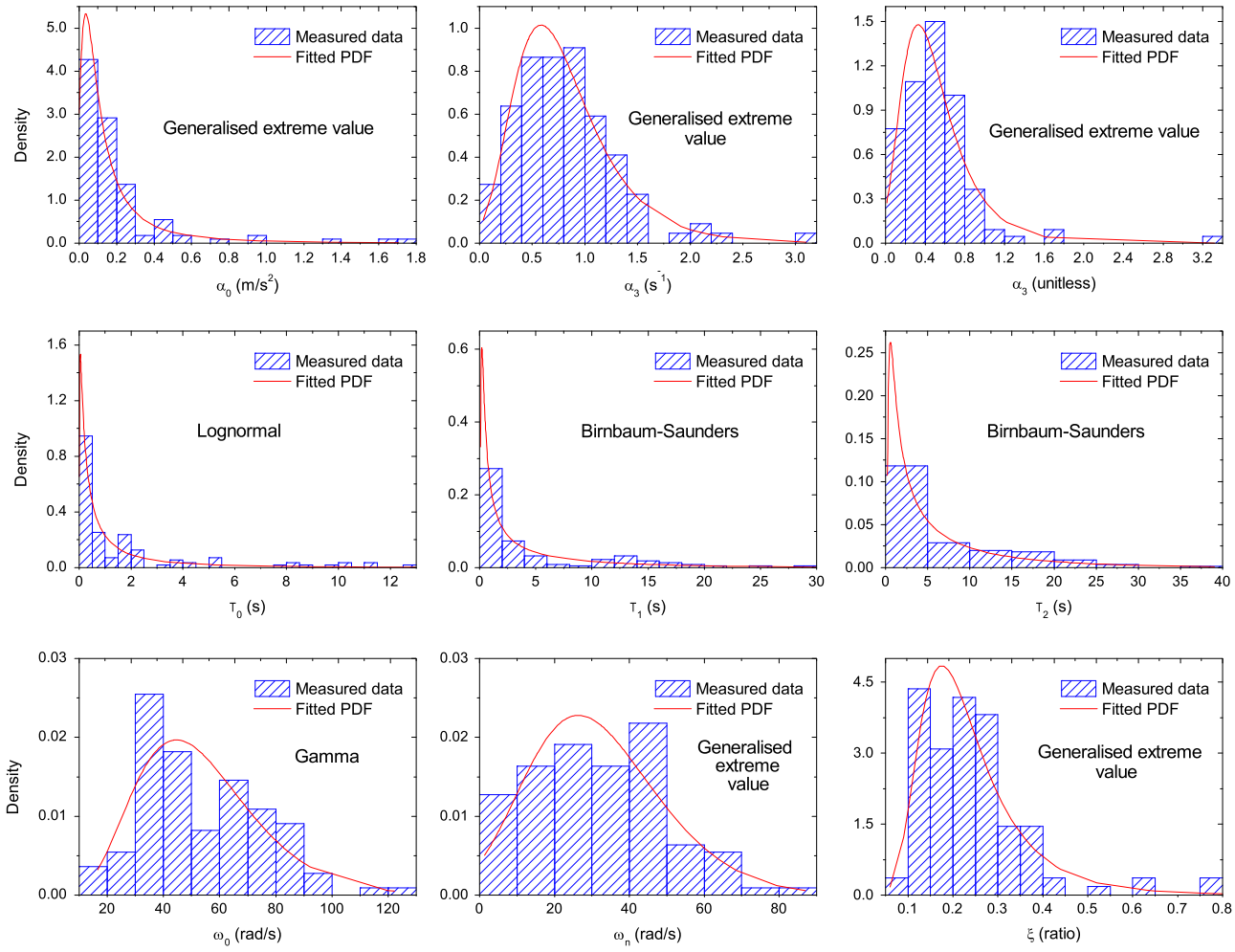

Fig. 8. Normalised histograms for each parameter of the stochastic process and their fitted marginal distributions for the major components of the accelerogram dataset.

Table 4
Fitted marginal distributions and results of hypothesis testing.

Parameter	**Fitted distribution**	Distribution parameters	Major		Intermediate	
			Value	*p*-value	Value	*p*-value
α_1 (m/s^2)	Generalised extreme value	k	0.635	0.325	0.603	0.718
		σ	0.082		0.078	
		μ	0.070		0.068	
α_2 (s^{-1})	Generalised extreme value	k	0.033	0.938	0.045	0.986
		σ	0.363		0.322	
		μ	0.597		0.587	
α_3 (unitless)	Generalised extreme value	k	0.093	0.725	−0.121	0.886
		σ	0.250		0.240	
		μ	0.353		0.403	
T_0 (s)	Lognormal	μ	−0.475	0.581	−0.433	0.833
		σ	1.664		1.570	
T_1 (s)	Birnbaum–Saunders	β	1.838	0.426	1.866	0.202
		γ	1.801		1.800	
T_2 (s)	Birnbaum–Saunders	β	3.310	0.481	3.425	0.590
		γ	1.435		1.392	
ω_0 (rad/s)	Gamma	a	6.014	0.254	5.933	0.644
		b	8.906		9.089	
ω_n (rad/s)	Generalised extreme value	k	−0.132	0.629	−0.125	0.921
		σ	16.296		17.076	
		μ	24.138		24.285	
ξ (ratio)	Generalised extreme value	k	0.143	0.889	0.214	0.983
		σ	0.077		0.084	
		μ	0.185		0.178	

[66]. However, as can be seen from Fig. 8, the dependent variables exhibit a non-normal statistical behaviour. Therefore, a transformation to the normal domain is required. The following change of variables was used [1]:

$$v_i = \Phi^{-1}\left[F_{\theta i}(\theta_i)\right] \quad i = 1, \ldots, 9 \tag{7}$$

In Eq. (7), v_i is the i-th transformed standard normal random variable; Φ^{-1} is the inverse standard normal cumulative distribution; θ_i is i-th parameter that defines the stochastic process, and $F_{\theta i}(\theta_i)$ is the marginal cumulative distribution function fitted for each θ_i. Once the nine dependent variables were transformed into normal distributions, empirical predictive equations were fitted to the measured data by means of regression analysis. As all data points of the dataset cannot be considered statistically independent observations, the random-effects regression technique by means of the algorithm proposed by Abrahamson and Youngs [67] was used to account for such an effect.

Regarding the functional form selected for the dependent variables, it is worth mentioning that models traditionally used for GMPEs are not necessarily valid for application in this work. Such models showed very little statistical significance in the regression analyses. This is due to the fact that GMPEs directly predict particular features of ground motions (e.g. peak ground acceleration) whereas the predictive equations proposed in this work determine nine single variables which are able to predict ground-motion accelerograms. As a consequence, the variable selection, and the form of such variables, played a crucial role in proposing a statistically meaningful functional form for the dependent variables. In this work, the forward stepwise method [66] was used to define the form of the variables and the functional form of the model. The main objective was to keep the number of explanatory variables as low as possible with the highest possible statistical significance, using only one functional form for all dependent variables. The functional form proposed for all parameters is given in Eq. (8), with the regression coefficients presented in Table 5.

$$v_i = \beta_{i,0} + \beta_{i,1} \cdot M_w + \beta_{i,2} \cdot \sqrt{R_{epi}} + \beta_{i,3} \cdot \ln\left(M_w \cdot R_{epi}\right) + \beta_{i,4} \cdot D_1 + \beta_{i,5} \cdot D_2 + n_i + \varepsilon_i \quad i = 1, \ldots, 9 \tag{8}$$

In Eq. (8), M_w and R_{epi} are the moment magnitude and epicentral distance (in km) for the seismic scenario to be simulated. The type of soil is modelled through two dummy variables D_1 and D_2: $D_1 = D_2 = 0$ for rock; $D_1 = 1$ and $D_2 = 0$ for stiff soil; and $D_1 = 0$ and $D_2 = 1$ for soft soil. Finally, n_i and ε_i are two normal random variables with zero mean and variances τ_i^2 and σ_i^2 that represent the residuals of the regressions for inter-event (random effect among different earthquakes) and intra-event (random effect among different accelerograms for the same earthquake) respectively. The total error of the model is then a normal random variable with zero mean and variance $\tau_i^2 + \sigma_i^2$. Table 5 also provides the standard deviations τ_i and σ_i. P-values in Table 5 are addressed in the following section.

3.3.4. Significance of regressions

In this section, the significance of the regressions are assessed for both the overall model adequacy and the coefficients obtained. Initially, the overall significance of the regression was assessed. For this case, the p-values for the f-test for the null hypothesis $H_0 : \beta_1 = \cdots = \beta_5 = 0$ are reported in Table 6. As all p-values are smaller than the standard 5% significance level, all null hypotheses are rejected. Also, the residual analysis was performed, and the total residuals were plotted against the model variables to check for deviations from normality. Figs. 9 and 10 show scatter plots of the total residuals for the nine dependent variables against M_w and R_{epi}, respectively. From this set of plots it is possible to observe that there are no apparent deviations from normality.

Tests on the significance of individual regression coefficients were also performed. P-values for the t-test for the null hypothesis $H_0 : \beta_i = 0$ are reported in Table 6 (β_0's are not included in this analysis as constants were not scrutinised).

Some p-values are higher than the standard 0.05 significance level, which means that the corresponding null hypothesis fails to be rejected. In such a case, the regression coefficients are of little value in explaining the variation of the corresponding dependent variable. However, as the functional form, in its entirety, is still able to represent the variation of the nine dependent variables (see p-values in Table 5), the regression coefficients of Table 5 were considered valid for simulations.

3.3.5. Correlations within principal axes

The variables v_i (either for the major or intermediate component) are correlated as they are derived using the same set of data, i.e. they are jointly normal random variables. Therefore, for consistency, such a correlation must be preserved when simulating

Table 5
Regression coefficients and standard deviations for the error random variables.

	Major component								
	β_0	β_1	β_2	β_3	β_4	β_5	τ	σ	p-value
v_1 (α_1)	0.7814	1.0668	0.2751	−1.6070	0.4110	0.0175	0.4852	0.5323	0.0000
v_2 (α_2)	4.1555	−0.2059	0.1435	−0.7665	−0.1218	0.2462	0.3564	0.8328	0.0008
v_3 (α_3)	0.9996	−0.0814	−0.0848	0.0069	0.0245	−0.6082	0.0781	0.9301	0.0215
v_4 (T_0)	−4.6028	−0.3342	−0.5952	1.9832	−0.2727	−0.1397	0.5740	0.7547	0.0075
v_5 (T_1)	−2.5345	−0.4945	−0.3979	1.4768	−0.0901	−0.0583	0.6754	0.7045	0.0231
v_6 (T_2)	−4.2075	−0.3931	−0.4153	1.7161	0.0544	0.0253	0.6779	0.6803	0.0114
v_7 (ω_0)	−0.7748	−0.8501	−0.4613	1.6332	−0.5170	−0.3077	0.1836	0.8411	0.0000
v_8 (ω_n)	−5.0464	−0.3083	−0.4932	1.9619	−0.6393	−0.2972	0.0141	0.8893	0.0001
v_9 (ξ)	−4.7793	−0.3850	−0.6217	2.1016	−0.2991	0.1322	0.1497	0.9501	0.0094
	Intermediate component								
v_1 (α_1)	0.5402	1.1438	0.3179	−1.6877	0.3794	−0.0083	0.4614	0.5215	0.0000
v_2 (α_2)	4.2933	−0.2351	0.2155	−0.8684	0.0720	0.1836	0.2663	1.0900	0.0081
v_3 (α_3)	1.7895	0.1881	0.0324	−0.5290	−0.3243	−0.6067	0.0374	0.9414	0.0353
v_4 (T_0)	−3.2093	−0.3599	−0.4034	1.5237	−0.4577	−0.0341	0.4960	0.8228	0.0255
v_5 (T_1)	−1.3461	−0.4227	−0.2670	1.0069	0.0036	−0.0502	0.8223	0.5098	0.0407
v_6 (T_2)	−4.7822	−0.4157	−0.5005	1.9481	0.0585	0.0649	0.7318	0.6281	0.0058
v_7 (ω_0)	0.1198	−0.7409	−0.3740	1.2472	−0.5771	−0.4125	0.2953	0.7965	0.0000
v_8 (ω_n)	−5.4575	−0.4664	−0.5289	2.2222	−0.4059	−0.2255	0.1628	1.0345	0.0000
v_9 (ξ)	−1.8771	−0.5859	−0.3816	1.4128	0.0405	0.3150	0.0640	0.9628	0.0194

Table 6
P-values for the *t*-test for the null hypothesis $H_0 : \beta_i = 0$.

	Major component					Intermediate component				
	β_1	β_2	β_3	β_4	β_5	β_1	β_2	β_3	β_4	β_5
ν_1 (α_1)	0.000	0.031	0.000	0.014	0.936	0.000	0.010	0.000	0.019	0.969
ν_2 (α_2)	0.202	0.367	0.167	0.558	0.370	0.239	0.275	0.206	0.780	0.589
ν_3 (α_3)	0.623	0.605	0.990	0.909	0.033	0.262	0.845	0.358	0.136	0.035
ν_4 (T_0)	0.049	0.001	0.001	0.212	0.626	0.037	0.018	0.010	0.040	0.907
ν_5 (T_1)	0.005	0.022	0.014	0.688	0.843	0.015	0.118	0.090	0.987	0.864
ν_6 (T_2)	0.023	0.015	0.004	0.805	0.931	0.017	0.004	0.001	0.792	0.824
ν_7 (ω_0)	0.000	0.003	0.002	0.010	0.239	0.000	0.013	0.018	0.004	0.110
ν_8 (ω_n)	0.053	0.002	0.000	0.002	0.270	0.013	0.005	0.001	0.094	0.477
ν_9 (ξ)	0.026	0.000	0.001	0.177	0.650	0.001	0.026	0.018	0.855	0.282

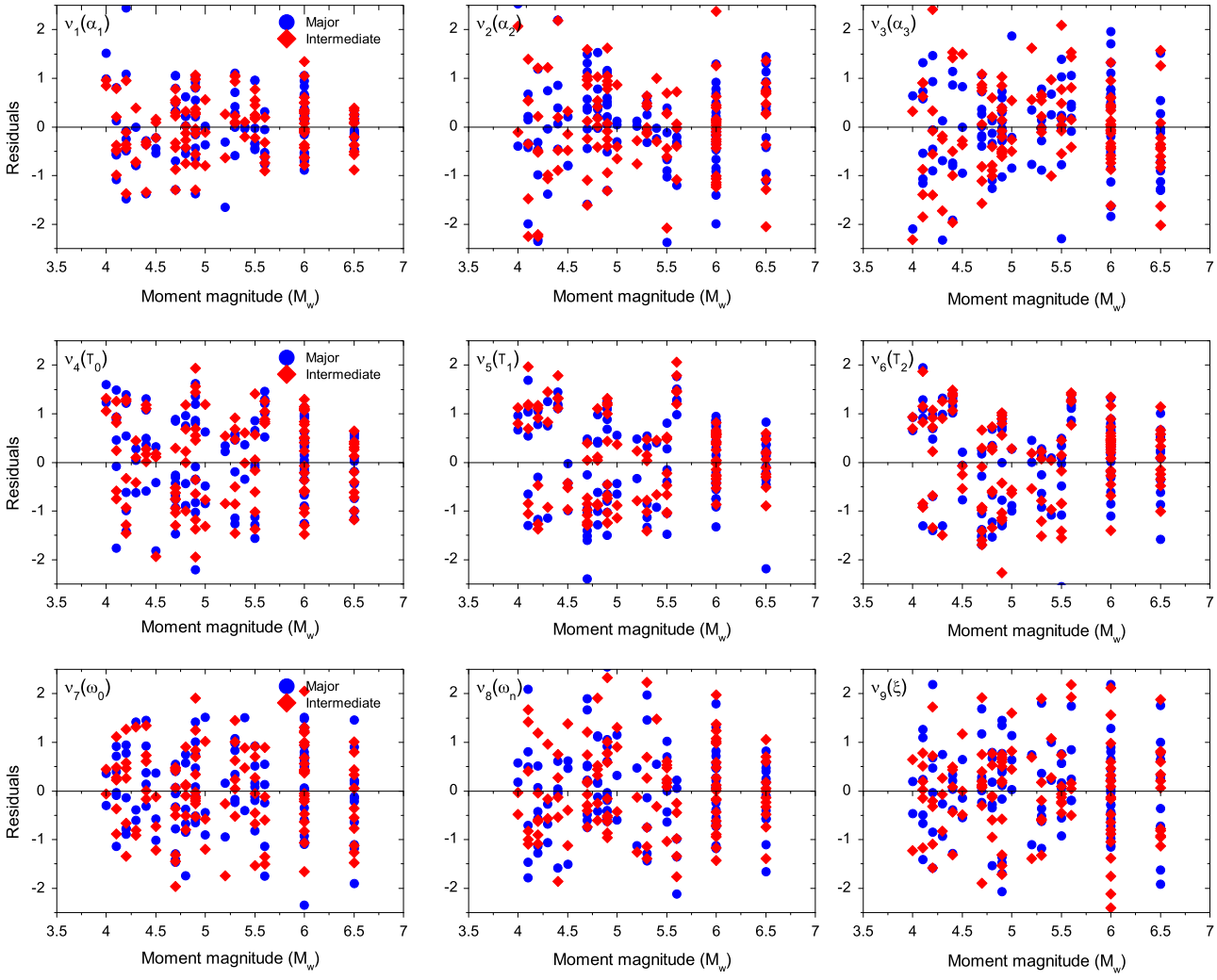

Fig. 9. Scatter plots of residuals against moment magnitude for the nine normalised variables.

accelerograms using the stochastic model and the predictive equations obtained from the regressions. This correlation can be estimated as the correlation coefficient between the inter-event η_i and the intra-event ε_i components of the total residual of regressions [1]. Table 7 shows the matrices of correlation coefficients for variables v_i for the major and intermediate components.

4. Simulation of accelerograms and model validation

In this section, the stochastic ground motion accelerogram model described in Section 3 is used to simulate accelerograms in order to validate its application against recorded accelerograms and GMPEs. The procedure involved in the generation of artificial accelerograms for any seismic scenario (moment magnitude, epicentral distance and type of soil) is summarised. Then, simulated accelerograms are compared with recorded accelerograms from the dataset. From this comparison, it is possible to see that the model is able to simulate the natural variability of accelerograms in terms of intensity, frequency content and time duration for a defined seismic scenario. In this sense, a recorded accelerogram can be seen as one data point from a wider range of accelerograms possible to be generated under a particular seismic

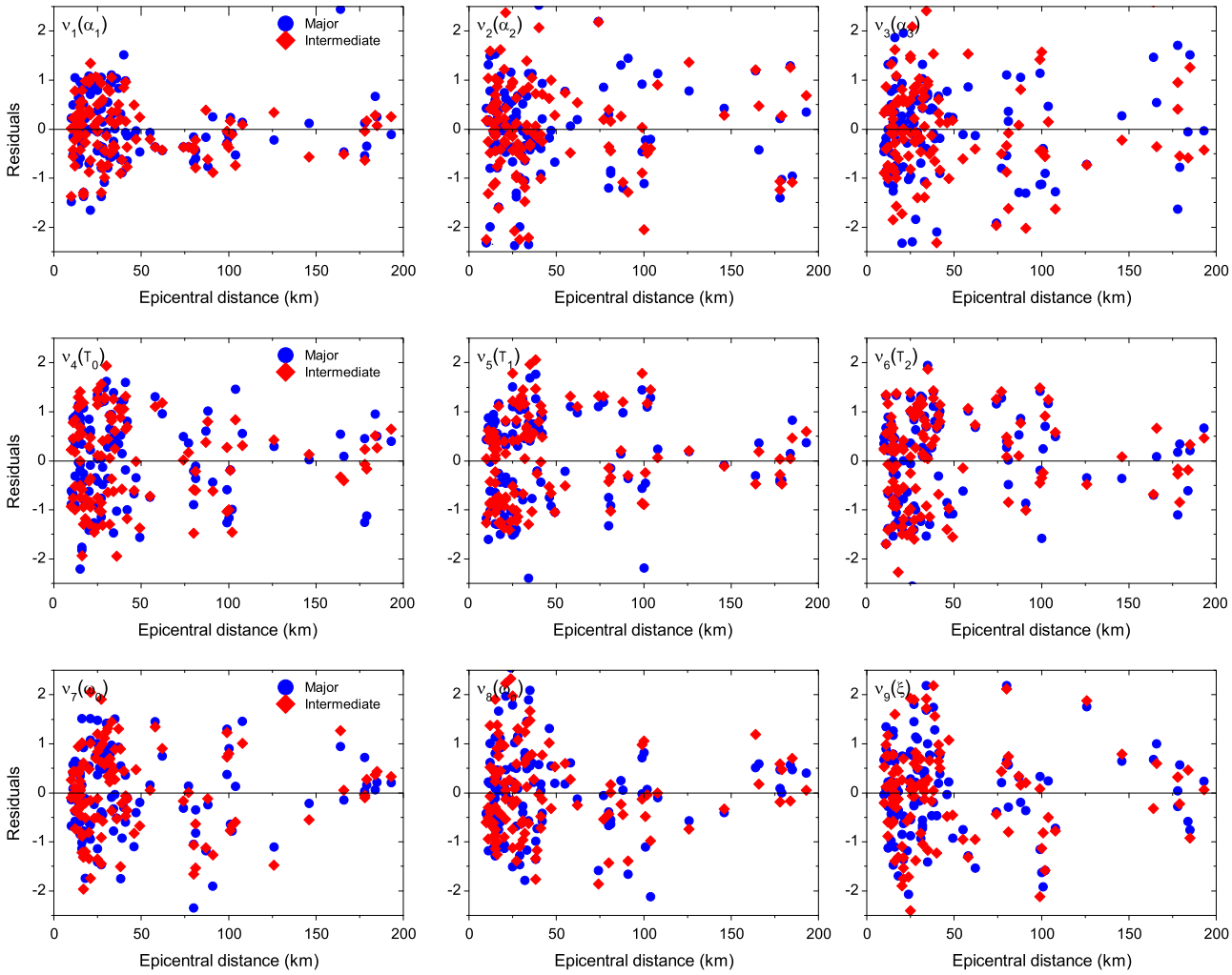

Fig. 10. Scatter plots of residuals against epicentral distance for the nine normalised variables.

Table 7
Correlation coefficients matrices for variables v_i for the major and intermediate component.

	Major component								
	$v1$	$v2$	$v3$	$v4$	$v5$	$v6$	$v7$	$v8$	$v9$
$v1$	1								
$v2$	0.4049	1							
$v3$	0.1551	−0.4909	1					Sym	
$v4$	−0.095	−0.0811	0.2381	1					
$v5$	−0.1872	−0.1506	0.2655	0.7648	1				
$v6$	−0.3815	−0.1849	0.1728	0.6766	0.883	1			
$v7$	0.081	−0.0557	0.0935	0.415	0.3592	0.2766	1		
$v8$	0.1741	−0.0108	0.0755	−0.1476	−0.1823	−0.2478	0.0998	1	
$v9$	−0.1388	−0.1155	0.0657	0.0959	−0.0167	−0.0003	−0.2352	−0.1544	1
	Intermediate component								
$v1$	1								
$v2$	0.479	1							
$v3$	0.095	−0.549	1						
$v4$	−0.093	−0.117	0.176	1				Sym	
$v5$	−0.235	−0.160	0.200	0.734	1				
$v6$	−0.379	−0.226	0.095	0.625	0.892	1			
$v7$	0.185	−0.048	0.258	0.405	0.366	0.308	1		
$v8$	0.195	0.091	0.050	−0.164	−0.180	−0.185	0.218	1	
$v9$	−0.252	−0.038	−0.068	0.097	0.013	0.021	−0.312	−0.337	1

scenario. A comprehensive set of accelerograms can be simulated containing as many accelerograms as required by the structural engineer to use for nonlinear time-history analyses. The model is validated in terms of peak ground acceleration, peak ground velocity and spectral accelerations. Accelerograms were simulated using the model proposed for a wide range of seismic scenarios

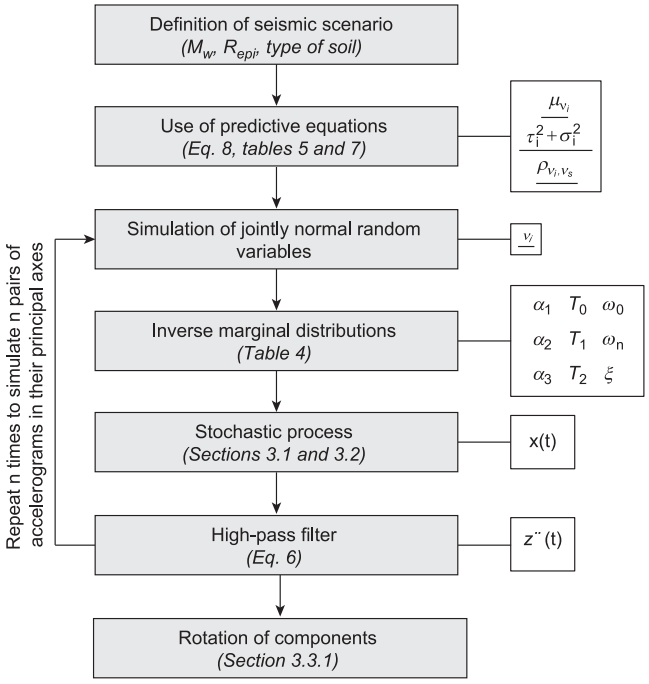

Fig. 11. Flowchart for the simulation of accelerograms compatible with a particular seismic scenario using the proposed model.

and compared with predictions made by GMPEs. The attenuation relations selected for these comparisons can be grouped in three main categories: (i) the UK, as a particular application of NW Europe, (ii) the broader region of Europe and the Middle East, and (iii) other Stable Continental Regions (SCRs) that possess a similar tectonic behaviour as NW Europe. The objective is to analyse the predictions made with the proposed model when compared with GMPEs whose target geographical regions can be considered comparable, to some extent, to the target region in this work.

4.1. Simulation of accelerograms

The flowchart in Fig. 11 summarises the steps to simulate accelerograms compatible with a particular seismic scenario (moment magnitude, epicentral distance and type of soil).

The procedure described in Fig. 11 was used to simulate accelerograms using a sample of four scenarios from the dataset outlined in Section 3.3, namely, the following events: (1) M_w 6, R_{epi}=32 km (ID: 140); (2) M_w 4, R_{epi}=40 km (ID: 1338); (3) M_w 6.5, R_{epi}=42 km (ID: 49); and (4) M_w 4.7, R_{epi}=15 km (ID: 259).

4.2. Validation for recorded accelerograms

Figs. 12 and 13 show the recorded traces of acceleration, velocity and displacement corresponding to the events selected that were recorded in rock condition and stiff soil conditions, respectively, and three stochastic simulations for each event. These figures show that for a single seismic scenario, a great variability in terms of intensity, frequency content and duration of the strong shaking phase is present in the simulated accelerograms. Such variability is likely to have a significant effect when assessing the seismic risk of civil structures for seismic scenarios of interest that dictate the seismic hazard of the selected site. Certainly, for structural engineering analyses, the zero acceleration history that may be obtained at the beginning of simulated accelerograms can be truncated to avoid unnecessary use of computer resources.

Fig. 14 shows the 5% damped acceleration response spectra for 30 simulations for the major component of each accelerogram defined above plus the response spectra for the four major components of the real records. It is observed that real accelerograms can be considered as only one record likely to be generated under the seismic scenario analysed. The variability present in the response spectra can be regarded as the natural variability associated with the earthquake generation phenomenon. Such variability should be properly accounted for when defining the seismic input for seismic probabilistic risk analysis. For NW European earthquakes, the proposed model seems to characterise reasonably well the natural variability of earthquakes for different scenarios defined by magnitudes, distances and types of soil.

4.3. Validation for GMPEs

4.3.1. Selection of GMPEs

A total of 15 GMPEs were selected for the three groups of comparisons, namely, (i) the UK, (ii) Europe and Middle East and (iii) other SCRs. Table 8 summarises these GMPEs and their main characteristics.

The following assumptions are made in order to perform meaningful comparisons between the GMPEs in Table 8 and the proposed model.

4.3.1.1. Scale magnitude. The moment magnitude scale (M_w) is used for the comparisons. GMPEs calibrated using the local magnitude (M_L) and the surface-wave magnitude (M_s) are transformed to M_w using the formulae calibrated by Johnston [49] for SCRs.

4.3.1.2. Distance metric. The epicentral distance (R_{epi}) is used for the comparisons. In order to allow transformations to R_{epi} from GMPEs calibrated using the Joyner–Boore distance (R_{JB}), hypocentral distance (R_{hyp}) and the rupture distance (R_{rup}), the following three assumptions are made: (i) only vertical faults are considered: in such a case, $R_{JB}=R_{epi}$; (ii) the focal depth is fixed to h=15 km; hence, the relationship between R_{epi} and R_{hyp} is analytical $\left(R_{hyp}=\sqrt{R_{epi}^2+h^2}\right)$ and (iii) the earthquake rupture is modelled as a point source: in such a case $R_{rup}=R_{hyp}$ and assumption (ii) can then be applied. It is worth mentioning that such a focal depth can be considered "average" for British earthquakes (Musson [52] provided a discussion on the focal depths for UK earthquakes) and it was also used by other researchers (e.g. the GMPE of Dahle et al. [73] for intraplate regions).

4.3.1.3. Type of soil. Comparisons are made either considering rock or hard rock conditions. Therefore, conversion factors between both types of soil are used. In any case, a rigorous adjustment would involve knowledge of the soil profile of the site of interest in terms of both shear-wave velocity and soil density [80]. As a rough estimation is intended in the following sections, simplified approaches are followed. One such approach, Cotton et al. [81], provided adjustment factors for hard rock conditions (V_{S30}=2880 m/s) and rock conditions (V_{S30}=618 m/s). A more recent model reported by Van Houtte et al. [82] provided adjustment factors derived for hard rock sites ($V_{S30}>2000$ m/s) and rock sites ($V_{S30}\sim800$ m/s). Either model could be used, however, the adjustment factors proposed by Van Houtte et al. [82] are arbitrarily selected. For those GMPEs that did not include site classification, it is assumed that they were calibrated for generic rock conditions, unless otherwise stated.

4.3.1.4. Style of faulting. GMPEs that include the style of faulting are set to strike-slip conditions. Even though the proposed model does not include style of faulting, strike-slip condition is chosen as it is most likely to occur in British earthquakes [31].

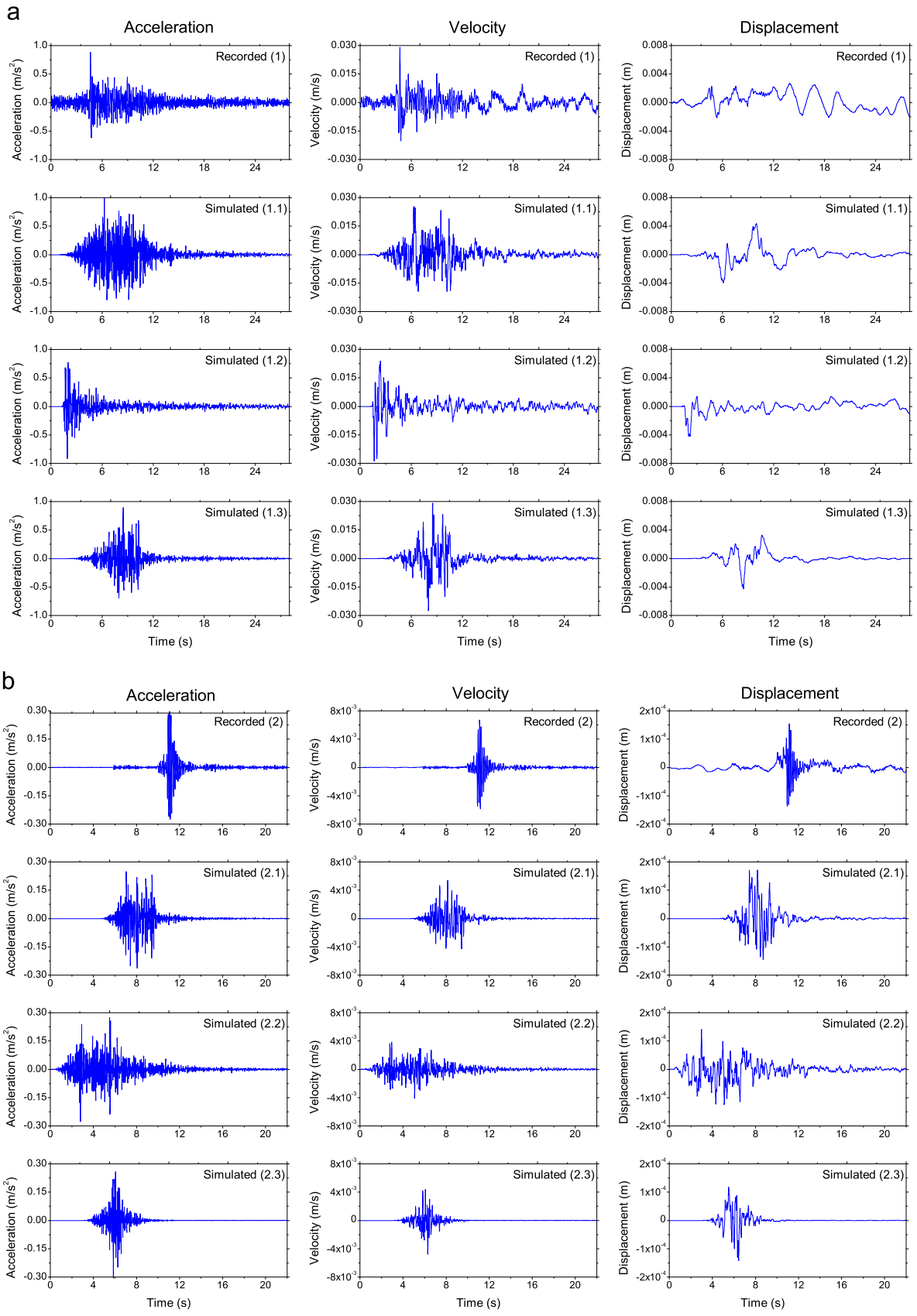

Fig. 12. Recorded (first row) and simulated traces (last three rows) of acceleration, velocity and displacement recorded in rock conditions. (a) M_w 6, R_{epi}=32 km (ID: 140). (b) M_w 4, R_{epi}=40 km (ID: 1338).

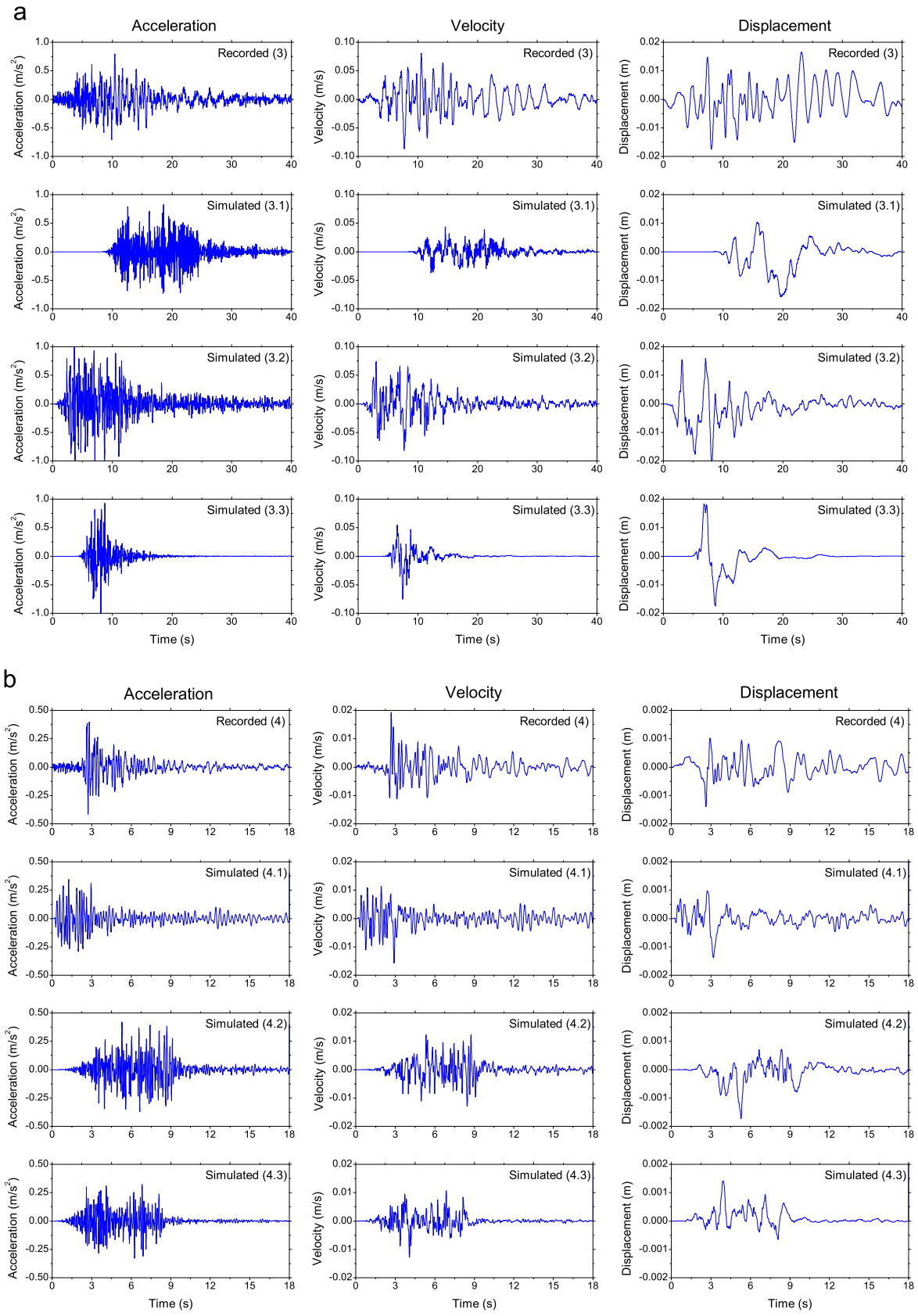

Fig. 13. Recorded (first row) and simulated traces (last three rows) of acceleration, velocity and displacement recorded in stiff soil conditions. (a) M_w 6.5, R_{epi}=42 km (ID: 49). (b) M_w 4.7, R_{epi}=15 km (ID: 259).

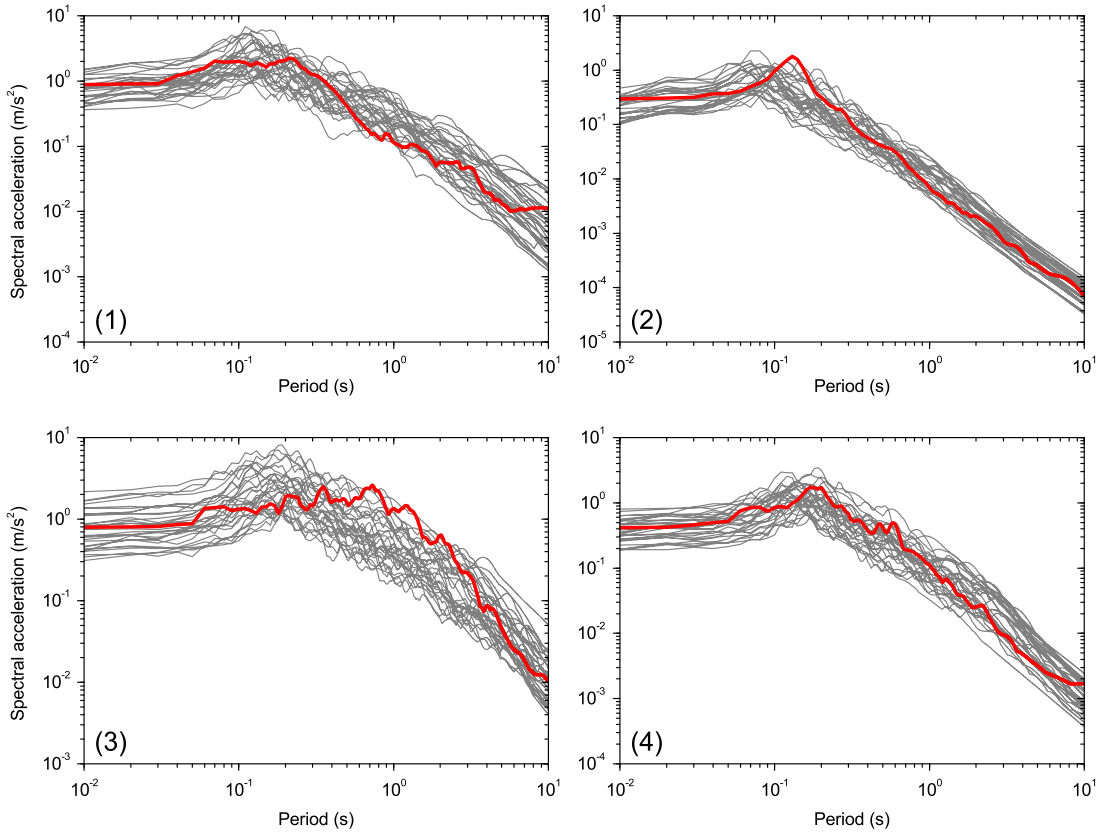

Fig. 14. 5% Damped acceleration response spectra for 30 simulations and real accelerograms (thick red line) for four real records (For interpretation of the references to color in this figure legend, the reader is referred to the web version of this article.).

4.3.1.5. Component of motion. Comparisons are made, either considering the larger horizontal (LH) component of motion, or the geometric mean (GM) of the two horizontal components of motion. Therefore, conversion factors between both types of components of motion are used. For this purpose, the coefficients proposed by Beyer and Bommer [83] are used. When making simulations with the proposed model, only the major component is used for LH comparisons and the geometric mean of the major and intermediate components $Sa_{GMxy}(T_i) = \sqrt{Sa_x(T_i) \cdot Sa_y(T_i)}$ [83] is used for GM comparisons.

Finally, two earthquake magnitudes are analysed throughout the following sections: (i) an earthquake M_w 6, that represents a "severe" event and (ii) an earthquake M_w 5, that represents a "moderate" event. The earthquake magnitude M_w 6 is selected as it is in line with the maximum magnitudes M_L 6.5–6.6 to be used in hazard analyses in the UK when considering a 10,000 years return period event [35] (an earthquake M_w 6 can be equivalent to an earthquake M_L 6.6 if the quadratic transformation formula of Johnston [49] is used). The choice of an earthquake M_w 5 as representative of a "moderate" event is made arbitrarily.

4.3.2. Peak ground acceleration estimation

Initially the effect of the number of simulations on the PGA estimation is studied. From this analysis, it was possible to conclude that the median PGA estimated with the proposed model tends to be reasonably stable when the number of simulations is equal or greater than 100. Differences when using more than 100 simulations can be considered negligible for structural engineering purposes. When 100 simulations are used several times to estimate the median PGA, there are slight differences in the final value as the accelerograms are stochastic in nature. Those differences, however, are numerically negligible. Consequently, analyses presented in the following sections are carried out considering the median of 100 simulations using the model proposed. Fig. 15 shows PGA estimation for earthquake magnitudes M_w 5 and 6, considering epicentral distances between 10 and 100 km for the UK (rock conditions), Europe and the Middle East (rock conditions) and SCRs (hard rock conditions). The standard deviation is shown for the results obtained with the proposed model and for one GMPE selected arbitrarily as the one that showed the closest behaviour to the proposed model for each group, namely, Rietbrock et al. [37] for the UK, Akkar et al. [72] for Europe and the Middle East, and Chen [79] for SCRs. Additionally, Table 9 provides a numerical summary of the data depicted in Fig. 15.

It is worth mentioning that the reason for taking the upper bound limit for epicentral distances as 100 km is due to the limitation of the proposed model to properly predict the rate of PGA attenuation for such distances. In other words, for epicentral distances longer than 100 km, the model tends to predict similar PGAs predicted for 90–100 km distance. This limitation of the model is due to the lack of information in the dataset (high epistemic uncertainty) of accelerograms recorded for epicentral distances longer than 100 km (see Fig. 2 for confirmation). Nevertheless, for structural engineering purposes, this limitation is relatively irrelevant: examples of disaggregation of hazard curves for the UK for a 10,000-years-return-period event [20,35,54], showed that earthquake distances longer than 100 km are of little or no significance in seismic hazard. Consequently, the upper bound of 100 km is considered sufficient for the purposes of risk analyses in the UK.

4.3.2.1. PGA estimation for the UK. GMPEs 1, 2, 3 and 4 in Table 8 are used for comparisons in the UK for the larger horizontal component of motion and consider generic rock conditions. GMPEs 1 and 2 are relevant in the UK as they have been extensively used for seismic hazard assessments of high-risk civil

Table 8
GMPEs selected for comparisons with the model proposed in this work.

N	Reference	Specific region	GMP[a]	HC[b]	M[c]	R[d]	Site classification	Style of faulting
	United Kingdom							
1	PML (1982) [68]	UK	PGA, PSV	LH	M_s	R_h	Rock, stiff soil and soft soil	Not included
2	PML (1985) [69]	UK	PGA, PSV	LH	M_s	R_h	Rock, stiff soil and soft soil	Not included
3	Musson et al. (1994) [70]	UK	PGA, PSV	LH	M_L	R_h	Not included	Not included
4	Rietbrock et al. (2013) [37]	UK	PGA, PGV, PSA	GM	M_w	R_{JB}	Hard rock (V_{s30}∼2300 m/s)	Not included
	Europe							
5	Akkar and Bommer (2010) [56]	Europe, Mediterranean Region and the Middle East	PGA, PGV, PSA	GM	M_w	R_{JB}	Rock ($V_{s30}>750$ m/s), Stiff soil ($360<V_{s30}<750$ m/s) Soft soil ($V_{s30}<360$ m/s)	Normal, strike-slip and reverse
6	Ambraseys et al. (2005) [50]	Europe and the Middle East	PGA, Sa	LH	M_w	R_{JB}	Rock ($V_{s30}>750$ m/s), Stiff soil ($360<V_{s30}<750$ m/s) Soft soil ($180<V_{s30}<360$ m/s) Very soft soil ($V_{s30}<180$ m/s)	Normal, strike-slip, thrust (reverse) and odd
7	Bommer et al. (2007) [71]	Europe and the Middle East	PGA, PSA	GM	M_w	R_{JB}	Rock ($V_{s30}>750$ m/s), Stiff soil ($360<V_{s30}<750$ m/s) Soft soil ($V_{s30}<360$ m/s)	Normal, strike-slip and reverse
8	Akkar et al. (2014) [72]	Europe and the Middle East	PGA, PSA	GM	M_w	R_{JB}, R_{ep}, R_{hyp}	Direct specification of V_{s30} (reference $V_{s30}=750$ m/s)	Normal, strike-slip and reverse
9	Dahle et al. (1990) [73]	Intraplate regions	PGA, PSV	LH	M_s	R_{hyp}	Not included	Not included
	Stable Continental Regions							
10	Toro et al. (1997) [74]	Central and Eastern North America	PGA, Sa	LH	M_w, m_{Lg}	R_{JB}	Hard rock (V_{s30}∼1800 m/s)	Not included
11	Campbell (2003) [75]	Eastern North America	PGA, PSA	GM	M_w	R_{rup}	Hard rock ($V_{s30}=2800$ m/s)	Not included
12	Liang et al. (2008) [76]	Australia	PGA, PGV, Sa	LH	M_L	R_{epi}	Generic rock	Not included
13	Kennedy et al. (2005) [77]	Australia	PGA,PGV	LH	M_L	R_{epi}	Generic rock	Not included
14	Raghu Kanth and Iyengar (2007) [78]	India	PGA, Sa	LH	M_w	R_{hyp}	Hard rock ($V_{s30}=3600$ m/s)	Not included
15	Chen (2008) [79]	Western China	PGA	LH, SH	M_L,M_s	R_{epi}	Not included	Not included

[a] Ground motion parameter predicted: PGA: peak ground acceleration; PGV, peak ground velocity; PSA: pseudospectral acceleration; PSV: pseudospectral velocity; Sa: spectral acceleration.
[b] Definition of the horizontal component: GM: geometric mean; LH: larger horizontal component; SH: smaller horizontal component.
[c] Magnitude scale used.
[d] Distance metric used.

structures. As mentioned by Lubkowski et al. [6], they have been used in the seismic risk assessment of "nuclear facilities, offshore oil and gas platforms, large dams, military installations and even the Channel Tunnel". Despite their widespread use, many concerns have been raised on the suitability of such predictive equations, calibrated about 30 years ago, and the necessity of upgrading earthquake estimation in the UK [34]. It is worth mentioning that the GMPEs 1, 2 and 3 were obtained indirectly through the comprehensive compilation of published GMPEs reported by Douglas [47]. GMPE 4 was the latest GMPE specifically calibrated for the UK found in the literature. This study calibrated two models based on the dependency/independency with magnitude of the stress parameter that defines the expected Fourier spectra of British earthquakes.

Fig. 15a shows that the PGAs estimated by the proposed model agree reasonably well with the magnitude-dependent stress parameter model reported by Rietbrock et al. [37]. In general, the models of PML [68–69] and Musson et al. [70] predicted higher values of PGAs, especially for epicentral distances shorter than 60–70 km. The constant stress parameter model of Rietbrock et al. [37] predicted systematically lower values of PGAs compared to the estimations made using the proposed model. The fact that the models of PML [68,69] estimated greater values of PGAs in the whole range of distances, compared to the proposed model, is a somewhat expected outcome. Such prediction equations were calibrated using datasets that comprised earthquakes from sites such as Central America, Greece, New Zealand and California. These zones belong to different tectonic regimes than those in Britain, and in general, they are more seismically active zones. This fact has raised many concerns on the validity of the PML equations and their current use in the British nuclear industry [34]. It is also likely that the use of PML equations may have led to an overestimation of seismic hazard analyses for nuclear sites in the UK.

4.3.2.2. PGA estimation for Europe and the Middle East. It is desirable to compare the proposed model with other models developed for the region of NW Europe. An early attempt was the model developed by Ambraseys [44] although the attenuation was modelled using the Medvedev–Sponheuer–Karnik (MSK) intensity scale. No PGA attenuation model is found in literature that has been calibrated with information exclusively taken from this region. Consequently, the closest models suitable for comparisons with the proposed model could be models calibrated using data from the wider region of Europe and the Middle East.

GMPEs 5, 6, 7, 8 and 9 in Table 8 are used for comparisons in Europe and the Middle East for the larger horizontal component of motion and consider generic rock conditions. GMPEs 5 to 7 are models widely and traditionally used in Europe; whereas GMPE 8 is part of the new generation of attenuation relations recently developed for Europe and the Middle East. This GMPE was randomly selected as representative from the five models that belong to the same project. Comprehensive comparisons among such five models can be found in Douglas et al. [57].

From Fig. 15b, it can be observed that the PGAs estimated by the proposed model, in general, fall below the predictions made by the selected GMPEs, especially for epicentral distances <60–

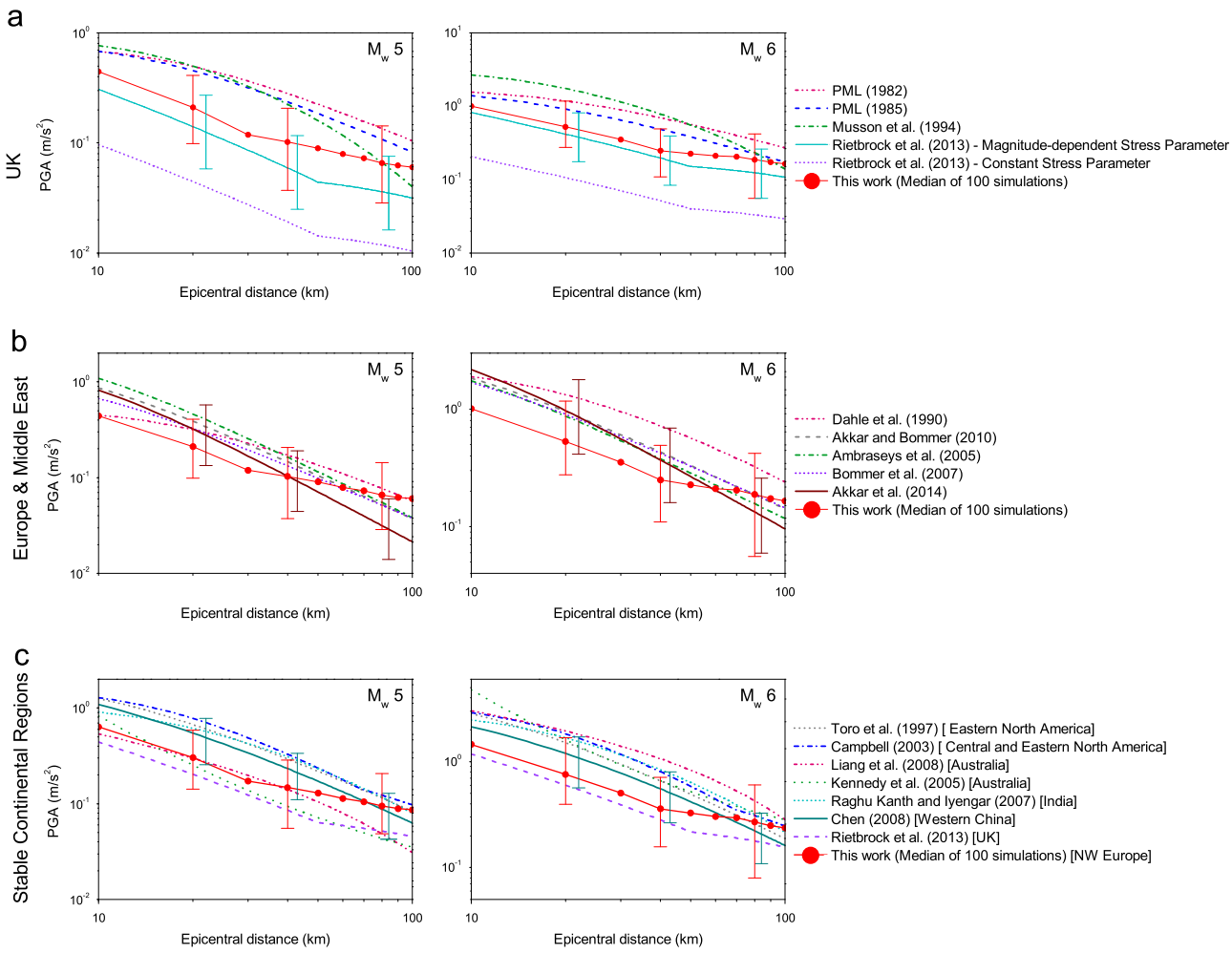

Fig. 15. PGA estimation for two earthquake magnitudes M_w 5 and 6, epicentral distances of 10 km $< R_{epi} <$ 100 km for (a) the UK in rock, (b) Europe and the Middle East in rock and (c) SCRs in hard rock. See text for details on adjustments.

70 km. For greater distances (up to 100 km), the predictions made by the two sets of models are in the same region. The proposed model, in general, tends to predict lower PGAs compared to GMPEs developed for Europe and intraplate regions, and this an expected outcome. The studies selected have broader target geographical regions, and therefore, they have been subjected to different and more active tectonic processes compared to NW Europe.

4.3.2.3. PGA estimation for SCRs. As discussed in Section 2, there is no total agreement as to what extent different SCRs can be considered equivalent in terms of their seismicity features. Johnston [36] defined nine major SCRs worldwide and this section focuses on five of them: Eastern North America (ENA), Australia, India, Western China and NW Europe.

The comparisons presented are for the geometric mean of the two horizontal components of motion and consider generic hard rock conditions. It is acknowledged that there is a high variability in the definition of hard rock made by the GMPEs selected (from V_{S30} = 1800 m/s made by Toro et al. [74] to V_{S30} = 3600 m/s made by Raghu Kanth and Iyengar [78]). Nevertheless, amplifications in such high range of velocities can be assumed negligible and comparisons can still be made in terms of generic site classes [37]. Even though the site classification of the Australian models reported by Liang et al. [76] and Kennedy et al. [77] is generic rock, it is unlikely that this coincides with the description of generic rock considered in this analysis. Rather, they seem to be more in agreement with generic hard rock conditions, as is suggested by the comparisons with ENA presented in Liang et al. [76]. Consequently, and for the sake of simplicity, both Australian models are not adjusted to generic hard rock conditions. For the model of Western China, developed by Chen [79], that does not include site classification, it is assumed that it was calibrated for generic hard rock conditions. Finally, the magnitude-dependent stress parameter model reported by Rietbrock et al. [37] is included in this analysis to observe differences in attenuation between the particular case of the UK and other SCRs.

Fig. 15c shows that there is a rather wide range of PGA intensities and attenuation rates among these SCRs. An explanation supporting this statement can be found in Johnston et al. [36]. All nine major SCRs share the same primary crustal features, but there are still differences between them as each continent has experienced its own particular geological/tectonic development. Nevertheless, from a broad point of view, it seems that ENA, Australia and India exhibit a rather similar behaviour; Western China can be considered to have an average behaviour whereas NW Europe has smaller intensities compared to other SCRs. These results are in reasonably good agreement with findings reported by Bakun and McGarr [84]. Although in their analysis the attenuation is modelled using the Modified Mercalli Intensity (MMI) scale, they suggested that ENA and NW Europe could be considered as the upper and lower limits of intensity

Table 9
Numerical summary for the PGA estimation shown in Fig. 15 (units in m/s^2).

Magnitude		M_w 5			M_w 6			σ[a]
R_{epi} (km)		20	40	80	20	40	80	
		United Kingdom						
1	PML (1982) [68]	0.496	0.281	0.135	1.176	0.698	0.347	0.543
2	PML (1985) [69]	0.454	0.237	0.108	0.919	0.486	0.226	0.49
3	Musson et al. (1994) [70]	0.499	0.225	0.067	1.742	0.784	0.232	0.65[b]
4	Rietbrock et al. (2013) [37] – Mod 1	0.045	0.019	0.012	0.107	0.052	0.033	0.436
5	Rietbrock et al. (2013) [37] – Mod 2	0.140	0.059	0.036	0.417	0.197	0.124	0.335
This work		**0.211**	**0.103**	**0.066**	**0.528**	**0.249**	**0.187**	**0.764–0.713**[c]
		Europe						
6	Akkar and Bommer (2010) [56]	0.387	0.146	0.052	0.956	0.432	0.186	0.279
7	Ambraseys et al. (2005) [50]	0.462	0.164	0.055	0.872	0.378	0.156	0.358–0.289
8	Bommer et al. (2007) [71]	0.325	0.133	0.051	0.903	0.421	0.187	0.352–0.286
9	Akkar et al. (2014) [72]	0.321	0.104	0.032	0.972	0.370	0.133	0.731
10	Dahle et al. (1990) [73]	0.317	0.172	0.077	1.327	0.721	0.322	0.83
This work		**0.211**	**0.103**	**0.066**	**0.528**	**0.249**	**0.187**	**0.764–0.713**[c]
		Stable Continental Regions						
11	Toro et al. (1997) [74]	0.672	0.293	0.115	1.511	0.659	0.258	0.65–0.71
12	Campbell (2003) [75]	0.779	0.329	0.123	1.834	0.805	0.310	0.69–0.59[c]
13	Liang et al. (2008) [76]	0.298	0.141	0.048	1.941	1.067	0.426	1.166
14	Kennedy et al. (2005) [77]	0.252	0.094	0.043	1.600	0.662	0.336	0.33
15	Raghu Kanth and Iyengar (2007) [78]	0.614	0.309	0.116	1.675	0.842	0.317	0.329
16	Chen (2008) [79]	0.548	0.233	0.088	1.193	0.555	0.222	0.240
17	Rietbrock et al. (2013) [37] – Mod 2	0.202	0.086	0.052	0.600	0.283	0.178	0.335
This work		**0.303**	**0.147**	**0.095**	**0.760**	**0.358**	**0.270**	**0.751–0.701**[c]

[a] Standard deviation in log units. Some models reported single values for σ (magnitude independent). Models that reported magnitude-dependent values for σ are shown for the two magnitudes selected for this comparison.
[b] It is a recommended value although not calculated in regression.
[c] Standard deviation is both magnitude- and distance-dependent. Values shown are the average for the three distances selected for this comparison.

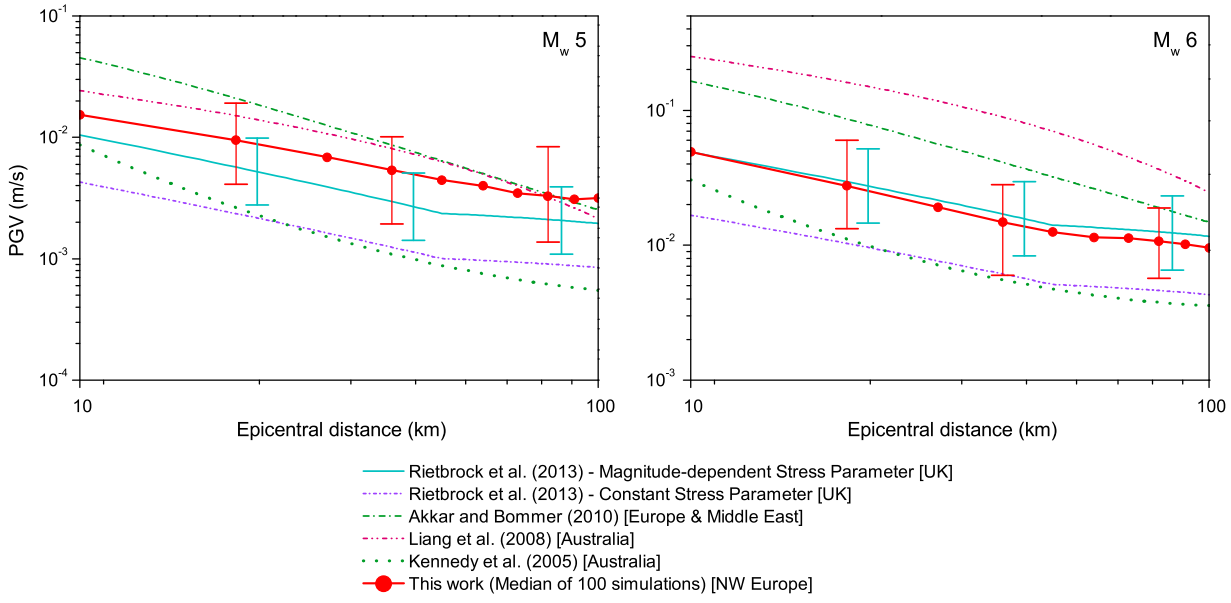

Fig. 16. PGV estimation for two earthquake magnitudes M_w 5 and 6, epicentral distances of 10 km < R_{epi} < 100 km for the UK, Europe and the Middle East and some SCRs in hard rock. See text for details on adjustments.

attenuation among SCRs, and the rest (a common SCR) might be somewhere in between.

4.3.3. *Peak ground velocity estimation*

PGV estimation was made considering the few GMPEs that reported it, i.e. GMPEs 4, 5, 12 and 13 in Table 8; consequently, comparisons were not possible to make using the same geographic categories as for the PGA. Fig. 16 shows the PGV estimation for the geometric mean of two horizontal components for earthquake magnitudes M_w 5 and 6, considering epicentral distances between 10 and 100 km in hard rock conditions for the UK, Europe and the Middle East, and SCRs. These predictions are compared to the median PGV of 100 simulations made with the proposed model using a corner frequency of $\omega_c = \pi$ (rad/s)in all simulated accelerograms. The standard deviation is shown for the results obtained with the proposed model and for one GMPE selected arbitrarily as the one that showed the closest behaviour to the proposed model, namely, Rietbrock et al. [37]. Additionally, Table 10 provides a numerical summary of the data depicted in Fig. 16.

Table 10
Numerical summary for the PGV estimation shown in Fig. 16 (units in m/s).

Magnitude		M_w 5			M_w 6			σ
R_{epi} (km)		20	40	80	20	40	80	
1	Rietbrock et al. (2013) [37] – Mod 1	2.35E-3	1.24E-3	9.05E-4	1.03E-2	6.12E-3	4.62E-3	0.347
2	Rietbrock et al. (2013) [37] – Mod 2	5.69E-3	2.95E-3	2.11E-3	2.95E-2	1.70E-2	1.26E-2	0.276
3	Akkar and Bommer (2010) [56]	2.10E-2	8.62E-3	3.42E-3	8.63E-2	4.11E-2	1.90E-2	0.278
4	Liang et al. (2008) [76]	1.51E-2	8.08E-3	3.21E-3	1.61E-1	8.91E-2	3.65E-2	1.3
5	Kennedy et al. (2005) [77]	2.63E-3	1.09E-3	6.18E-4	1.11E-2	5.54E-3	3.77E-3	0.423
This work		**9.46E-3**	**5.41E-3**	**3.30E-3**	**2.75E-2**	**1.48E-2**	**1.15E-2**	**0.336–0.373**[a]

[a] Standard deviation is both magnitude- and distance-dependent. Values shown are the average for the three distances selected for the corresponding magnitudes used in this comparison.

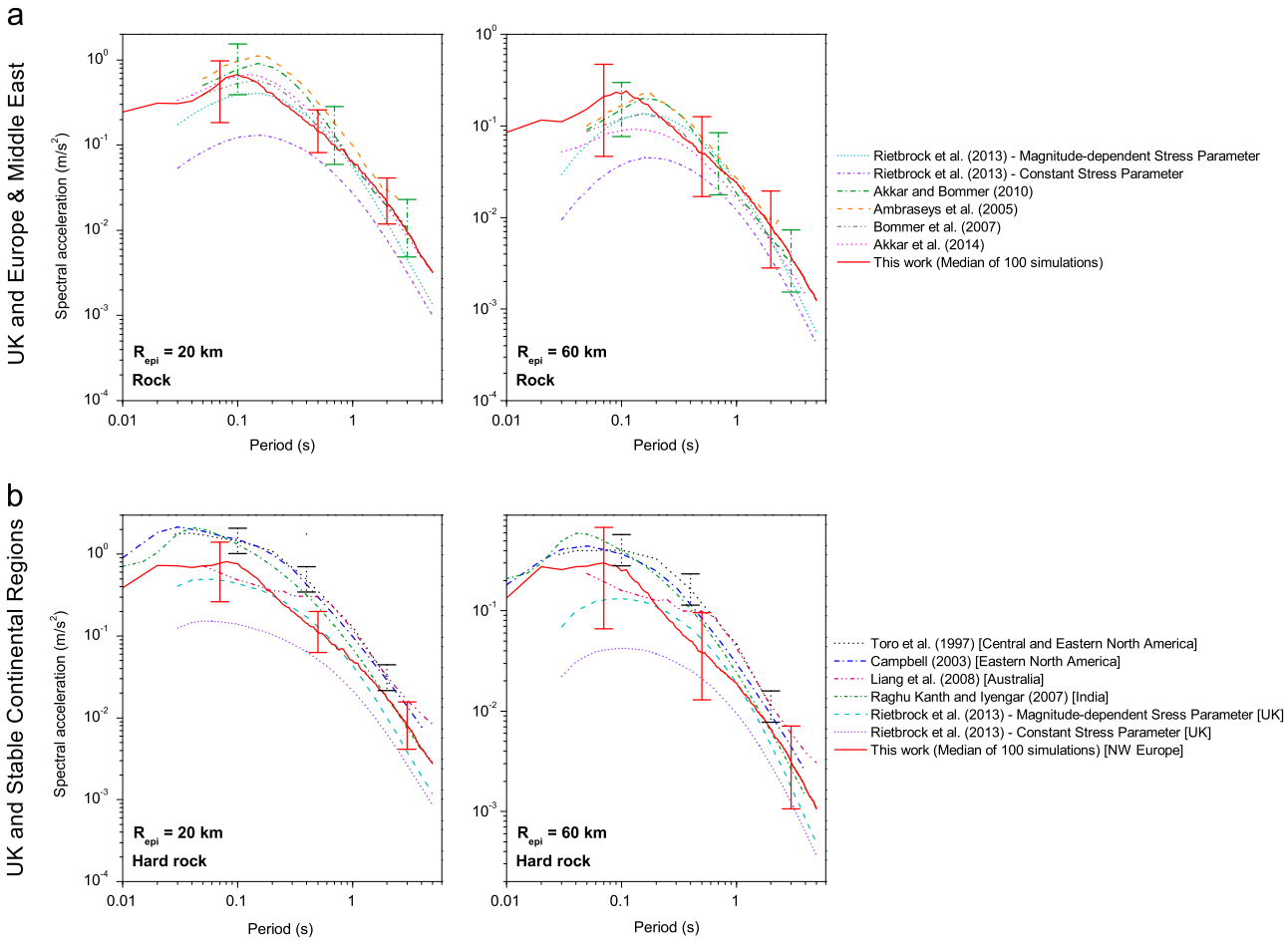

Fig. 17. Spectral acceleration estimation for an earthquake magnitude M_w 5, R_{epi}=20 and 60 for (a) UK and Europe and the Middle East in rock; (b) UK and SCRs in hard rock. See text for details on adjustments.

Fig. 16 shows that the PGVs estimated by the proposed model agree reasonably well with the magnitude-dependent stress parameter model reported by Rietbrock et al. [37]. In general, the European model of Akkar and Bommer [56] and the Australian model of Liang et al. [76] predicted higher values of PGVs in the whole range of distances. The constant stress parameter model of Rietbrock et al. [37] and the Australian model of Kennedy et al. [77] predicted systematically lower values of PGVs compared to the estimations made with the proposed model. This overall behaviour is similar to what was obtained for PGA estimations.

4.3.4. Spectral acceleration estimation

As the two models developed by Rietbrock et al. [37] are the only models found in literature that predict spectral accelerations calibrated exclusively for the UK, the comparisons presented in this section are simultaneously made for UK-Europe and the Middle East, and UK-SCRs, both in terms of the geometric mean of two horizontal components. Figs. 17 and 18 show the acceleration response spectra for earthquake magnitudes M_w 5 and 6 with two different epicentral distances, R_{epi}=20 and 60 km for UK/Europe & the Middle East (rock conditions) and UK/SCRs (hard rock conditions). These predictions are compared to the median spectrum of 100 simulations made with the proposed model using a corner frequency of $\omega_c = \pi$ (rad/s)in all simulated accelerograms. The standard deviation is shown for the results obtained with the proposed model and for one GMPE selected arbitrarily as the one that showed the closest behaviour to the proposed model for each group, namely, Akkar and Bommer [56] for Europe and Toro et al.

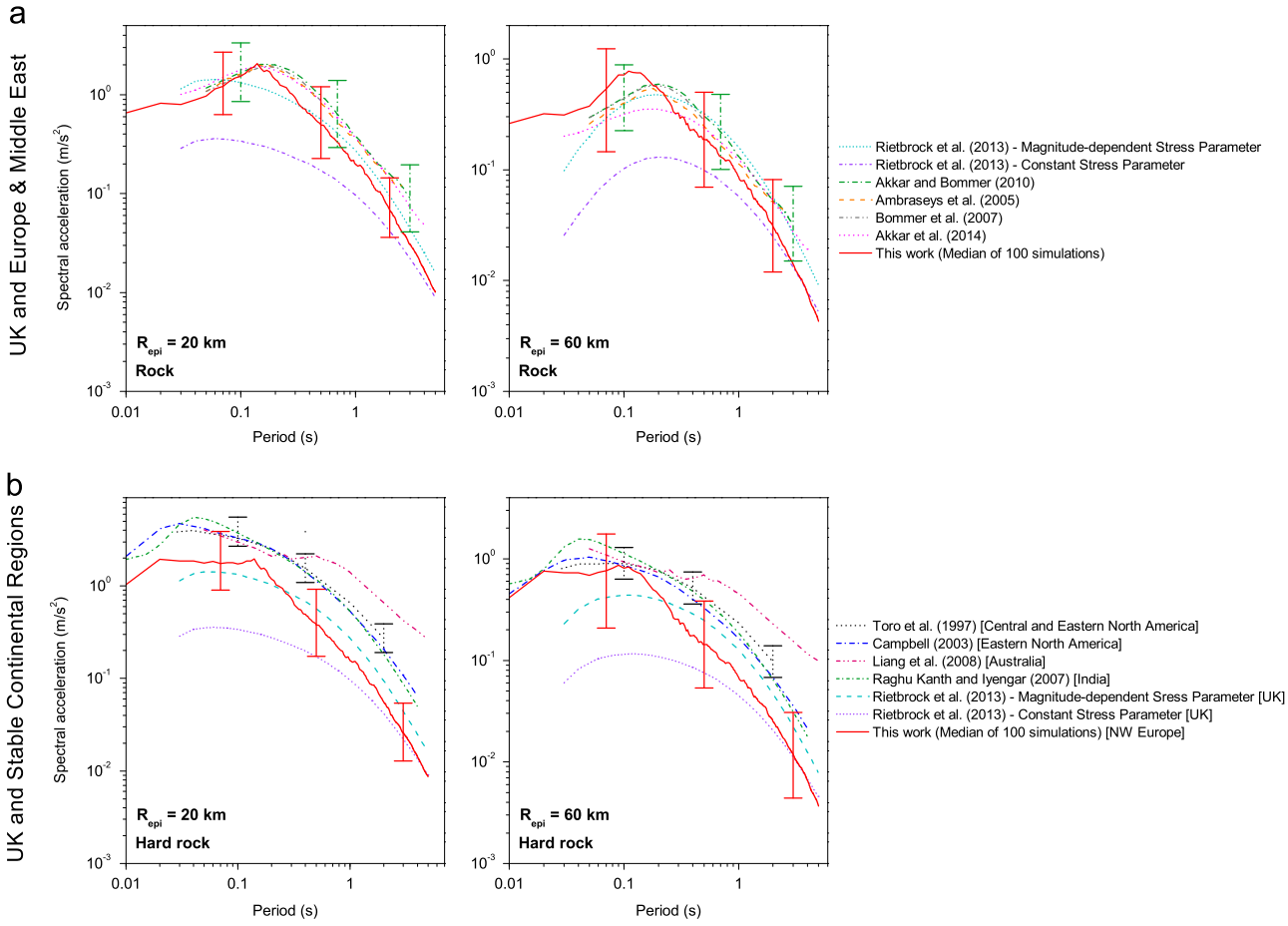

Fig. 18. Spectral acceleration estimation for an earthquake magnitude M_w 6, R_{epi}=20 and 60 for (a) UK and Europe and the Middle East in rock; (b) UK and SCRs in hard rock. See text for details on adjustments.

Table 11
Numerical summary for the spectral acceleration estimation shown in Fig. 17 (units in m/s^2).

R_{epi} (km)		20–60			σ		
Period (s)		**0.1**	**0.5**	1	**0.1**	**0.5**	1
		UK and Europe					
1	Rietbrock et al. (2013) [37] – Mod 1	0.123–0.038	0.067–0.028	0.027–0.012	0.428	0.378	0.350
2	Rietbrock et al. (2013) [37] – Mod 2	0.393–0.118	0.169–0.069	0.055–0.024	0.325	0.282	0.268
3	Akkar and Bommer (2010) [56]	0.777–0.151	0.244–0.064	0.062–0.018	0.297	0.329	0.325
4	Ambraseys et al. (2005) [50]	0.965–0.164	0.313–0.075	0.099–0.027	0.392	0.422	0.323
5	Bommer et al. (2007) [71]	0.534–0.119	0.161–0.047	–	0.381	0.388	–
6	Akkar et al. (2014) [72]	0.645–0.088	0.202–0.042	0.065–0.017	0.802	0.788	0.798
This work		**0.676–0.223**	**0.147–0.051**	**0.064–0.024**	**0.463**	**0.573**	**0.660**
		UK and Stable Continental Regions					
7	Rietbrock et al. (2013) [37] – Mod 1	0.139–0.042	0.052–0.021	0.022–0.009	0.428	0.378	0.350
8	Rietbrock et al. (2013) [37] – Mod 2	0.442–0.133	0.130–0.053	0.043–0.019	0.325	0.282	0.268
9	Toro et al. (1997) [74]	1.454–0.401	0.493–0.164[a]	0.130–0.046	0.66	0.69	0.70
10	Campbell (2003) [75]	1.497–0.368	0.300–0.084	0.099–0.030	0.715	0.683	0.661
11	Liang et al. (2008) [76]	0.489–0.160	0.301–0.099	0.118–0.043	–	–	–
12	Raghu Kanth and Iyengar (2007) [78]	1.321–0.398	0.228–0.077	0.070–0.024	0.285	0.247	0.222
This work		**0.761–0.251**	**0.112–0.039**	**0.050–0.019**	**0.455**	**0.563**	**0.649**

[a] Results shown are for a structural period of 0.4 s.

[74] for SCRs. Additionally, Tables 11 and 12 provide a numerical summary of the data depicted in Figs. 17 and 18.

Fig. 17 shows that the predictions for an earthquake magnitude M_w 5 made with the proposed model tend to be in between those from the magnitude-dependent stress parameter model of Rietbrock et al. [37] and the other models calibrated for Europe and the Middle East, and SCRs for the whole range of structural periods in the epicentral distances considered. Fig. 18 shows that for an earthquake magnitude M_w 6, for shorter periods, say 0.05 to 0.2 s, the predictions made with the proposed model tend to be in relatively close agreement with other models calibrated for Europe and the Middle East, and SCRs. However, for longer periods, say 0.5 to 5 s, the predictions made with the proposed model are mostly in between the two UK models developed by Rietbrock et al. [37].

Table 12
Numerical summary for the spectral acceleration estimation shown in Fig. 18 (units in m/s^2).

R_{epi} (km)		20–60			σ		
Period (s)		**0.1**	**0.5**	1	**0.1**	**0.5**	1
		UK and Europe					
1	Rietbrock et al. (2013) [37] – Mod 1	0.301–0.102	0.224–0.099	0.122–0.057	0.428	0.378	0.350
2	Rietbrock et al. (2013) [37] – Mod 2	1.181–0.392	0.741–0.322	0.344–0.160	0.325	0.282	0.268
3	Akkar and Bommer (2010) [56]	1.687–0.447	0.980–0.305	0.382–0.132	0.297	0.329	0.325
4	Ambraseys et al. (2005) [50]	1.608–0.397	0.820–0.246	0.364–0.113	0.313	0.340	0.328
5	Bommer et al. (2007) [71]	1.575–0.44	0.867–0.279	–	0.308	0.363	–
6	Akkar et al. (2014) [72]	1.781–0.317	0.883–0.239	0.368–0.123	0.802	0.788	0.798
This work		**1.543–0.720**	**0.493–0.187**	**0.199–0.086**	**0.935**	**0.811**	**0.755**
		UK and Stable Continental Regions					
7	Rietbrock et al. (2013) [37] – Mod 1	0.338–0.115	0.171–0.076	0.097–0.045	0.428	0.378	0.350
8	Rietbrock et al. (2013) [37] – Mod 2	1.329–0.441	0.566–0.247	0.272–0.126	0.325	0.282	0.268
9	Toro et al. (1997) [74]	3.268–0.902	1.556–0.517[a]	0.657–0.233	0.709	0.735	0.753
10	Campbell (2003) [75]	3.293–0.857	1.142–0.330	0.533–0.166	0.625	0.597	0.593
11	Liang et al. (2008) [76]	2.894–0.935	2.115–0.694	1.402–0.457	–	–	–
12	Raghu Kanth and Iyengar (2007) [78]	3.744–1.127	1.176–0.396	0.533–0.185	0.285	0.247	0.222
This work		**1.737–0.811**	**0.377–0.143**	**0.157–0.068**	**0.920**	**0.797**	**0.742**

[a] Results shown are for a structural period of 0.4 s.

5. Discussion

On the definition of NW Europe: Though different definitions of NW Europe have been used in the literature, it is acknowledged that the F–E regionalisation scheme [45] is only intended to set clear boundaries among different regions of the Earth and not necessarily based on their tectonic features. However, the NW European area defined by the F–E scheme is contained within the borders of the European SCR defined by Johnston [36]; hence, a relatively similar tectonic behaviour may be expected within this constrained area. It may be argued that the F–E definition of NW Europe includes areas of high seismic activity (in relative terms), such as the Alps and the Pyrenees. However, this was deemed suitable as it was necessary to include areas that possessed recorded accelerograms from strong earthquake magnitudes, say M_w 6–6.5. In this light, the model proposed would be calibrated using data from strong earthquakes (for NW European standards) that were recorded in areas that could be assumed to be comparable due to geographical proximity. This would avoid the use of accelerograms from such high earthquake magnitudes recorded in areas that possess more available information (e.g. active crustal regions) but whose characteristics may not be directly applied in NW Europe, as discussed in Section 2.

Underlying assumption of the model proposed: The database of British earthquakes is mainly composed of small magnitude events whose features are unsuitable for predicting the characteristics of moderate-to-large earthquake accelerograms. For this reason, it is assumed that the inherent features of accelerograms (intensity, frequency content and time duration), caused by moderate-to-strong earthquakes in Britain, would be similar to those in the Stable Continental Region to which the UK belongs, namely NW Europe. In terms of PGA, estimations made with the proposed model closely follow predictions made with the latest GMPEs calibrated for the UK in the range of magnitudes and distances of interest in probabilistic seismic hazard analysis in Britain. Also, estimations made with the proposed model confirm a result that has been earlier reported in the literature: i.e. NW Europe has associated smaller PGA intensities than other SCRs covered in earthquake engineering research. When compared with GMPEs calibrated for the wider region of Europe, it is expected that lower PGA estimations are obtained with the proposed model, as the European region comprises more seismically active zones than NW Europe. In general, this result is confirmed from the validation analyses performed.

Comparison with a NGA model: The stochastic accelerogram model reported by Rezaeian and Der Kiureghian [1,2] calibrated using a subset of the NGA database is used for a general comparison with the proposed model. Table 13 shows a detailed comparison in terms of the dataset, mathematical formulation, variable selection and marginal distributions, and regression analysis between the two models. Although both share the same mathematical model, Table 13 shows several differences between their developments. The various modifications introduced in this work were necessary to adopt in order to define a suitable model for NW European accelerograms' features.

Limitations: One of the limitations of the model proposed that could be envisaged *a priori* is related to the lack of information of the dataset for accelerograms recorded at epicentral distances longer than 100 km. As stated in Section 4.3, the model proposed was not able to appropriately capture the attenuation rate of PGAs, PGVs and spectral accelerations when simulating seismic scenarios for such distances. For this reason, in this article the applicability of the model was set to a maximum epicentral distance of 100 km. In this light, it is acknowledged that the model presented in this work possesses a rather high epistemic uncertainty. The epistemic uncertainty of this model can only be reduced by adding more accelerograms to the dataset; therefore, the model should be subjected to revisions/updates when more data are available.

GMPEs vs stochastic accelerogram models: As GMPEs do not primarily aim to provide ground motion accelerograms, nonlinear time-history analysis in the context of SPRA, could not rationally be performed based solely on such predictive models. For seismic assessment of critical structures, such as nuclear power stations, comprehensive sets of accelerograms compatible with the local seismicity are required. In this sense, the main objective of the model proposed is to establish a mathematical model able to simulate any number of accelerograms for any seismic scenarios (magnitude, distance, type of soil) within NW Europe. However, as GMPEs are widely used and recognised by practitioners/researchers, they can also be used as a validation framework of the model presented in this work.

6. Conclusions

A fully non-stationary stochastic ground motion accelerogram model for use in the NW European areas is developed, based on the

Table 13
Comparison between an NGA accelerogram model and this work.

	Rezaeian and Der Kiureghian [1,2]	**This work**
Target geographical region	Active crustal regions	Northwest Europe
Dataset		
Database	NGA	ISESD
Number of accelerograms	203	220
Magnitudes (M_w)	6.1–7.7	4–6.5
Distances	$10 < R_{rup} < 100$ km	$10 < R_{epi} < 100$ km
Type of soil	$V_{s30} > 600$ m/s	Rock, stiff and soft soil
Style of faulting	Strike-slip, reverse	Not included
Mathematical formulation		
Mathematical model	Rezaeian and Der Kiureghian [2]	Rezaeian and Der Kiureghian [2]
Time-modulating function	Gamma type (3 parameters)	Piece-wise type (6 parameters)
Linear filter	PSA SDOF (3 parameters)	PSA SDOF (3 parameters)
Total variables to simulate accelerograms	6	9
Variable selection		
Time-modulating function	1. Arias intensity, $\boldsymbol{I_a}$ 2. Effective duration, $\boldsymbol{D_{5-95}}$ 3. Middle time of the strong-shaking phase, $\boldsymbol{t_{mid}}$	1. Maximum intensity, α_1 2, 3. Controllers of decaying intensity, α_2, α_3 4. Start time, $\boldsymbol{T_0}$ 5, 6. Start and end time of strong-shaking phase, $\boldsymbol{T_1}$, $\boldsymbol{T_2}$
Filter parameter	1. Frequency at t_{mid}, $\omega_{\boldsymbol{mid}}$ 2. Rate of frequency change, ω' 3. Damping ratio, $\xi_{\boldsymbol{f}}$	1. Frequency at beginning, $\omega_{\boldsymbol{0}}$ 2. Frequency at end, $\omega_{\boldsymbol{f}}$ 3. Damping ratio, $\xi_{\boldsymbol{f}}$
Matching procedure for parameters of dataset's accelerograms	Nonlinear optimisation	Monte Carlo simulation
Marginal distributions of variables		
Time-modulating function	$\boldsymbol{I_a}$: Normal $\boldsymbol{D_{5-95}}$: Beta $\boldsymbol{t_{mid}}$: Beta	α_1, α_2, α_3: Generalised extreme value (GEV) $\boldsymbol{T_0}$: Lognormal $\boldsymbol{T_1}$, $\boldsymbol{T_0}$: Birnbaum–Saunders
Filter parameter	$\omega_{\boldsymbol{mid}}$: Gamma ω': Two-sided exponential $\xi_{\boldsymbol{f}}$: Beta	$\omega_{\boldsymbol{0}}$: Gamma $\omega_{\boldsymbol{f}}$: GEV $\xi_{\boldsymbol{f}}$: GEV
Regression analysis		
Modelling of random-effects regression	Rezaeian and Der Kiureghian's [1] algorithm	Abrahamson and Youngs's [67] algorithm
Type of functional form	Linear	Nonlinear
Functional form	$\nu_i = \beta_{i,0} + \beta_{i,1} \cdot F + \beta_{i,2} \cdot (M/7) + \beta_{i,3} \cdot (R/25) + \beta_{i,4} \cdot (V_{s30}/750)$ $i = 2, \ldots, 6$	$\nu_i = \beta_{i,0} + \beta_{i,1} \cdot M + \beta_{i,2} \cdot \sqrt{R} + \beta_{i,3} \cdot \ln(M \cdot R) + \beta_{i,4} \cdot D_1 + \beta_{i,5} \cdot D_2$ $i = 1, \ldots, 9$
Explanatory variables of functional form	$\boldsymbol{F}$=type of faulting $\boldsymbol{M}$=moment magnitude $\boldsymbol{R}$=distance-to-site $\boldsymbol{V_{s30}}$=shear-wave velocity (type of soil is modelled **quantitatively**)	$\boldsymbol{M}$=moment magnitude $\boldsymbol{R}$=epicentral distance $\boldsymbol{D_1}$ and $\boldsymbol{D_2}$=dummy variables (type of soil is modelled **qualitatively**)

time-modulated filtered white noise process proposed by Rezaeian and Der Kiureghian [1,2]. A functional form of predictive equations for such a process is presented which in turn is calibrated using a subset of the European database composed of 220 accelerograms recorded in NW Europe. This model simulates accelerograms compatible with seismic scenarios defined by earthquake magnitudes $4 < M_w < 6.5$, distance-to-site $10 \text{ km} < R_{epi} < 100$ km and different types of soil (rock, stiff and soft soil). The calibration of the predictive equations was performed by means of regression analysis. The statistical significance of the regressors proposed are considered appropriate to simulate accelerograms as it has been seen that the model is able to capture the natural variability of accelerograms for a specified seismic scenario. The conclusions from this research are summarised as follows:

* The definition of the boundaries for a NW European region that possesses uniform tectonic behaviour, which in turn could be considered representative for UK standards, seems to be a matter open to discussion as different definitions were found in the literature. The approach used in this work, based on the Flinn–Engdhal regionalisation scheme, was initially found to be a reasonable alternative to define an area of moderate-to-low seismic activity. This area includes recorded accelerogram data from earthquakes of magnitudes and distances relevant for structural engineering purposes.
* The predictive equations calibrated by means of the random-effects regression technique are able to account for the sample-dependency of the dataset used. Several functional forms for these predictive equations were tested. For simplicity, only one functional form, with the least possible number of explanatory variables, was chosen for all parameters that govern the stochastic process. This implies that different levels of statistical significance for the predictive equations were obtained. However, all predictive equations proposed were appropriate for explaining the statistical behaviour of the dependent variables at the standard 5% significance level normally used in statistical hypothesis testing.
* The model proposed requires three input variables typically used in structural engineering applications, namely, earthquake magnitude, distance-to-site and type of soil for a design seismic scenario. Once this information is set, the simulation of accelerograms is entirely made in the time domain and essentially involves the generation of random variables. In this light, this model is considered to be straightforward to define seismic inputs for nonlinear time-history analysis of structures.

* The predictive model proposed in this work was found to capture the natural variability of accelerograms produced by different seismic scenarios. Verifications using recorded accelerograms from NW Europe show that a real recording can be considered to be one accelerogram likely to be produced by a specific seismic scenario. The artificial recordings are able to simulate the natural dispersion associated to the earthquake generation phenomenon.
* Regarding PGA estimations obtained with the model proposed, it is found that there is a reasonably good agreement with the latest predictive models calibrated for the UK and Europe, for the magnitudes and distances of interest in seismic hazard and risk analysis. However, when compared with the models used in hazard assessments in the UK [68,69], the proposed model systematically estimates lower PGAs. This may support some concerns reported in the literature on the validity of such equations, especially for their use in the British nuclear industry. Even though further evidence is required to support this statement, it is likely that such models may have led to conservative results for nuclear sites in the UK. Additionally, comparisons made with other SCRs show that PGA intensities and attenuation rates are somewhat different. This may be explained by the fact that each SCR has experienced its own tectonic evolution. Nevertheless, results obtained in this work suggest that Eastern North America, Australia and India possess a rather similar behaviour and have associated higher PGA intensities. On the other hand, NW Europe can be considered to have associated smaller PGA intensities. Finally, Western China could be regarded as possessing an average behaviour.
* Regarding estimations on spectral acceleration, there is also a reasonably good agreement between the model proposed and predictive models calibrated for the UK, Europe and other SCRs. This is valid for a wide range of periods for the magnitudes and distances of interest for time-history analyses of structures. Consequently, it can be concluded that the proposed model is suitable to rationally define the loading input in structural engineering analyses for the NW European regions.

Acknowledgments

The authors would like to thank Dr Brian Ellis, Ellis Consultant, for his constructive comments on the manuscript.

References

[1] Rezaeian S, Der Kiureghian A. Simulation of synthetic ground motions for specified earthquake and site characteristics. Earthq Eng Struct Dyn 2010;39:1155–80.
[2] Rezaeian S, Der Kiureghian A. A stochastic ground motion model with separable temporal and spectral nonstationarities. Earthq Eng Struct Dyn 2008;37:1565–84.
[3] McGuire RK. Seismic hazard and risk analysis. Oakland, California, USA: Earthquake Engineering Research Institute; 2004.
[4] Huang Y-N, Whittaker AS, Luco N. A probabilistic seismic risk assessment procedure for nuclear power plants: (I) Methodology. Nucl Eng Des 2011;241:3996–4003.
[5] Huang Y-N, Whittaker A, Luco N. A probabilistic seismic risk assessment procedure for nuclear power plants: (II) Application. Nucl Eng Des 2011;241:3985–95.
[6] Lubkowski Z, Bommer JJ, Baptie B, Bird J, Douglas J, Free M, Hancock J, Sargeant S, Sartain N, Strasser F. An evaluation of attenuation relationships for seismic hazard assessment in the UK. In: Proceedings of the 13th World conference on earthquake engineering. Vancouver (Canada); 2004. p. 1422.
[7] Musson RMW. UK seismic hazard assessments for strategic facilities: a short history. In: Proceedings of the 30th national GNGTS conference (Gruppo Nazionale di Geofisica della Terra Solida). Trieste (Italy); 2011.
[8] Katsanos EI, Sextos AG, Manolis GD. Selection of earthquake ground motion records: a state-of-the-art review from a structural engineering perspective. Soil Dyn Earthq Eng 2010;30:157–69.
[9] NIST. Selecting and scaling earthquake ground motions for performing response-history analyses. Gaithersburg, Maryland, USA: National Institute of Standards and Technology (NIST); 2012.
[10] Huang Y-N, Whittaker A, Luco N, Hamburger. Scaling earthquake ground motions for performance-based assessment of buildings. J Struct Eng 2011;137:311–21.
[11] Luco N, Bazzurro P. Does amplitude scaling of ground motion records result in biased nonlinear structural drift responses? Earthq Eng Struct Dyn 2007;36:1813–35.
[12] Grant DN, Diaferia R. Assessing adequacy of spectrum-matched ground motions for response history analysis. Earthq Eng Struct Dyn 2013;42:1265–80.
[13] Hancock J, Bommer JJ, Stafford PJ. Numbers of scaled and matched accelerograms required for inelastic dynamic analyses. Earthq Eng Struct Dyn 2008;37:1585–607.
[14] Ay BÖ, Akkar S. A procedure on ground motion selection and scaling for nonlinear response of simple structural systems. Earthq Eng Struct Dyn 2012;41:1693–707.
[15] Baker JW. Conditional mean spectrum: tool for ground-motion selection. J Struct Eng 2011;137:322–31.
[16] Watson-Lamprey J, Abrahamson N. Selection of ground motion time series and limits on scaling. Soil Dyn Earthq Eng 2006;26:477–82.
[17] Bozorgnia Y, Abrahamson NA, Atik LA, Ancheta TD, Atkinson GM, Baker JW, Baltay A, Boore DM, Campbell KW, Chiou BSJ, Darragh R, Day S, Donahue J, Graves RW, Gregor N, Hanks T, Idriss IM, Kamai R, Kishida T, Kottke A, Mahin SA, Rezaeian S, Rowshandel B, Seyhan E, Shahi S, Shantz T, Silva W, Spudich P, Stewart JP, Watson-Lamprey J, Wooddell K, Youngs R. NGA-West2 research project. Earthq Spectra 2014;30:973–87.
[18] Douglas J. Preface of special issue: a new generation of ground-motion models for Europe and the Middle East. Bull Earthq Eng 2014;12:307–10.
[19] Atkinson GM. Integrating advances in ground-motion and seismic-hazard analysis. In: Proceedings of the 15th World conference on earthquake engineering. Lisbon (Portugal); 2012.
[20] Musson RMW. The use of Monte Carlo simulations for seismic hazard assessment in the U.K.; 2000.
[21] Assatourians K, Atkinson GM. EqHaz: an open-source probabilistic seismic-hazard code based on the Monte Carlo Simulation Approach. Seism Res Lett 2013;84:516–24.
[22] Weatherill G, Burton PW. An alternative approach to probabilistic seismic hazard analysis in the Aegean region using Monte Carlo simulation. Tectonophysics 2010;492:253–78.
[23] Douglas J, Aochi H. A survey of techniques for predicting earthquake ground motions for engineering purposes. Surv Geophys 2008;29:187–220.
[24] Halldórsson B, Mavroeidis G, Papageorgiou A. Near-fault and far-field strong ground-motion simulation for earthquake engineering applications using the specific barrier model. J Struct Eng 2011;137:433–44.
[25] Liu P, Archuleta RJ, Hartzell SH. Prediction of broadband ground-motion time histories: hybrid low/high- frequency method with correlated random source parameters. Bull Seismol Soc Am 2006;96:2118–30.
[26] Mobarakeh AA, Rofooei FR, Ahmadi G. Simulation of earthquake records using time-varying Arma (2,1) model. Probab Eng Mech 2002;17:15–34.
[27] Rofooei FR, Mobarake A, Ahmadi G. Generation of artificial earthquake records with a nonstationary Kanai–Tajimi model. Eng Struct 2001;23:827–37.
[28] Sgobba S, Stafford PJ, Marano GC, Guaragnella C. An evolutionary stochastic ground-motion model defined by a seismological scenario and local site conditions. Soil Dyn Earthq Eng 2011;31:1465–79.
[29] Graves RW, Pitarka A. Broadband ground-motion simulation using a hybrid approach. Bull Seismol Soc Am 2010;100:2095–123.
[30] Boore DM. Stochastic simulation of high-frequency ground motions based on seismological models of the radiated spectra. Bull Seismol Soc Am 1983;73:1865–94.
[31] Baptie B. Seismogenesis and state of stress in the UK. Tectonophysics 2010;482:150–9.
[32] Musson RMW. The seismicity of the British Isles. Ann Geophys 1996;39.
[33] Ambraseys NN, Smit PM, Douglas J, Margaris B, Sigjornsson R, Olafsson S, Suhadolc P, Costa G. Internet site for European strong-motion data. Boll Geofis Teor Ed Appl 2004;45:113–29.
[34] Bommer JJ, Papaspiliou M, Price W. Earthquake response spectra for seismic design of nuclear power plants in the UK. Nucl Eng Des 2011;241:968–77.
[35] Musson RMW. Design earthquakes in the UK. Bull Earthq Eng 2004;2:101–12.
[36] Johnston AC, Coppersmith KJ, Kanter LR, Cornell CA. The earthquakes of stable continental regions, in: TR-102261. Palo Alto, California, USA: Electric Power Research Institute; 1994.
[37] Rietbrock A, Strasser F, Edwards B, Stochastic A. Earthquake ground-motion prediction model for the United Kingdom. Bull Seismol Soc Am 2013;103:57–77.
[38] Musson RMW. The case for large $M > 7$ earthquakes felt in the UK in historical times. In: Fréchet J, Meghraoui M, Stucchi M, editors. Historical seismology. Netherlands: Springer; 2008. p. 187–207.
[39] Baptie B, Ottemoller L, Sargeant S, Ford G, O'Mongain A. The Dudley earthquake of 2002: a moderate sized earthquake in the UK. Tectonophysics 2005;401:1–22.
[40] Ottemöller L, Baptie B, Smith NJP. Source parameters for the 28 April 2007 *Mw* 4.0 earthquake in Folkestone, United Kingdom. Bull Seismol Soc Am 2009;99:1853–67.

[41] Ottemöller L, Sargeant S. Ground-motion difference between two moderate-size intraplate earthquakes in the United Kingdom. Bull Seismol Soc Am 2010;100:1823–9.
[42] Musson RMW, Sargeant S. Eurocode 8 seismic hazard zoning maps for the UK. Technical Report, CR/07/125N. Keyworth, Nottingham, UK: British Geological Survey; 2007.
[43] Goes S, Loohuis JJP, Wortel MJR, Govers R. The effect of plate stresses and shallow mantle temperatures on tectonics of northwestern Europe. Glob Planet Chang 2000;27:23–38.
[44] Ambraseys NN. Intensity-attenuation and magnitude-intensity relationships for northwest european earthquakes. Earthq Eng Struct Dyn 1985;13:733–78.
[45] Young JB, Presgrave BW, Aichele H, Wiens DA, Flinn EA. The Flinn–Engdahl regionalisation scheme: the 1995 revision. Phys Earth Planet Inter, 96; 1996. p. 223–97.
[46] Akkar S, Sandıkkaya MA, Şenyurt M, Azari Sisi A, Ay BÖ, Traversa P, Douglas J, Cotton F, Luzi L, Hernandez B, Godey S. Reference database for seismic ground-motion in Europe (RESORCE). Bull Earthq Eng 2014;12:311–39.
[47] Douglas J. Ground-motion prediction equations 1964–2010. Final Report BRGM/RP-59356-FR. Orléans, France: BRGM; 2011.
[48] Ambraseys NN, Free MW. Surface-wave magnitude calibration for European Region Earthquakes. J Earthq Eng 1997;1:1–22.
[49] Johnston AC. Seismic moment assessment of earthquakes in stable continental regions—I. Instrumental seismicity. Geophys J Int 1996;124:381–414.
[50] Ambraseys NN, Douglas J, Sarma SK, Smit PM. Equations for the estimation of strong ground motions from Shallow Crustal Earthquakes using data from europe and the middle east: horizontal peak ground acceleration and spectral acceleration. Bull Earthq Eng 2005;3:1–53.
[51] Abrahamson N, Shedlock KM. Overview. Seismol Res Lett 1997;68:9–23.
[52] Musson RMW. British earthquakes. Proc Geol' Assoc 2007;118:305–37.
[53] Mavroeidis GP, Papageorgiou AS. A mathematical representation of near-fault ground motions. Bull Seismol Soc Am 2003;93:1099–131.
[54] Goda K, Aspinall W, Taylor CA. Seismic hazard analysis for the U.K.: sensitivity to spatial seismicity modelling and ground motion prediction equations. Seismol Res Lett 2013;84:112–29.
[55] Gregor N, Abrahamson NA, Atkinson GM, Boore DM, Bozorgnia Y, Campbell KW, Chiou BSJ, Idriss IM, Kamai R, Seyhan E, Silva W, Stewart JP, Youngs R. Comparison of NGA-West2 GMPEs. Earthq Spectra 2014;30:1179–97.
[56] Akkar S, Bommer JJ. Empirical equations for the prediction of PGA, PGV, and spectral accelerations in Europe, the Mediterranean Region, and the Middle East. Seismol Res Lett 2010;81:195–206.
[57] Douglas J, Akkar S, Ameri G, Bard P-Y, Bindi D, Bommer J, Bora S, Cotton F, Derras B, Hermkes M, Kuehn N, Luzi L, Massa M, Pacor F, Riggelsen C, Sandıkkaya MA, Scherbaum F, Stafford P, Traversa P. Comparisons among the five ground-motion models developed using RESORCE for the prediction of response spectral accelerations due to earthquakes in Europe and the Middle East. Bull Earthq Eng 2014;12:341–58.
[58] Boore DM, Joyner WB, Fumal TE. Estimation of response spectra and peak accelerations from Western North American Earthquakes: an interim report. Menlo Park, California, USA: USGS; 1993.
[59] Douglas J, Halldórsson B. On the use of aftershocks when deriving ground-motion prediction equations. In: Proceedings of the 9th U.S. national and 10th Canadian conference on earthquake engineering. Toronto, Ontario (Canada); 2010.
[60] Papadimitriou K. Stochastic characterization of strong ground motion and applications to structural response. In: Pasadena, California: Earthquake Engineering Research Laboratory, California Institute of Technology; 1990.
[61] Liao S, Zerva A. Physically compliant, conditionally simulated spatially variable seismic ground motions for performance-based design. Earthq Eng Struct Dyn 2006;35:891–919.
[62] Brune JN. Tectonic stress and the spectra of seismic shear waves from earthquakes. J Geophys Res 1970;75:4997–5009.
[63] Arias A. A measure of earthquake intensity. In: Hansen RJ, editor. Seismic design for nuclear power plants. Cambridge, Massachusetts, USA and London, UK: MIT Press; 1970.
[64] Penzien J, Watabe M. Characteristics of 3-dimensional earthquake ground motions. Earthq Eng Struct Dyn 1975;3:365–73.
[65] Kubo T, Penzien J. Time and frequency domain analyses of three dimensional ground motions San Fernando Earthquake. Berkeley, California, USA: Earthquake Engineering Research Center; 1976.
[66] Rawlings JO, Pantula SG, Dickey DA. Applied regression analysis: a research tool. Springer; 1998.
[67] Abrahamson N, Youngs R. A stable algorithm for regression analyses using the random effects model. Bull Seismol Soc Am 1992;82:505–10.
[68] PML. British earthquakes, Technical Report 115/82, Principia Mechanica Ltd., London; 1982.
[69] PML. Seismological studies for UK hazard analysis, Technical Report 346/85, Principia Mechanica Ltd., London; 1985.
[70] Musson RMW, Marrow PC, Winter PW. Attenuation of earthquake ground motion in the UK. Report AEA/CS/16422000/ZJ745/004. AEA Technology Consultancy Services; 1994. p. 30.
[71] Bommer JJ, Stafford PJ, Alarcón JE, Akkar S. The Influence of magnitude range on empirical ground-motion prediction. Bull Seismol Soc Am 2007;97:2152–70.
[72] Akkar S, Sandıkkaya MA, Bommer JJ. Empirical ground-motion models for point- and extended-source crustal earthquake scenarios in Europe and the Middle East. Bull Earthq Eng 2014;12:359–87.
[73] Dahle A, Bungum H, Kvamme LB. Attenuation models inferred from intraplate earthquake recordings. Earthq Eng Struct Dyn 1990;19:1125–41.
[74] Toro GR, Abrahamson NA, Schneider JF. Model of strong ground motions from earthquakes in Central and Eastern North America: best estimates and uncertainties. Seismol Res Lett 1997;68:41–57.
[75] Campbell KW. Prediction of strong ground motion using the hybrid empirical method and its use in the development of ground-motion (attenuation) relations in Eastern North America. Bull Seismol Soc Am 2003;93:1012–33.
[76] Liang JZ, Hao H, Gaull BA, Sinadinovski C. Estimation of strong ground motions in Southwest Western Australia with a combined green's function and stochastic approach. J Earthq Eng 2008;12:382–405.
[77] Kennedy J, Hao H, Gaull B. Earthquake ground motion attenuation relations for SWWA. New South Wales, Australia: Earthquake Engineering in Australia; 2005 pp. Paper 15.
[78] Raghu Kanth STG, Iyengar RN. Estimation of seismic spectral acceleration in Peninsular India. J Earth Syst Sci 2007;116:199–214.
[79] Chen L. Ground motion attenuation relationships based on Chinese and Japanese strong ground motion data. Pavia, Italy: European School for Advanced Studies in Reduction of Seismic Risk, ROSE School; 2008.
[80] Boore DM, Joyner WB. Site amplifications for generic rock sites. Bull Seismol Soc Am 1997;87:327–41.
[81] Cotton F, Scherbaum F, Bommer J, Bungum H. Criteria for selecting and adjusting ground-motion models for specific target regions: application to central europe and rock sites. J Seismol 2006;10:137–56.
[82] Van Houtte C, Drouet S, Cotton F. Analysis of the origins of κ (Kappa) to compute hard rock to rock adjustment factors for GMPEs. Bull Seismol Soc Am 2011;101:2926–41.
[83] Beyer K, Bommer JJ. Relationships between median values and between aleatory variabilities for different definitions of the horizontal component of motion. Bull Seismol Soc Am 2006;96:1512–22.
[84] Bakun WH, McGarr A. Differences in attenuation among the stable continental regions. Geophys Res Lett 2002;29:2121.

Appendix C

Seismic probabilistic risk analysis based on stochastic simulation of accelerograms for nuclear power plants in the UK

Progress in Nuclear Energy 91 (2016) 373–388

Contents lists available at ScienceDirect

Progress in Nuclear Energy

journal homepage: www.elsevier.com/locate/pnucene

Seismic probabilistic risk analysis based on stochastic simulation of accelerograms for nuclear power plants in the UK

Carlos Medel-Vera*, Tianjian Ji

School of Mechanical, Aerospace and Civil Engineering, Pariser Building, Sackville Street, The University of Manchester, Manchester M13 9PL, UK

ARTICLE INFO

Article history:
Received 5 January 2016
Received in revised form
15 May 2016
Accepted 6 June 2016

Keywords:
Seismic risk analysis
Probabilistic methods
Nuclear power plants
Fragility curves
United Kingdom

ABSTRACT

This article presents an approach to probabilistically assess the seismic risk of nuclear power plants (NPPs) in the UK. The approach proposed is based on direct stochastic simulation of the seismic input to conduct nonlinear dynamic analysis of a structural model of the NPP analysed. Therefore, it does not require the use of ground motion prediction equations and scaling/matching procedures to define suitable accelerograms as is done in conventional approaches. Additionally, as the structural response is directly calculated, it does not require the use of Monte Carlo-type algorithms to simulate the damage state of the NPP analysed. However, it demands longer use of computer resources as a relatively large number of nonlinear dynamic analyses are needed to perform. The approach is illustrated using an example of a 1000 MW Pressurised Water Reactor building located in a representative UK nuclear site. A comparison of risk assessment is made between the conventional and proposed approaches. Results obtained are reasonable and well constrained by conventional procedures; hence, it can confidently be used by the UK New Build Programme in the next two decades to generate 16 GWe of new nuclear capacity.

© 2016 Elsevier Ltd. All rights reserved.

1. Introduction

The UK nuclear industry has gained an established reputation due to nearly 60 years of successful and safe exploitation of low-carbon nuclear power plants. At present, around 20% of the total electricity supply in the UK is provided by nuclear power (HM Government, 2013). Although no NPP has been built in the UK since 1995 and the majority of UK plants are on their way to be decommissioned, the industry is in the early stages of a long-lasting renaissance. The New Build Programme, intended to build 16 GWe of new nuclear capacity by 2030 involving the construction of at least 12 new reactors plus its likely expansion until 2050 with the development of Generation III+, IV and Small Modular Reactors, is currently under way (NIA, 2012). The necessity of correctly assessing all safety aspects of the new generation NPPs buildings in the UK has become a vital issue for the industry, including their seismic performance. Although the UK is a tectonically stable continental region that possesses medium-to-low seismic activity (Musson, 1996), its seismic hazard is non-negligible as strong ground motions capable of jeopardising the structural integrity of NPPs, although infrequent, can still occur (Musson, 2014). In addition, the occurrence of the Fukushima Dai-ichi nuclear accident (Hirano et al., 2012) in 2011 rose major questions on the seismic safety of nuclear installations worldwide, certainly including the UK. As a response of this accident, Her Majesty's Chief Inspector of Nuclear Installations (Weightman, 2011) recommended that the British nuclear industry should conduct further studies to continue the validation of methodologies for analysing the seismic performance of structures, systems and safety-related components of NPPs. This article is intended to make a contribution towards that aim.

In order to conduct seismic probabilistic risk analysis (SPRA), it is necessary to perform non-linear time history (NLTH) analysis of a structural model. The main obstacle for conducting NLTH analysis of structures is the scarcity of accelerograms compatible with the seismic scenarios that contribute most strongly to the hazard of the site selected. This is an even more remarkable problem for areas of medium-to-low seismicity because: (i) strong earthquakes rarely occur, and (ii) those areas have limited monitoring networks (Lubkowski et al., 2004). These recordings need to be able to realistically represent the frequency content, intensity distribution, and time duration of the strong shaking phase of accelerograms

* Corresponding author.
E-mail addresses: carlos.medelvera@postgrad.manchester.ac.uk (C. Medel-Vera), tianjian.ji@manchester.ac.uk (T. Ji).

http://dx.doi.org/10.1016/j.pnucene.2016.06.005
0149-1970/© 2016 Elsevier Ltd. All rights reserved.

associated with the seismic scenarios that contribute most strongly to the hazard of the site selected (Rezaeian and Der Kiureghian, 2010; Rezaeian and Der Kiureghian, 2008). The paucity of accelerograms has led structural engineers to using techniques on selecting, scaling and matching procedures applied to available records (Huang et al., 2011a; Katsanos et al., 2010; NIST, 2012). In general, these procedures are intended to match a spectral shape predicted by *ad-hoc* ground motion prediction equations (GMPEs). Currently, GMPEs play a critical role in seismic hazard and risk analysis and much research effort has been placed on the development of such models (Bozorgnia et al., 2014; Douglas et al., 2014). However, as SPRA requires the direct specification of sets of accelerograms, promising trends in earthquake engineering have been developed aiming at considering alternatives to GMPEs (Musson, 2000; Atkinson, 2012). This article presents an alternative and straightforward approach that does not make use of GMPEs to conduct SPRA for NPPs in the UK, through an example of application. In this procedure, a large set of accelerograms are generated by direct stochastic simulation by means of a predictive model developed previously by the authors (Medel-Vera and Ji, 2016) that are compatible with seismic scenarios of magnitude $4 < M_w < 6.5$, distance-to-site $10 < R_{epi} < 100$ km in rock, stiff and soft soil conditions. Such a model was calibrated using a dataset of accelerograms recorded in the same stable continental region that the UK belongs to, namely NW Europe. A hypothetical UK nuclear site was selected as a representative of a high seismic demand area (for British standards) and the risk is assessed using a simplified model of a 1000 MW Pressurised Water Reactor building. For completion, the alternative procedure is compared to the usual GMPE-based procedure to perform SPRA for nuclear facilities, in order to highlight that the risk assessment procedure becomes remarkably more straightforward when using the approach proposed.

This article is organised as follows: Section 2 provides a general comparison to define seismic inputs and calculate structural outputs in SPRA between the conventional GMPE-based approach and the alternative approach proposed based on direct stochastic simulation. Section 3 describes the structural model used to perform risk assessments that is based on a 1000 MW Pressurised Water Reactor building and the selection of its critical components. It also presents the choice of the nuclear site and a description of its seismic hazard for nuclear design. Then, it shows a detailed comparison to define accelerograms suitable for use in SPRA between the conventional and the alternative approach proposed. Section 4 explains in detail the determination of the fragility curves used to characterise the critical components of the sample NPP. Later, it explains how the structural response is handled when using both approaches and summarises the calculations of risk performed. Section 5 discusses further aspects regarding the appropriateness of the approach proposed and Section 6 presents the conclusions from this study.

2. Description of methodologies

This work is based on the approach to perform SPRA for nuclear power plants reported by Huang et al. (2011b, 2011c, 2010). which in turn was based on the methodology for seismic performance assessment of *buildings* reported in FEMA-P-58 (FEMA, 2012). This methodology involves performing five steps: (i) perform plant-system and accident-sequence analyses, (ii) characterise seismic hazard, (iii) calculate and simulate structural response, (iv) assess damage of NPP components, and (v) compute the risk. These steps are graphically summarised in Fig. 1.

As seen in Fig. 1, such a methodology considers three types of assessments: (i) intensity-based, (ii) scenario-based and (iii) time-based assessments. Intensity-based assessments are intended to estimate the probability of unacceptable performance when a NPP is subjected to a specific intensity of shaking (e.g. PGA = 0.25 g). Scenario-based assessments estimate the probability of unacceptable performance of a NPP under a specific earthquake, defined by a pair of magnitude and distance (e.g. M_w 6 and epicentral distance $R_{epi} = 25$ km). Finally, time-based assessments estimate the annual frequency of unacceptable performance of a NPP taking into account all potential damaging earthquakes that may occur in the selected nuclear site. This work is focused on scenario-based assessments, although the methodology proposed could also be used for applications in the two other assessments.

When performing scenario-based assessments, it is required to define the seismic input for the single scenario (or all scenarios of interest) that contributes most strongly to the hazard of the nuclear site. Such a scenario can be obtained by means of the deaggregation of the hazard curve of the site (Goda et al., 2013). Then, a spectral shape predicted by *ad-hoc* GMPE(s) compatible with such scenario is estimated and few available accelerograms are scaled to match such a spectral shape. The scaled accelerograms are then used to perform nonlinear time-history analysis of a suitable structural model in order to estimate the damage state of the NPP. However, in order to estimate the probability of unacceptable performance with high statistical confidence, a great number of observations of the damage state are required. This leads to the necessity of sampling the structural response (i.e. the *output* of nonlinear time-history analysis) by means of Monte Carlo-type procedures. Such an approach for the simulation of structural response in probabilistic analysis is a known and used technique in earthquake engineering research (see for example Basim and Estekanchi (2015), Gencturk et al. (2016), Spence et al., Fragiadakis et al. (2015), among others). For illustration purposes, Fig. 2 summarises the steps involved to define the seismic input and calculate the structural output in scenario-based SPRA when using the traditional GMPE-based procedure.

The procedure summarised in Fig. 2 is somewhat cumbersome as a number of intermediate steps are required in order to obtain both suitable accelerograms and a great number of observations of the damage state of the NPP studied. The approach presented in this work that makes use of a stochastic accelerogram model previously calibrated by the authors (Medel-Vera and Ji, 2016) is more direct than the traditional procedure. Indeed, once the seismic scenario (or all scenarios of interest) that contributes most strongly to the hazard of the nuclear site is determined, an unlimited number of accelerograms compatible with such a scenario can be simulated. In this light, neither GMPEs nor scaling/matching procedures are necessary. In this approach, the ground motion *input* is sampled and the damage state is directly calculated rather than sampled. Clearly, no Monte Carlo-type procedures would be required to simulate the structural output. For illustration purposes, Fig. 3 summarises the steps involved to define the seismic input and calculate the structural output in SPRA when using the proposed procedure.

The following sections are devoted to present a step-by-step comparison of SPRA between the traditional GMPE-based methodology and the proposed alternative approach through a particular application for NPPs in the UK. For both analyses performed, the seismic hazard curve of the nuclear site was considered to be known.

3. Reactor building, seismic hazard and input definition

3.1. Sample nuclear reactor building

Risk assessments conducted in this article were performed considering a sample NPP based on a 1000 MW Pressurised Water

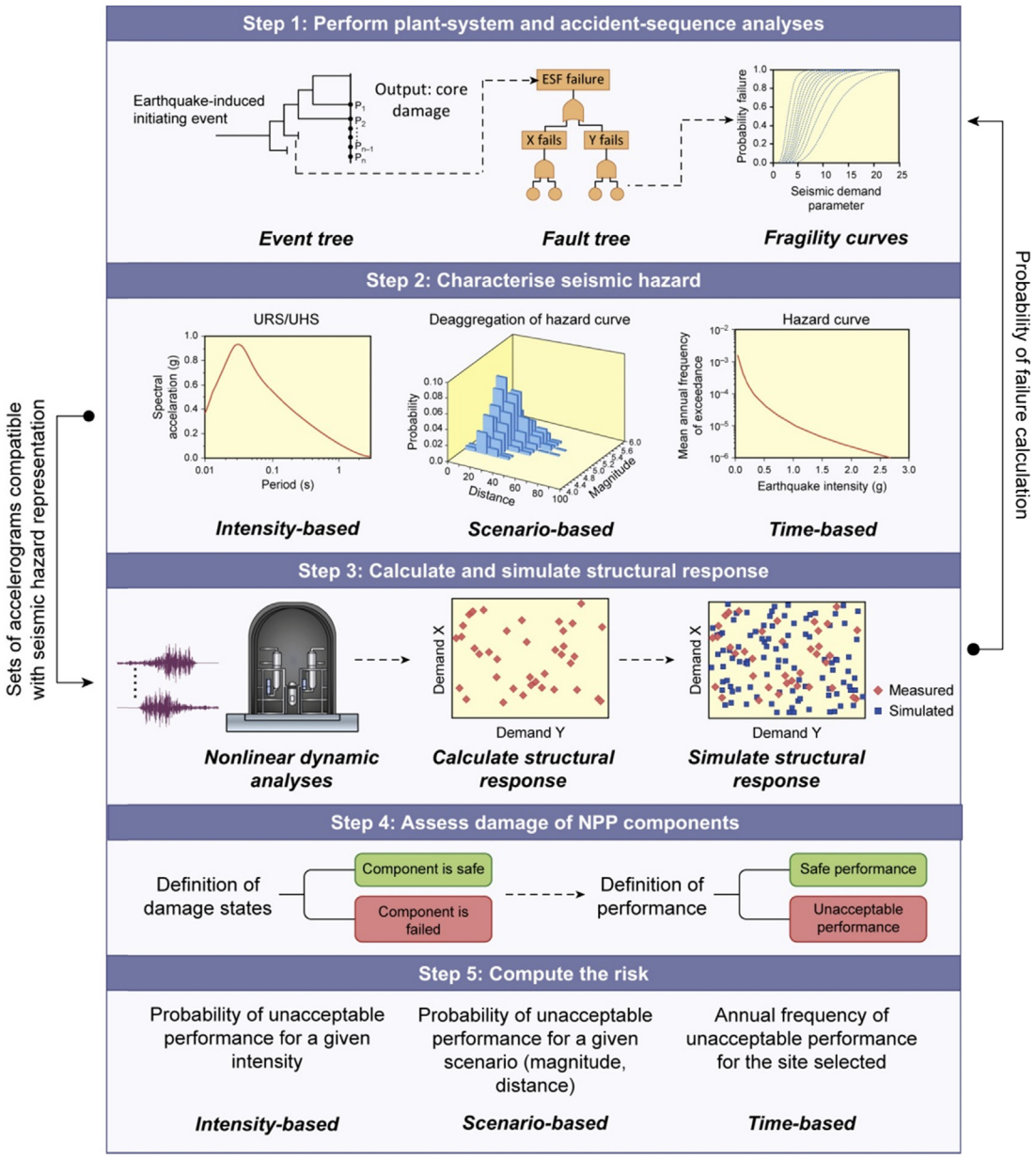

Fig. 1. Graphical summary of steps to conduct SPRA for NPPs proposed by Huang et al. (2011b, 2011c, 2010).

Reactor (PWR) shown schematically in Fig. 4a. This sample nuclear reactor building is composed of two structural units: (i) the containment structure (CS), composed of a post-tensioned concrete cylindrical wall, and (ii) the internal structure (IS), to which the critical key components/equipment/machinery of the NPP are attached. These structural units are independent from each other; hence, they are only connected at the foundation level. The height of the CS and IS are 60 and 39 m, respectively, whereas the total weight of the reactor building is approximately 62,000 ton. Fig. 4b shows the simplified structural model of the sample NPP used in this work to perform time-history analysis. Both the CS and IS are modelled as lumped-mass stick models that are the same in both horizontal directions. Masses of each node, stiffness and geometry properties of each stick element, and material properties were taken from Li et al. (2005). Fundamental periods of vibration of the CS and IS are 0.23 s and 0.18 s, respectively. It is worth mentioning that this type of structural model, although simplified, has been extensively used in nuclear engineering research (Huang et al., 2010; Choi et al., 2008; Ozaki et al., 1998; Yoo et al., 2000; Huang et al., 2007).

Following Huang et al. (2010, 2011c), risk assessments of NPPs are focused on their critical components supported by the IS. These components control the cost of a NPP project in terms of design, analysis, construction, testing and regulatory aspects. As for the CS, it is designed to withstand large internal pressures in order to provide shield against potential radiation release; hence, it is expected to remain within the elastic range during seismic events. The critical components of the sample NPP, node assignment in the structural model and their location related to the foundation level are summarised in Table 1.

In this work, unacceptable performance of the sample NPP is defined as the failure of any of the critical components indicated in Table 1. Consequently, the simplified fault tree used for risk assessments conducted in this work is shown in Fig. 5. This fault tree

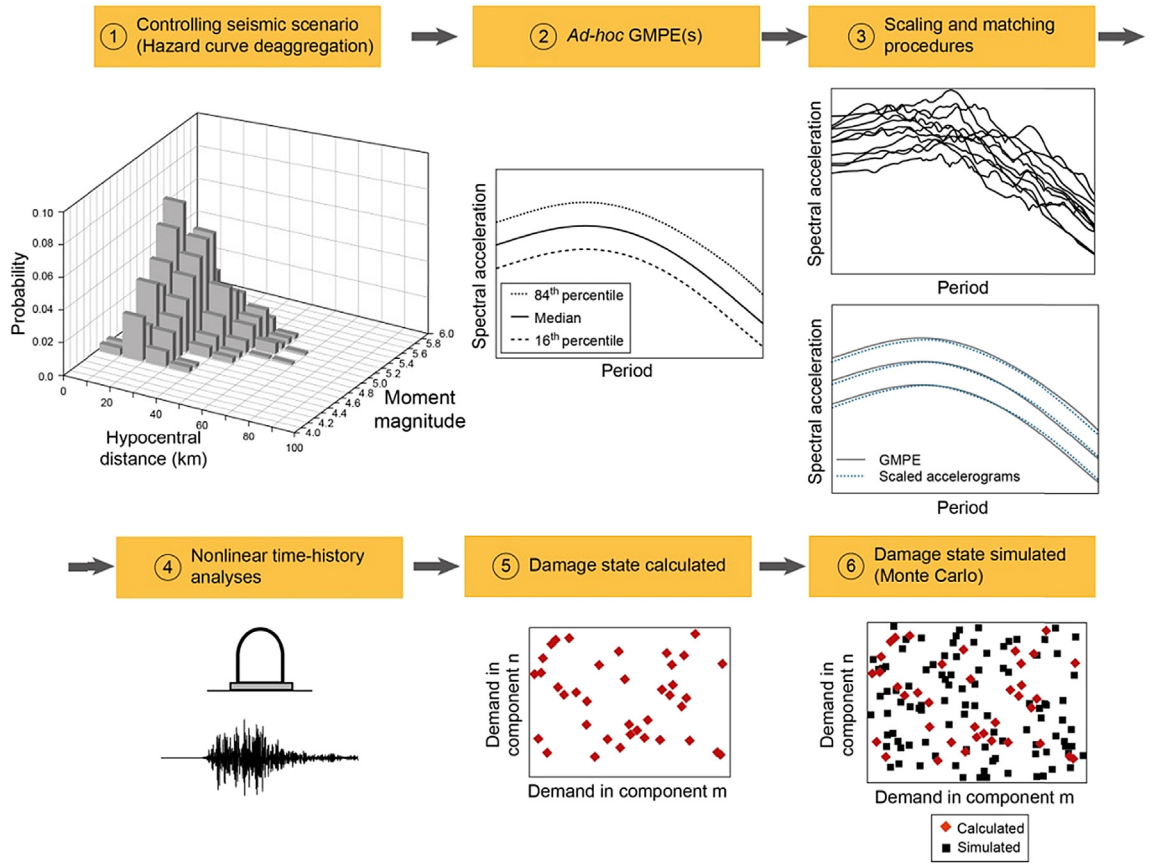

Fig. 2. Using the GMPE-based approach: steps to define seismic input and calculate structural output in scenario-based SPRA.

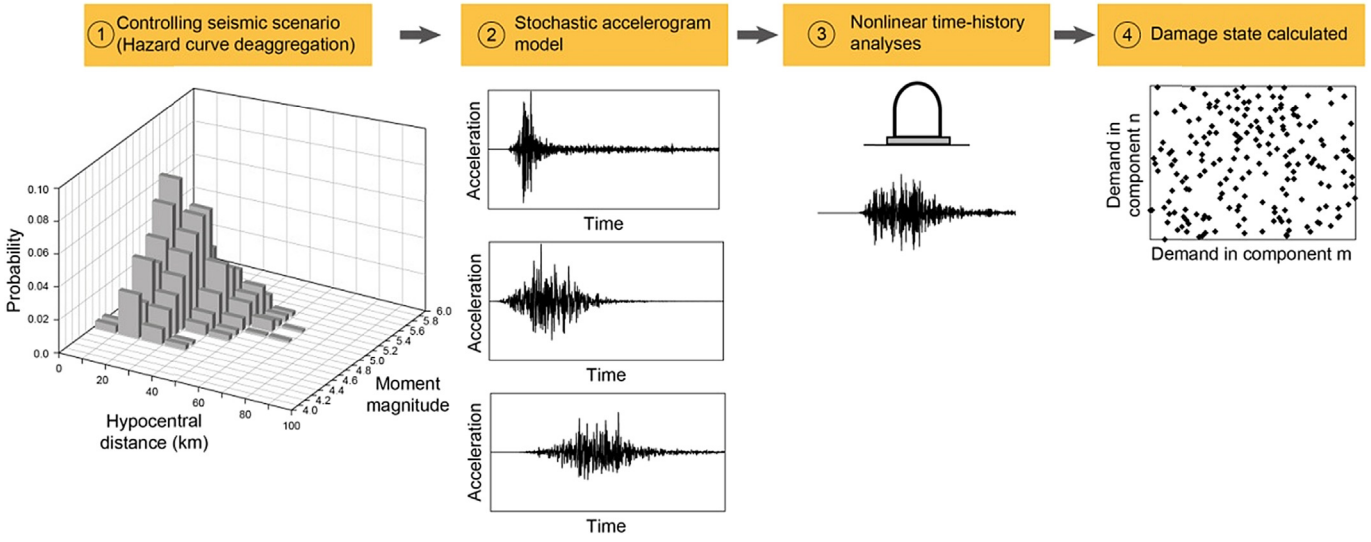

Fig. 3. Using the proposed approach: steps to define seismic input and calculate structural output in scenario-based SPRA.

possesses one 'OR' gate in which the failure of *one or more* events below it defines the failure of the event above it. Failure of each critical component is expressed by means of fragility curves. Estimation of such fragility curves are discussed in detail in Section 4.1.

As it will be seen in Section 4.2, nonlinear time-history analyses of the structural model shown in Fig. 4b were performed. In this work, the same inelastic definition for the structural model used by Huang et al (2010, 2011c). was used for simplicity. In this definition, bilinear shear hinges with 3% post-yield stiffness were assigned to all stick elements of the IS. The yield capacity of each hinge was estimated as $0.5 \cdot \sqrt{f'_c} \cdot A_s$, where f'_c is the compression concrete strength (assumed as 35 N/mm^2) and A_s is the shear area of each stick of the IS as indicated in Li et al. (2005).

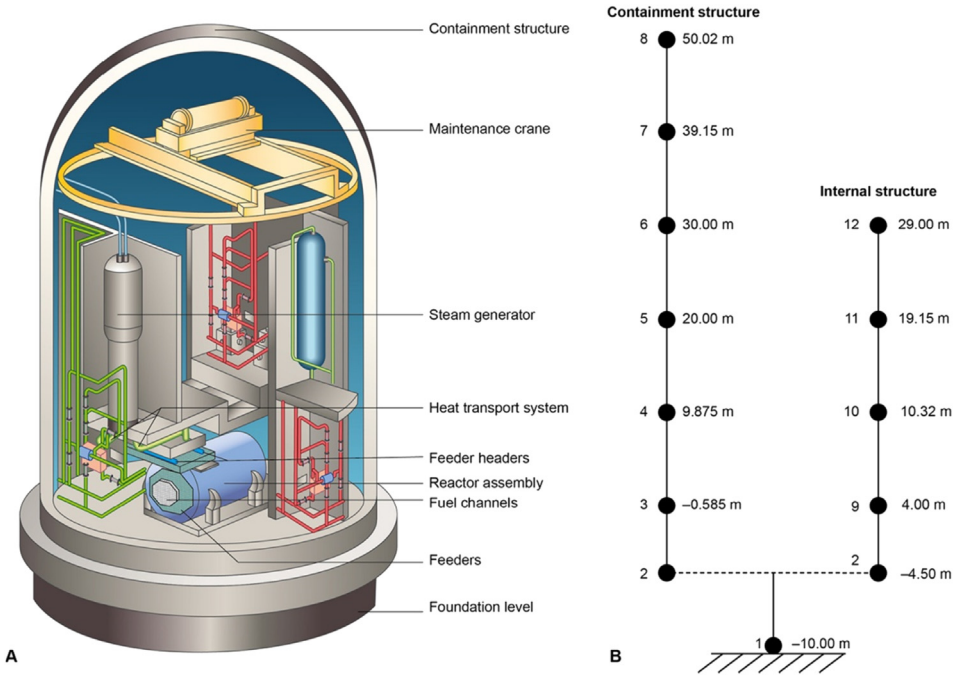

Fig. 4. Sample NPP reactor building: (a) schematic view; (b) lumped-mass stick model (Li et al., 2005).

Table 1
Critical components and their location within the sample NPP.

Critical component	Node number	Elevation (m)
Reactor assembly and fuel channels	2	−4.50
Feeders and feeder headers	9	4.00
Heat transport system	10	10.32
Steam generator	11	19.15
Maintenance crane	12	29.00

as the Wylfa Nuclear Power Station was built in a nearby location in Anglesey (Magnox, 2011). The estimation of the dominant seismic scenario was taken from the deaggregation of the hazard curve of Holyhead proposed by Goda et al. (2013). for 10,000 years return period at a structural period of 0.2s, shown in Fig. 6b (for simplicity, the hazard defined for a structural period of 0.2s was assumed to be valid for the fundamental period of the IS = 0.18 s). From this figure, it is possible to see that the scenario that contributes most strongly

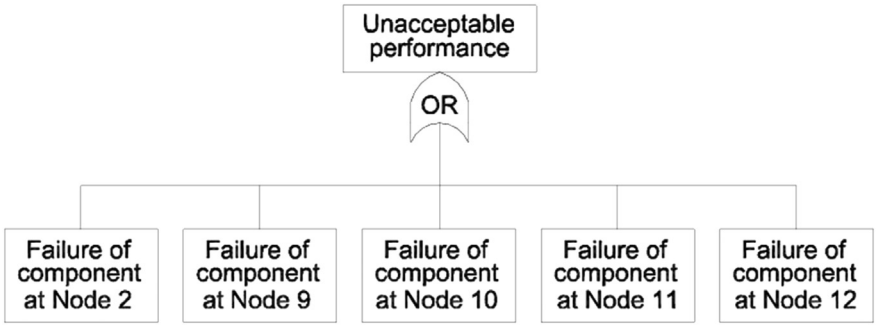

Fig. 5. Fault tree used for risk assessments conducted in this work.

3.2. Seismic hazard of the nuclear site

A hypothetical UK nuclear site was necessary to select. The level of seismic hazard of nuclear sites in the UK is defined by a seismic event of an annual frequency of exceedance of 10^{-4}, corresponding to a return period of 10,000 years (HSE, 2011). Therefore, it is of interest to determine the scenario (magnitude, distance) that contributes most strongly to the site's hazard for a 10,000 years return period at the fundamental period of the IS of the sample NPP. The hypothetical nuclear site selected for risk assessments in this work was the town of Holyhead, Anglesey (shown in Fig. 6a). This site was considered to be representative of an actual UK nuclear site the site's hazard is an earthquake magnitude M_w 5.3 at a hypocentral distance of 15 km (average between 10 and 20 km). Accelerograms compatible with such a scenario will be later required to perform time history analysis of the structural model of the sample NPP.

3.3. Definition of seismic inputs: GMPEs vs stochastic model

3.3.1. Ground motion prediction equations (GMPEs)

The GMPEs selected for this purpose were the same used to define current national seismic hazard maps for the UK in Musson and Sargeant (2007), namely, Bommer et al. (2007). and Campbell

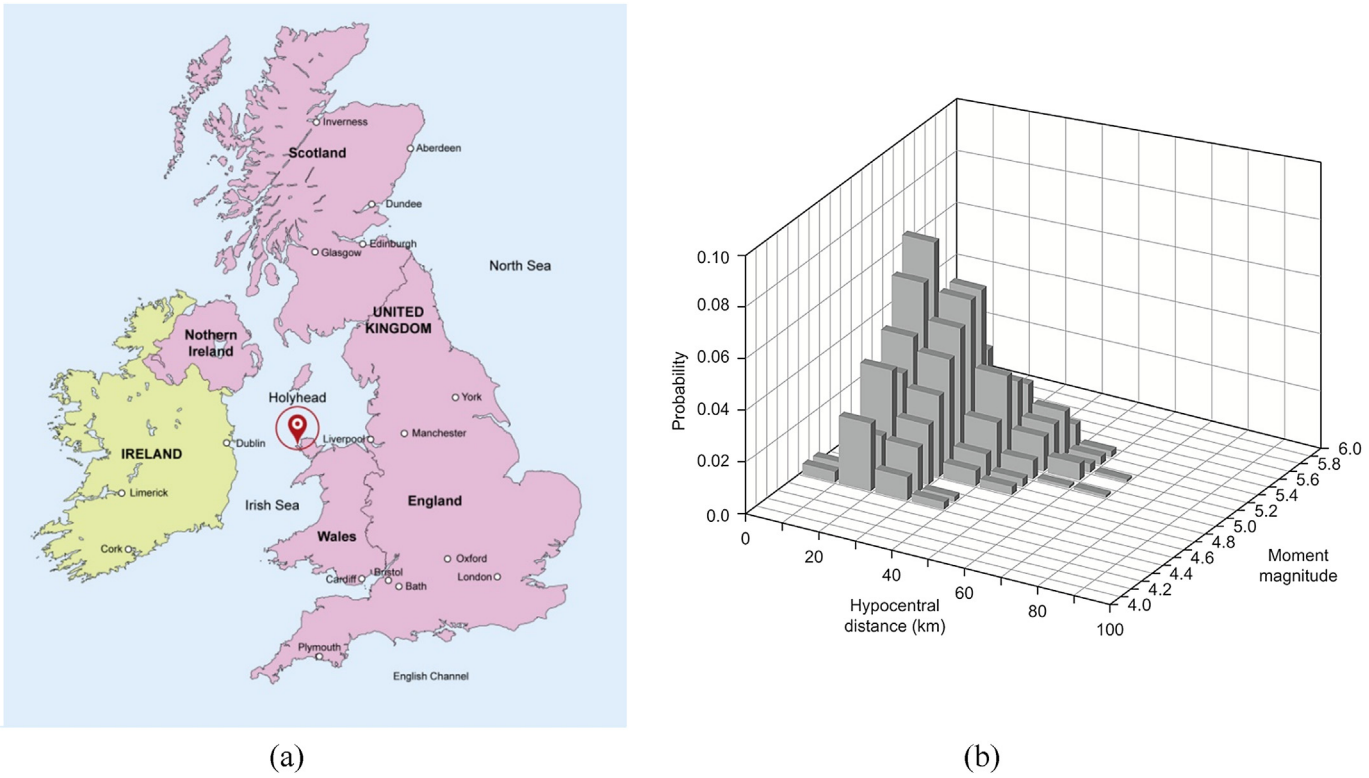

Fig. 6. Hypothetical UK nuclear site selected: (a) location of Holyhead; (b) deaggregation of the hazard curve for Holyhead, UK for 10,000 years return period at a structural period of 0.2s (redrawn from Goda et al. (2013).

and Bozorgnia (2008). The underlying basis for the use of the model of Bommer et al. (2007). was geographical proximity as it was calibrated using earthquake data from Europe and the Middle East, whereas the model of Campbell and Bozorgnia (2008), although calibrated using earthquake data from active crustal zones, was deemed to be suitable for the UK (Goda et al., 2013). Additionally, the model of Rietbrock et al. (2013). was also included as it is a UK-based model calibrated using weak-motion data from British earthquakes. Table 2 shows the GMPEs selected for comparisons and their principal features.

The following conditions/assumptions were made in order to be consistent in the generation of sets of accelerograms compatible with the seismic scenario defined in Section 3.2.

1. *Scale magnitude*: The moment magnitude scale (M_w) was used. All GMPEs selected are consistent with such a scale.
2. *Distance metric*: The epicentral distance (R_{epi}) was used. For simplicity in these calculations, the earthquake rupture was modelled as a point source, the fault was assumed to be vertical, and a very small focal depth was assumed; hence all distance metrics could be considered approximately equivalent. These assumptions are considered to be conservative.
3. *Type of soil*: It was assumed rock type conditions. As the model of Rietbrock et al. (2013). was calibrated for hard rock conditions, the modification factors proposed by Van Houtte et al. (2011). were used to adjust it to rock conditions.
4. *Style of faulting*: The type of faulting was not considered. However, strike-slip conditions were set to those GMPEs that included style of faulting as this type is the most likely to occur in British earthquakes (Baptie, 2010).
5. *Component of motion*: The larger horizontal (LH) component of motion was used. As the GMPEs selected were calibrated considering the geometric mean (GM) of the two horizontal

Table 2
GMPEs selected for risk assessments in this section.

N	Reference	Specific region	GMP[a]	HC[b]	M[c]	R[d]	Site classification	Style of faulting
1	Rietbrock et al. (2013)	UK	PGA, PGV, PSA	GM	M_w	R_{JB}	Hard rock (Vs30 ~ 2300 m/s)	Not included
2	Bommer et al. (2007)	Europe and the Middle East	PGA, PSA	GM	M_w	R_{JB}	Rock (Vs30 > 750 m/s), Stiff soil (360 < Vs30 < 750 m/s) Soft soil (Vs30 < 360 m/s)	Normal, strike-slip and reverse
3	Campbell and Bozorgnia (2008)	Active crustal zones	PGA, PGV,PSA, PGD	GM	M_w	R_{rup}	Rock (Vs30 > 750 m/s), Stiff soil (360 < Vs30 < 750 m/s) Soft soil (180 < Vs30 < 360 m/s) Very soft soil (Vs30 < 180 m/s)	Normal, strike-slip and reverse

[a] Ground motion parameter predicted: PGA: peak ground acceleration; PGV, peak ground velocity; PGD, peak ground displacement; PSA: pseudospectral acceleration.
[b] Definition of the horizontal component: GM: geometric mean.
[c] Magnitude scale used.
[d] Distance metric used.

components, the coefficients proposed by Beyer and Bommer (2006) were used to estimate LH.

Following Huang et al. (2011b, 2011c), 11 accelerograms for each GMPE of Table 2 were scaled by means of the Distribution-Scaling Method (Huang et al., 2011a) to match the spectral shape and variability predicted by the corresponding GMPE. For this purpose, it was decided to use recorded accelerograms that were used in the calibration of their corresponding GMPE, where possible, compatible with the scenario of interest. This was done as an attempt to preserve the natural features of frequency content and time duration of real records from the location of interest for the corresponding GMPE. The criterion for selecting accelerograms was to use records from earthquake magnitude $5.2 < M_w < 5.4$, epicentral distance $10 < R_{epi} < 20$ km, and rock conditions ($V_s \geq 750$ m/s). For the model of Rietbrock et al. (2013), no such accelerograms were available; therefore, the 11 accelerograms were simulated using the stochastic model calibrated by the authors for NW Europe (Medel-Vera and Ji, 2016). For the model of Bommer et al. (2007), the 11 recorded accelerograms selected are summarised in Table 3. For the model of Campbell and Bozorgnia (2008), only 3 accelerograms fell into the selection criterion defined. These records are indicated in Table 3. The remaining 8 accelerograms were obtained through simulations. As the stochastic model calibrated for by the authors (Medel-Vera and Ji, 2016) is not suitable to simulate accelerograms from active crustal regions, it was used the computer code "Strong Ground Motion Simulation (SGMS)" (Halldórsson, 2004). SGMS is based on the Specific Barrier Model (Halldorsson and Papageorgiou, 2005) which is a complete and self-consistent description of the earthquake faulting process. In this case, the tectonic regime selected to simulate accelerograms with SGMS was "inter-plate" (rather than "intra-plate" or "extensional" regimes) as it is more consistent with the corresponding GMPE. Table 3 is a general summary of the 11 accelerograms selected for each GMPE used for risk assessments in this work.

Fig. 7a shows the spectral accelerations of the 11 scaled accelerograms for each GMPE whereas Fig. 7b shows the median, 84th and 16th percentiles for the 11 scaled accelerograms and their corresponding GMPEs. From Fig. 7b, it is possible to see that the scaled accelerograms are able to capture reasonably well the spectral shape and variability predicted by the GMPEs selected. Consequently, the scaled accelerograms were considered suitable to perform nonlinear time-history analysis with the structural model of the sample NPP.

3.3.2. Stochastic ground motion accelerogram model for NW Europe

Complete details on the stochastic accelerogram model for NW Europe developed by the authors can be found in Medel-Vera and Ji (2016). The necessity for developing such a model lies on three key characteristics: (i) the underlying tectonic mechanism causing earthquakes in the UK is not yet fully understood (Baptie, 2010); (ii) there is little correlation between the pattern of earthquake occurrence and structural geology of Britain (Musson, 1996); and (iii) the database of British earthquakes is mainly composed of small magnitude earthquakes, say, M_w 2–4.5. Therefore the nature of accelerograms (intensity, frequency content and time duration) is relatively unknown for earthquake magnitudes of interest for UK nuclear design, say magnitude M_w 5–6 (Bommer et al., 2011).

The model is a set of predictive equations of parameters that define a time-modulated filtered white noise process. Such a stochastic process is defined by: (i) a 6-parameter time-modulating function and (ii) a 3-parameter time-varying linear filter. The set of predictive equations for these parameters were calibrated by means of the random-effects regression technique using a small dataset of 220 accelerograms recorded in the stable continental region of NW Europe. The model simulates accelerograms compatible with seismic scenarios defined by earthquake magnitudes $4 < M_w < 6.5$, distance-to-site $10 < R_{epi} < 100$ km and different types of soil (rock, stiff and soft soil). Certainly, the underlying assumption of using this model is that the nature of accelerograms caused by moderate-to-strong earthquakes in Britain would be similar to those caused in the broader region of NW Europe due to geographical proximity.

For the stochastic model, the generation of accelerograms compatible with the seismic scenario of interest is significantly more straightforward. As the model proposed is an unlimited source of accelerograms compatible with the dominant seismic

Table 3
Summary of the 11 accelerograms associated to each GMPE selected.

No	Earthquake name	Location[a]	Wave ID[b]	Year	Mw	Distance (km)[c]
Rietbrock et al. (2013)						
1–11	Simulated accelerograms using the stochastic model for NW Europe, considering a scenario M_w 5.3, R_{epi} = 15 km and rock conditions.					
Bommer et al. (2007)						
1	Friuli	Northern Italy	981	1977	5.4	11
2	Calabria	Southern Italy	169	1978	5.2	10
3	Montenegro	Albania	193	1979	5.4	15
4	Kalamata	Southern Greece	1900	1987	5.3	17
5	Javakheti Highland	Turkey-Georgia-Armenia	487	1990	5.4	20
6	Umbria Marche	Central Italy	765	1997	5.2	11
7	Umbria Marche	Central Italy	826	1997	5.2	14
8	Umbria Marche	Central Italy	791	1997	5.2	18
9	Mt. Hengill Area	Iceland	5085	1998	5.4	15
10	Mt. Hengill Area	Iceland	5086	1998	5.4	15
11	Mt. Hengill Area	Iceland	5078	1998	5.4	18
Campbell and Bozorgnia (2008)						
1	Lytle Creek	California, USA	43	1970	5.33	16.7
2	Whittier Narrows-02	California, USA	715	1987	5.27	16.5
3	Anza (Horse Canyon)-01	California, USA	225	1980	5.19	12
4–11	Simulated accelerograms using the SGMS computer code, considering a scenario M_w 5.3, R_{epi} = 15 km and rock conditions.					

[a] Location for accelerograms used for Bommer et al. (2007) is the Flinn-Engdhal region.
[b] Wave ID for accelerograms used for Bommer et al. (2007) are given by the ISESD database and Campbell and Bozorgnia (2008) are given by the PEER database
[c] Distance metric for accelerograms used for Bommer et al. (2007) is R_{epi} and Campbell and Bozorgnia (2008) is R_{JB}.

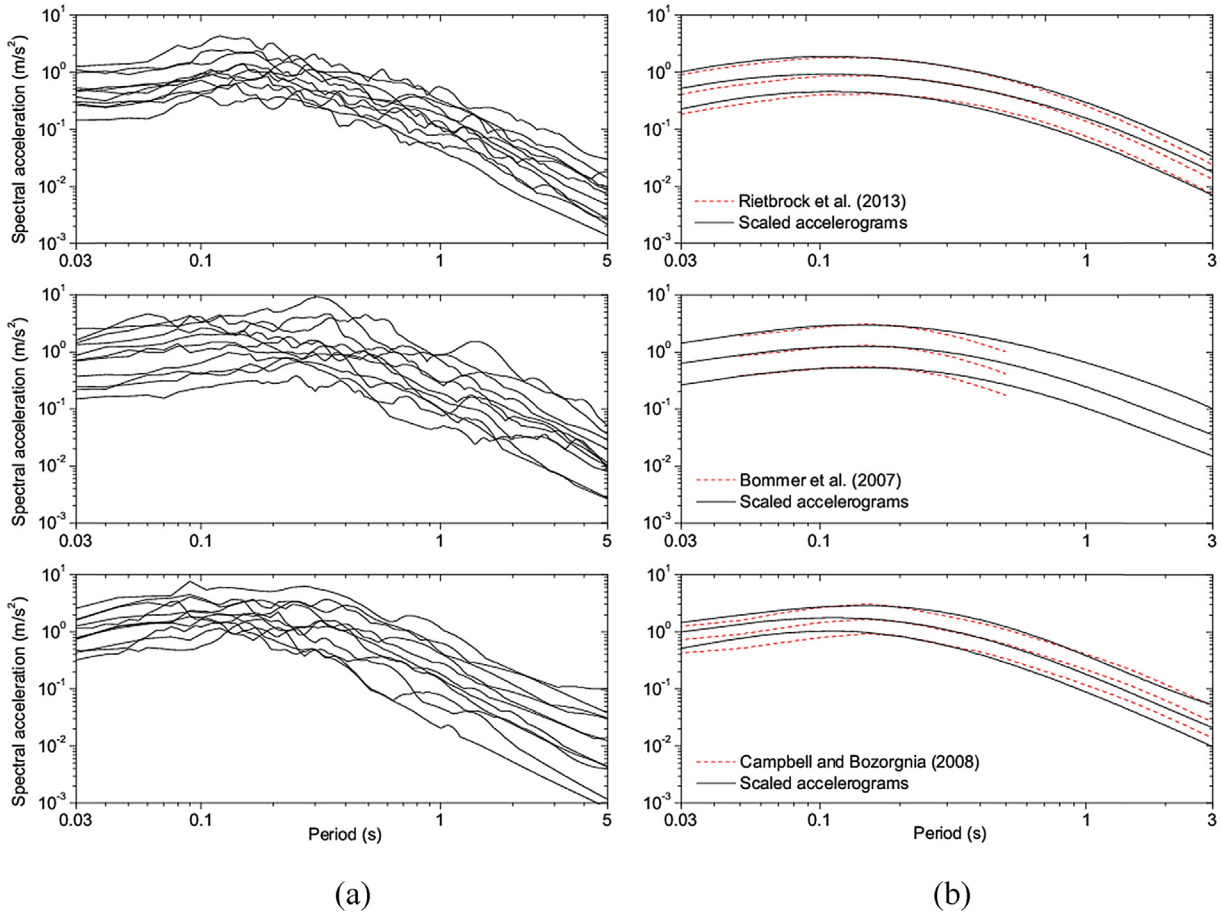

Fig. 7. (a) Spectral accelerations of the 11 accelerograms scaled for each GMPE; (b) median, 84th and 16th percentiles of spectral accelerations predicted by each GMPE and their corresponding scaled accelerograms.

scenario, there is no need of using intermediate steps towards obtaining suitable records. Selection of GMPE(s) suitable to use in the UK and scaling-matching procedures are not needed when using the stochastic model. For illustration purposes, Fig. 8a shows five simulated accelerograms and Fig. 8b shows the spectral acceleration of 50 simulated accelerograms for a scenario M_w 5.3 and epicentral distance $R_{epi} = 15$ km.

Before performing nonlinear-time history analysis using the

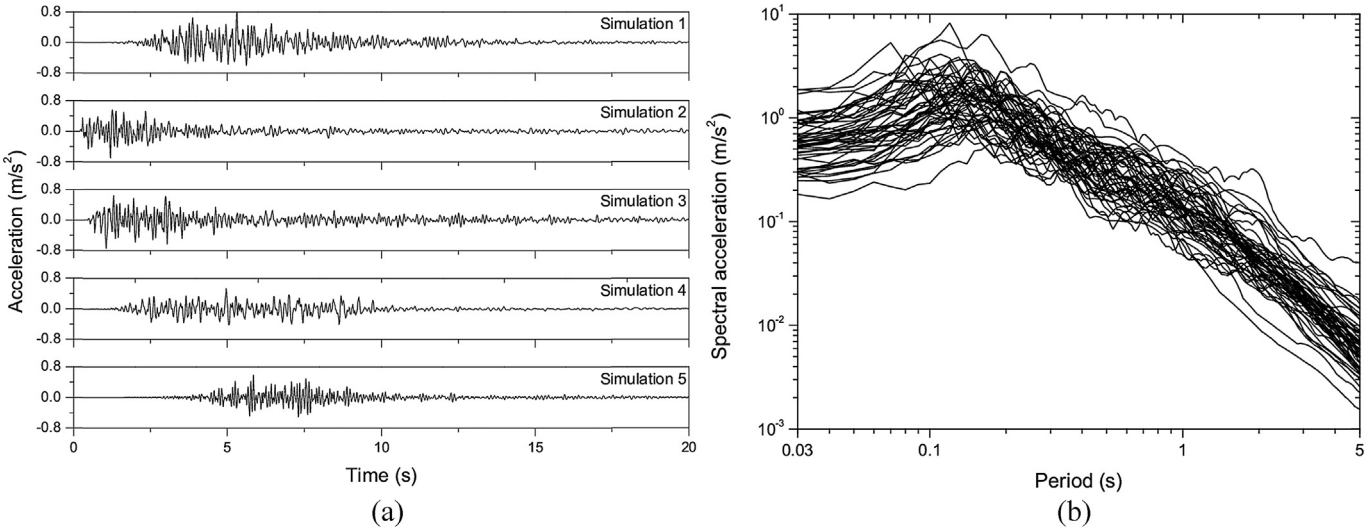

Fig. 8. Sample input compatible with a scenario M_w 5.3 and epicentral distance $R_{epi} = 15$ km: (a) five simulated accelerograms and (b) spectral acceleration of 50 simulated accelerograms.

accelerograms defined in this section, it is necessary to define the vulnerability of the sample nuclear reactor building against seismic actions. In the next section, the fragility analysis of the sample NPP is discussed.

4. Fragility curves, structural analysis and risk calculations

4.1. Fragility analysis

Fragility analysis of NPP components is largely based on the so-called "Zion method" initially described in Kennedy and Ravindra (1984) and Kennedy et al. (1980). Thorough guidelines for conducting such analysis were later reported in EPRI (1994) and then updated in EPRI (2002). In this methodology, fragility curves are used to characterise the conditional probability of failure of a component under seismic loads; such failure occurs when its capacity, defined as a function of a predefined demand parameter, is exceeded. The capacity of a component is defined by the double lognormal model as follows:

$$A = \overline{A} \cdot \varepsilon_r = \widehat{a} \cdot \varepsilon_u \cdot \varepsilon_r \tag{1}$$

In this model, the capacity A is modelled as a random variable in which $\overline{A}$ is the median value of the capacity and ε_r is a lognormal random variable with unit median and logarithmic standard deviationβ_r. The random variable ε_r accounts for the inherent randomness (aleatory uncertainty) naturally present in the seismic demand when determining the capacity of a component. As another source of uncertainty is the lack of complete knowledge (epistemic uncertainty) to determine the median capacity of the component, $\overline{A}$ is also modelled as a random variable in which $\widehat{a}$ is a deterministic value that represents the best estimation for $\overline{A}$ and ε_u is a lognormal random variable with unit median and logarithmic standard deviation β_u. Using the capacity model indicated in (1), the probability of failure of a component for a given intensity a of the selected seismic demand parameter is

$$f = \Phi\left(\frac{\ln\left(a \Big/ \widehat{a}\right) + \Phi^{-1}(Q)\cdot\beta_u}{\beta_r}\right) \tag{2}$$

where Φ is the standardised normal distribution function and Q is the probability (confidence level) that the median capacity of the component exceeds a predetermined value of the demand parameter. Using Eq. (2), a family of fragility curves can be defined for different confidence levels Q required by the analyst.

In order to determine the best estimator for the capacity of a component $\widehat{a}$, the seismic margin approach is frequently used in practice. This methodology estimates the minimum seismic capacity of a component by defining its high-confidence-of-low-probability-of-failure (HCLPF) capacity level. HCLPF is defined as the capacity in which the analyst has 95% confidence that the failure probability is less than 5%. Therefore, considering Q = 0.95 and f = 0.05 in Eq. (2), the relationship between $\widehat{a}$ and HCLPF is

$$\widehat{a} = HCLPF \cdot e^{1.65(\beta_r+\beta_u)} \tag{3}$$

The fragility parameters $\widehat{a}$, β_r, β_u (and *HCLPF*) were estimated following a simplified approach. It is initially defined the seismic demand parameter used to characterise fragility curves for the critical components of the sample NPP. It is acknowledged that the following parameters have been previously analysed in the literature for this purpose: peak ground acceleration, peak ground velocity, pseudo-spectral acceleration, Arias intensity, cumulative absolute velocity intensity, etc. (Kim et al., 2011). However, in this work the average floor spectral acceleration (AFSA) over a frequency range from 1 to 33 Hz was selected (i.e. the average of 33 floor spectral ordinates at frequencies from 1 to 33 Hz with increments of 1 Hz). This demand parameter was selected for two reasons: (i) damage of NPP components is better correlated to structural response parameters rather than ground-motion parameters (Huang et al., 2011b) and (ii) seismic demands on NPP components are usually characterised by means of floor response spectra (Huang et al., 2010). The frequency range 1–33 Hz to calculate AFSA was selected as most frequencies of NPP components are comprised within such a range (see Pisharady and Basu (2010) for a complete summary of typical frequency ranges for NPP components).

The *HCLPF* capacity for the critical components of the sample NPP defined in Section 3.1 were estimated by means of linear dynamic analysis of the structural model using a large set of accelerograms compatible with the seismic hazard of the selected nuclear site. The number and nature of input accelerograms, range of earthquake magnitudes and distances, and type of analysis used to determine fragility parameters are all matters open to discussion. Table 4 shows some examples reported in the literature showing a wide variety of criteria among researchers. However, it is apparent that the majority of such studies intended to use accelerograms (either recorded or simulated or a combination of both) that at some extent are representatives of the nuclear site's seismic hazard.

In this work, a different approach to estimate the *HCLPF* capacity for the critical components was used. As the stochastic model used is an unlimited source of accelerograms compatible with any seismic scenario required by the analyst, a large database of simulated recordings compatible with the site's hazard was used. For simplicity purposes, the seismic hazard of the site selected was characterised by means of its dominant events (Dehghani and Tremblay, 2012), i.e. the scenarios that are most likely to contribute to the hazard which are directly obtained from the disaggregation of the hazard curve. From Fig. 6b, it is possible to see that the dominant events for the nuclear site selected are earthquakes magnitude $4.5 < M_w < 5.5$ at hypocentral distances of $10 < R_{hyp} < 30$ km. For simplicity in these calculations, it was assumed a very small focal depth; hence $R_{hyp} \approx R_{epi}$. A large set of scenarios within such ranges (magnitude, distance) was sampled. For each scenario, a single corresponding accelerogram was simulated with the model proposed and a linear time-history analysis of the sample NPP structural model was performed. Then, AFSAs for each node were calculated. This procedure was repeated until convergence on the median value for AFSAs for all nodes was reached. Following Huang et al. (2010), this median value for AFSAs for each node was assigned as their HCLPF capacity level. Fig. 9a shows the simulated seismic scenarios and Fig. 9b shows the convergence of the median value of AFSAs for each node, which is reached after performing approximately 200 simulations.

From Fig. 9b, it is obtained that the HCLPF for the critical components are: 0.71, 0.76, 0.87, 1.12 and 1.65 m/s^2 for Nodes 2, 9, 10, 11 and 12, respectively. The logarithmic standard deviations β_r and β_u are normally calculated following the factor of safety methodology reported in Kennedy and Ravindra (1984). For equipment, this methodology involves calculating the variability of three factors of safety: capacity factor (F_C), structure response factor (F_{RS}) and equipment response factor (F_{RE}). Due to the simplified nature of the structural model used in this work, it was not possible to appropriately calculate the total variability associated to them. In cases where no theoretical derivation is available, they are suggested to be selected form the published literature (Pisharady and Basu, 2010), for example, from the comprehensive review reported by

Table 4
Examples of the nature of seismic inputs used to determine fragility curves of NPP structures and components.

Reference	Application (country)	Number and nature of accelerograms	Range of magnitudes (scale)	Range of distances (km)	Nature of time-history analyses
Cho and Joe (2005)	Containment & component cooling water buildings – Standard NPP (Korea)	**87** recorded in southeast Korean peninsula	2.7–4.8[a]	Unspecified	Linear
Choi et al. (2008)	CANDU containment structure (Korea)	**30** recorded around the world	5.7–7.6 (M_w)	0.10–18.3 (R_{rup})	Nonlinear
Huang et al. (2010)	Components of a sample NPP (Eastern United States)	**11** simulated compatible with local tectonic regime	5.3 (M_w)	7.5[b]	Linear
Kennedy et al. (1990)	Diablo Canyon NPP (Western United States)	**52** (24 recorded in WUS + 28 simulated from WUS motions)	6.5–7.5 (M_w)	0.1–25[b]	Linear
Nakamura et al. (2010)	PWR-type building (Japan)	**1** simulated matched with site UHS	Unspecified	Unspecified	Nonlinear
Ozaki et al. (1998)	PWR-type building (Japan)	**12** simulated based on local standard motions	Unspecified	Unspecified	Linear and nonlinear
Zentner (2010)	Reactor coolant system – Standard NPP (France)	**50** simulated matched with site response spectrum	Unspecified	Unspecified	Nonlinear

[a] Unspecified earthquake magnitude scale.
[b] Unspecified distance metric.

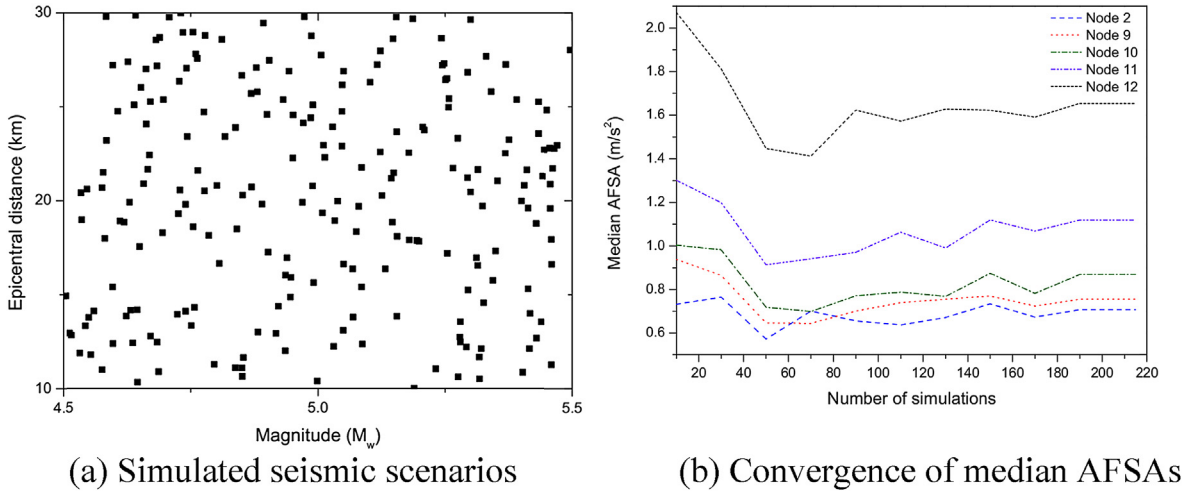

Fig. 9. Estimation of the HCLPF capacity level for the critical components of the sample NPP.

Park et al. (1998). However, in this work, generic values recommended by Kennedy and Ravindra (1984) were directly used. As in this work the parameter used to characterise fragility curves is a structural response parameter rather than a ground motion parameter, uncertainties related to F_{RS} are not needed to take into account. In this light, the upper limits for the variability of F_C and F_{RE} proposed by Kennedy and Ravindra (1984) were conservatively taken, giving a combined final value of $\beta_r = 0.31$ and $\beta_u = 0.41$. These values are considered to be on the safe side: the sum of both logarithmic standard deviations should conservatively be $(\beta_r + \beta_u) \approx 0.7 - 0.8$ (Ellingwood, 1994; Prassinos et al., 1986). Therefore, the values for the deterministic estimator for the capacity of the critical components $\hat{a}$ expressed in terms of AFSA between 1 and 33 Hz are: 2.32, 2.48, 2.85, 3.67 and 5.43 m/s^2 for Nodes 2, 9, 10, 11 and 12 respectively. As an example, and Fig. 10a and b show families of 11 fragility curves for the critical components at Nodes 2 and 12. These curves were built using Eq. (2) considering confidence levels Q from 1/22 to 21/22 with increments of 1/11. The median fragility curve ($Q = 0.5$) is shown in the solid bold line. Fig. 10c shows the median fragility curves for critical components at all nodes of the IS.

4.2. Structural response

Nonlinear time-history analyses were performed on the structural model of the sample NPP using the 11 accelerograms selected for each GMPE described in Section 3.3.1. For the stochastic model proposed, a databank of 600 accelerograms were simulated as described in Section 3.3.2 and then used to conduct nonlinear time-history analysis. It is worth mentioning that the size of the databank of 600 nonlinear dynamic analyses and their associated results of the structural response is only intended to have a statistically large collection of data to choose from. This does not mean that 600 nonlinear dynamic analyses are needed to perform to make a statistically significant estimation of the seismic risk as it will be seen in Section 4.3. The structural response of all analyses was calculated in all nodes of the IS in terms of the same demand parameter used to define fragility curves, i.e. AFSA over a frequency range from 1 to 33 Hz. Consequently, for each GMPE a matrix of results of order 11 × 5 (11 accelerograms and 5 nodes) was obtained, whereas for the stochastic model proposed, such matrix of results is of order 600 × 5. Table 5 summarises the matrices of results associated to each GMPE. Additionally, as an example of these results, Fig. 11 shows the median floor spectral accelerations between 1 and 33 Hz for Node 2 (reactor assembly) and Node 12 (maintenance crane).

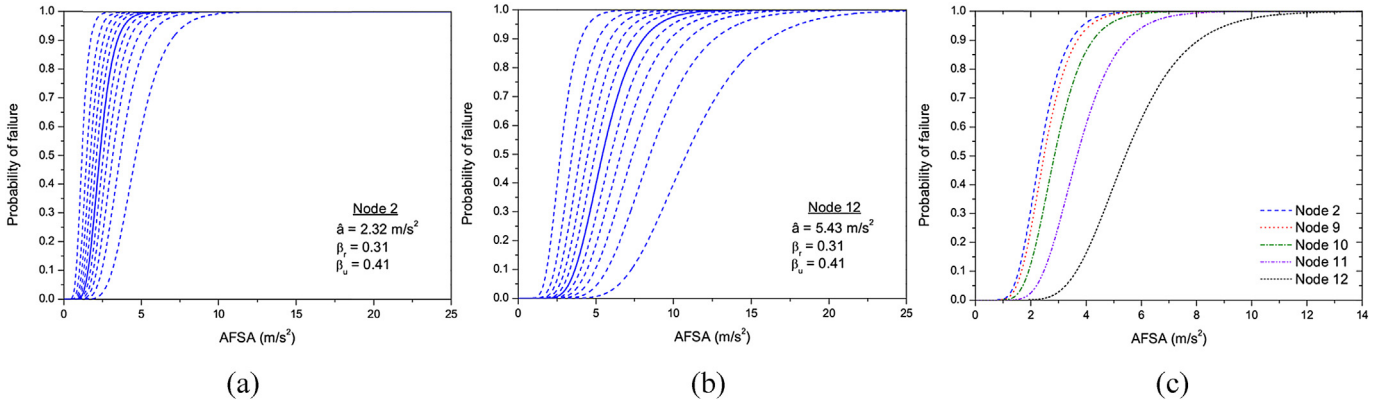

Fig. 10. Family of fragility curves for the critical components at (a) Node 2; (b) Node 12; (c) median fragility curves for critical components at all nodes of the IS.

Table 5
AFSAs obtained for each set of accelerograms associated to the GMPEs selected.

GM	Rietbrock et al. (2013)					Bommer et al. (2007)					Campbell and Bozorgnia (2008)				
	Node 2	Node 9	Node 10	Node 11	Node 12	Node 2	Node 9	Node 10	Node 11	Node 12	Node 2	Node 9	Node 10	Node 11	Node 12
1	0.346	0.405	0.449	0.507	0.589	0.191	0.244	0.257	0.272	0.290	0.709	0.933	1.057	1.168	1.339
2	0.212	0.264	0.285	0.312	0.350	0.327	0.423	0.453	0.486	0.529	0.501	0.889	0.972	1.058	1.197
3	0.337	0.444	0.481	0.515	0.565	0.332	0.393	0.426	0.459	0.512	1.542	1.260	1.402	1.587	1.870
4	0.496	0.579	0.637	0.702	0.799	0.524	0.697	0.747	0.793	0.849	0.599	0.694	0.751	0.811	0.873
5	0.398	0.527	0.565	0.599	0.644	0.958	1.139	1.226	1.319	1.428	1.098	1.258	1.385	1.505	1.628
6	0.657	0.845	0.921	0.985	1.069	1.233	1.510	1.683	1.847	2.014	1.121	1.423	1.547	1.663	1.775
7	0.632	0.858	0.928	0.997	1.073	0.952	1.101	1.178	1.246	1.331	1.194	1.478	1.605	1.714	1.831
8	1.175	1.449	1.639	1.816	2.011	2.427	2.284	2.559	2.829	3.095	2.226	2.616	2.874	3.101	3.302
9	0.683	0.925	1.004	1.069	1.141	2.440	2.888	3.158	3.435	3.708	2.475	2.723	2.929	3.126	3.343
10	1.275	1.713	1.852	1.987	2.151	1.944	2.287	2.489	2.684	2.907	1.724	2.387	2.589	2.765	2.952
11	1.949	2.585	2.875	3.143	3.441	3.191	4.583	4.847	5.074	5.306	3.930	4.742	5.152	5.522	5.888

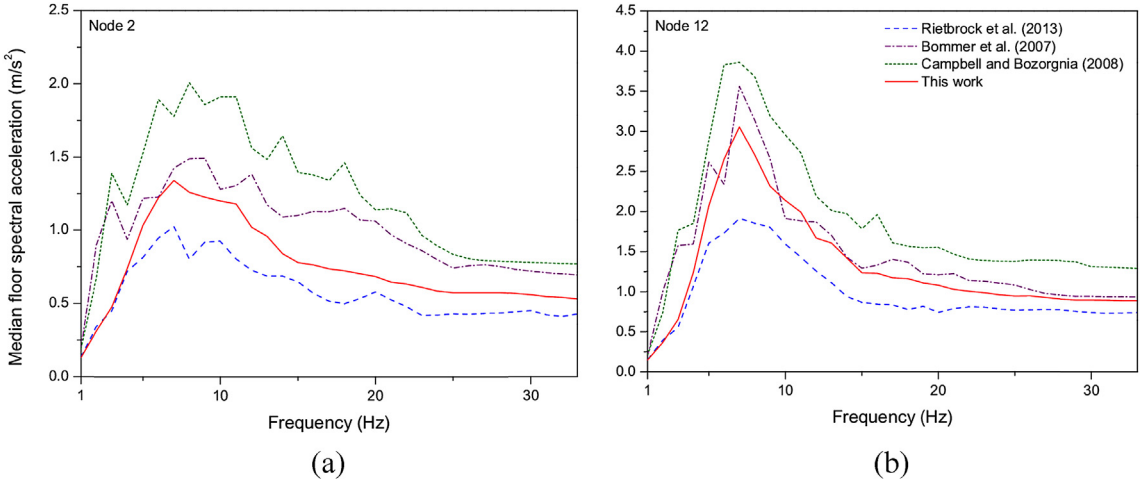

Fig. 11. Median floor spectral acceleration at: (a) Node 2 (reactor assembly) and (b) Node 12 (maintenance crane).

As the matrices of results associated to each GMPE are comprised of only 11 rows, it is required to sample the structural response (output) in order to enlarge the number of row vectors to hundreds or thousands to estimate the probability of unacceptable performance of the sample NPP with high confidence. Such simulations of the structural response were performed using the Monte Carlo-based algorithm indicated in Appendix G of FEMA P-58 (FEMA, 2012). This algorithm simulates hundreds of vectors of demands that preserve the original statistical correlation present in the underlying matrix of demands. For comparison, Fig. 12a–c shows some results obtained from the augmentation of the matrices of results from 11 to 200 rows. This figure shows the vector of demands (AFSAs) for Nodes 2 and 9 for the three GMPEs selected. Additionally, 200 direct results (randomly selected from the databank of 600) obtained from performing time-history analysis using accelerograms simulated with the model proposed are shown in Fig. 12d. Certainly, when using the proposed model, no Monte Carlo simulations of the structural response are required to perform.

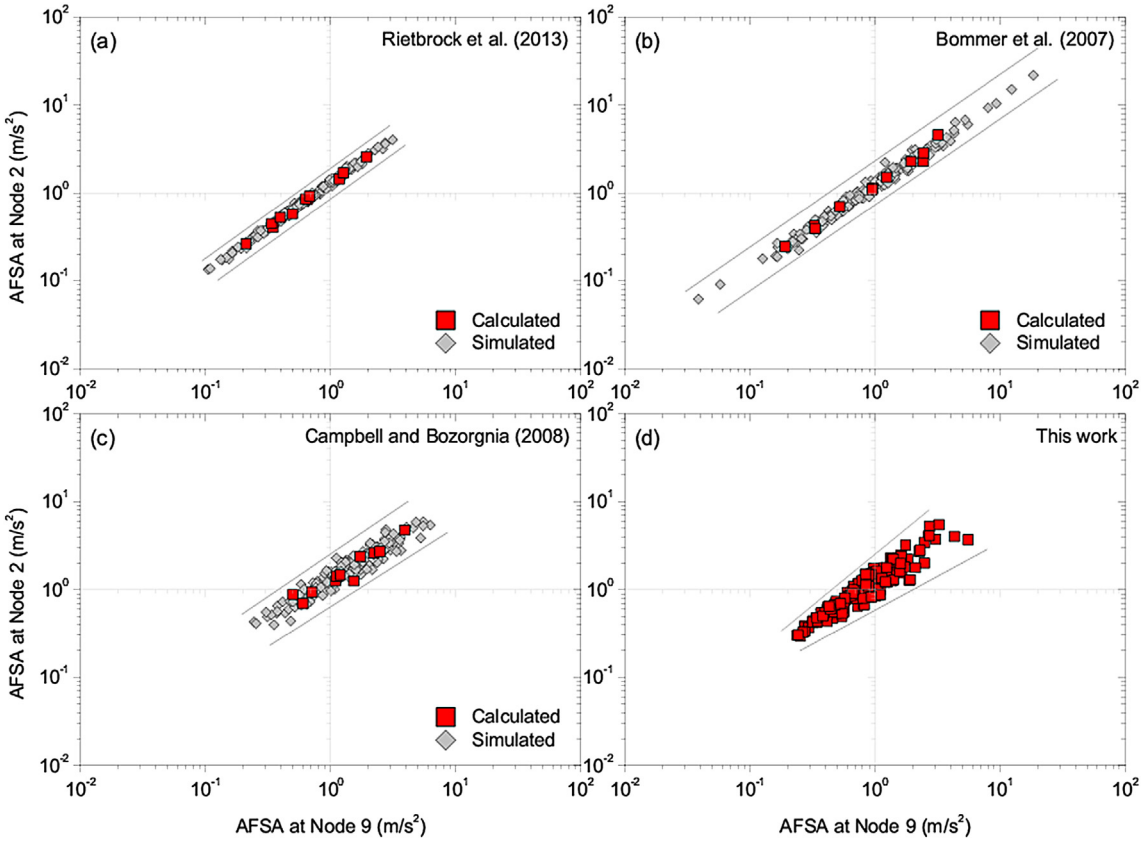

Fig. 12. AFSAs at Nodes 2 vs 9 for the three selected GMPEs and the proposed model.

4.3. Risk assessment calculations

Risk assessment calculations were based on the methodology proposed by Huang et al. (2011b, 2011c). Fig. 13 shows the flowchart that summarises such a methodology. From this flowchart, it is possible to see that it requires three variables: (i) the number (k) of fragility curves (FC) for each component, (ii) the number (m) of row vectors (RV) in the demand-parameter matrix and, (iii) the number (n) of trials (T) required to estimate the statistical distribution of the probability of unacceptable performance.

A sensitivity analysis was carried out in order to obtain the number for each variable that produces a numerically stable value for the probability of unacceptable performance. Table 6 summarises this sensitivity analysis. This table informs two benchmark values of the statistical distribution of the probability of unacceptable performance: the mean and median values of such distributions. However, the median value was arbitrarily selected as the final benchmark associated to each distribution. In Table 6, the number of FC, RV and T highlighted in yellow are the ones that produced the highest median value, whereas their associated median value has been highlighted in blue. Among the three values highlighted in blue for each GMPE and the model proposed, the highest was selected as the final benchmark (highlighted in bold) for the probability of unacceptable performance for each approach.

The results of the sensitivity analysis are as follows: for Rietbrock et al. (2013): 21 FC, 1000 RV and 3000 T; for Bommer et al. (2007): 21 FC, 200 RV and 2000 T; for Campbell and Bozorgnia (2008): 101 FC; 200 RV and 2000 T; and for the model proposed in this work: 21 FC, 200 RV (i.e. 200 accelerograms) and 2000 T. Finally, the median probabilities of unacceptable performance obtained are (mean values are indicated in parenthesis): 16.0% (17.2%), 36.0% (36.2%) and 50.5% (50.4%) when using the GMPEs of Rietbrock et al. (2013), Bommer et al. (2007). and Campbell and Bozorgnia (2008), respectively; whereas a value of 22.0% (24.0%) was obtained when using the model proposed. Fig. 14 shows the corresponding cumulative distribution functions for each approach studied.

5. Discussion

* *Conservatism of using active crustal models for the UK*: When assessing seismic risk of high critical structures in the UK, such as NPPs, it seems that there may be an unnecessarily excessive conservatism if models from active crustal regions are used. These models have been customarily applied in seismic hazard analysis in the UK (Goda et al., 2013; Musson and Sargeant, 2007). This is mainly due to the naturally high epistemic uncertainty of ground motion models of any nature developed for the UK. Such uncertainty is intended to overcome by using data from areas with a wealth of available data. However, an upper limit imposed by ground motion models calibrated for the broader region of Europe and the Middle East seem to be a more reasonable alternative for hazard and risk assessments in the UK. It is acknowledged that NGA attenuation relations have been described to be suitable to be applied in the Euro-Mediterranean region as there is a generally good fit between both types of models (Stafford et al., 2008; Campbell and Bozorgnia, 2006). However, as the results reported in Sections 4.2 and 4.3 imply, it seems that the intrinsic nature of accelerograms in terms of their content of frequencies and intensities could have a different effect when estimating the damage state of critical components of NPPs. For future applications of nuclear facilities,

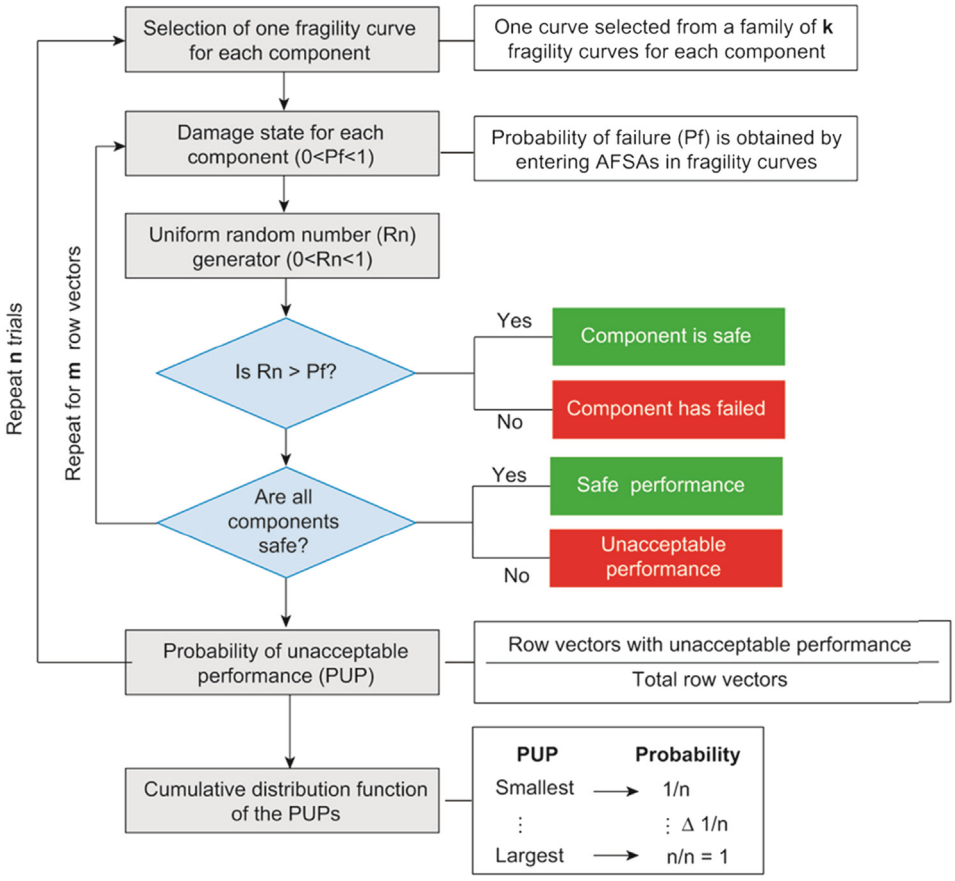

Fig. 13. Flowchart for risk assessment calculations (Huang et al., 2011b; Huang et al., 2011c).

Table 6
Sensitivity analysis for risk assessment calculations.

Fragility curves	Row vectors	Trials	Median	Mean	Fragility curves	Row vectors	Trials	Median	Mean
Rietbrock et al. (2013)					Bommer et al. (2007)				
	200		0.155	0.164		200		0.358	0.359
	1000		0.159	0.167		1000		0.355	0.356
11	2000	2000	0.154	0.164	11	2000	2000	0.357	0.359
21			**0.160**	0.172	21			**0.360**	0.362
101			0.160	0.177	101			0.355	0.364
201	200	2000	0.155	0.172	201	200	2000	0.360	0.369
		2000	0.155	0.170			2000	0.360	0.362
		3000	0.157	0.170			3000	0.358	0.361
21	1000	4000	0.156	0.170	21	200	4000	0.360	0.361
Campbell and Bozorgnia (2008)					This work				
	200		0.495	0.493		200		0.220	0.235
	1000		0.493	0.492		300		0.207	0.222
11	2000	2000	0.494	0.490	11	400	2000	0.220	0.231
21			0.500	0.500	21			**0.220**	0.240
101			**0.505**	0.504	101			0.215	0.239
201	200	2000	0.495	0.502	201	200	2000	0.215	0.241
		2000	0.505	0.504			2000	0.220	0.240
		3000	0.495	0.503			3000	0.220	0.239
101	200	4000	0.500	0.503	21	200	4000	0.220	0.238

Yellow shade represents the number of either fragility curves, or row vectors, or trials that produce the maximum median value.
Blue shade represents the actual maximum median value.
Highlighted in bold is the maximum of maxima median values.

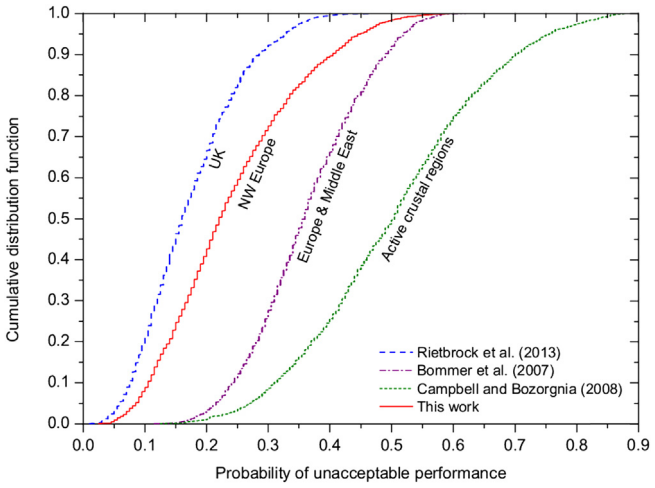

Fig. 14. Statistical distributions of the probability of unacceptable performance of the sample NPP for the three GMPEs selected and the model proposed.

it seems reasonable to discard the use of active crustal models available in the literature (mainly based on data from California and Taiwan) for estimating their seismic risk in the UK.

* *Comparison with a NPP in Eastern United States*: Huang et al. (2010). reported a SPRA of a sample NPP of similar characteristics as the reactor building examined in this work located in Eastern United States, a zone classified as Stable Continental Region as well as NW Europe. The seismic scenario that controlled the hazard of the site selected was an earthquake magnitude M_w 5.3 at distance-to-site of 7.5 km, i.e. a scenario controlled by near-fault conditions. The reported probability of unacceptable performance of such sample NPP was 51%. This higher value can be explained by intrinsic characteristics present in near-fault accelerograms, such as forward directivity and permanent translation causing velocity pulses (Mavroeidis and Papageorgiou, 2003), that can have a significant influence on the content of frequencies and intensities of accelerograms. These particular features of near-fault accelerograms will have a direct effect when assessing the damage state of critical components of NPPs. In any case, the seismic risk for sample NPPs reported for Eastern United States and the results obtained in this work for the UK, although different in absolute terms, they are of the same order of magnitude. As Huang et al. (2010). also showed, the seismic risk for a conventional NPP can be drastically reduced, in the region of 5 orders of magnitude, by the use of seismic isolation devices. A similar outcome could be inferred for a nuclear facility in the UK. The use of seismic protection technology for a NPP in Britain aimed at reducing the seismic risk to values that could be considered negligible for a design event of 10,000 years return period may be worth considering for potential future applications. A systematic review of seismic protection devices suitable for nuclear deployments can be found in Medel-Vera and Ji (2014).
* *Comparison of assessment methods and outcome*: The seismic risk result obtained with the proposed methodology seems to be well constrained by the GMPEs selected for comparisons. Indeed, the UK model used (Rietbrock et al., 2013) was calibrated using weak ground motion data from the UK. As it is not clear to what extent data from low magnitude earthquakes can be used to predict features of moderate-to-large earthquakes, the risk may be underestimated when using this model. On the other hand, the model for Europe and the Middle East used for comparisons (Bommer et al., 2007) was calibrated using data from a broader region possessing a wider variety of tectonic regimes compared to data used to calibrate the model used in this work. Therefore, a higher value of risk was expected to obtain with such a model. Another aspect worth mentioning is regarding the artificial enlargement of observations of the damage state by simulation procedures. The Monte Carlo procedure used for this purpose uses a few seed observations to extrapolate them aimed at creating a statistically robust databank of observations. As this is a rather statistics-based treatment of data, it does not necessarily consider how the nonlinear response of a given structure changes for stronger seismic demands. When using the proposed procedure this effect is included in nature. This effect might be even more important when a NPP is subjected to stronger earthquakes as the nature of accelerograms (intensity, frequency content and time duration) changes considerable for increasing magnitudes. Therefore, it could have a significant influence in the final assessment of risk. This assertion is by no means conclusive and it is therefore left as a matter of further research. Finally, one disadvantage of the proposed approach is that it is computationally more demanding than conventional approaches. The major task contributing to the use of computer resources is the execution of a large number of nonlinear time-history analyses of a structural model of the NPP analysed. For real NPP projects, structural models could reach several thousands of degrees of freedom possessing a significant amount of systems, equipment and critical components whose seismic response need to be analysed in detail. Nevertheless, the extremely high criticality of NPPs projects are deemed worthy of investing such resources. Nowadays, powerful computational resources are available to the technical community to perform such extremely demanding tasks, e.g. ARCHER, the UK National Supercomputing Service, a system that possesses 118,080 processor cores enabling it to perform 3×10^{14} instructions per second.

6. Conclusions

The work conducted for this article has led to the following conclusions:

* The use of the stochastic model calibrated for NW Europe (Medel-Vera and Ji, 2016) seems to produce reasonable seismic risk results for nuclear applications in Britain. It can be inferred that the true value for the seismic risk of the sample NPP analysed here is somewhere in between: (a) the UK model of Rietbrock et al. (2013), and (b) the European model of Bommer et al. (2007). and/or similar models that have used the same target geographical region (such as the new generation of GMPEs calibrated for Europe (Douglas et al., 2014)). In this light, the model proposed can be considered as a reasonable approach for use in risk assessments of nuclear facilities in the UK. The use of the model for active crustal regions of Campbell and Bozorgnia (2008) is likely to produce excessively conservative results for UK seismic conditions. The use of such a model and similar ones (e.g. the GMPES of the projects NGA (Power et al., 2008) and NGA-West2 (Bozorgnia et al., 2014)) to assess the seismic risk of nuclear applications in the UK may not be adequate and may lead to unrealistic results.
* The proposed approach effectively simplifies the methodology for assessing seismic risk which is more rational and more direct to generate sets of accelerograms compatible with the controlling scenario of the seismic hazard at the site. Although not analysed in this article, the stochastic model used (Medel-Vera

and Ji, 2016) could also be applied in the framework of probabilistic seismic hazard analysis for NW European sites.

* The pattern of the nonlinear structural response obtained with the proposed approach differs in shape compared with those from the conventional procedure performed. When using Monte Carlo procedures to simulate and enlarge the damage state of the NPP, the observations of the structural response seem to be enclosed by parallel lines. On the other hand, when using the proposed approach, the observations of the structural response seem to follow a rather divergent pattern, i.e. the stronger the seismic demand, the greater the incursion in the inelastic structural response; hence, greater scattering of observations. This behaviour seems reasonable from a structural engineering point of view and it can be intuitively expected.

References

Musson, R.M.W., 1996. The seismicity of the British Isles. Ann. Geophys. 39.

Atkinson, G.M., 2012. Integrating advances in ground-motion and seismic-hazard analysis. In: 15th World Conference on Earthquake Engineering, Lisbon, Portugal.

Baptie, B., 2010. Seismogenesis and state of stress in the UK. Tectonophysics 482, 150–159.

Basim, M.C., Estekanchi, H.E., 2015. Application of endurance time method in performance-based optimum design of structures. Struct. Saf. 56, 52–67.

Beyer, K., Bommer, J.J., 2006. Relationships between median values and between aleatory variabilities for different definitions of the horizontal component of motion. Bull. Seismol. Soc. Am. 96, 1512–1522.

Bommer, J.J., Stafford, P.J., Alarcón, J.E., Akkar, S., 2007. The influence of magnitude range on empirical ground-motion prediction. Bull. Seismol. Soc. Am. 97, 2152–2170.

Bommer, J.J., Papaspiliou, M., Price, W., 2011. Earthquake response spectra for seismic design of nuclear power plants in the UK. Nucl. Eng. Des. 241, 968–977.

Bozorgnia, Y., Abrahamson, N.A., Atik, L.A., Ancheta, T.D., Atkinson, G.M., Baker, J.W., Baltay, A., Boore, D.M., Campbell, K.W., Chiou, B.S.J., Darragh, R., Day, S., Donahue, J., Graves, R.W., Gregor, N., Hanks, T., Idriss, I.M., Kamai, R., Kishida, T., Kottke, A., Mahin, S.A., Rezaeian, S., Rowshandel, B., Seyhan, E., Shahi, S., Shantz, T., Silva, W., Spudich, P., Stewart, J.P., Watson-Lamprey, J., Wooddell, K., Youngs, R., 2014. NGA-West2 research project. Earthq. Spectra 30, 973–987.

Campbell, K., Bozorgnia, Y., 2006. Next Generation Attenuation (NGA) empirical ground motion models: can they be used in Europe?. In: First European Conference on Earthquake Engineering and Seismology, Geneva, Switzerland.

Campbell, K.W., Bozorgnia, Y., 2008. NGA ground motion model for the geometric mean horizontal component of PGA, PGV, PGD and 5% damped linear elastic response spectra for periods ranging from 0.01 to 10. Earthq. Spectra 24, 139–171.

Cho, S.G., Joe, Y.H., 2005. Seismic fragility analyses of nuclear power plant structures based on the recorded earthquake data in Korea. Nucl. Eng. Des. 235, 1867–1874.

Choi, I.-K., Choun, Y.-S., Ahn, S.-M., Seo, J.-M., 2008. Probabilistic seismic risk analysis of CANDU containment structure for near-fault earthquakes. Nucl. Eng. Des. 238, 1382–1391.

Dehghani, M., Tremblay, R., 2012. Standard dynamic loading protocols for seismic qualification of BRBFs in Eastern and Western Canada. In: 15th World Conference on Earthquake Engineering, Lisbon, Portugal.

Douglas, J., Akkar, S., Ameri, G., Bard, P.-Y., Bindi, D., Bommer, J., Bora, S., Cotton, F., Derras, B., Hermkes, M., Kuehn, N., Luzi, L., Massa, M., Pacor, F., Riggelsen, C., Sandıkkaya, M.A., Scherbaum, F., Stafford, P., Traversa, P., 2014. Comparisons among the five ground-motion models developed using RESORCE for the prediction of response spectral accelerations due to earthquakes in Europe and the Middle East. Bull. Earthq. Eng. 12, 341–358.

Ellingwood, B., 1994. NUREG/GR-0008-Validation of Seismic Probabilistic Risk Assessments of Nuclear Power Plants. US Nuclear Regulatory Commission, Washington, DC.

EPRI, 1994. TR-103959-Methodology for Developing Seismic Fragilities. Electric Power Research Institute, California, USA.

EPRI, 2002. TR 1002988-Seismic Fragility Application Guide. Electric Power Research Institute, California, USA.

FEMA, 2012. FEMA P-58: Seismic Performance Assessment of Buildings. California & Washington DC, USA.

Fragiadakis, M., Vamvatsikos, D., Karlaftis, M.G., Lagaros, N.D., Papadrakakis, M., 2015. Seismic assessment of structures and lifelines. J. Sound Vib. 334, 29–56.

Gencturk, B., Hossain, K., Lahourpour, S., 2016. Life cycle sustainability assessment of RC buildings in seismic regions. Eng. Struct. 110, 347–362.

Goda, K., Aspinall, W., Taylor, C.A., 2013. Seismic hazard analysis for the U.K.: sensitivity to spatial seismicity modelling and ground motion prediction equations. Seismol. Res. Lett. 84, 112–129.

B. Halldórsson, <http://civil.eng.buffalo.edu/engseislab/products.htm>, in, Engineering Seismology Laboratory, State University of New York, Buffalo, New York, 2004.

Halldorsson, B., Papageorgiou, A.S., 2005. Calibration of the specific barrier model to earthquakes of different tectonic regions. Bull. Seismol. Soc. Am. 95, 1276–1300.

Hirano, M., Yonomoto, T., Ishigaki, M., Watanabe, N., Maruyama, Y., Sibamoto, Y., Watanabe, T., Moriyama, K., 2012. Insights from review and analysis of the Fukushima Dai-ichi accident. J. Nucl. Sci. Technol. 49, 1–17.

HM Government, 2013. Report: Nuclear Industrial Strategy - the UK's Nuclear Future. HM Government & Nuclear Industry Association, London.

HSE, 2011. Health and Safety Executive - Office for Nuclear Regulation. T/AST/013-Issue 4. Technical Assessment Guide - External Hazards.

Huang, Y.-N., Whittaker, A.S., Constantinou, M.C., Malushte, S., 2007. Seismic demands on secondary systems in base-isolated nuclear power plants. Earthq. Eng. Struct. Dyn. 36, 1741–1761.

Huang, Y., Whittaker, A.S., Luco, N., 2010. Seismic performance assessment of base-isolated safety-related nuclear structures. Earthq. Eng. Struct. Dyn. 39, 1421–1442.

Huang, Y.-N., Whittaker, A., Luco, N., Hamburger, R., 2011. Scaling earthquake ground motions for performance-based assessment of buildings. J. Struct. Eng. 137, 311–321.

Huang, Y.-N., Whittaker, A.S., Luco, N., 2011. A probabilistic seismic risk assessment procedure for nuclear power plants: (I) Methodology. Nucl. Eng. Des. 241, 3996–4003.

Huang, Y.-N., Whittaker, A., Luco, N., 2011. A probabilistic seismic risk assessment procedure for nuclear power plants: (II) Application. Nucl. Eng. Des. 241, 3985–3995.

Katsanos, E.I., Sextos, A.G., Manolis, G.D., 2010. Selection of earthquake ground motion records: a state-of-the-art review from a structural engineering perspective. Soil Dyn. Earthq. Eng. 30, 157–169.

Kennedy, R.P., Ravindra, M.K., 1984. Seismic fragilities for nuclear power plant risk studies. Nucl. Eng. Des. 79, 47–68.

Kennedy, R.P., Cornell, C.A., Campbell, R.D., Kaplan, S., Perla, H.F., 1980. Probabilistic seismic safety study of an existing nuclear power plant. Nucl. Eng. Des. 59, 315–338.

Kennedy, R.P., Sarkar, B.E., Cluff, L.S., 1990. On some aspects of seismic fragility evaluation for Diablo Canyon seismic PRA. Nucl. Eng. Des. 123, 167–188.

Kim, J.H., Choi, I.-K., Park, J.-H., 2011. Uncertainty analysis of system fragility for seismic safety evaluation of NPP. Nucl. Eng. Des. 241, 2570–2579.

Li, Z.X., Li, Z.C., Shen, W.X., 2005. Sensitivity analysis for floor response spectra of nuclear reactor buildings. Nucl. Power Eng. 26 (in Chinese).

Lubkowski, Z., Bommer, J.J., Baptie, B., Bird, J., Douglas, J., Free, M., Hancock, J., Sargeant, S., Sartain, N., Strasser, F., 2004. An evaluation of attenuation relationships for seismic hazard assessment in the UK. In: 13th World Conference on Earthquake Engineering, Vancouver, Canada. Paper 1422.

Magnox, 2011. Wylfa: Response to EU Stress Tests Following the Events at Fukushima, Japan.

Mavroeidis, G.P., Papageorgiou, A.S., 2003. A mathematical representation of near-fault ground motions. Bull. Seismol. Soc. Am. 93, 1099–1131.

Medel-Vera, C., Ji, T., 2014. Seismic protection technology for nuclear power plants: a systematic review. J. Nucl. Sci. Technol. 52, 607–632.

Medel-Vera, C., Ji, T., 2016. A stochastic ground motion accelerogram model for northwest Europe. Soil Dyn. Earthq. Eng. 82, 170–195.

Musson, R.M.W., 2000. The use of Monte Carlo simulations for seismic hazard assessment in the U.K. Ann. Geophys. 43.

Musson, R.M.W., 2014. UK seismic hazard assessments for strategic facilities: a short history. Boll. Geofis. Teor. Appl. 55, 165–173.

Musson, R.M.W., Sargeant, S., 2007. Eurocode 8 Seismic Hazard Zoning Maps for the UK, British Geological Survey. Technical Report, CR/07/125N.

Nakamura, N., Akita, S., Suzuki, T., Koba, M., Nakamura, S., Nakano, T., 2010. Study of ultimate seismic response and fragility evaluation of nuclear power building using nonlinear three-dimensional finite element model. Nucl. Eng. Des. 240, 166–180.

NIA, 2012. Capability Report: Capability of the UK Nuclear New Build Supply Chain,. Nuclear Industry Association, London.

NIST, 2012. Selecting and Scaling Earthquake Ground Motions for Performing Response-history Analyses. National Institute of Standards and Technology (NIST).

Ozaki, M., Okazaki, A., Tomomoto, K., Iba, T., Satoh, R., Nanba, H., Seya, H., Moriyama, K., Ugata, T., 1998. Improved response factor methods for seismic fragility of reactor building. Nucl. Eng. Des. 185, 277–291.

Park, Y.J., Hofmayer, C.H., Chokshi, N.C., 1998. Survey of seismic fragilities used in PRA studies of nuclear power plants. Reliab. Eng. Syst. Saf. 62, 185–195.

Pisharady, A.S., Basu, P.C., 2010. Methods to derive seismic fragility of NPP components: a summary. Nucl. Eng. Des. 240, 3878–3887.

Power, M., Chiou, B., Abrahamson, N., Bozorgnia, Y., Shantz, T., Roblee, C., 2008. An overview of the NGA project. Earthq. Spectra 24, 3–21.

Prassinos, P.G., Ravindra, M.K., Savy, J.B., 1986. NUREG/CR-4482-Recommendations to the Nuclear Regulatory Commission on Trial Guidelines for Seismic Margin Reviews of Nuclear Power Plants. Lawrence Livermore National Laboratory, Livermore, CA, USA.

Rezaeian, S., Der Kiureghian, A., 2008. A stochastic ground motion model with separable temporal and spectral nonstationarities. Earthq. Eng. Struct. Dyn. 37, 1565–1584.

Rezaeian, S., Der Kiureghian, A., 2010. Simulation of synthetic ground motions for specified earthquake and site characteristics. Earthq. Eng. Struct. Dyn. 39, 1155–1180.

Rietbrock, A., Strasser, F., Edwards, B., 2013. A stochastic earthquake ground-motion

prediction model for the United Kingdom. Bull. Seismol. Soc. Am. 103, 57–77.
Spence, S.M.J., Gioffrè, M., Kareem, A., 2016. An efficient framework for the reliability-based design optimization of large-scale uncertain and stochastic linear systems. Probabilistic Eng. Mech. 44, 174–182.
Stafford, P., Strasser, F., Bommer, J., 2008. An evaluation of the applicability of the NGA models to ground-motion prediction in the Euro-Mediterranean region. Bull. Earthq. Eng. 6, 149–177.
Van Houtte, C., Drouet, S., Cotton, F., 2011. Analysis of the origins of κ (kappa) to compute hard rock to rock adjustment factors for GMPEs. Bull. Seismol. Soc. Am. 101, 2926–2941.
Weightman, M., 2011. Japanese earthquake and tsunami: implications for the UK nuclear industry. In: Office for Nuclear Regulation - HM Chief Inspector of Nuclear Installations, Bootle, Merseyside. ONR-FR-REP-11-002 Revision 2.
Yoo, B., Lee, J.-H., Koo, G.-H., Lee, H.-Y., Kim, J.-B., 2000. Seismic base isolation technologies for Korea advanced liquid metal reactor. Nucl. Eng. Des. 199, 125–142.
Zentner, I., 2010. Numerical computation of fragility curves for NPP equipment. Nucl. Eng. Des. 240, 1614–1621.